Physiological importance of various NFκB family members in regulating intestinal responses to injury

Thesis submitted in accordance with the requirements of the University of Liverpool for the degree of Doctor in Philosophy

by Abdalla Farj Hanedi

March 2013

Acknowledgements

I am truly indebted and thankful to Professor D Mark Pritchard who has supported me throughout my thesis, and without his patience, guidance and immense knowledge, this doctoral thesis would not have been completed. I would like to thank him for teaching me scientific writing and for the opportunity to participate in international conferences. I am also grateful to my second supervisor, Professor Rod Dimaline for his supervision, advice and valuable technical support. This work would not have been possible without the generous donation of mouse colonies by Dr Jorge Caamano from the University of Birmingham. I gratefully acknowledge Jonthan Williams for his pathological reporting of AOM/DSS colitis associated tumours. Thanks also to Dr Carrie Duckworth and Dr Michael Burkitt for their valuable advice, discussions and constructive criticism and all members of the Henry Wellcome Laboratories at the University of Liverpool for their help. I would like to acknowledge the University of Tripoli via the Ministry of Higher Education in Libya for my PhD funding.

Last but not the least, I would like to thank my father, my mother and my wife for their sincere encouragement and inspiration throughout this study.

Table of contents

List of figures

List of tables

Abbreviations

ACF	Aberrant crypt foci
ANOVA	Analysis of variance
AOM	Azoxymethane
APES	3-aminopropyltriethoxysilane
APS	Ammonium persulfate
Ascl2	Achaete scute-like 2
BAFF	B cell activating factor
BAK	Bcl-2 homologous antagonist/killer
BAX	Bcl-2–associated X protein
BCL2	B-cell lymphoma 2
BCL-XL	B-cell lymphoma-extra large
Bmi-1	B lymphoma Mo-MLV insertion region 1 homolog
BrdU	Bromodeoxyuridine
CAC	Colitis-associated cancer
CD	Crohn's disease
cDNA	Complementary DNA
CIN	Chromosomal instability
c-IAP2	Baculoviral IAP repeat-containing protein 3
COX	Cyclooxygenase
CRC	Colorectal cancer
DAB	Diaminobenzidine
DAI	Disease activity index

Dcamkl1	Doublecortin and CaM kinase-like-1
DNAse	Deoxyribonuclease
DR	Decoy receptor
DSS	Dextran sulphate sodium
EDTA	Ethylenediaminetetraacetic acide
EMSA	Electrophoretic mobility shift assay
FADD	Fas-associated protein with death domain
FAB	Familial adenomatous polyposis
FCS	Foetal calf serum
H/E	Hematoxylin and eosin
Hes-1	Hairy and enhancer of split-1
HNPCC	Herediatory non-polyposis colorectal cancer
IAPs	Inhibitors of apoptosis proteins
IBD	Inflammatory bowel disease
IEC	Intestinal epithelial cells
IFN	Interferon
IKK	IκB kinase
IκB	Inhibitor of NFκB
IL	Interleukin
iNOS	Inducible nitric oxide synthases
i.p	Intraperitoneal
JNK	Janus kinase
Klf4	Kruppel-like factor 4
LGr5	Leucine-rich repeat-containing G-protein coupled receptor 5

MMR	Mismatch repair
mRNA	Messenger RNA
MSI	Microsatellite instability
Msi-1	Musashi-1
NFκB	Nuclear factor κB
Ngn	Neurogenin
NIK	NFκB-inducing kinase
NLRs	NOD-like receptors
NO	Nitric oxide
NSAID	Non-steroidal anti-inflammatory drug
PBS	Phosphate buffered saline
PCNA	Proliferating cell nuclear antigen
PRRs	Pattern recognition receptors
P/S	Penicillin/streptomycin mixture
PUMA	p53 upregulated modulator of apoptosis
RAG	Recombination activating gene
RANKL	Receptor activator of NFκB ligand
RHD	Rel homology domain
RIPA	Radio-Immunoprecipitation Assay
RNAse	Ribonuclease
ROS	Reactive oxygen species
RT-PCR	Real time polymerase chain reaction
SEM	Standard error of the mean
SD	Standard deviation

SDS	Sodium dodecyl sulphate
siRNA	Small interfering RNA
SMAC	Second mitochondria-derived activator of caspases
SOX9	SRY (sex determining region Y)-box 9
TAD	Transcription activation domain
TBS	Tris-buffered saline
TEMED	Tetramethylethylenediamine
Th	T-cell helper
TLRs	Toll-like receptors
TNBS	2,4,6-trinitrobenzene sulphonic acid
TNF	Tumour necrosis factor
TRAF	TNF receptor-associated factor
TRAIL	TNF-related apoptosis inducing ligand
TUNEL	Terminal deoxynucleotidyl transferase dUTP nick end labelling
TWEAK	TNF-related weak inducer of apoptosis
UC	Ulcerative colitis
XIAP	X-linked inhibitor of apoptosis protein

Physiological importance of various NFκB family members in regulating intestinal responses to injury

Abdalla Farj Hanedi

Abstract

As key regulators of cell survival, proliferation and immune responses, the NFκB family of transcription factors, which signal via the classical and alternative activation pathways, play important roles in intestinal physiology. The pro-inflammatory function of the classical NFκB activation pathway has previously been demonstrated in various animal models of intestinal inflammation. Persistent activation of this pathway has also been detected in the colonic mucosa of patients with inflammatory bowel diseases (IBD). Conversely, several studies in transgenic mice have shown that disruption of the classical NFκB activation pathway specifically in intestinal epithelial cells renders these cells more susceptible to undergoing apoptosis and also results in increased susceptibility to developing colitis. However, the specific roles of individual members of the NFκB family and in particular the role of the alternative NFκB activation pathway in regulating the susceptibility of the intestine to apoptosis, inflammation and colitis associated colon cancer have not been well defined. We therefore hypothesised that individual members of the NFκB family of proteins which signal via the classical and alternative activation pathways specifically regulate intestinal epithelial cell proliferation, apoptosis and colonic inflammation, consequently modulating susceptibility to developing inflammation associated colon cancer.

Most of these aims were addressed using transgenic mice with germline deletions of c-Rel, NFκB1, and NFκB2, along with their wild-type counterparts. Intestinal

epithelial apoptosis was induced using either γ-irradiation or irinotecan administration. Colitis was induced using dextran sulphate sodium (DSS) and colitis associated cancer by a combination of azoxymethane (AOM) and DSS. *In vitro* studies were performed in HCT116 colon carcinoma cells.

Disruption of classical NFκB signalling by deletion of NFκB1 but not c-Rel sensitised intestinal epithelial cells to undergo apoptosis following γ-irradiation and irinotecan administration. Deleting either c-Rel or NFκB1 also exacerbated the severity of experimental acute and chronic DSS-induced colitis in mice. However, only c-Rel-null mice showed an increase in AOM/DSS induced colonic tumours. This was associated with c-Rel, but not NFκB1 deletion resulting in persistent colonic epithelial mitosis and increased crypt regeneration following DNA damage.

Disruption of the alternative NFκB activation pathway by either deleting NFκB2 (*in vivo*) or suppressing its expression (*in vitro*) also increased the susceptibility of intestinal epithelial cells to undergo apoptosis following DNA damaging stimuli. Conversely and intriguingly however, deleting NFκB2 also protected mice from developing colitis and colitis associated colon cancer.

Specific members of the NFκB family therefore play different roles in regulating the intestinal responses to various types of cellular injury. NFκB2 in particular appears to be essential for developing colitis and its associated cancer. Pharmacological inhibition of NFκB2 may therefore be a promising novel therapeutic strategy for IBD, whereas inhibition of c-Rel signalling may increase susceptibility to developing colitis and its associated colon cancer.

1 Introduction

The intestinal tract forms a mucosal barrier which separates the host's cells from the outside world. Although this intestinal mucosal barrier allows the absorption of various nutrients, it also prevents water loss and protects the body from environmental toxins, harmful luminal contents and microbial insults. The outermost element of this barrier is a single layer of epithelial cells. In order to sense intestinal microbes and mount appropriate responses to maintain homeostasis, epithelial cells express pattern recognition receptors (PRRs) such as Toll-like receptors (TLRs) and NOD-like receptors (NLRs). Once bacteria have been detected, the TLRs and NLRs are ligated and this eventually leads to the activation of NFκB signalling as one of their main downstream effectors. NFκB activation induces the expression of various inflammatory mediators (such as pro-inflammatory cytokines and chemokines) and anti-microbial factors, which are required for the elimination of invading bacteria (1).

As a key regulator of cell survival and proliferation, and of the immune responses which are mediated by PRRs, NFκB signalling plays important roles in regulating intestinal epithelial homeostasis and pathophysiology. As a consequence, dysregulated NFκB signalling has been detected in several intestinal disorders such as chronic inflammatory intestinal diseases (2, 3). However, NFκB signalling has various functions depending on cell context and it can also modulate other key pathways involved in cancer development such as apoptosis and proliferation. This therefore complicates the prediction of the outcomes of dysregulated NFκB signalling on development of intestinal diseases. Hence, dissecting the roles of NFκB

signalling pathways in the intestine is essential to improve our understanding of the pathogenesis of many intestinal diseases.

Several lines of evidence have suggested that the classical NFκB activation pathway is involved in the pathogenesis of inflammatory bowel disease and its associated colorectal cancer. However, most previous investigations have involved generic disruption of this pathway (by disrupting upstream components of the classical signalling pathway such as IKKβ). The NFκB family however consists of 5 transcription factors. Therefore, it is important to investigate and define the importance of these individual members of the NFκB family of proteins in regulating intestinal homeostasis, intestinal responses to injury and the development of inflammatory and neoplastic intestinal disorders.

In this thesis the consequences of deleting three individual members of the NFκB family on intestinal responses to injury and development of colonic inflammation and colitis associated cancer have been assessed using murine models. In order to understand the studies described later in this thesis, I will begin by briefly outlining the major elements involved. These include: structure and functions of the intestine; cell apoptosis and proliferation, particularly in intestinal epithelia; inflammatory bowel disease and its associated colorectal cancer and NFκB signalling pathways.

1.1 Structure and function of the intestinal tract

Anatomically, the intestinal tract is composed of two parts, the small and large intestines. Each part plays a particular role in the digestion and absorption of food.

Ultimately energy and nutrients are extracted from ingested food and the remaining waste is expelled. Additionally, the intestinal tract constitutes a prominent part of the immune system. It is the first line of defence against harmful microbes and toxins. This function is achieved through many factors such as mucus containing secreted IgA antibodies and the gut associated lymphoid tissue (GALT). These vital processes within the intestinal tract are tightly controlled and their disturbance contributes to the development of many local and systemic diseases. All parts of the intestinal tract share a similar general structure, but there are some differences which reflect the specialisation of each section. Histologically, the intestinal tract generally consists of four concentric layers which are as follows from the inside (lumen) of the tract to the outside: mucosa, submucosa, muscularis externa and serosa.

The mucosa is a mucous membrane that lines the inner surface of the intestinal tract and consists of three layers. The innermost is a simple columnar epithelium. The second layer of mucosa is the lamina propria which is composed of loose connective tissue including blood and lymphatic vessels. The muscularis mucosae is the outermost layer of the mucosa and is a thin layer of smooth muscle. The folds in the small intestine are formed by contractions and movements of this smooth muscle layer.

1.1.1 Small intestine

The small intestine which extends from the gastric pylorus to the ileocaecal junction is divided into three segments from proximal to distal; duodenum, jejunum and ileum. The duodenum is about 25 cm in length in humans and this is the place

where the stomach contents are emptied and where pancreatic juice and bile enter from the pancreas and liver respectively. The second segment is the jejunum, which is about 2.5 m long in man. The last section (ileum) is about 3.5 m long and extends until the ileocecal valve. The boundaries of these three segments are not observable either by the naked eye or microscopically. Nevertheless, there are histological differences between them. In some animals including mouse and rat, discrimination between small intestinal segments is less important and the anatomical description is based on the percentage of length. The entire small intestinal mucosa forms finger-like projections called villi which are approximately 1mm in length in man and consist of a core composed of lamina propria. Villi are covered by a layer of simple columnar epithelium (absorptive enterocytes) that have at their luminal side a brushlike surface formed by micro-villi. These villi and micro-villi hugely increase the absorptive surface area. The enterocytes are interspersed with goblet cells that secrete mucus and protect the epithelial cells from digestion. In the space between the bases of villi, there are deep tubular cavities called intestinal crypts (crypts of Lieberkühn) that extend to the muscularis mucosae through the lamina propria (Figure 1.1). These crypts are lined predominantly by less differentiated epithelial cells. At the base of crypts is a zone that is believed to contain the tissue's stem cells, which continually divide to eventually produce all the types of differentiated epithelial cells in the crypts and on the villi. Enteroendocrine cells are scattered individually among the absorptive cells, most commonly in the lower parts of the crypts. These cells secrete various hormones that stimulate intestinal motility and secretion. Additionally, there are secretory epithelial cells located at the bottom of intestinal crypts called Paneth

cells. These are thought to provide protection for stem cells by releasing anti-microbial substances into the gut lumen.

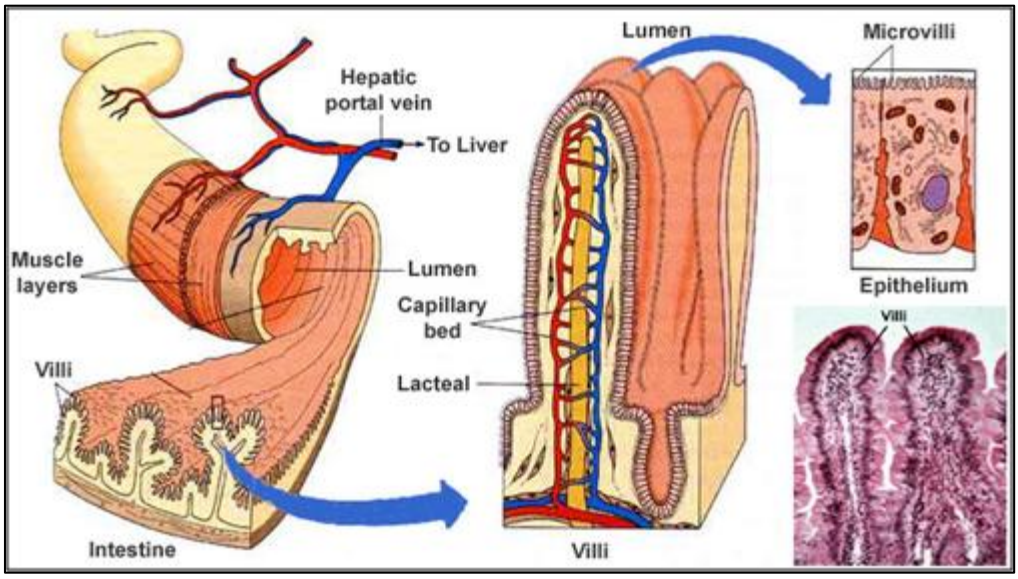

Figure 1.1: Small intestinal cross section and illustration of the structure of villi and crypts of Lieberkühn (adapted from http://www.daviddarling.info/encyclopedia/S/small_intestine.html).

1.1.2 Large intestine

The distal part of the digestive system includes the caecum, appendix, colon, rectum and anal canal. The colon of humans is subdivided into the ascending, transverse, descending and sigmoid colon. However, in mouse these divisions are not well defined and subdivisions have simply been designated as proximal and distal colon in this thesis. The main function of the large intestine is the reabsorption of ions and water from the food that has already passed through the small intestine.

All parts of the large intestine share a common histological structure with the exception of the anal canal. The mucosa consists of a layer of simple columnar epithelium that is configured into deep invaginations called crypts. In contrast to the small intestine, the luminal surface is flat and does not contain villi. The region between the crypts is called the inter-crypt table. The cellular composition of the mucosa is similar to that of the small intestine with the exception that there are no Paneth cells. Additionally, the crypts of the colon contain more cells than those of the small intestine and the proportion of goblet cells is higher.

1.2 Intestinal epithelial stem cells

Cell generation and replacement in intestinal crypts is regulated by stem cells that divide constantly. Intestinal stem cells are morphologically indistinguishable from intestinal epithelial cells. Generally, there are two characteristic features of stem cells. The first is longevity such that they are able to maintain the tissue for long periods of time. The second feature is multipotency which refers to the ability of tissue stem cells to generate all types of differentiated cells within that tissue. In addition to these characteristic properties, stem cells are believed to be quiescent and divide very infrequently. A stem cell divides into one daughter stem cell and a rapidly cycling daughter cell which provides a large number of proliferating cells which subsequently undergo differentiation (4). Several experimental approaches have been used to try to identify candidate intestinal stem cells. These include long term label retention, transplantation and *in vivo* lineage tracing studies. However, there are a number of limitations for each of these methods.

Intestinal stem cells are now thought to be localised near the crypt base. The precise location of small intestinal stem cells however remains uncertain and two schools of thought have been proposed, the "+4 position" model and the "stem cell zone" model (Figure 1.2). The "+4 position" model suggests that stem cells reside at cell position +4 in the crypt axis starting from the bottom with the lower three positions being occupied by differentiated Paneth cells. This model has been supported by several studies conducted by Potten and colleagues. For example they showed that label retaining cells specifically exist at the +4 cell position (5). In addition, they also demonstrated that the cells which reside at the +4 cell position are highly radio-sensitive, an essential function acquired by stem cells to protect them from genetic damage (6). However, the multipotency of these +4 cells has not yet been proven in the literature. By contrast the "stem cell zone" model proposes that the small undifferentiated Crypt Base Columnar (CBC) cells that are located between the Paneth cells are actually the small intestinal epithelial stem cells (7-9). This model relied originally on morphological considerations, but has recently been supported by clonal marking techniques (10).

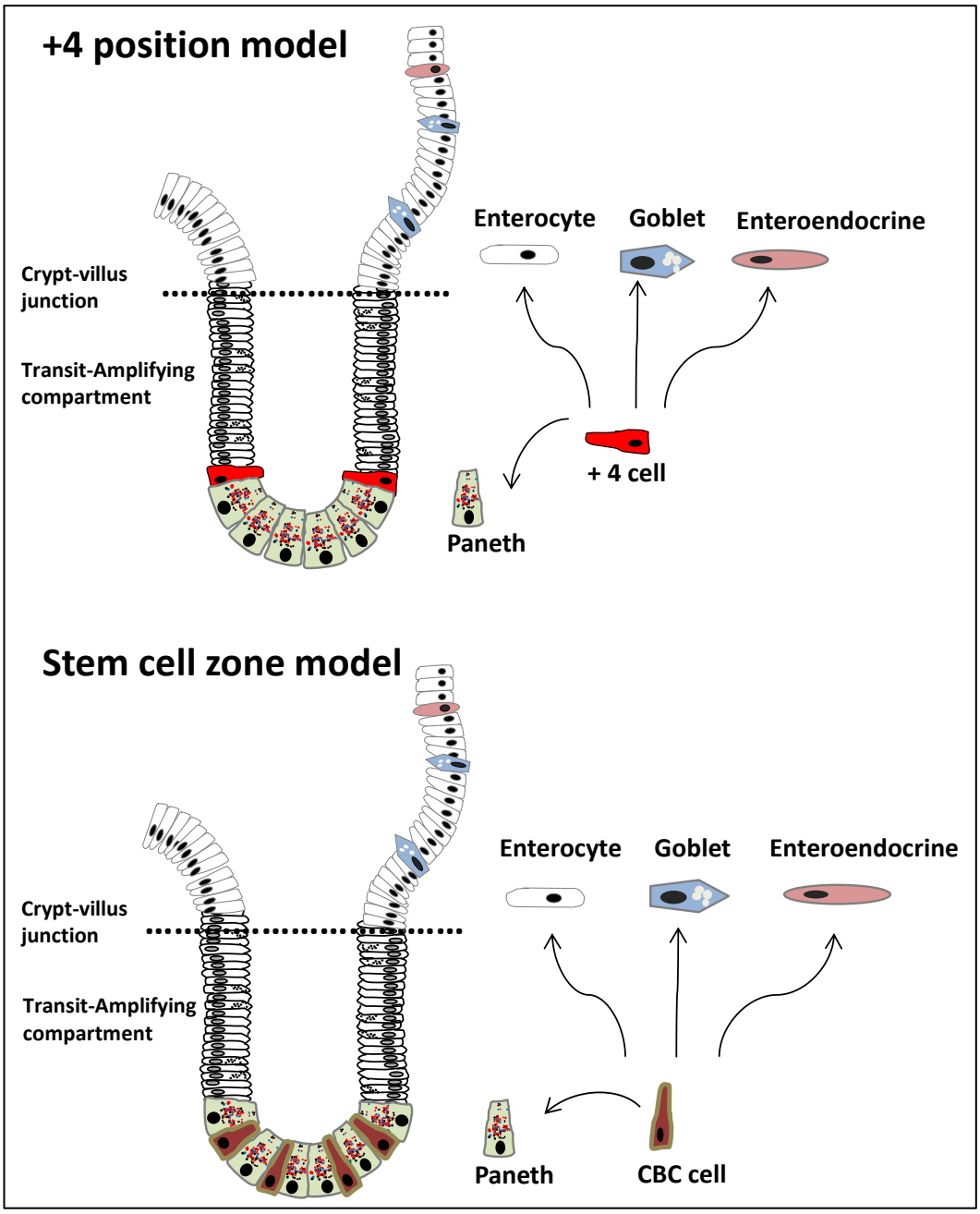

Figure 1.2: Location of the small intestinal stem cells as proposed by two models, "+4 position" model and "stem cell zone" model (CBC cell means Crypt Base Columnar cell). Modified from Barker *et al*, 2008 (4).

Several studies have investigated the number of epithelial stem cells that are present within each crypt. Mathematical models have suggested that there are 4-6 stem cells per crypt in the murine small intestine (11). However, there is currently considerable debate about this. Some studies have proposed that all proliferative cells in the crypt are stem cells, whereas other researchers have suggested that there is only one stem cell present in each crypt. These differences in stem cell number have been attributed to the fact that stem cell number varies in response to crypt injury (12). It is unlikely that there is only one stem cell per crypt, as this might lead to crypt asymmetry and might result in crypt extermination if that stem cell were to die (13). In the colon, stem cells are thought to be located at the very bottom of colonic crypts (at cell positions 1-2) (12, 14). There are no Paneth cells in the colon in the normal state (15), but in chronically inflamed colon such as ulcerative colitis, Paneth cells can be found (11, 16, 17).

Although long term retention, transplantation and *in vivo* lineage tracing methods have demonstrated important aspects of intestinal stem cells, the lack of a unique marker of stem cells hindered the exact identification of intestinal stem cells for many years (18). Recent studies have however identified various potential intestinal epithelial stem cell markers and several of these are summarised in Table 1.1. LGr5/GPR49 has been recently identified as a novel potential marker for intestinal stem cells. It is the first marker to have identified cells that are situated between the Paneth cells. LGr5 positive cells were also observed at the base of colonic crypts. These cells actively divide approximately once every 24 hours and are capable of producing all types of differentiated intestinal epithelial cells (19, 20). Additionally,

it has been shown that Bmi-1 is expressed in a few cells which are located predominantly at cell position 4 in small intestinal crypts, but this protein is also occasionally expressed in the cells that are located between Paneth cells. Bmi-1 positive cells have been shown to proliferate and can generate all differentiated cell lineages within the small intestinal epithelium. However, the observation of Bmi-1 positive cells only in proximal small intestinal crypts suggests the existence of Bmi-1 negative intestinal stem cells in other parts of the intestine (13, 21). Mushashi-1 (Msi-1) has also been suggested as a marker of intestinal stem cells. It is expressed in cells which are distributed at cell positions 4-5 and also in a few cells at the base of the crypt in the adult small intestine and colon respectively (11, 13, 22). Other potential intestinal stem cell markers include doublecortin and CaM kinase-like-1 (Dcamkl1) and SOX9. Dcamkl1 has been found to colocalize with Msi-1 staining and is expressed mainly in the upper stem cell zone (20).To date, it has not yet been confirmed whether the stemness of these cells is intrinsically acquired or is due to the influence of the microenvironment in which they reside.

Marker	Method of discovery	Expression	Evidence for stem cell properties	Evidence against stem cell properties
Lgr5	*In vivo* lineage tracing	Only in CBC cells	Lgr5+ cells are proven to be multipotent cells *in vivo* and *in vitro*	None to date
Bmi1	*In vivo* lineage tracing	Predominantly in +4 cells	Bmi1+ cells are multipotent and targeted deletion of Bmi1+ cells results in crypt extermination	Bmi1 is expressed only in crypts of the proximal small intestine
Ascl2	Microarray profiling of Lgr5+ cells	Only in CBC cells	In addition to restricted expression of Ascl2 in the CBC compartment, Ascl2 is required for survival of Lgr5+ stem cells	Not supported by *in vivo* lineage tracing
Sox9	*In vivo* lineage tracing	Crypt base and sporadically in villus. High expression at +4 to +6, low expression in CBC and Paneth cells	In addition to restricted expression of Sox9 in CBC cells, Sox9+ cells are multipotent *in vitro*	Sox9 is expressed in Paneth cells
Musashi1	Positional information based on expression analysis	In +4 and CBC cells	Msi1 activates some known active pathways in stem cells and colocalises with Dcamkl1	Msi1 is expressed in non stem cells at the crypt base
Dcamkl1	Positional information based on laser capture microdissection of +4 cells	Sporadic expression along crypt-villus axis	Dcamkl1 labels +4 cells	Sporadic expression along crypt-villus axis

Table 1.1: Some potential markers for intestinal stem cells. Adapted from Lin *et al*, 2011 (18).

1.3 Proliferation and differentiation of the intestinal epithelium and the crypt/villus hierarchy

By the process of proliferation, the murine intestinal epithelium renews itself approximately every 5 days. Intestinal epithelial cell proliferation is confined to the crypt compartment and is initiated by asymmetric stem cell division which results in the production of an identical stem cell (retaining the original DNA strand as a protective mechanism against replication errors) and a differentiated progenitor cell (a committed transit-amplifying cell). The transit-amplifying cell cycles very quickly compared to the original stem cell. As the transit-amplifying cell undergoes several divisions, it migrates upwards along the crypt-villus axis in the small intestine and along the crypt axis in the colon, before undergoing differentiation (23). The first few of about 6 cell generations in the small intestine and 8 cell generations in the colon cells retain some stemness and are capable of replacing the ultimate stem cells when they die. These cells are referred to as clonogenic cells and constitute a reserve force to supply additional stem cells to preserve crypt survival. The clonogenic cell population is about 30-40 cells per crypt while about 124 dividing transit committed cells completely lose their stemness (24). As these committed precursor cells migrate upwards, they gradually differentiate when they reach the crypt-villus junction in the small intestine and the upper part of the large intestinal crypt. They differentiate predominantly into absorptive enterocytes and secretory lineages, particularly goblet cells and enteroendocrine cells (4, 12, 24-26). Paneth cells represent the fourth cell lineage in the small intestine and result from the downward migration of committed precursor cells. Paneth cells reside in the crypt base for around 20 days (27). The upwardly migrating epithelial cells are

organised in coherent lines from the upper third of the crypt until they reach the villus tip in the small intestine and inter-crypt table in the colon where they are eventually removed by apoptosis (26).

Regulation of proliferation and differentiation is very important for maintaining homeostasis within intestinal epithelia. This equilibrium is dynamic and depends upon tissue conditions. For instance, tissue injury triggers more proliferation through rapid division of precursor cells and an increase in clonogenic cell number (28). Two vital signalling pathways that appear to control intestinal proliferation and differentiation are the Wnt/β-catenin and Notch pathways.

1.3.1 Wnt/β-catenin signalling pathway

Wnt/β-catenin(canonical Wnt) signals influence cell proliferation by regulating progression through the cell cycle. Active Wnt/β-catenin signalling at the bottom of crypts maintains transit amplifying progenitors in a proliferative state. Inactivating Wnt signalling by over expression of the inhibitor DKK1 results in loss of crypt proliferation (29, 30). Conversely, a constitutively active Wnt/β-catenin/TCF pathway keeps intestinal epithelial cells in a proliferative state and suppresses differentiation (31). A cytoplasmic protein β-catenin is a key element of the canonical Wnt signalling pathway. It translocates into the nucleus and stimulates the subsequent transcriptional regulation of Wnt target genes such as the *c-myc* oncogene. Therefore, nuclear accumulation of β-catenin is considered to be a hallmark of an activated canonical Wnt signalling. When the trigger of Wnt disappears, β-catenin is removed from the nucleus and is degraded by the tumour

suppressor gene product Adenomatous Polyposis Coli (APC). APC therefore acts as a suppressor of Wnt/β-catenin signalling (26).

The role of Wnt signalling in influencing cell proliferation is probably mediated by suppressing the expression of *p21*$^{CIP1/WAF1}$. Additionally, it has been shown that Wnt-dependent down regulation of p21$^{CIP1/WAF1}$ is mediated by c-Myc. Therefore, it has been suggested that Wnt signalling regulates cell cycle progression through up-regulation of c-Myc, which subsequently leads to down-regulation of p21$^{CIP1/WAF1}$ (31, 32).

1.3.2 Notch signalling pathway

Whereas both Wnt and Notch signals are important for maintaining a proliferative state in the lower crypt, many studies have suggested that the key determinant of cell fate and differentiation in the intestinal epithelium is the Notch signalling pathway. This pathway is stimulated by the interaction between Notch receptors and their ligands. This leads to cleavage of an intracellular domain (ICD) from the transmembrane domain of the receptor and the subsequent translocation of ICD into the nucleus, where it binds to the DNA binding protein RBP-J. Subsequently this complex activates the transcription of Notch target genes such as *Hes1* (33, 34). These Notch signalling pathway elements, ligands, receptors and the target gene *Hes1,* are expressed in the proliferative cell compartment of the intestinal crypt (35). Inhibiting Notch signalling through intestinal-specific deletion of RBP-J resulted in increased expression of *Math1* (which is usually repressed by active Notch signalling), and the replacement of the transit amplifying (proliferative) compartment by goblet cells. This was associated with repression of all epithelial

cell division while Wnt signalling stayed active (36, 37). Interrupting the Notch signalling pathway in Zebrafish by mutating *DeltaD* (which is a Notch ligand) and *mind bomb* (in which all Delta-Notch signalling is blocked) also resulted in an increase in goblet cell number in the gut epithelium (35, 38). Murine intestinal epithelium deficient in *Hes1* displayed an increase in the number of secretory cell types (goblet cells, entero-endocrine cells and Paneth cells) and a decrease in enterocytes. This suggests that Hes1 functions as a negative regulator of secretory cell type differentiation (39). Additionally, Hes1 inhibits *Math1* which is a positive regulator of secretory cell lineage differentiation. *Math1* deletion in mice caused a reduction in intestinal epithelial goblet cells, entero-endocrine cells and Paneth cells without affecting enterocytes (40). Therefore, the commitment choice of progenitor cells to differentiate into either absorptive or secretory cell types depends to a certain extent on the balance between Hes1 and Math1 expression (Figure 1.3). However, further downstream regulation of Math1-specified secretory cell lineages is necessary for the differentiation of individual secretory cell lineages. This downstream choice involves the zinc-finger transcriptional repressor Gfi1 which is shown to be lost in *Math1*-null embryonic intestines. Deleting *Gfi1* in mice was shown to cause loss of Paneth cells and a reduction in the number of goblet cells and an increase in the number of enteroendocrine cells. This suggests that Gfi1 is essential for the differentiation of Paneth and goblet cells and that it is a negative regulator of the differentiation of enteroendocrine cells (41). Deleting neurogenin 3 (Ngn3) in mice resulted in complete loss of enteroendocrine cells, while the other three cell types (enterocytes, goblet cells and Paneth cells) developed normally. This suggests that Ngn3 is specifically essential for the enteroendocrine cell fate decision

in intestinal multipotent stem cells (42). Homozygous Kruppel-like factor 4 (*Klf4*)-null mice die within 15 hours of birth. The colon of these *Klf4*-null mice showed a 90% decrease in goblet cell numbers. Therfore Klf4 is likely to be a goblet cell-specific differentiation factor (43). Sox9 has been shown to be crucial for the differentiation of Paneth cells (44) (Figure 1.3).

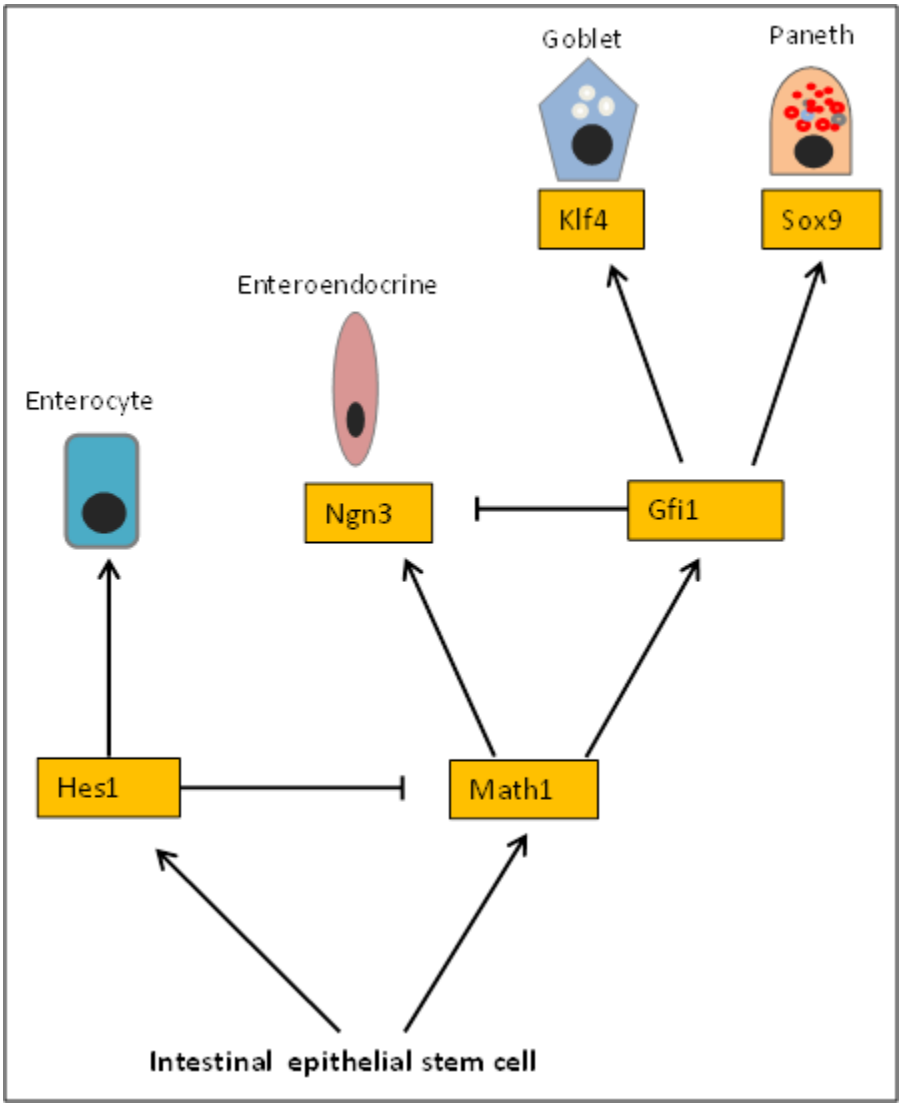

Figure 1.3: Schematic diagram showing the contribution of several regulators to fate decision from intestinal epithelial stem cells.

1.4 Apoptosis

Currently there are thought to be four main distinct modalities of cell death, apoptosis, autophagy, cornification and necrosis. Cornification is a morphologically and biochemically distinct form of programmed cell death that occurs in the epidermis and results in the formation of corneocytes. Autophagic cell death is a self-degradative process which is thought to be required during critical times of insufficient energy availability during development and nutritional stress. Autophagy is morphologically characterised by massive accumulation of two-membrane autophagic vacuoles in the cytoplasm and the absence of chromatin condensation (45). Unlike other forms of cell death, necrosis is morphologically characterised by cell swelling, dilatation of cytoplasmic organelles, plasma membrane rupture and the release of cellular contents which can subsequently evoke an inflammatory response. Apoptosis is a morphologically and biochemically distinct form of physiological cell deletion. It is the process whereby unwanted healthy, damaged and deleterious cells are removed from tissues (46). Apoptosis also plays a central role in tissue morphogenesis during development and in tissue homeostasis in adult animals. Many pathophysiological conditions have been attributed to a disturbance in the regulation of apoptosis. In the intestinal epithelium, homeostasis is ultimately determined by a balance between cell proliferation and cell death. The cells that are lost from the small intestine villus tip or from the inter-crypt colonic table into the gut lumen are replaced by equal number of cells through cell proliferation in the crypt. In pathological conditions such as colon cancer, impaired apoptosis may result in failure to delete mutated

cells, which subsequently may accumulate and result in progression to colon cancer and resistance to chemotherapeutic drugs (47).

1.4.1 Molecular mechanisms that regulate apoptosis

Apoptosis is mediated mainly by two pathways, extrinsic and intrinsic. The extrinsic pathway is activated through the binding of pro-apoptotic ligands to pro-apoptotic receptors, such as Tnfsf10/Apo2L/TRAIL to DR4 and DR5 receptors or FasL to the Fas receptor. As a result, two intracellular protease enzymes termed caspase-8 and caspase-10 are released in their active forms. This signal leads to activation of caspases-3, 6 and 7, which are the enzymes responsible for apoptosis (48, 49). This pathway is independent of p53 expression (50). The intrinsic pathway is initiated within the cell in response to cellular stress. It basically depends on the equilibrium between pro-apoptotic and anti-apoptotic proteins of the BCL2 superfamily (51). The cell senses stress through p53 and activates the pro-apoptotic BH3-only proteins PUMA and NOXA, which augment the stimulation of multi-domain pro-apoptotic proteins such as BAX or BAK. As a result, these proteins proceed to the mitochondrial membrane where they counteract the function of the anti-apoptotic BCL2 proteins which suppress the permeability of the mitochondrial membrane. As a consequence, mitochondrial permeability is increased and cytochrome c and the pro-apoptotic protein SMAC/DIABLO escape from the mitochondria into the cytosolic space. Through this process, cytochrome c activates caspase 9, which in turn activates caspases-3, 6 and 7 that carry out apoptosis. The SMAC/DIABLO protein has a pro-apoptotic role by interacting with inhibitor of apoptosis proteins (IAPs) and preventing their ability to inhibit caspases (52, 53) (Figure 1.4).

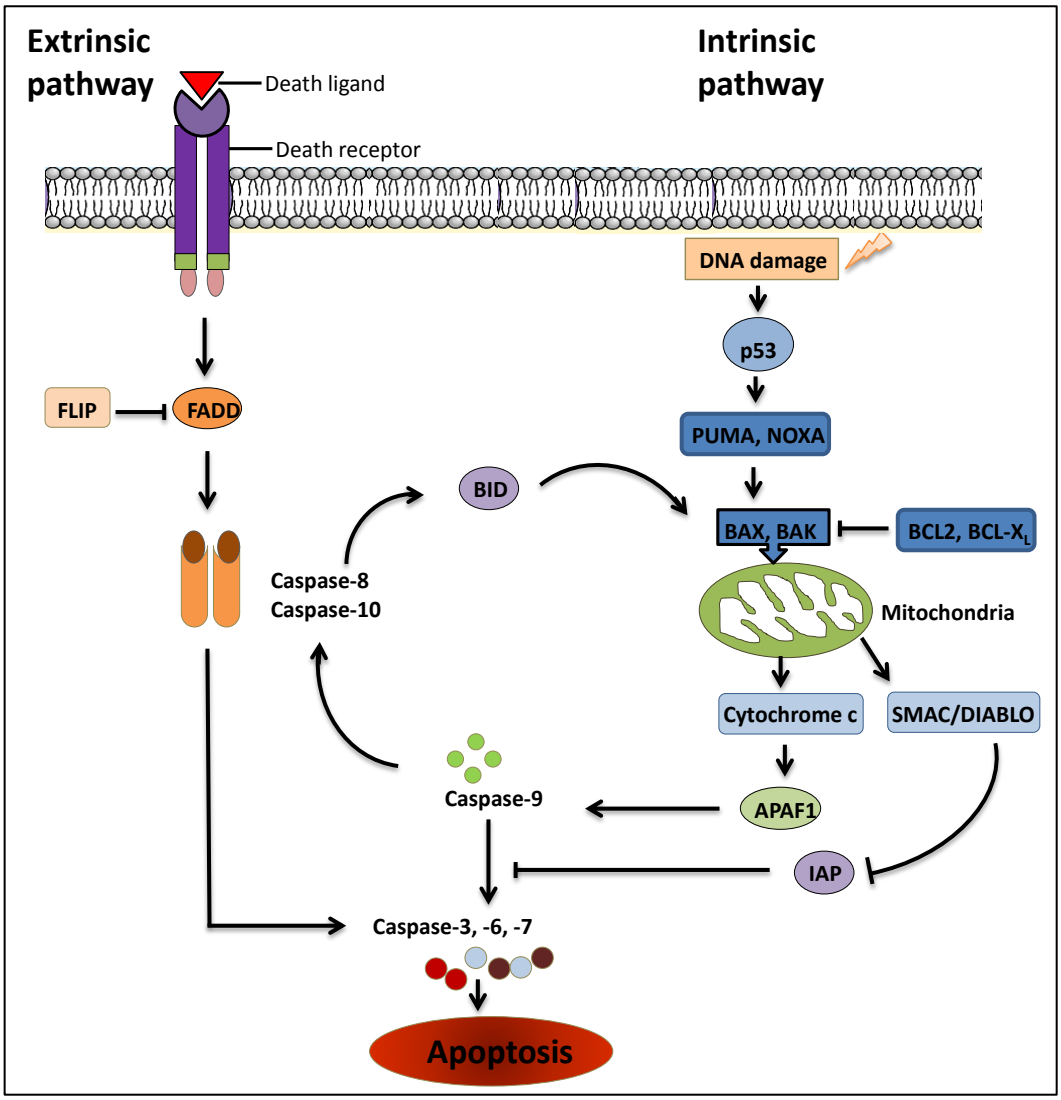

Figure 1.4: Extrinsic and intrinsic pathways of apoptosis. Modified from Ashkenazi, 2002 (48).

1.4.2 Detecting apoptosis in intestinal epithelium

Apoptosis is characterised by well-defined morphological and biochemical changes. These include shrinking of the cell, disappearance of microvilli and condensation of chromatin at the nuclear margins. Eventually, the cell fragments into separate membrane-bound bodies termed apoptotic bodies which are ultimately phagocytosed by adjacent epithelial cells and phagocytic cells (54). Most of these features can be seen in adequately fixed, processed, embedded and well oriented hematoxylin and eosin (H/E) stained paraffin embedded tissue sections (55). However, there are some problems associated with interpreting apoptotic indices obtained in this way as discussed by Potten (56). The number of apoptotic cells in the normal intestinal epithelium is relatively small, hence most biochemical methods for detecting apoptosis are insensitive in this setting.

1.4.3 Spontaneous apoptosis in the normal intestinal epithelium

1.4.3.1 Small intestine

The small intestinal epithelium has a high turnover rate. In healthy murine intestinal epithelium, the number of apoptotic cells is very small (<1%) relative to the total epithelial cell number. This spontaneous apoptosis is predominately located at crypt cell positions 4 to 5 just above the Paneth cells, where the stem cells have been proposed to reside in one hypothesis (57). The apoptotic cell number, expressed as a percentage of all cells at cell position 4, reaches about 10% (55). Comparable amounts of spontaneous apoptosis levels are observed in mutant mice in which the *p53* gene has been deleted. This p53-independent process may therefore function

as a regulatory mechanism to delete excess stem cells and maintain stem cell number (57-60).

1.4.3.2 Large intestine

The large intestine shows significantly lower rates of spontaneous apoptosis than the small intestine. Furthermore, the apoptotic cells observed in murine colonic crypts do not predominate in the proposed stem cell zone (cell position 1-2), but are located throughout the proliferative compartment of the crypt. Therefore, spontaneous apoptosis may not be the sole mechanism for the regulation of stem cell number in the large bowel. Unlike the small intestine, the antiapoptotic gene *BCL2* is expressed at the base of murine and human colonic crypts. This may contribute to the relative lack of spontaneous apoptosis in the stem cell zone of colonic crypts (55, 59, 61, 62).

1.4.3.3 Genetic determinants of spontaneous intestinal apoptosis

The trigger that induces spontaneous intestinal epithelial apoptosis has not yet been identified. However, its genetic regulation has been assessed using knockout mice. As mentioned above, spontaneous apoptosis does not depend on p53 expression. In addition, homozygous BCL2-null mice do not show any differences in the amounts of spontaneous apoptosis in the small intestine relative to control mice (46, 63). However, BCL2 knockout mice do demonstrate higher rates of spontaneous colonic apoptosis, located predominantly at cell positions 1-2 at the bottom of the crypt (61). These findings suggest that BCL2 is involved in regulating the homeostasis of normal colonic epithelium. Bax-null mice showed similar levels of spontaneous apoptosis to their wild-type counterparts in both the small intestine

and midcolon. This is consistent with the known distribution of Bax expression which is confined to differentiated Paneth cells and villus enterocytes that are not responsible for cell renewal (46, 64, 65). Additionally, Bcl-w does not appear to be involved in the regulation of spontaneous intestinal apoptosis (66). However, it has been demonstrated that BAK regulates spontaneous apoptosis at the colonic intercrypt table region, but it is not involved in regulating spontaneous apoptosis in the small intestine (67).

1.4.4 Damage–induced intestinal apoptosis

Several studies have investigated the apoptosis that is induced in gastrointestinal epithelia by cytotoxic agents such as irradiation and cytotoxic drugs. As a result of double strand breaks in DNA due to γ-irradiation, p53-dependent apoptosis is initiated (60, 68). The mechanism of apoptosis induction in intestinal epithelium following DNA damage has not however been completely clarified. The DNA glycosylase MBD4 has been implicated in the cellular response to DNA damage and the subsequent initiation of cell apoptosis in $APC^{Min/+}$ mice (69). Radiation-induced apoptosis occurs mainly in cells above the Paneth cell zone in small intestinal crypts. This suggests that cells within this potential stem cell zone and thus probably the actual stem cells are highly sensitive to apoptosis. Intestinal apoptosis induced by γ-irradiation increases as the dose increases until it reaches a plateau at doses greater than 1Gy in the small intestine and 6-8Gy in the mid-colon (59). This early wave of apoptosis reaches peak levels within 3-6h of radiation exposure. p53 appears to be the main regulator of this early wave of intestinal apoptosis following γ-irradiation as *p53*-null mice demonstrate complete absence of this response (68). However,

p53-null mice demonstrate a significant increase in small intestinal apoptotic cells 24h following 8Gy, but not 1Gy γ-irradiation. Therefore, a p53-independent mechanism appears to function to delete damaged cells following exposure to high doses of radiation several hours after the p53-dependent wave of apoptosis (60). Other studies have also demonstrated that induction of apoptosis by doses of γ-irradiation less than 10Gy is mediated by p53 and BAK, but inhibited by BCL2 and BCL-w (60, 61, 64, 66, 67).

The cell positional distributions of apoptosis induced in the intestinal epithelium by 18 cytotoxic agents, 5 sources of radiation (70, 71) and 4 mutagens was systematically assessed by Ijiri and Potten (72, 73). Each agent tends to induce apoptosis within a particular region of the crypt, however apoptosis could be induced in any region (59). Irinotecan (CPT-11) is a relatively a new chemothereuptic drug used to treat various tumours particularly colon cancer. Its mechanism of action is by inhibiting DNA topoisomerase I (74, 75), which prevents DNA from unwinding. Chemically, it is a semisynthetic analogue of the natural alkaloid camptothecin. In several studies, irinotecan has been shown to display distinctive concentration-dependent effects such as apoptosis and differentiation induction, in addition to its cytotoxic activity (76, 77). An increase in apoptosis has been observed throughout the intestinal epithelium in mice following intraperitoneal administration of irinotecan (77). Irinotecan-induced apoptosis has however not previously been well defined on a cell positional basis in the murine small intestine and colon.

1.5 Inflammatory bowel diseases

The inflammatory bowel diseases (IBD) are characterised by chronic inflammation of the intestinal tract. Ulcerative colitis (UC) and Crohn's disease (CD) are the two main disorders that constitute IBD. Clinically, patients with IBD present with symptoms such as loss of body weight, diarrhoea and rectal bleeding. The histological hallmark of IBD is chronic and uncontrolled inflammation of the intestinal mucosa characterised by distortion of the normal crypt architecture and the presence of a mixed inflammatory cell infiltrates. This architectural distortion distinguishes IBD from the chronic inflammation that occurs in the gut of healthy individuals or patients with bacterial colitis (78).

1.5.1 Aetiology and pathogenesis of IBD

The aetiological factors that are involved in the pathogenesis of IBD have not yet been fully determined. However, accumulating evidence suggests that both genetic and environmental factors contribute to the pathogenesis of IBD (79, 80). The current hypothesis for the pathogenesis of IBD suggests that it results from the interaction of environmental factors, mainly the intestinal microbiota, and inappropriate immune responses in genetically predisposed individuals (81). Recent genome-wide association studies have identified approximately 100 genomic loci that confer susceptibility to IBD. These susceptibility loci contain candidate genes that encode proteins that are required for various crucial cellular functions such as microbial recognition, cytokine signalling and epithelial barrier function. Among these genes is *Rel* that encodes the NFκB family member c-Rel (82, 83). Several of the identified candidate genes have been shown to be specifically associated with Crohn's Disease such as *NOD2* (84)*, ATG16L1* (85) and *IRGM* (86). These genes

encode key proteins involved in microbial recognition (eg NOD2) and autophagy (eg NOD2, ATG16 and IRGM). NOD2 is expressed in immune and epithelial cells of the intestine and it is important for microbial sensing and subsequent NFκB activation to initiate an adequate innate immune response which required for bacterial clearance (87). Moreover, autophagy (intracellular bacterial processing) is also required for the clearance of invading bacteria (88) and polymorphisms of NOD2, ATG16 and IRGM which are key regulators of this process (86, 89, 90) have been strongly associated with Crohn's Disease.

In addition to defective bacterial sensing and autophagy, impairment of the intestinal mucosal barrier is also a key pathophysiological process that leads to intestinal inflammation and has been linked to the pathogenesis of IBD (91, 92). The mucosal barrier consists of several layers of protection, including outer mucosal barrier elements (such as commensal microbiota, the mucus layer and immunoglobulin A), intestinal epithelial cells and subepithelial immune cells. These elements communicate with and affect each other. The normal commensal microbiota contribute to maintaining a functional intestinal mucosal barrier. This results from inhibition of the colonisation of pathogenic bacteria and by influencing the development of both the intestinal epithelium and the gut associated lymphoid tissues (81, 93, 94). However, this beneficial relationship between the microbiota and host can break down and this may result in chronic intestinal inflammation. This abnormal reaction may occur as a consequence of dysbiosis and an altered gut microbial ecosystem which are common findings in IBD. Several studies have shown that the gut microbiota represent a crucial factor in inducing inflammation in IBD

(95, 96). Several environmental factors have also been shown to be associated with IBD such as diet and life style (eg smoking). These factors also influence the composition of the gut microbiota (96, 97). Defects in the intestinal epithelial cell barrier have been shown to be essential for the abnormal response of the mucosal immune system to microbiota that leads to chronic intestinal inflammation (98). Disruption of the intestinal epithelium is a hallmark of IBD and is associated with increased intestinal epithelial cell apoptosis (81). As a consequence, subepithelial immune cells are exposed to luminal bacteria resulting in an uncontrolled inflammatory response (98). Indeed, a large body of evidence from human studies has indicated the importance of these factors in the pathogenesis of IBD. However, animal models have also provided insights into the pathogenesis of IBD.

In order for an animal to act as a model of IBD, several characteristic features of human IBD should be demonstrated such as characteristic histopathology and accompanying clinical features. Although none of the available animal models is exactly identical to human IBD, they do represent several aspects of the human disease. They can therefore provide valuable information about the pathogenesis of the disease and are useful tools for evaluating the therapeutic potential of new therapies for IBD before they are tested in human clinical trials. In the last two decades, a large number of animal models of IBD have been developed. These can be classified into four categories: spontaneous models, genetically engineered models, inducible models and adoptive transfer models in immunocompromised hosts (99-101). Colitis develops spontaneously in certain strains of mice. For instance, C3H/HejBir mice spontaneously develop colitis by the age of 3 - 4 weeks

and this disappears by the time they reach 10 - 12 weeks old (102). A spontaneous IBD animal model has been also demonstrated in SAMP1/Yit mice, which develop chronic terminal ileitis, resembling Crohn's disease (103). The genetically engineered models include two subgroups, knockout and transgenic. IL-7 transgenic mice develop chronic colitis when they are 4-11 weeks old and this resembles ulcerative colitis in humans (104). Genetic deletion of IL-10 has also been shown to induce spontaneous chronic colitis in mice (105). In adaptive transfer models, intestinal inflammation occurs as a result of selective transfer of certain cell types to immunodeficient host animals such as the adoptive transfer of CD45 RB^{high} T-helper cells into SCID mice (severe combined immunodeficient mice) (106). Inducible colitis models are however probably the most widely used by researchers for studying IBD pathogenesis and the effects of new therapeutic agents. Therefore, we have focused on inducible models in this thesis as described below.

1.5.2 Inducible colitis models

Acute and chronic inflammation of an animal's intestine can be induced by mechanical or chemical disruption of the mucosal barrier. Induction of colitis in this model is thought to be due to the activation of the mucosal immune system on exposure to luminal contents particularly the microbiota (107). Induced models, particularly chemically induced forms of colitis are therefore widely used.

1.5.2.1 Dextran sulphate sodium induced colitis

Chemically induced colitis in mice, particularly dextran sulphate sodium (DSS) induced colitis is one of the most frequently used animal models of IBD. This is because it has low cost, is simple to use and the severity of the resultant colonic

inflammation can be easily controlled (107). It has also been shown that administration of azoxymethane (AOM) prior to DSS treatment results in the development of several colorectal tumours in areas which have developed colonic inflammation. This suggests that experimental DSS induced colitis can also be used as a model for studying the potential molecular mechanisms that may link inflammation to inflammation associated carcinogenesis in the colon (108) and thus the pathogenesis of IBD and IBD associated colon cancer. The murine model of DSS-induced colitis is thus a valid model to translate mouse data to human diseases (109). In contrast to other models, acute, chronic and relapsing colitis can be induced easily by changing the DSS concentration and the number of DSS cycles. Therefore, the DSS induced colitis model was chosen in this thesis for studying the individual contribution of individual NFκB family members to the pathogenesis of colitis and colitis associated colonic cancer.

1.5.2.1.1 Induction of colitis using DSS

Colitis is induced in animals by adding DSS to their drinking water. Animals can develop acute or chronic colitis. This depends on the concentration, duration and frequency of administered DSS (110). It has been shown that mice exposed to one DSS cycle of 5 days develop acute colitis which resolves after approximately 2 weeks following DSS removal, with the exception C57BL/6 mice in which colitis may progress to chronicity. Chronic colitis can be induced by subjecting the mice to three to five DSS cycles and this is manifested by monocyte and lymphocyte infiltration and architectural distortion of crypts (111).

1.5.2.1.2 Clinical and histological features of DSS induced colitis

DSS induced colitis has similar clinical and histological manifestations to IBD (particularly UC) in humans. These include body weight loss, diarrhoea, bloody stool and compromised general health. Severe DSS induced colitis may eventually lead to death. As a result of administrating 3-5% DSS for a few days, C57BL/6 mice develop acute colitis which is characterised by epithelial and crypt loss, infiltration of neutrophils into the mucosa and submucosa and shortening of the colon. Consistent with IBD in humans, cryptitis and crypt abscesses may also be observed in DSS induced colitis, particularly in C57BL/6 mice (112).

1.5.2.1.3 Important factors that influence DSS induced colitis

Various factors have been shown to influence the susceptibility, onset and severity of DSS induced colitis and these factors can be divided into three categories. The first category is related to the nature of DSS itself and its mode of administration. These include the molecular weight, concentration, duration, manufacturer and batch of administered DSS. It has been shown that the severity of colitis and colitis associated carcinogenesis varies following administration of different molecular weights of DSS ranging from 5 to 500 kDa. It appears that DSS with a molecular weight around 50 kDa is optimal for inducing severe colitis and enhancing the carcinogenic activity of AOM in the colon (113, 114). The second category is related to the animal species, strain and gender and reflects the importance of genetic factors in the pathogenesis of DSS induced colitis, similar to the contribution of genetic factors during the development of IBD in humans (111, 115). The third category involves environmental factors such as housing conditions and the

intestinal microbiota. The importance of the intestinal microbiota in the pathogenesis of DSS induced colitis is supported by the observation that mice did not develop colitis when maintained in germ free conditions, but colitis appeared immediately after mice had been reconstituted with commensal bacteria (116). Thus, similar to IBD in humans, both genetic and environmental factors contribute to the pathogenesis of DSS-induced colitis.

Despite evidence for the involvement of all the above mentioned factors in the pathogenesis of DSS induced colitis, the exact mechanism by which DSS induces colitis remains unknown. It is believed that the toxic effect of DSS on colonic epithelial cells results in impairment of the epithelial barrier. This is evident in the acute stage of DSS induced colitis, where crypt loss, increased epithelial apoptosis, decreased epithelial proliferation and altered expression of tight junction proteins are observed in the colon along with inflammation following DSS administration (117, 118). Hence, defects in the epithelial layer, which functions as a physical and immunological barrier, permit the uncontrolled entry of commensal bacteria and toxins into the mucosa. Consequently, this leads to an overwhelming inflammatory response (115). Given the importance of inflammatory mediators such as cytokines, chemokines and nitric oxide in the pathogenesis of colitis, it has been shown that DSS induced colitis is associated with up-regulation of these mediators. The acute phase of DSS induced colitis is dominated by a Th1 response, whereas during the chronic phase both Th1 and Th2 responses are observed (119).

In summary, the simplicity of induction of colitis and colitis associated carcinogenesis, the low cost and the similarities between DSS induced colitis and

human IBD suggest that the murine model of DSS induced colitis is suitable for studying the specific roles of individual members of the NFκB family of transcription factors in the pathogenesis of both colitis and colitis associated cancer. However, as mentioned above, several factors may affect the susceptibility to DSS; it is therefore important to report details of all the conditions that may alter the susceptibility to DSS such as mouse strain, gender, animal housing conditions, and the molecular weight, manufacturer, concentration and duration of DSS treatment.

1.5.2.2 Other inducible models of colitis

Several other models of induced colitis have also been established such as acetic acid induced colitis, indomethacin induced enterocolitis, 2,4,6-trinitrobenzene sulphonic acid (TNBS) induced colitis and oxazolone induced colitis. Rectal administration of a diluted acetic acid results in epithelial damage and mucosal and submucosal inflammation in the colon (120). It has been suggested that this model is suitable for studying the early phase of colonic inflammation and wound healing (121, 122). Indomethacin induced enterocolitis is based on subcutaneous injection or addition of dissolved indomethacin to the diet, and results in inflammation in the small intestine and colon of rodents (120, 123). Acute colitis can be induced in mice by luminal intracolonic instillation of TNBS or oxazolone in ethanol. Repeated enema administration of TNBS or skin sensitisation by subcutaneous injection of oxazolone before administration of oxazolone enema can result in chronic colitis (124, 125). In contrast to the DSS model however, these models do not show such high reproducibility (126).

1.5.3 Risk of colorectal cancer in IBD

The risk of colorectal cancer (CRC) development is increased in patients with IBD compared to the general population. Although a multitude of epidemiological studies have been conducted, the exact magnitude of this risk remains difficult to determine. This has been attributed to several biases and methodological errors (127, 128). Due to geographical and study variations, the risk of developing CRC in patients with UC and CD ranges between a 2 to 8.2-fold increase compared to the general population (129). Eaden *et al* extracted data from 116 published studies which involving around 55,000 patients with UC. CRC was diagnosed in 1,700 patients. Using meta-analysis, Eaden *et al* estimated the risk of developing CRC in patients with UC and found it to be 2% at 10 years, 8% at 20 at years and 18% at 30 years (irrespective of disease extent) (130). In another more recent meta-analysis of the results of 34 published studies involving 60,122 patients with CD, the estimated risk of developing CRC was 2.59 times and the risk of developing small intestinal carcinoma was 28.4 times compared to the normal population (131). In general, several risk factors have been found to be associated with an increased risk of developing CRC in UC such as the severity of inflammation, duration, extent of the disease, family history of CRC, presence of pseudopolyposis and smoking (132, 133). Chronic colonic inflammation has been strongly linked to an increased susceptibility to developing colorectal cancer. This has been supported by several lines of evidence. For example, a positive association has been found between the increased susceptibility to CRC and the duration and extent of colitis. This is further supported by the fact that the use of several anti-inflammatory drugs that reduce the severity of inflammation is associated with reduced risk the development of CRC

(133, 134). Additionally, the production of cytokines (which are regulated by NFκB) and oxidative stress, which are both enhanced in UC, are considered to be important risk factors that contribute to colorectal carcinogenesis (135, 136).

1.6 Colorectal cancer

1.6.1 Epidemiology of colorectal cancer

Colorectal cancer (CRC) is the one of most common malignancies worldwide and has a high mortality and morbidity. CRC is more prevalent in Europe, North America, Australia and Japan (137). The incidence of CRC is still increasing and it represents the most common cancer and the second leading cause of cancer deaths in Europe, where 436,000 new cases of CRC were diagnosed and 212,000 deaths were reported in 2008 (138). The majority of cases of CRC present with advanced disease at diagnosis (139).

Genetic and environmental risk factors have been identified and linked to the development of CRC. The lifetime risk of developing CRC is 5% in the general population and this risk increases with age (140). Family history of CRC in one first degree relative imposes a 2-fold increase in risk of developing CRC and this risk increases to 4-fold when three or more of first degree relatives have been affected compared to individuals with no family history (141). Individuals with inherited conditions such as familial adenomatous polyposis (FAP) and hereditary non-polyposis colorectal cancer (HNPCC) have 100% and 80% lifetime risks of developing CRC respectively (142). Personal and environmental factors have been also implicated in the development of CRC. Obesity, high consumption of red and processed meats, and low dietary fibre increase the risk of developing CRC (143). In

contrast, negative associations have been shown between physical activity, calcium intake, vitamin D intake, aspirin use and the development of CRC (144).

1.6.2 Types of colorectal cancer

CRC can be categorised by aetiology into three types: sporadic, hereditary and inflammation associated.

1.6.2.1 Sporadic CRC

Sporadic CRC is the most predominant type and accounts for more than 80% of all cases. Sporadic colorectal cancers show a variety of genetic mutations which have been identified as underlying causes. Inactivating somatic mutations in the adenomatous polyposis coli (*APC*) gene have been detected in approximately 70-80% of sporadic colorectal cancers. Subsequent mutations of the oncogene *K-ras* and tumour suppressor gene *p53* are often observed in the later stages of cancer development (142, 145, 146). Other mutations have also been reported in sporadic colorectal cancers particularly mutations of the mismatch repair (*MMR*) genes, but these occur in only 10-15% of sporadic colorectal cancers (147, 148). The contributions of mutated *APC* and *MMR* genes in the pathogenesis of carcinogenesis will be discussed below.

1.6.2.2 Hereditary CRC

There are several forms of hereditary CRC. However, familial adenomatous polyposis (FAP) and hereditary nonpolyposis colorectal cancer (HNPCC) (also termed the Lynch syndrome) are the most frequent forms. Both of these hereditary syndromes are inherited as autosomal dominant diseases. FAP accounts for less than 1% of all CRC cases (149). The major cause of FAP has been attributed to

germline mutation of the *APC* gene. Individuals with FAP present with multiple adenomatous polyps in the colon and rectum during childhood and the number increases to hundreds or thousands of polyps by the age of 30-40 years. These adenomatous polyps eventually transform into CRC if they not treated (150, 151). HNPCC is caused by germline mutations in one of the MMR genes and the tumours which develop in these patients are characterised by the presence of microsatellite instability (152). 80% of patients with HNPCC develop colorectal cancer and this can occur by the age of 45 years (142).

1.6.2.3 Colitis associated colorectal cancer

Colitis-associated colorectal cancer describes a subtype of CRC that arises as a complication of the chronic colonic inflammation that occurs in inflammatory bowel disease. Chronic inflammation has been implicated in the development of colitis associated colorectal cancer as described above in section 1.5.3. Although this type of cancer accounts for only 1-2% of CRC, it is aggressive in nature and has a high mortality. A milestone meta-analysis study performed by Eaden *et al* showed that the cumulative risk of developing colitis associated cancer in ulcerative colitis patients is approximately 2% at 10 years, 8% at 20 years, and 18% at 30 years and 50% of those patients die from their cancer (130). However, more recent population based studies have showed this risk to be decreased by time (153-155). Various genetic alterations which contribute to the pathogenesis of sporadic CRC are also observed in colitis associated cancer. These include the two forms of genomic instability chromosomal instability (CIN) and microsatellite instability (MSI), inactivating mutations in tumour suppressor genes such as *APC* (resulting in

overactivation of Wnt/β-catenin signalling pathway) and *p53*, activating mutations in oncogenes such as K-*ras* and defects in MMR genes.

1.6.3 Molecular pathogenesis of colorectal cancer

CRC occurs as a result of the accumulation of genetic and epigenetic alterations that eventually cause the transformation of normal colonic epithelial cells into colonic adenocarcinoma cells. The loss of genomic stability is recognised as an early event in colorectal carcinogenesis. Genomic instability in turn provides the mechanism for the occurrence and accumulation of genetic mutations. These are the early key molecular pathogenic processes that occur during carcinogenesis. A sufficient accumulation of genetic alterations involving tumour suppressor genes, oncogenes and DNA repair genes permits cells to escape from growth and regulatory control mechanisms. This promotes cell transformation and tumour progression. However, the exact timing of genomic instability during the carcinogenesis process remains elusive. Inactivating mutations of the tumour suppressor gene *APC*, resulting in overactivation of the Wnt/β-catenin signalling pathway have been proposed as the early initiating event in most cases of sporadic colorectal cancer. In addition to activation of the Wnt/β-catenin signalling pathway, the resultant truncated APC protein has been shown to cause genomic instability during the early phase of colonic carcinogenesis (156). The finding of genomic instability in adenomas has provided supportive evidence for the proposed important role of genomic instability in tumour formation (157, 158).

1.6.3.1 Genomic instability

In colon cancer, two genomic instability pathways have been identified, chromosomal instability (CIN) and microsatellite instability (MSI). CIN is the predominant form of genomic instability. It occurs in 80% of all colorectal cancers and is particularly more frequent in sporadic and colitis associated cancers (159). CIN is characterised by an increased rate of chromosome missegregation in mitosis and results in the gain or loss of whole chromosomes (aneuploidy) or fractions of chromosomes, a characteristic feature of solid cancers. This pathway is manifested by inactivating mutations of tumour suppressor genes such as *APC* and *p53*, or activation of oncogenes such as Kirsten rate sarcoma viral oncogene homolog (K-*ras*) (160). The second form of genomic instability is MSI which is manifested by alterations in the length of microsatellites in genomic DNA. This pathway is caused by dysfunction of the mismatch repair (MMR) system which fails to correct errors that may occur in short repeat sequences during DNA replication (161). This promotes mutations in the downstream target genes of MSI that are important in tumour progression such as *TGFβRII* (which encodes TGF-β receptor type II) and *BAX* (146, 162). MSI is observed in most cases of HNPCC (which have germline mutations in a particular MMR gene) (163), in 15-20% of sporadic colorectal cancer cases (147) and at a variable frequency in colitis associated cancer (164). A multi-step model of colorectal carcinogenesis was firstly proposed by Vogelstein *et al* (165) who described the genetic changes associated with colorectal oncogenesis. This is referred to as the adenoma-carcinoma sequence as described below.

1.6.3.2 Adenoma-carcinoma sequence

This describes a sequences of progressive genetic mutations that results in the histopathological changes from normal epithelium to colonic adenoma to carcinoma. These genetic mutations involve tumour suppressor genes and oncogenes. Among the earliest genetic events that trigger the progression towards these pathogenic changes are inactivating mutations of the *APC* gene. Mutated *APC* gene is a characteristic feature in FAP and is also observed in most cases of sporadic colorectal cancer. The APC protein is an important regulator of the Wnt signalling pathway and loss of APC function leads to activation of this pathway and subsequent nuclear accumulation of β-catenin. This leads to transcriptional activation of several Wnt target genes that regulate cell cycle progression and apoptosis such as *c-Myc* and *Cyclin D1* (166). In addition, *APC* mutation has been shown to result in chromosomal instability (140). These early genetic alterations facilitate activating mutations of oncogenic *K-ras* and inactivating mutations of the tumour suppressor genes deleted in colorectal carcinoma (*DCC*) and *TP53* leading to cancer development (167, 168). These key stages of genetic and histopathological events during malignant transformation are similar between colitis associated colorectal cancer and non-inflammatory colorectal cancer. However, several differences in the sequence of molecular events have been demonstrated in colitis associated cancer as illustrated in Figure 1.5. This involves progression from inflammation induced dysplasia to carcinoma without the development of well-defined adenomas (169, 170). Although colitis associated cancer shows similar genetic mutations to those observed in sporadic and hereditary CRC, there are some differences in the sequence of these genetic events. For example, in sporadic

colorectal carcinogenesis, inactivating mutations of the *APC* gene are considered to be early genetic events. By contrast, in colitis associated colorectal carcinogenesis these mutations occur at a later stage (170).

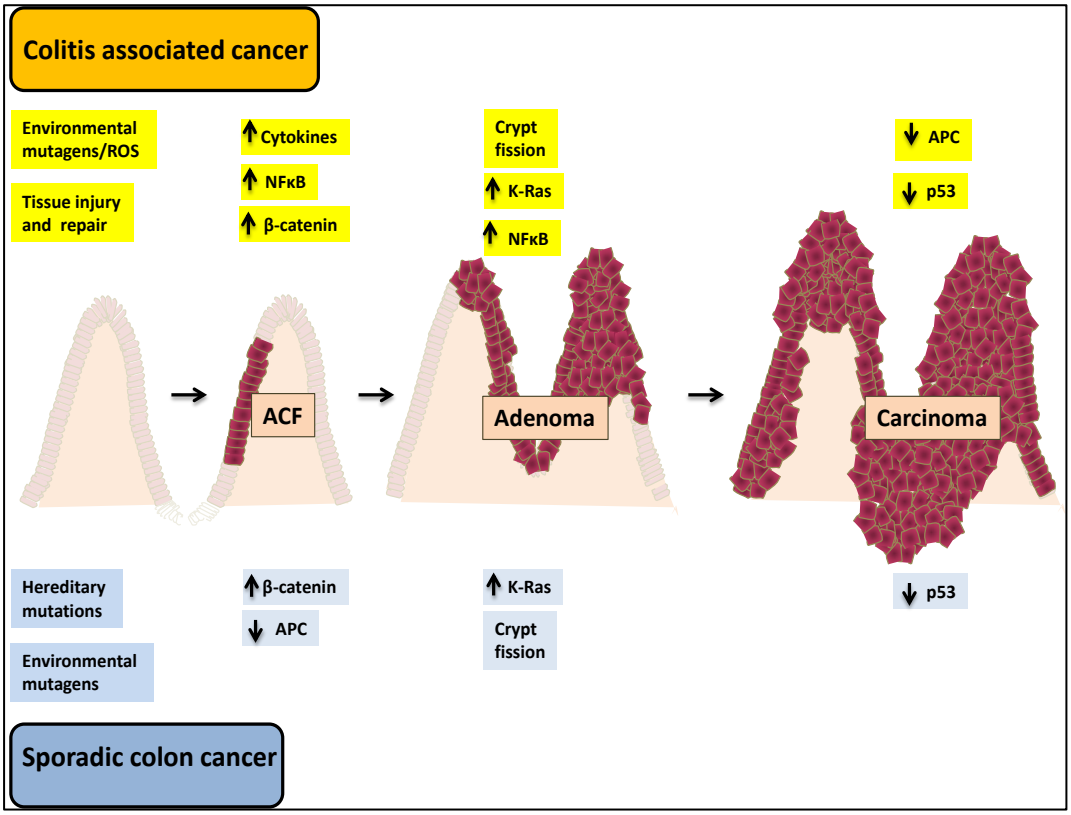

Figure 1.5: Comparison of the molecular alterations that occur in sporadic colon cancer and colitis associated colon cancer development. Modified from Terzic *et al*, 2010 (169).

1.6.4 Colitis associated colorectal carcinogenesis

Various epidemiological, pharmacological and genetic studies have linked inflammation to carcinogenesis. This is evident in IBD where patients have an increased risk of developing colorectal cancer as discussed in section 1.5.3. As mentioned above, several of the molecular alterations that are responsible for the development of sporadic colon cancer have also been implicated in pathogenesis of colitis associated cancer, including the two major forms of genomic instability (CIN and MSI) and functional alterations in key proteins that regulate cell proliferation and apoptosis (APC, K-ras and p53). Additionally, increased activation of NFκB (as a crucial element of the inflammatory pathway), immune cell infiltration and increased expression of proinflammatory cytokines have also been observed in sporadic colorectal tumours (171-173). These findings suggest a large overlap in the mechanisms responsible for the development of colitis associated colon cancer and sporadic colon cancer (169). Chronic colonic inflammation contributes to colorectal carcinogenesis by multiple mechanisms such as induction of genomic instability and alteration of DNA methylation patterns, oxidative DNA damage, enhancement of proliferation of initiated preneoplastic cells and suppression of apoptosis of those cells with DNA damage or mutation (174). NFκB is a crucial mediator of all these inflammation induced processes that drive normal cells toward malignant transformation and finally cancer development. NFκB, which is constitutively active in inflamed tissues and frequently detected in tumours, has been recognised as a key molecular factor that links inflammation to cancer (175). For instance, various proinflammatory cytokines (e.g. IL-1β, IL-6 and TNF-α), chemokines, inducible nitric oxide synthase (iNOS), cyclooxygenase-2 (COX-2) and adhesion molecules are

transcriptionally regulated by NFκB. Data from numerous studies support the notion that all these inflammatory mediators can promote colitis associated colorectal carcinogenesis via several mechanisms. These mechanisms include induction of oxidative DNA damage, genomic instability and functional and genetic alterations of key regulatory genes which are implicated in the process of carcinogenesis (174, 176-180). Oxidative DNA damage that occurs as a result of overproduction of reactive oxygen species (ROS) during colonic inflammation is considered to be a major contributor to the development of colitis associated cancer in patients with IBD. Various inflammatory mediators enhance ROS production by infiltrating inflammatory cells and also induce ROS generation within epithelial cells. ROS induced DNA damage leads to genomic instability and inactivation of tumour suppressor genes and/or activation of oncogenes, which are considered to be important initial genetic events for tumourigenesis (180-182). Apoptotic and DNA repair responses to oxidative damage-induced telomere shortening might not be initiated and senescence associated secretory phenotypes may be acquired by epithelial cells (183). These cells have been shown to secrete more proinflammatory cytokines and ROS, which further promotes malignant transformation (182, 184).

1.6.5 Animal models of colitis associated colorectal cancer

Numerous animal models of inflammation associated colorectal cancer have been established. Studies using these animal models have provided insights into the pathogenesis and risk factors for colitis associated colorectal cancer and have estabilished the chemopreventive potential of various drugs for this condition. These animal models can again be classified into genetically modified and chemically induced types. Several knockout animal models of colitis have been

shown to develop colitis associated colorectal cancer. Deleting certain genes that are involved in the immune response has been shown to result in the development of a disease in animals similar to IBD in humans. Development of adenocarcinoma in these animal models has however been documented with variable frequency. These knockout animal models that have also been demonstrated to be models of colitis associated colorectal cancer include IL10-null (185), IL2-β_2-M-null (186) and RAG2-null mice (187). Abrogation of genes that encode important proteins involved in maintaining the physiological intestinal barrier have also been shown to represent another type of animal models that develop colitis and colonic adenocarcinomas such as Muc2-null mice (188) .

Chemically induced animal models of colitis associated colorectal cancer are also widely employed. DSS is the most commonly used substance to induce colitis particularly in mice and this murine model of colitis has been discussed in detail in section 1.5.2 (110). To promote colorectal carcinogenesis as seen in chronic ulcerative colitis in humans, several cycles of DSS administration which are separated by periods of free water are required. The number of DSS cycles ranges from 4 to 15 cycles depending on DSS dose and duration, and mouse strain. However, the incidence and multiplicity of tumours are low in the DSS induced colitis model (189). A novel murine model of colitis associated colorectal cancer (AOM/DSS model) has therefore recently been established and validated by Tanaka *et al* (190) as described below.

1.6.5.1 AOM/DSS model

This model involves an initial single low dose intraperitoneal administration of the genotoxic colon carcinogen azoxymethane (AOM) followed by oral administration of DSS using different protocols. For example in the original study conducted by Okayasu *et al* (108), a dose of 7.4mg/kg AOM was injected intraperitoneally 2 weeks prior to DSS administration. This was followed by exposure to three cycles of alternating administration of 3% DSS in the drinking water for 7 days, followed by 14 days of ordinary water intake. 11 weeks following AOM pre-treatment, mice developed multiple tumours seen as polypoid or flat elevated lesions in the distal colon. Most of these tumours were adenomas with high-grade dysplasia, but a few invasive adenocarcinomas were also observed. The location of these tumours corresponded to the areas of the colon that showed the greatest inflammation and damage. This provided evidence for inflammation driven colorectal carcinogenesis in this model (108).

Similar to the standard UC model (DSS-induced colitis), the AOM/DSS model depends on DSS administration to produce chronic colitis as the main promoter of carcinogenesis. Pre-treatment with the carcinogen AOM may recapitulate the chronic exposure to low doses of environmental mutagens and carcinogens that initiates colorectal cancer development in humans (191). Data from several studies support the notion that the AOM/DSS model is relevant for investigating various aspects of colitis associated cancer in humans. For example, the clinical and histopathological features of the colitis induced in the AOM/DSS model are similar to those observed in patients with ulcerative colitis. These features include body

weight loss, diarrhoea, rectal bleeding, distortion of colonic crypts, colonic mucosal ulceration and diffuse inflammatory cell infiltrate. These changes can be observed from the third week of the AOM/DSS regimen.

In addition to the presence of inflammation as a predisposing factor for cancer development, the early molecular and genetic alterations that occur in colitis associated colorectal cancer are also observed in the AOM/DSS model. For example increased expression and mutation of the β-catenin gene, which occurs in inflammation related colorectal cancer in humans, are also detected in tumours induced by AOM/DSS treatment in mice (190). This was also shown to be associated with increased expression of target genes of the Wnt/β-catenin pathway such as c-Myc both in humans and in AOM/DSS treated mice (192). Similar to humans, activating mutations in the oncogene *K-ras* have been identified and shown to contribute to the early phases of colorectal carcinogenesis in the AOM/DSS model (193). In contrast to colitis associated colorectal carcinogenesis in humans, however, no immunoreactivity to p53 is observed in the neoplastic lesions that develop in the AOM/DSS model (190). Other key molecular changes that are involved in the development of inflammation related colorectal carcinogenesis in humans such as up-regulations of Cox-2, iNOS and several pro-inflammatory cytokines have been also observed in the dysplastic and neoplastic colonic lesions that develop in the AOM/DSS model. Due to these close similarities between colitis associated colorectal cancer in humans and AOM/DSS induced tumours in rodents, the AOM/DSS model has been described as a valuable and practical tool for investigating the pathogenesis of colitis associated colon cancer (194). Therefore,

the AOM/DSS murine model was employed to study inflammation associated colorectal carcinogenesis in this thesis.

1.7 Nuclear Factor κB (NFκB)

The mammalian nuclear factor κB (NFκB) complex consists of a family of five related transcriptional factors, RelA (also called p65), c-Rel, RelB, NFκB1 (p50 and its precursor p105), and NFκB2 (p52 and its precursor p100). These proteins share the ability to bind DNA in a specific manner and to regulate the expression of a diverse range of NFκB-dependent genes. These NFκB-dependent genes are involved in regulating various physiological processes and functions including cell division, differentiation, cell survival and immunity, and have therefore been implicated in the development of several diseases (195).

1.7.1 Structure and forms

Structurally, all the NFκB transcription factors are characterised by the presence of an N-terminal Rel homology domain (RHD), which is responsible for DNA binding and homo- and heterodimerisation through a conserved dimerisation interface in the RHD. Dimerisation of NFκB subunits is a fundamental characteristic and is essential for DNA binding (196). However, only RelA, c-Rel and RelB contain a C-terminal transcription activation domain (TAD) that is required for the positive regulation of gene expression. p50 and p52 are synthesised as large precursor proteins named p105 and p100 respectively and proteolytic cleavage of ankyrin repeats at their C terminus leads to the release p50 and p52. Therefore, the p52 and p50 subunits which lack TAD, depend on interactions with other family

members to positively regulate gene transcription, otherwise they may function to repress transcription (197).

RelA and c-Rel heterodimerise mainly with p50 (197-199) while RelB preferentially heterodimerises with p100 and its processed form p52 (197, 200). Additionally, RelB has a unique property owing to the presence of a leucine zipper (LZ) motif in its N terminus which has a transcriptional regulatory function (201). All the mammalian NFκB subunits can form homodimers or heterodimers *in vivo,* with the exception of RelB which can only heterodimerise with other proteins *in vivo*. These various combinations and forms are thought to be responsible for regulating the expression of distinct and overlapping sets of genes (202).

1.7.2 NFκB signalling

A diverse range of stimuli that include endogenous and exogenous ligands, and different physical and chemical stresses can trigger NFκB signalling. In unstimulated cells, NFκB dimers are sequestered in a latent form by the attachment of their RHD to NFκB inhibitory proteins termed IκBs. However, the unprocessed NFκB1 and NFκB2 precursor proteins p105 and p100 act as IκBs which upon processing produce the active proteins p50 and p52 respectively (203-205). NFκB activation is mediated by two pathways, classical (canonical) and alternative (noncanonical). The dominant and most extensively investigated of these is the canonical pathway. It involves RelA, c-Rel and NFκB1 proteins that are found mainly as RelA:p50 and c-Rel:p50 heterodimers. The main initiating event in this pathway is the activation of the IκB kinase (IKK) complex which is composed of two catalytic subunits (IKKα and IKKβ) and a regulatory subunit (IKKγ, also called NEMO) (197, 206, 207). Activated IKK

phosphorylates IκBα (this is mainly by IKKβ although a role for IKKα has also been proposed in this process)(203) and results in IκBα polyubiquitination. This in turn leads to its proteasomal degradation and the subsequent release of associated NFκB subunits, which translocate into the nucleus where they regulate the transcription of target genes (Figure 1.6).

The alternative NFκB activation pathway is activated by only certain members of the TNF receptor superfamily including lymphotoxin-β receptor, CD40L, BAFF (B cell activating factor), RANKL (receptor activator of NFκB ligand) and TWEAK (TNF-related weak inducer of apoptosis) (197-199, 203, 208, 209). Once any of these receptors engages with its corresponding ligand it activates NFκB-inducing kinase (NIK), which then phosphorylates and activates IKKα homodimers (not associated with the NEMO subunit) (202, 210). The latter NIK-activated IKKα dimers phosphorylate two serine residues adjacent to the ankyrin repeat at the C-terminal IκB domain of p100 (211). As a result of this phosphorylation, the $SCF^{I\kappa B}$E3 ligase complex detects p100 and leads to its polyubiquitination and subsequent partial proteolysis. The partial proteolysis is due to the presence of a STOP signal located between the p100 C-terminal ankyrin repeat domain and the p52 N-terminal part. Subsequently, the p52:RelB dimer liberates and translocates into the nucleus (197, 212) (Figure 1.6).

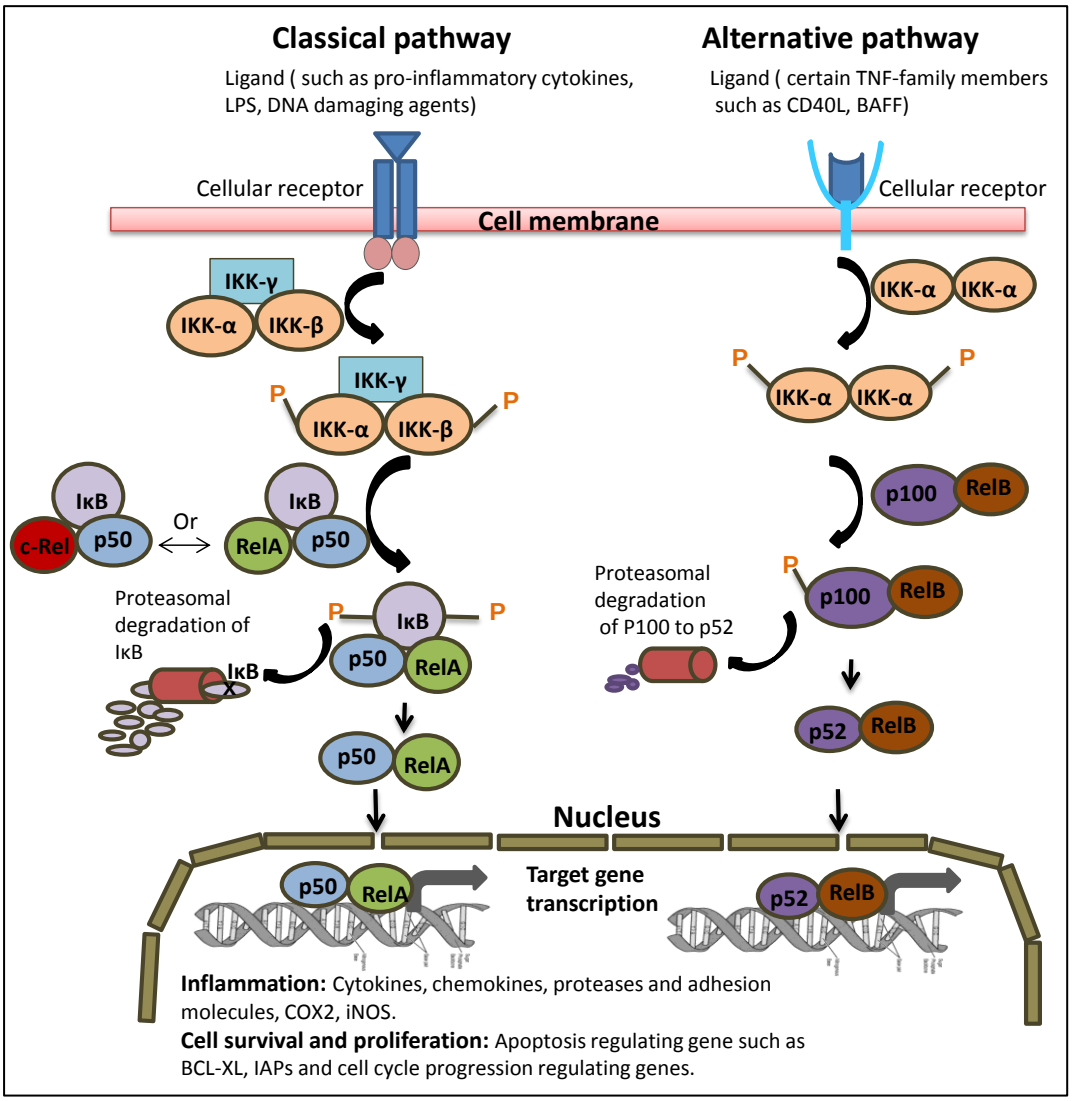

Figure 1.6: NFκB activation pathways: two pathways (classical and alternative) lead to activation of NFκB. Activation of the classical pathway is triggered by a wide range of stimuli such as pro-inflammatory cytokines and DNA damaging stimuli. These stimuli result in IKK-β and IKK-γ-dependent phosphorylation of IκB and its subsequent proteasomal degradation and liberation of NFκB subunits (which are commonly p50:RelA or p50:c-Rel dimers) that translocate into the nucleus where they regulate the transcription of a wide array of target genes. The alternative pathway is activated by certain TNF family members such as CD40 and BAFF. This triggers IKK-β and IKK-γ-independent, but IKK-α dependent phosphorylation of p100 that is bound to RelB. This results in the partial proteasomal degradation of p100 to p52. As a consequence, p52 and RelB dimers liberate and translocate into the nucleus for target gene transcription.

Approximately 500 different target genes for NFκB signalling have been gathered from the literature by the Gilmore Laboratory at Boston University (213). Based on biological functions, these genes that are under NFκB transactional regulation can be generally divided into four groups: (1) Apoptosis regulating genes that encode both pro-apoptotic proteins such as BAK, FAS and FAS-L (214), and anti-apoptotic genes such as BCL-2 (215) and BCL-XL (216). (2) Cell cycle progression regulating genes which encode proteins that control cell cycle progression. Some of these proteins facilitate cell cycle progression such as cyclin dependent kinases (217) and others suppress or arrest cell cycle progression such as the cyclin dependent kinase inhibitor p21 and p53 (218). (3) Inflammation mediating genes which include cytokines such as TNF-α (219), IL-1β (220) and IL-6 (221) which can further enhance NFκB activity and result in a positive feedback loop, various adhesion molecules and inducible nitric oxide synthase iNOS (222). (4) NFκB inhibitory genes which encode various proteins (such as IκB) that inhibit NFκB activity and hence provide a negative feedback regulatory mechanism that balances the pro-inflammatory function of NFκB (223).

1.7.3 Functions of individual NFκB family proteins

The apparent functions of the transcriptional factors RelA, c-Rel, NFκB1, NFκB2 and RelB have been demonstrated using knockout mouse models. Investigating these mice that have been rendered homozygously null for individual NFκB family members has demonstrated several functions of these transcription factors in various tissues. The phenotypes of these knockout mouse models are summarised in Table 1.2

Genotype	Phenotype	Reference
RelA-null mice	Embryonic lethal as a result of extensive TNFα-mediated fetal hepatocyte apoptosis.	(224)
	Defects in secondary lymphoid organ development when this strain of mice was crossed with TNFR1 deficient mice.	(225)
c-Rel-null mice	Mice are fertile and have a normal lifespan under standard housing conditions.	
	Defects in the proliferation and responses of B and T cells.	(226)
	Impaired neuronal survival.	(227)
NFκB1-null mice	Mice are fertile and have a normal lifespan under standard housing conditions.	
	Impaired innate and adaptive immune functions.	(228)
	More susceptible to irradiation induced intestinal apoptosis.	(229)
	Enhanced colonic epithelial proliferation.	(230)
	Resistant to unloading-induced muscle atrophy.	(231)
NFκB2-null mice	Mice are fertile and have a normal lifespan under standard housing conditions.	
	Defects in secondary lymphoid structures.	(232)
	Impaired B cell maturation; abnormal T and dendritic cell functions.	(212)
RelB-null mice	Survive to maturity with T cell mediated inflammation in multiple organs and impaired cell-mediated immunity.	(233)
	Defects in secondary lymphoid structures.	(234)
	Absence of certain dendritic cell populations.	(235)

Table 1.2: Phenotype of knockout mouse strains for individual members of the NFκB family of proteins.

1.7.4 NFκB and apoptosis

NFκB is an inhibitor of the two main types of cell death (apoptosis and necrosis). This physiological role of NFκB is important during development and for the homeostasis of several systems (236, 237). The anti-apoptotic function of NFκB is highlighted by the observation that deletion of RelA in mice leads to embryonic death as a result of extensive tumor necrosis factor α (TNFα)-mediated fetal hepatocyte apoptosis (195, 224). NFκB has also been shown to suppress apoptosis and necrosis in various adult mouse models of liver damage. This pro-survival role of NFκB has now been demonstrated in various tissues and cell types (238-240). However, NFκB can also promote apoptosis in other cell types under certain conditions. For example NFκB is usually a cell protective factor in the nervous system, but in microglia it has the opposite effect. Therefore, the effect of NFκB appears to be dependent on the cell type and the nature of the death-triggering stimulus (241, 242). The antiapoptotic functions of NFκB apply to apoptosis induced via both extrinsic and intrinsic pathways (238, 243, 244).

Various transgenic mouse models have clarified the importance of NFκB family members in regulating apoptosis and proliferation. As mentioned above, *RelA* knockout mice die at embryonic day 15 as a result of extensive hepatocyte apoptosis (224). This apoptotic liver damage is rescued by deleting the *TNF-R1* gene, suggesting that hepatocyte apoptosis is induced by TNFα in the absence of RelA (245). Similar findings have been demonstrated in IKKβ and IKKγ (NEMO) deficient mice (246-248). In order to avoid embryonic lethality, researchers have conditionally deleted IKKβ in the intestine and have demonstrated that IKKβ

activation (classical pathway) protects the intestinal epithelium from apoptosis as well as systemic inflammation following ischemia-reperfusion injury (249). Moreover, absence of intestinal epithelial IKKβ was associated with increased intestinal apoptosis and reduced tumour incidence following induction of colitis-associated cancer, whereas IKKβ deletion in myeloid cells caused a significant decrease in tumour size which was attributed to decreased levels of pro-inflammatory cytokines (250). Additionally, blocking the classical pathway of NFκB activation selectively in intestinal epithelial cells *in vivo* by the deletion of IKKβ resulted in a significant increase in small intestinal epithelial apoptosis after irradiation. This was associated with an increase in p53 and a decrease in anti-apoptotic BCL2 family member expression (251). Azoxymethane (AOM) did not cause an increase in epithelial cell apoptosis in the colon of IKKβ-deleted mice (250). Specific intestinal epithelial cell inhibition of NFκB via conditional knockout of IKKγ or both IKKα and IKKβ subunits, spontaneously resulted in severe chronic intestinal inflammation in mice as a result of increased epithelial colonic apoptosis, impaired expression of antimicrobial peptides and translocation of bacteria into the mucosa (252).

$p50^{-/-}$ mice also showed a significant increase in intestinal epithelial cell apoptosis following exposure to total body irradiation compared to wild-type mice. This indicates that selective NFκB activation can protect the small intestine from radiation-induced damage (229). However, the effects of deleting other individual members of NFκB family or of disrupting the alternative pathway of NFκB signalling upon intestinal apoptosis have not yet been well defined.

1.7.5 Regulation of mechanisms of apoptosis by NFκB

1.7.5.1 Inhibition of apoptosis by NFκB

1.7.5.1.1 Activation of transcription of antiapoptotic genes

NFκB regulates the transcriptional activation of a number of apoptosis-regulating genes resulting in the subsequent up-regulation of their protein products. These include the inhibitors of apoptosis proteins (IAPs) such as c-IAP1, c-IAP2, XIAP which prevent the activation of procaspase-9 and suppress caspase-3 and -7 activities (241, 253, 254). In addition, IAPs exert an antiapoptotic role by inducing the degradation of Smac/Diablo (255, 256). XIAP also has an inhibitory effect on the persistent activation of JNK (241, 257).

The second group of proteins that is upregulated by NFκB includes the antiapoptotic BCL2 family members BCL-XL, BCL2, Bfl-1/A1 and NR13. These proteins compete with pro-apoptotic BCL2 family proteins to prevent the release of cytochrome c and Smac/Diablo from mitochondria, thus preventing the activation of effector caspases and apoptosis (215, 241, 258, 259). Other NFκB target genes which encode proteins that promote cell survival include c-FLIP, TRAF1, TRAF2, TRAIL decoy receptor 1 (DcR1) and GADD45β. c-FLIP suppresses apoptosis through inhibition of caspase-8 activation (260). The adaptor molecules TRAF1 and TRAF2 inhibit TNF-induced apoptosis through augmenting NFκB activation and therefore represent a positive feedback mechanism. DcR1 is involved in the inhibition of TRAIL-induced apoptosis (261) whereas GADD45β suppresses JNK signalling and hence inhibits cell death (241, 262).

1.7.5.1.2 Repression of transcription of proapoptotic genes

The second mechanism by which NFκB can promote cell survival is by downregulation of apoptosis inducing proteins and receptors such as caspase-8, TRAIL receptors DR4 and DR5, and hypoxia-inducible protein BNIP3. Additionally, NFκB can promote cell survival by inducing p53 degradation through the upregulation of Mdm2 (E3 ligase for p53) (241, 263).

1.7.6 NFκB's role in intestinal inflammation

Although inflammation is a key physiological process that protects the host against microbial challenges, it can also cause tissue damage and other complications if activated inappropriately or excessively. Altered NFκB signalling has been linked to the development of cancer, inflammatory and autoimmune diseases. NFκB plays a fundamental role in regulating the inflammation response. NFκB expression is up-regulated in several inflammatory conditions such as the inflammatory bowel diseases (IBD) ulcerative colitis and Crohn's disease, hence NFκB is thought to be involved in the pathogenesis of these conditions. This has been attributed to its pro-inflammatory role via transcriptional regulation of several genes which encode proteins that are involved in inflammation, including pro-inflammatory cytokines (such as TNFα, IL-1β, IL-6), chemokines, cyclooxygenase 2 (COX2), inducible nitric oxide synthase (iNOS), surface receptors and adhesion molecules (2). Additionally, these NFκB regulated cytokines enhance NFκB activity, leading to further production of inflammatory mediators (264). A recent study which used topological proteomic analysis identified NFκB as one of the key proteins that regulates the formation of various molecular networks responsible for different cellular functions

linked to IBD (265). This pro-inflammatory function of NFκB has also been previously documented in various experimental models of intestinal inflammation. For example, inhibition of the classical NFκB activation pathway by an antisense oligonucleotide for RelA (P65) (266) or by a small-molecule inhibitor of IKKβ (267) has been shown to attenuate inflammation in a murine model of colitis.

Although several lines of evidence have linked NFκB activity to intestinal inflammation, several recent studies that have addressed the cell specific functions of NFκB have unexpectedly demonstrated a protective function for intestinal epithelial cell derived NFκB activity in the intestine. For instance, mice with specific deletions of IKKγ (NEMO) or both IKKα and IKKβ subunits in intestinal epithelial cells develop spontaneous colitis (252) and selective deletion of IKKβ from intestinal epithelial cells resulted in increased inflammation in the DSS-induced colitis model (250, 268). In humans, mutations in NEMO are associated with several disorders such as immunodeficiency, osteopetrosis and colitis. Those patients with mutations in NEMO who underwent allogeneic haematopoietic stem cell transplantation were shown to recover from immunodeficiency and osteopetrosis disorders, but colitis persisted and actually worsened. These findings suggest that dysregulated NFκB signalling in non-immune intestinal epithelial cells is crucial for colitis development (269, 270). In the normal intestine, the intraluminal microbiota are separated from the mucosal immune system by a single layer of epithelial cells. This physical barrier and antimicrobial factors produced by intestinal epithelial cells prevent the invasion of commensal bacteria into the mucosa, where they can be recognised by immune cells and induce inflammation. It has been shown that enterocyte derived NFκB

activity contributes to maintenance of the integrity of this barrier by promoting intestinal epithelial cell survival and proliferation (243). For example, IKK-β deficient enterocytes have been shown to be more susceptible to irradiation induced (251) and DSS induced apoptosis, thus sensitising mice to DSS induced colitis (268). Most of the studies that have elucidated the dual functions of NFκB were based on defects in upstream components particularly of the classical NFκB activation pathway. There is only one study that has evaluated the consequences of specific intestinal epithelial cell deletion of one of the classical NFκB proteins RelA on DSS induced colitis. Similarly to mice with IKK-β deficient enterocytes, these mice showed increased intestinal epithelial apoptosis, a disrupted intestinal barrier and increased susceptibility to DSS induced colitis (271). Another study has investigated the consequences of deleting other NFκB family members on parasite infection. Infestation with helminth parasites such as *Trichuris muris* (a natural parasite which inhabits the caecum and large intestine of mice) is associated with intestinal inflammation and crypt hyperplasia. Unlike c-Rel-null mice, NFκB1 and NFκB2 deficient mice failed to clear infection with this parasite, but only chronically infected NFκB1-null mice developed destructive colitis-like pathology. Therefore, a direct role of NFκB1 and an indirect role of NFκB2 in Th2 responses have been suggested. This has provided evidence of nonoverlapping functions of NFκB family members in the development of Th2 cytokine-mediated resistance to *T. muris* and the regulation of infection-induced intestinal inflammation (272). Apart from parasite infection and RelA, the specific roles of NFκB family proteins and the role of the alternative NFκB activation pathway in intestinal inflammation have not been well defined to date.

1.7.7 The impacts of NFκB's role in apoptosis and inflammation regulation on inflammation related colorectal carcinogenesis

The contribution NFκB signalling to the process of carcinogenesis has now been documented in many studies. NFκB is considered to be a key factor in the pathogenesis of many human tumours and their resistance to chemotherapeutic agents. NFκB plays an important role in inflammation related colorectal carcinogenesis via different mechanisms. The first mechanism appears to be via promoting cell survival of tumour or cells targeted by carcinogens through the transcriptional activation of anti-apoptotic genes. For example, in a mouse model of colitis associated cancer, specific ablation of IKKβ in intestinal epithelial cells resulted in a marked decrease in tumour incidence without a reduction in tumour size or composition. An increase in epithelial apoptosis was observed during tumour promotion and no difference in inflammation was noticed between animal groups (250). Thus, NFκB's ability to promote cancer in the intestine does not appear to be related to its pro-inflammatory properties, but rather to its role in inhibiting apoptosis (273).

In addition to the central role of NFκB in promoting cancer cell survival, it also functions in a paracrine manner to enhance cancer cell growth. Recently, NFκB has been shown to act as a molecular link between inflammation and cancer (175). NFκB activity in tumour or pre-neoplastic cells and in inflammatory cells up-regulates the expression of genes encoding pro-inflammatory cytokines, chemokines, adhesion molecules, COX2 and iNOS. The cytokines further induce NFκB activation in tumour or pre-neoplastic cells and in tumour associated

inflammatory cells, thus a sustained chronic inflammatory microenvironment is formed (274). This chronic inflammatory state promotes colorectal cancer development as described in section 1.6.4. This is illustrated by several mouse models of inflammation-associated cancer (241, 250). The mouse model of colitis associated colorectal cancer provides direct evidence that NFκB (particularly IKKβ-dependent NFκB activation) links inflammation and cancer. In this model, deleting IKKβ only in myeloid cells reduced tumour number and size without affecting apoptosis. This decrease in tumour size resulted from reduced expression of the pro-inflammtory cytokines which are required for tumour growth (250). The expression of major inflammatory factors such as TNFα, IL-1, IL-6, IL-8 is regulated by NFκB and these cytokines in turn activate NFκB expression. This therefore represents a positive feedback loop whereby cellular and DNA damage promote cell proliferation and transformation, ultimately leading to the initiation, promotion and progression of cancer (175, 273, 275). The previous findings suggest that IKKβ-driven NFκB activation participates in the development of colitis associated cancer via distinct cell-type-specific mechanisms. Thus, in enterocytes, it activates antiapoptotic genes which in turn inhibit the process of apoptotic elimination of pre-neoplastic cells, whereas in myeloid cells, it enhances the production pro-inflammatory cytokines that act as growth factors for transformed enterocytes (276). These NFκB-dependent mechanisms that are involved in inflammation associated colorectal carcinogenesis are summarised and illustrated in Figure 1.7. However, in certain contexts NFκB can also play a major anti-inflammatory role in the intestine. This opposite effect may lead to suppression of inflammation driven colorectal carcinogenesis rather than promoting this type of carcinogenesis.

Together these previous studies have provided evidence that the classical NFκB activation pathway plays a role in regulating susceptibility towards developing intestinal inflammation and inflammation associated colorectal cancer. However, the specific roles of individual members of the NFκB family of proteins or of the alternative signalling pathway in regulating the development of colonic inflammation and colitis associated colorectal cancer have not previously been addressed.

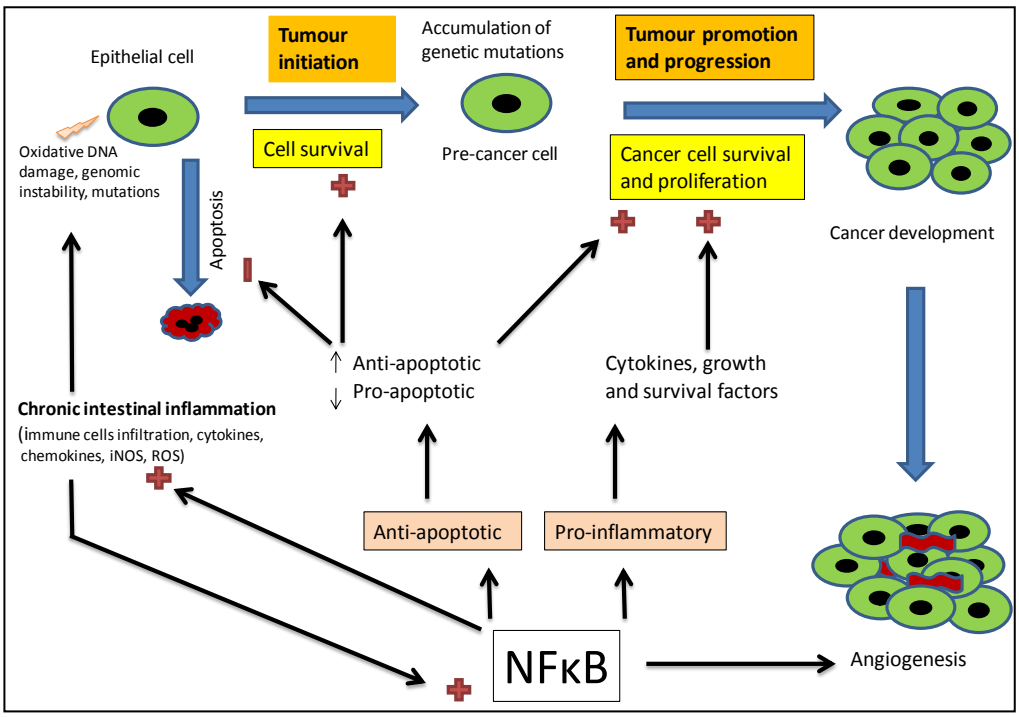

Figure 1.7: NFκB-dependent mechanisms that are involved in inflammation associated colorectal carcinogenesis. NFκB is a key factor in mediating inflammation by inducing the production of various inflammatory mediators such as pro-inflammatory cytokines which in turn further enhance NFκB activity. ROS and other reactive species derived from inflammation stress cause oxidative DNA damage, genomic instability and mutations in various genes such as tumour suppressor genes and oncogenes and this leads to tumour initiation. This event is also facilitated by the anti-apoptotic function of NFκB. The pro-inflammatory cytokines, growth and survival factors induced by NFκB are also involved in tumour promotion and progression stages by enhancing the survival and proliferation of pre-cancer cells leading to cancer development. (+) symbol means promotion effect and (–) symbol means inhibition effect.

1.8 Hypothesis

In several previous studies, the classical NFκB activation pathway has been shown to regulate intestinal epithelial cell proliferation, apoptosis and colonic inflammation. This regulation of cell proliferation, apoptosis and intestinal inflammation by the classical NFκB activation pathway has also been implicated in the development of inflammation associated colorectal cancer. Previous studies have predominantly involved disrupting the upstream components of the classical NFκB activation pathway such as IKK-β and IKK-γ. However, the specific roles of individual NFκB family proteins (as downstream components of both the classical and alternative NFκB activation pathways) and the roles of the alternative NFκB activation pathway itself in intestinal epithelial cell proliferation and apoptosis, intestinal inflammation and inflammation related intestinal carcinogenesis have not been well defined to date. We therefore hypothesise that:

Individual members of the NFκB family which signal via the classical and alternative activation pathways specifically regulate intestinal epithelial cell proliferation, apoptosis and colonic inflammation, consequently modulating susceptibility to developing inflammation associated colon cancer.

1.9 Aims

1. To investigate whether individual members of the NFκB family of transcription factors specifically regulate murine intestinal epithelial cell turnover during physiological conditions.

2. To assess the specific roles of individual members of the NFκB family of transcription factors in regulating the susceptibility of intestinal epithelial cells to undergo apoptosis following induction of cellular injury.
3. To investigate the consequences of *in vitro* suppression of the expression of the NFκB family members NFκB2 or RelB (which signal via the alternative activation pathway) upon proliferation and apoptosis in human colon cancer (HCT116) cells.
4. To determine how individual members of the NFκB family of transcription factors regulate susceptibility to developing colonic inflammation and inflammation associated colorectal cancer *in vivo*.

2 Materials and methods

Unless otherwise stated, reagents were provided by Sigma-Aldrich (Gillingham, UK).

2.1 Animals

All animals were adult 10-12 weeks old male mice which were housed under conventional conditions with food and water *ad libitum*. Animals were kept on a 12:12 hour light-dark cycle. Groups of 5 to 10 male mice were used for each experiment.

2.1.1 Wild-type C57BL/6 mice

In-bred, wild-type C57BL/6 mice were purchased from Charles River Laboratories (Margate, UK), and were acclimatised under standard animal house conditions for a minimum of 1 week prior to being used in experimental procedures.

2.1.2 c-Rel-null mice

This strain of mice was generated on the C57BL/6 genetic background and provided by Dr Jorge Caamano of the University of Birmingham. Exons 4-9 of the c-Rel gene encoding amino acid residues 145-588 have been targeted with a PGKNeo cassette. This disruption truncates the *c-rel* protein, removing sequences required for DNA binding, Rel/NFκB dimerisation, nuclear transport, and transcriptional *trans*-activation (226). The c-Rel-null mice were fertile and had a normal lifespan when maintained under standard conditions. The correct genotype of these mice was confirmed in our laboratory by Dr Mike Burkitt using conventional PCR.

2.1.3 NFκB1-null mice

This strain of mice was generated on the C57BL/6 genetic background and donated to our laboratory by Dr Jorge Caamano of the University of Birmingham. This null colony was originally generated by Sha *et al* in 1995 (228). Targeted disruption of the NFκB1 gene was achieved by insertion of a PGK-*neo* cassette into exon 6 of the NFκB1 gene. Exon 6 encodes residues 134-187 that lie within the Rel homology domain that extends from residues 30-330. This disruption was shown to produce a functionally inactive protein that is unable to dimerise with other NFκB proteins or bind to DNA. This genetic alteration efficiently inhibits the synthesis of NFκB1 p105 and p50 and does not affect the transcription of IKK-γ which is encoded also by the same gene through an alternative promoter site (228). NFκB1-null mice survive to maturity and are fertile. This null colony was maintained under standard animal house conditions. The genotype of this null colony was verified in our laboratory by Dr Mike Burkitt using conventional PCR.

2.1.4 NFκB2-null mice

This strain of mice was generated on a C57BL/6 genetic background and provided by Dr Jorge Caamano, University of Birmingham, UK. Exon 4 of the NFκB2 gene has been targeted with a PGKNeo cassette, effectively interrupting the production of both p100 and p52 (232). The generated NFκB2-null mice were fertile and were maintained under conventional conditions. Confirmation of the genotype of these mice was again performed in our laboratory by Dr Mike Burkitt using conventional PCR.

2.2 Animal procedures

Experiments were conducted with UK Home Office approval under a project licence as specified by the Animals (Scientific Procedures) Act 1986. All experiments were performed by the author as a UK Home Office personal licensee and conducted within the University of Liverpool in specified rooms for animal procedures. All experiments were conducted during the daytime starting between 9-11am.

2.2.1 Induction of apoptosis

2.2.1.1 γ-irradiation

Protocols for investigating apoptosis induction and mitosis suppression by γ-radiation including dosages and time points have previously been established by Potten and Grant, 1998 (277). These protocols have determined the doses and time points that induce maximal differences in apoptosis between different groups of mice. A dose of 8Gy γ-radiation at a rate of 2.6Gy/min from a ^{137}Cs closed source was therefore used in these studies and the irradiated mice were sacrificed 4.5 hours after exposure using a schedule 1 approved method.

2.2.1.2 Irinotecan

In previous studies, a marked increase in the number of apoptotic crypt cells and a marked decrease in the total number of crypt cells were observed in murine small intestine and colon, 24 hours following intraperitoneal (i.p.) administration of 280mg/kg irinotecan. Administration of a second dose of irinotecan 24 hours later was associated with approximately 25% mortality of mice along with extensive damage of intestinal mucosa 24 hours following this second dose (278). Therefore,

the consequences of a single dose of 250mg/kg of irinotecan (irinotecan solution 20mg/ml, RLBUH NHS Trust, Pharmacy Dept., Liverpool, UK) were assessed in C57BL/6 wild-type mice (5 mice per group). Intestinal apoptosis and mitosis and intestinal damage were assessed during a time course. Mice received a subcutaneous (s.c) injection of 0.01mg/kg Atropine (Atropine 600mg/ml, RLBUH NHS Trust, Pharmacy Dept., Liverpool, UK) 2 minutes prior to administration of the single i.p. dose of irinotecan to reduce any cholinergic reactions (279, 280). Mice were sacrificed after 6, 12, 24, 48, 72 and 96 hours. 6 hours was considered as an early time point that showed a significant increase in epithelial apoptosis particularly in the small intestine and 48 hours was considered as a late time point that showed maximal intestinal damage. These time points were therefore chosen for subsequent experiments involving c-Rel-null, NFκB1-null mice and NFκB2-null mice.

2.2.1.3 Azoxymethane (AOM)

It has been shown in previous studies that maximal induction of intestinal apoptosis and maximal suppression of mitosis were observed 8 hours and 24 hours respectively after a dose of 10mg/kg azoxymethane (AOM) (281, 282). Mice were therefore administrated interaperitoneally with a dose of 10mg/kg AOM (Cat#A5486, Sigma-Aldrich, UK).and mice were culled either 8 or 24 hours later.

2.2.2 Crypt regeneration assay

Mice were exposed to a dose of 12Gy γ-radiation at a rate of 2.6Gy/min from a ^{137}Cs closed source and culled 96 hours later to allow for detection of regenerating crypts.

2.2.3 Colitis induction

Mice were administrated 2% dextran sulphate sodium (DSS) (M.W= 36,000 – 50,000; Catalogue number: 160110; Lot number: 6683K; MP Biomedicals, LLC, UK) in their drinking water for 5 days to induce colitis. This was followed by one day of DSS-free water and mice were sacrificed on day 6 from the start of the experiment.

2.2.4 Induction of Colitis associated colonic cancer using AOM/DSS

According to the findings observed in DSS induced colitis experiments (see section 2.2.3), some strains of mice particularly the c-Rel-null and NFκB1 null mice were highly susceptible to 2% DSS and mice were not able to recover and were severely ill at day 6 from the start of the experiment. Therefore, the experiment was terminated at day 6. In order to choose a suitable DSS concentration that induced colitis with less than 20% mortality rate, lower DSS concentrations were given (1.5%, 1%, 0.75% and 0.5% DSS) to 5-6 mice per group of the susceptible strains and mice were monitored for 12 days. 0.5% and 0.75% DSS effectively induced colitis and most mice were able to recover (only one c-Rel-null mouse failed to recover following 0.75% DSS). However, 1.5% and 1% DSS resulted in higher mortality rates. Therefore, 0.5% and 0.75% DSS concentrations were used in the subsequent experiments using a murine model of colitis associated cancer (CAC). Mice were injected (i.p) with 12.5mg/kg AOM (Cat#A5486, Sigma-Aldrich, UK). After 5 days, DSS (0.5%) was given in the drinking water for 5 days followed by 16 days of ordinary water. This cycle was repeated twice with 0.75% DSS and mice were sacrificed 12 days after the last DSS cycle as described by Greten *et al* (250) (Figure 2.1).

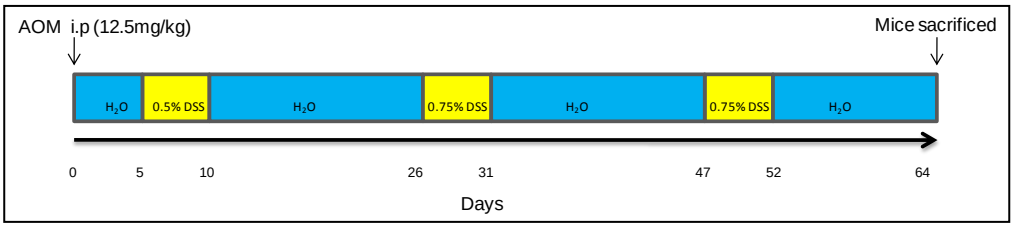

Figure 2.1: Schematic overview of murine model of colitis associated cancer. 5 days following the initial AOM (i.p) injection (12.5mg/kg), DSS was provided in drinking water (yellow areas) followed by ordinary tap water (blue areas) as indicated above.

2.3 Tissue dissection and preparation

Following sacrifice, standard dissection techniques were used to excise the small intestine and colon. Faecal matter was removed by flushing with PBS and the excised intestines were immersed in 4% formalin solution overnight. Tissues were then stored in 70% ethanol prior to gut bundling.

2.3.1 Gut bundling

The entire fixed small intestine was bundled, however the colon was first divided into halves designated proximal and distal colon. The small intestine and colon were placed into loops of 3M micropore surgical tape. Following bundling by squeezing the tape around the tissue, they were cut into about 0.6cm lengths and excess tape and tissue was cut off using a Swann-Morton size 22 scalpel blade (VWR international Ltd, Lutterworth, UK). Bundles were placed in histology cassettes and stored in 70% ethanol prior to processing and embedding in paraffin wax. During the embedding step, bundles were oriented vertically in order to obtain transverse sections during tissue cutting.

2.3.2 Haematoxylin and eosin staining

Transverse tissue sections of 4µm thickness were attached to glass microscope slides. Following drying at 37°C, slides were dewaxed in xylene for 10 minutes and rehydrated by passing through a series of decreasing ethanol concentrations to distilled water. Nuclei were stained by immersing in haematoxylin (Sigma-Aldrich Co, Dorset, UK) for 3 minutes and then washed in running tap water for 10 minutes. To stain the cytoplasm, sections were placed in eosin (Sigma-Aldrich Co, Dorset, UK) for 4 minutes. The excess eosin was removed and sections were dehydrated by dipping the slides briefly (twice, 4 seconds each) in 95% ethanol and (twice, 4 seconds each) in 100% ethanol. After clearing in xylene for 10 minutes, the slides were mounted with DPX, coverslipped and examined under a light microscope.

2.3.3 Immunohistochemical staining

2.3.3.1 Primary antibody incubation

Several treatments were applied to the samples prior to primary antibody incubation. Tissue sections were placed on APES coated slides and left to dry at 37°C in a fan assisted drying oven overnight. Following de-waxing in 2 changes of xylene, sections were dehydrated by passing them through different concentrations of ethanol from 100% to 70%. After that, endogenous peroxidase activity was abolished by immersing the slides in 3% H_2O_2 diluted in methanol for 4 minutes. Following washing in distilled water, sections were subjected to antigen retrieval process by placing them in citric acid buffer (10mM, pH6) and microwaved for 20 minutes at 800W. Slides were allowed to cool for 10 minutes at room temperature and were rinsed in slow running tap water for 10 minutes before being washed in

50mM Tris buffered saline (150mM NaCl) with 0.1% Tween20 (TBS-tween) solution. Sections were blocked by 5% rabbit serum in TBS-tween for Ki67 staining for 40 minutes before being incubated with primary antibody overnight at 4°C (primary antibody concentration is shown in Table 2.1. Following 2 washes in TBS-tween for 5 minutes each, sections were incubated with a suitable secondary antibody.

Primary antibody	concentration	provider	Catalogue number	Species raised in
Anti-Ki67	1 : 25	Dako	M7249	Rat

Table 2.1: Primary antibody which was used in immunohistochemistry.

2.3.3.2 Secondary antibody and chromagen application using streptavidin / biotin based assay

The Envision+ detection kit was not appropriate for sections which were stained with the anti-Ki67 primary antibody. Hence, a biotinylated anti-Rat secondary antibody raised in rabbit was used (E0468, Dako, Ely, UK) at a dilution of 1:200 in blocking solution for 30 minutes. Sections were washed twice in TBS for 5 minutes each before being incubated with Vectastain ABC Kit (Vector Laboratories, Peterborough, UK) solution for 30 minutes. The ABC solution conjugates multiple horseradish peroxidase molecules to each biotinylated secondary antibody moiety, thereby amplifying the primary antibody signal for chromagen detection. Sections

were incubated in 0.07% DAB in TBS with 5µl 30% hydrogen peroxide for 5 minutes in the dark and following a wash step they were counterstained with Gill's haematoxylin for 3.5 minutes before being dehydrated and mounted with DPX.

2.4 Cytological and histological scoring methods

Various techniques were applied to quantify physiological and pathophysiological responses following different treatments. All scoring procedures were performed by the author who was blinded to the treatment and genotype of the samples being scored. In order to validate the scoring procedure and the accuracy of scoring, inter- and intra-scorer variability were both assessed during the training process for scoring and this is demonstrated in the examples shown in Figure 2.2 and Figure 2.3 respectively. Also, the degree of variability between individual animals within a treatment group is shown in Figure 2.4.

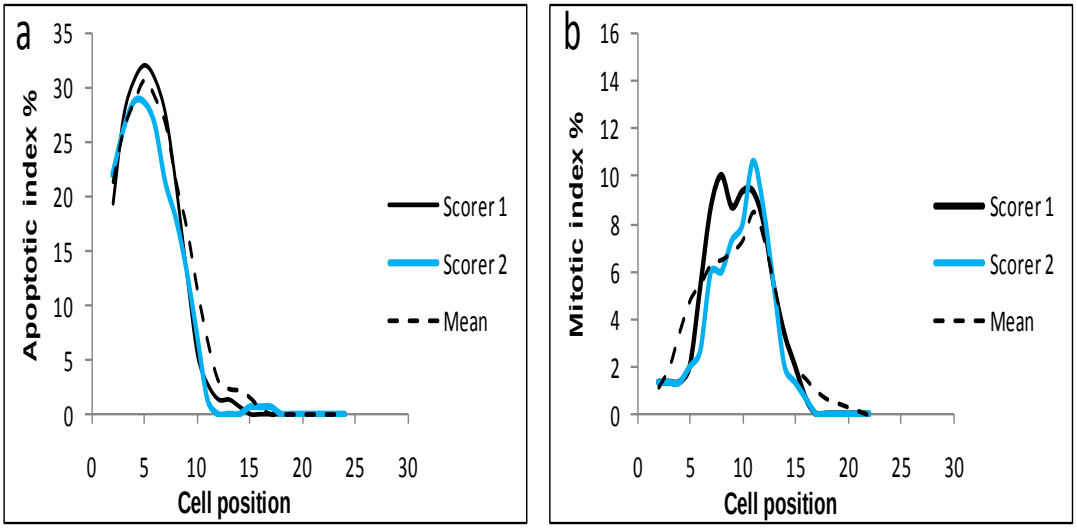

Figure 2.2: Inter-scorer variability shown in the small intestine. C57BL/6 wild-type male mice were assessed for apoptotic index following 8Gy γ-irradiation (a) and basal mitotic index (b) by scorer 1 (black) (an individual previously trained in this technique) and scorer 2 (light blue) (author). Mean apoptotic index from 4 mice following 8Gy γ-irradiation and mean basal mitotic index from 4 mice were also assessed by scorer 2 (black dotted line) (author). No statistical differences were found by modified median test.

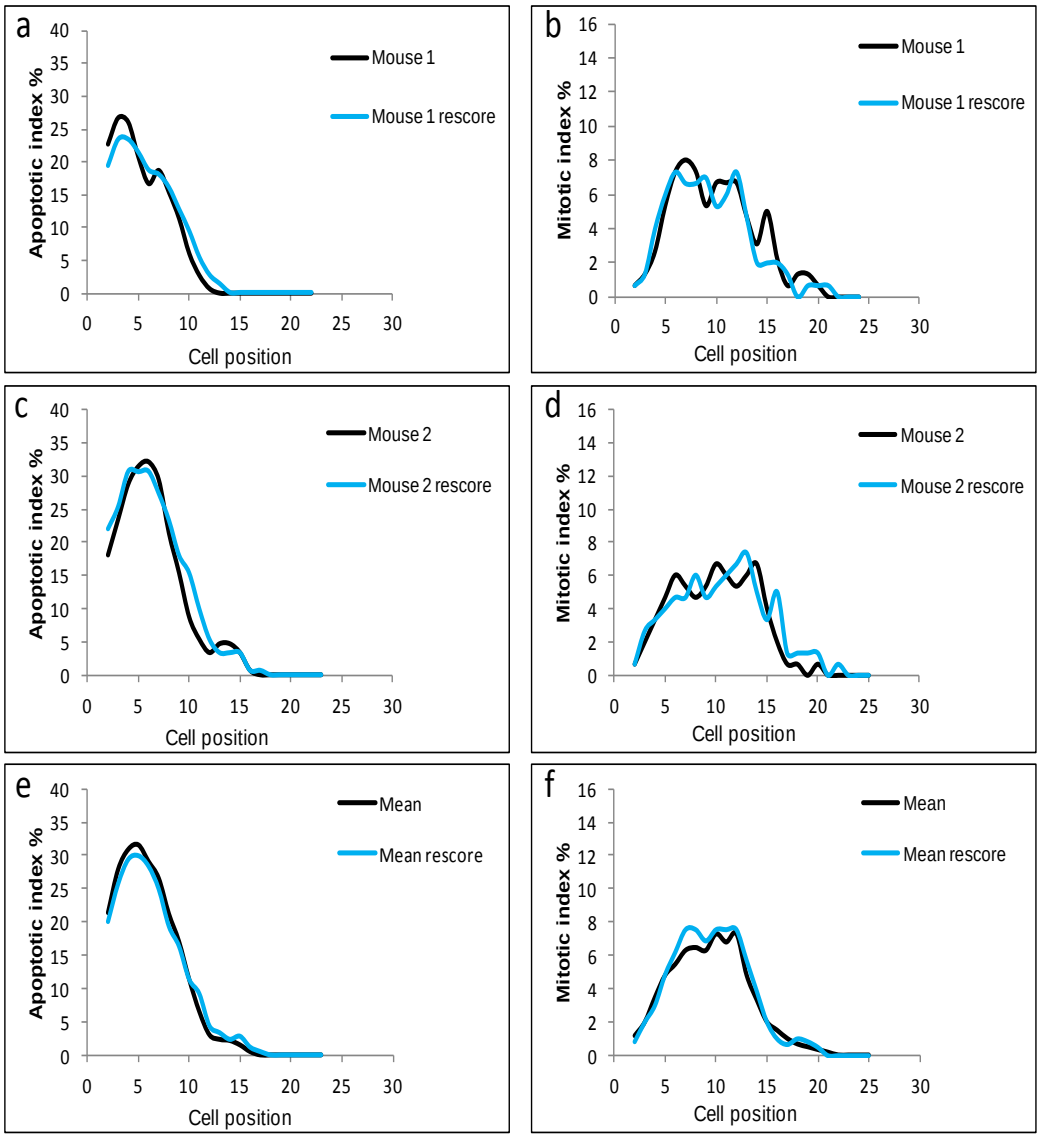

Figure 2.3: Intra-scorer variability in the small intestine. C57BL/6 wild-type male mice were assessed for apoptotic index following 8Gy γ-irradiation (a, c and e) and basal mitotic index (b, d and f). 2 examples of apoptotic index (a and c) and basal mitotic index (b and d) from individual mice are demonstrated after assessment and reassessment of the same H and E stained small intestinal section on two separate days by the same scorer. Mean apoptotic index from 4 mice following 8Gy γ-irradiation (e) and mean basal mitotic index from 4 mice (f) were also scored on two separate occasions. No statistical differences were found by modified median test.

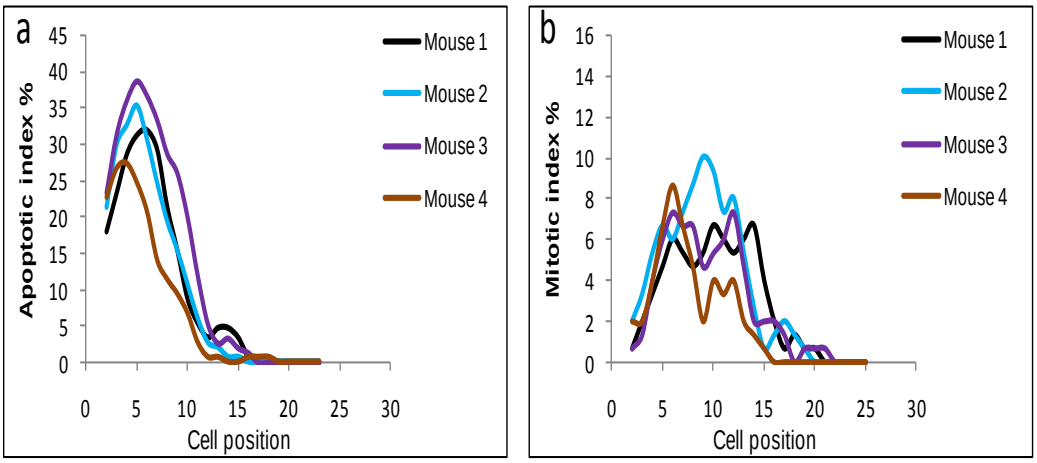

Figure 2.4: Individual mouse variability in apoptosis and mitosis levels within the same group and treatment. Small intestinal apoptotic index were assessed from 4 individual C57BL/6 wild-type mice following 8Gy γ-irradiation (a) and basal mitotic index were also assessed from 4 individual C57BL/6 wild-type mice (b).

2.4.1 Cell positional scoring of crypt apoptosis and mitosis

Apoptosis and mitosis have distinguishable morphological features which can be obviously seen in H and E stained intestinal tissue. Apoptosis is characterised by cellular shrinking, fragmentation and nuclear chromatin condensation which appears in H and E sections as spherical eosinophilic areas around dark condensed genetic material usually in place of a cell nucleus. Mitotic cells are characterised by visibly separating chromosomes and tend to be larger than normal cells and located towards the lumen of the crypt as demonstrated in Figure 2.5 (a). A cell positional scoring system was used to quantify crypt intestinal apoptosis and mitosis. This scoring system which relies upon the observation of well oriented intestinal crypts has been previously validated (61, 64). Assessment of apoptosis and mitosis within each hemi-crypt was performed on a cell positional basis in which the cell at the crypt base was designated cell position 1 and the next cell above was designated

cell position 2 and so on until the crypt-villus junction or inter-crypt table were reached in the small intestine and colon respectively. These cell positions were classified as normal, apoptotic or mitotic according to the histological findings on H and E stained sections. It has been shown that scoring 200-300 well oriented hemi-crypts from 4-6 mice produces reliable and reproducible results (60). Therefore, we scored 50 hemi-crypts per mouse from a minimum of 5-6 mice per experimental group (Figure 2.5 b). Inter-scorer variability, intra-scorer variability and inter-mouse variability are illustrated in Figure 2.2, Figure 2.3 and Figure 2.4 respectively.

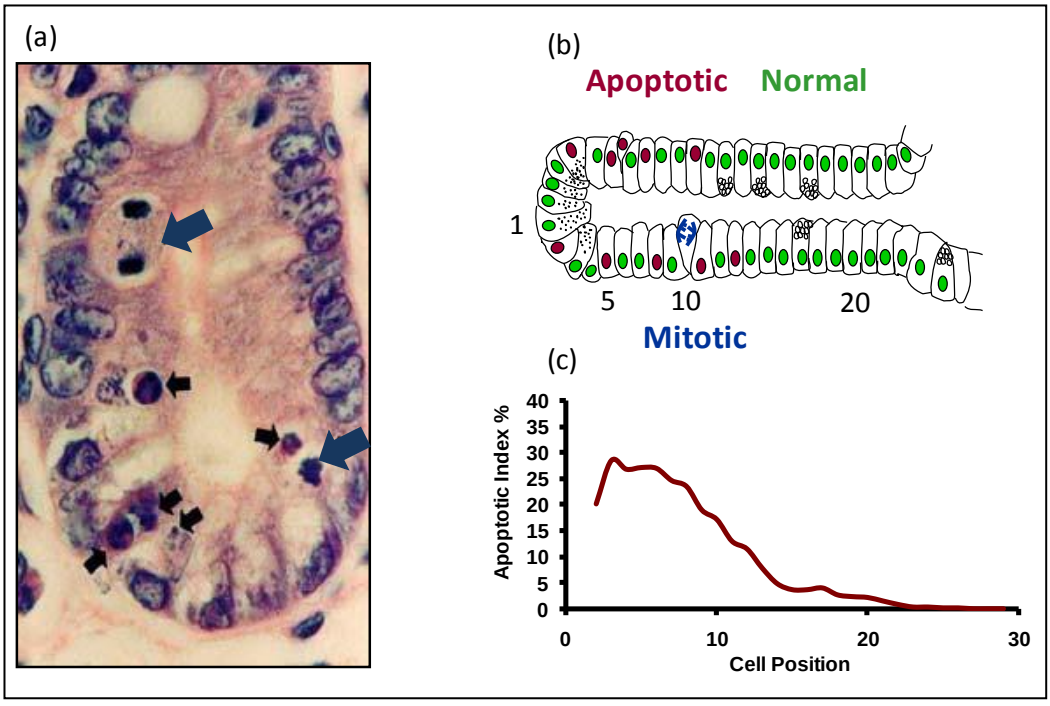

Figure 2.5: Cell positional scoring procedure from H and E stained intestinal tissue. (a) apoptotic bodies are shown by black arrows and mitotic bodies are shown by blue arrows in an H and E stained intestinal crypt. (b) schematic representation of a crypt and (c) subsequent analysis of apoptosis on a cell positional basis.

2.4.2 Measurement of AOM/DSS induced colon tumour number and size

At the end of the AOM/DSS experiment described previously in section 2.2.4, mice were sacrificed and the whole colon was dissected and flushed with PBS. The colon was cut open longitudinally along its main axis and gently washed by PBS to remove any remaining faecal content. The opened colon was carefully inspected macroscopically for the presence and location of polyps. The size and the number of polyps were then carefully measured as previously described (283).

2.4.3 Disease activity index scoring in DSS induced colitis

To evaluate the clinical signs of colitis severity, a disease activity index (DAI) was determined on a daily basis by assessing the following clinical parameters: body weight loss, stool consistency and presence of rectal bleeding. These parameters provide comprehensive functional measures similar to the clinical symptoms observed in human IBD. DAI was scored using a validated method described in previous studies (284-286). The method of scoring is shown in Table 2.2.

Score	Weight loss (%)	Stool consistency	Occult/gross bleeding
0	none	Normal	Normal
1	1 – 5	–	–
2	5 – 10	Loose stools	Hemoccult +
3	10 – 15	–	–
4	> 15	Diarrhoea	Gross bleeding

Table 2.2: Disease activity index (DAI) scoring. DAI = (combined score of weight loss, stool consistency and bleeding)/3. Normal stool = well formed pellets; loose stools = pasty stools that do not stick to the anus; and diarrhoea = liquid stools that stick to the anus.

2.4.4 Histological scoring of colitis severity

Mice were sacrificed on day 6 from the start of DSS induced colitis, the colon was removed and colonic length was measured. Following fixation in 4% formalin and embedding in paraffin, sections were stained with H and E as described previously in section 2.3.2. In order to quantify inflammatory changes following DSS administration, a histological scoring system was applied as described by Bauer *et al* (287). The histological colitis severity score (range from 0 to 6) was determined as shown in Table 2.3.

Score	Cell infiltration	Tissue damage
0	None	None
1	Focally increased numbers of inflammatory cells in the lamina propria	Discrete epithelial lesions
2	Confluence of inflammatory cells extending into the submucosa	Mucosal erosions
3	Transmural extension of the infiltrate	Extensive mucosal damage and/or extension through deeper structures of the bowel wall

Table 2.3: Histological scoring of colitis severity. The combined histological colitis severity score which ranges from 0 to 6 is the sum of the two equally weighted subscores (cell infiltration and tissue damage).

2.4.5 Determination of tumour proliferation (Ki67) index

In order to estimate the growth rate of AOM/DSS induced colonic tumours, the proliferation marker Ki67 was used. AOM/DSS induced tumours from each mouse were firstly scanned under a light microscope using a 10x objective lens for areas with the highest Ki67 labelling. Because of the small size of the tumours that developed in NFκB2-null mice, only one area of 0.25mm^2 could be evaluated in each animal. Hence, the proliferation index for each mouse colonic tumour section was determined manually by counting the number of positively labelled neoplastic cells per 0.25mm^2 area (which showed the highest Ki67 staining) using a light microscope (at 40x objective) using a 0.25 mm^2 optical grid reticule and a manual cell counter as described previously (288). For the accuracy and validation of the scoring procedure for Ki67 index, the intra-scorer variability was assessed as shown in Figure 2.6. In

addition, the degree of variability between individual tumours within the same mouse and the degree of variability between individual animals within the same experimental group were assessed and this is demonstrated in Figure 2.7.

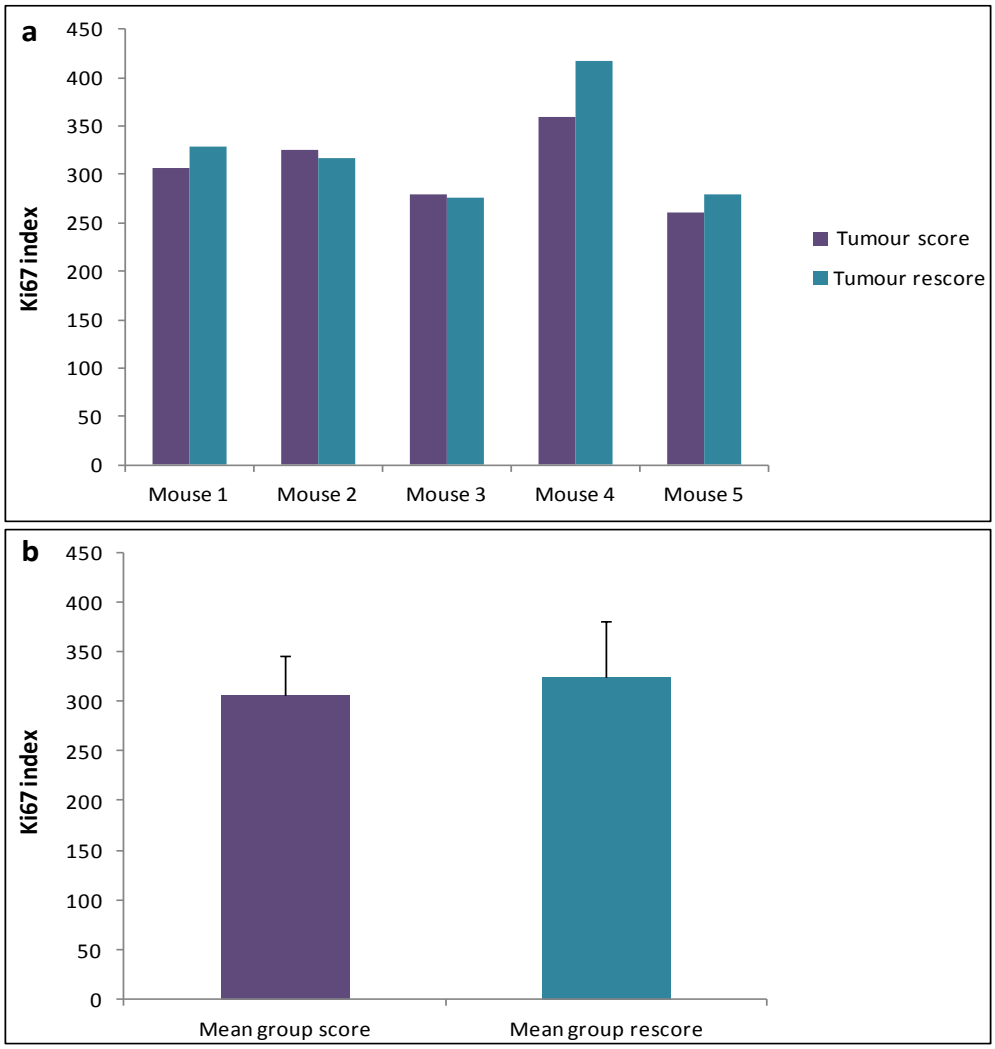

Figure 2.6: Intra-scorer variability in Ki67 index. (a) Ki67 index for AOM/DSS induced tumour from 5 individual C57BL/6 wild-type mice is demonstrated after assessment and reassessment of the same area of the same tumour by the same investigator (Author). (b) mean Ki67 index of these mice after assessment and reassessment was also determined. No statistical differences were found between the initial scores and rescores of Ki67 positively stained neoplastic cells by student's t-test.

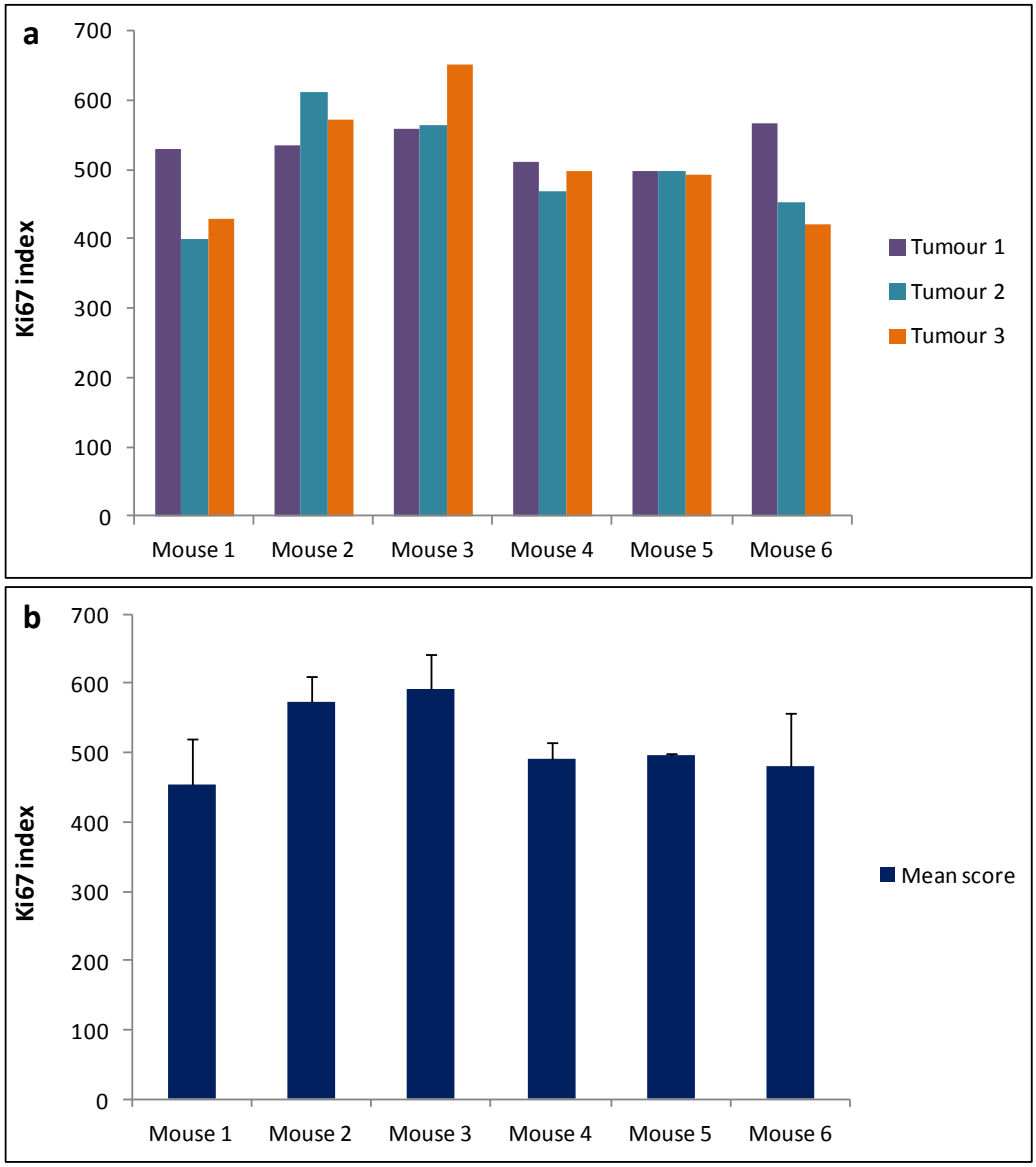

Figure 2.7: Individual tumour and mouse variabilities in Ki67 index. (a) Ki67 index was assessed in 3 individual AOM/DSS induced colonic tumours within the same animal in 6 individual c-Rel-null mice. This demonstrates the degree of variability of Ki67 index between individual tumours within the same mouse. (b) mean Ki67 index of these 3 tumours within each c-Rel-null mouse was determined. This shows the degree of variability between individual animals within the same strain of mice.

2.5 Cell culture

2.5.1 Cell line maintenance

The human colon adenocarcinoma cell line HCT116 was obtained from John Hopkins Medical Institute, MD, USA. Cells were grown as monolayers in McCoy's 5A media supplemented with 10% foetal calf serum (FCS-Gibco® Invitrogen Ltd, Paisley, UK), 0.5% 2mM L-glutamine (L-glu) and 0.4% pencillin/streptomycin mixture (P/S). The cells were cultured in T75 flasks (Appleton Woods Ltd, Birmingham, UK) at 37^{O}C and 5% CO_2 in a humidified atmosphere. Cells were maintained by sub-culturing at 80% confluence using trypsin/ethylenediaminetetaacetic acid (EDTA) in phosphate buffered saline (PBS).

2.5.2 Calculation of cell number

Floating cell number was counted by adding 40µl of the media that contained floating cells to a coverslipped haemocytometer. Following trypsinisation, 40µl of the cell suspension was added to a coverslipped haemocytometer to allow the number of attached cells to be counted.

2.5.3 Small interfering RNA transfection (siRNA) of HCT116 cells

RNA interference technologies have provided a tool for genetic manipulation *in vitro* and *in vivo* at the level of gene transcription and consequent protein translation. Therefore, siRNA inhibition of target gene expression with subsequent reduction in the level of the encoded protein translation can be a powerful tool for investigating gene-specific functions (289).

2.5.3.1 SiRNA transfection optimisation in HCT116 cell line

To achieve effective silencing with minimum cell toxicity, experimental conditions were initially optimised. When this work started, siRNA transfection of the HCT116 cell line was not among the previously validated protocols from Dharmacon and there was no detailed protocol available in the literature. Optimisation of the experimental conditions (such as transfection reagent (lipid) type, siRNA type, siRNA concentration, siRNA : lipid ratio) procedures was therefore conducted in our laboratories by Dr. Fei Song using the transfection efficiency control si*TOX*, a non-target siRNA negative control and DharmaFECT 1 Transfection Reagent. The siRNA along with transfection reagents were selected from Dharmacon. The criteria to select the appropriate siRNA : lipid ratio were to identify the lowest cell viability in si*TOX* treatment with minimal reduction of cell viability in the no siRNA control (water) and siGENOME not-target siRNA control. Following these optimisation procedures, the recommended optimal conditions were established as illustrated in Table 2.4.

Cell line	Flask size	Cell density	Type of lipid	Lipid volume	siRNA volume /20µM stock	Incubation volume
HCT116	T25 flasks	10×10^5 per flask	DharmaFECT 1	10µl	25µl	5000µl

Table 2.4: Recommended optimal experimental conditions for siRNA transfection of the HCT16 cell line.

2.5.3.2 NFκB2 siRNA and RelB siRNA transfection of HCT116 cells

The optimal experimental conditions developed by Dr. Fei Song were employed in NFκB2 siRNA and RelB siRNA transfection procedures as described in Table 2.4. A suspension of HCT116 cells ($10x10^5$) was seeded into T25 flasks (Appleton Woods Ltd, Birmingham, UK) and the total volume was made up to 5ml with complete McCoy's media lacking P/S. The cells were allowed to adhere for 24 hours before transfection with siRNA.

For each flask to be transfected, 25µl of 20µM targeting siRNA (siGENOME SMARTpool, Thermo Scientific Dharmacon Products, Epsom, UK) was added to 475µl of antibiotic and serum free media and allowed to mix for 5 minutes at room temperature (RT). 10µl of DharmaFECT 1 Transfection Reagent (Thermo Scientific Dharmacon Products, Epsom, UK) was added to 490µl of antibiotic and serum free media and allowed to mix for 5 minutes at RT. Following addition of the siRNA mixture to DharmaFECT 1 mixture, the resultant 1ml solution was allowed to mix for 20 minutes at RT. 4ml of antibiotic free complete media was then added to this solution to give 5ml total volume. Then the media in the flasks was replaced by this transfection media and the cells were incubated as mentioned above for a predetermined period according to the experimental protocol.

A non-targeting siRNA (siGENOME Non-Targeting siRNA Pool, Thermo Scientific Dharmacon Products, Epsom, UK) (25µl of 20µM) was also used as described to transfect a duplicate flask (so that each targeting siRNA flask had a corresponding control siRNA flask). This represented a control to demonstrate any off-target effects of siRNA transfection. Following the incubation period, the media was

removed and the floating cells were counted to give an estimate of apoptosis. The attached cells were liberated by 1ml of trypsin and then neutralised by adding 4ml of complete media. The total number of attached cells was counted to give a measure of cellular proliferation.

A time course of 24, 48 and 72 hours incubation was performed in duplicate for each time point using both NFκB2 siRNA and RelB siRNA transfection to initially determine the time point of maximal knock down of the expression of NFκB2 and RelB respectively. Also, longer time points (5 and 6 days) were performed for NFκB2 siRNA transfection to confirm successful depletion of p52 (the processed and active form of NFκB2) protein stores.

The 48 hour time point showed maximal reduction in the expression of NFκB2 and RelB following NFκB2 siRNA and RelB siRNA transfection respectively. This 48 hour time point was therefore initially chosen for the subsequent experiments that assessed apoptosis and proliferation following either knocking down the expression of NFκB2 or RelB in presence or absence of Etoposide as shown in Figure 2.8.

2.5.4 Etoposide treatment

For further assessment of the effects of knocking down NFκB2 and RelB gene expression on apoptosis and proliferation in the HCT116 cell line, Etoposide (a chemotherapeutic agent which inhibits topoisomerase II) was used to induce apoptosis. The cells were treated with Etoposide (final concentration, 20μM) for 24 hours following 24 hours of siRNA transfection (Figure 2.8).

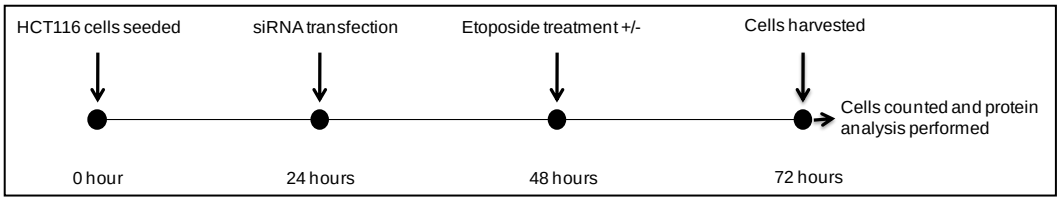

Figure 2.8: Schematic overview of experimental design for siRNA transfection (for 48 hours) and Etoposide treatment using HCT116 cells. Cells was seeded and allowed to attach for 24 hours before being transfected with siRNA. 24 hours after siRNA transfection, Etoposide was added and cells were harvested 24 hours later.

2.6 Western blot analysis

Following trypsinization, the cell suspension was centrifuged to produce a cell pellet which was then lysed using lysis buffer (5ml RIPA buffer, 50µl protease inhibitor and 3.5µl β-mercaptoethanol) and kept on ice for 20 minutes. After centrifugation of this suspension at 15,000 rpm for 15 minutes at 4^0C, the supernatant was removed and its protein concentration was determined by the BradFord method (Bio-Rad). Twenty micrograms of protein from each sample were diluted to a final volume of 20µl using lysis buffer and this was mixed with 5µl of 4-times loading buffer before denaturing at 100^oC for 2 minutes and placing on ice until use. Protein samples were then run on SDS gels that included a stacking gel (6.17ml dH_2O, 1.33ml acrylamide, 2.5ml 0.5M TRIS buffer (pH6.8), 100µl 10% SDS, 50µl 10% APS and 10µl TEMED) and a 10% running gel (8.4ml dH_2O, 6.6ml acrylamide, 5ml 1.5M TRIS buffer (pH8.8), 200µl 10% SDS, 100µl 10% APS and 10µl TEMED) in 1x running buffer (5mM Tris, 38.4mM Glycine, 0.02% SDS) at 50V then at 120V when the samples had run through the stacking gel. This was followed by transferring the proteins onto a nitrocellulose membrane using the Bio-Rad Trans blot cell apparatus at 100V in 1x

transfer buffer (14.4g glycine, 3.03g Tris, 800ml H_2O, 200ml methanol) for 1 hour. After this, the membranes were incubated in a blocking solution (0.1% Tween-20 and 5% dry milk in PBS) to prevent non-specific antibody binding for 1 hour, followed by incubation in primary antibody diluted in 2ml of the blocking solution overnight at 4^{o}C. Prior to incubation with horseradish peroxidase-congugated secondary antibody diluted in 2ml of blocking solution for 1 hour at room temperature, membranes were washed 3 times with PBS 0.01% Tween. The membranes were developed by enhanced chemiluminescence reagent and chemiluminescence was visualized using a Fluor-S^{TM} molecular imager (BIO-RAD, Hertfordshire, UK). Protein densitometry was quantified using Quantity One Software (BIO-RAD, Hertfordshire, UK). Details of the antibodies used are shown in Table 2.5.

Antigen	Primary Antibody	Dilution	Secondary Antibody	Dilution
NFκB2	1 Mouse monoclonal	1:1000	10 Rabbit anti-mouse HRP	1:1000
	2 Rabbit polyclonal	1:200	11 Swine anti-rabbit HRP	1:1000
	3 Rabbit polyclonal (k-27)	1:200	11 Swine anti-rabbit HRP	1:1000
RelB	4 Rabbit polyclonal	1:200	11 Swine anti-rabbit HRP	1:1000
P53	5 Mouse monoclonal (ab-6)	1:1000	10 Rabbit anti-mouse HRP	1:1000
Cyclin D1	6 Mouse monoclonal (ab-3)	1:100	10 Rabbit anti-mouse HRP	1:1000
$P21^{WAF-1/CIP1}$	7 Mouse monoclonal (ab-1)	1:300	10 Rabbit anti-mouse HRP	1:1000
BCL-2	8 Mouse monoclonal	1:100	10 Rabbit anti-mouse HRP	1:1000
(pan) Actin	9 Mouse monoclonal (ab-5)	1:1000	10 Rabbit anti-mouse HRP	1:1000

Table 2.5: Antigens and the details of the corresponding antibodies used for Western blotting.

1- It is raised against the amino acids 1-82 epitope of mouse p100 (NFκB2) and it was used by Caamano *et al*, 1996. It was donated by Dr Jorge Caamano, University of Birmingham, UK.
2- Abcam, ab7972-1
3- Santa Cruz, sc-298
4- Santa Cruz (c-19), sc-226
5- Oncogene research products, CAT#OP43-100UG
6- Oncogene research products, CAT#CC12-100UG
7- Oncogene research products, CAT#OP64-20UG
8- Dako, Ref M0887
9- NeoMarkers (Fremont, CA), CAT# ACTN05
10- Dako, Cat#P0161
11- Dako, Cat#P0217

2.7 RNA sample collection

Mice were sacrificed and both small intestine and colon were excised. To isolate epithelial-only cells, a modified version of the Weiser method was employed for both small intestine and colon (290) as described below.

2.7.1 Weiser technique

The intestine was cut longitudinally and opened out to expose the mucosal surface. Tissue was then washed two times with ice cold Weiser solution before harvesting crypts and each time the Weiser solution was substituted with clean solution (constituents of Weiser solutions: 5.56mM disodium hydrogen orthophosphate, 8mM potassium dihydogen orthophosphate, 96mM sodium chloride, 1.5mM potassium chloride, 27mM tri-sodium citrate, 0.5mM dithiothreitol (DTT), 1.5% sucrose, 1% D-sorbitol, 6.07mM EDTA, 4mM EGTA, Ph 7.3). The intestine was transferred into a new universal tube with clean Weiser solution and shaken gently for 5 minutes to release crypts and villi from the intestine into the solution. The detached crypts and villi were viewed under a light microscope. The intestine was then removed into another tube with clean Weiser solution and the Weiser solution which contained the dissociated crypts was collected in a tube and kept on ice. This cycle was repeated until most of the crypts and villi had been detached and collected. Following centrifuging the collecting tube with crypts for 5 minutes at 2400rpm and 4^{o}C, the Weiser solution was removed and ice cold PBS was added to the crypt pellet and it was centrifuged again. Finally, the PBS was discarded and the pellet was resuspended in 1ml of RNA later and stored at 4^{o}C for 24 hours then at -20^{o}C until RNA extraction.

2.7.2 RNA extraction and purification

Epithelial enriched intestinal cell suspensions were centrifuged and the RNA later supernatant was removed. RNA was extracted from tissue samples using the High Pure RNA Tissue Kit (Roche, Burgess Hill, UK) according to the manufacturer's instructions. An appropriate volume of the provided lysis buffer containing the chaotropic salt guanidine hydrochloride was used to lyse the tissue using a mechanical tissue homogeniser. Following this, nucleic acids were bound to a glass fleece filter column and contaminating salts and proteins were washed away. DNA was digested on the column using DNAse I, and fragments were subsequently washed through the column. Purified RNA was then eluted in TE buffer or RNAse free water.

2.7.3 RNA quantification (NanoDrop)

RNA samples were quantified using a NanoDrop spectrophotometer (Thermo Scientific NanoDrop 2000c). Following adding 1µl of RNA sample (RNase free water was added first as a reference) to the NanoDrop, the operating software was used to initiate a spectral measurement. Sample concentration and quality were also determined by the software. Only samples with a 260nm/280nm ratio >1.9 were accepted as good quality RNA for subsequent use in assays.

2.7.4 Reverse transcription of RNA to cDNA

1µg of RNA was used for the reverse transcription process using the Transcriptor reverse transcriptase kit (Roche, Burgess Hill, UK) and the protocol of the manufacturer was followed. This kit was optimised for use with RNA extracted using

the High Pure RNA kit; 1µg of template RNA was incubated in the presence of *anchored*-Oligo (dT) primers to allow non-specific reverse transcription of mRNAs. The resulting reaction mixture was used as template cDNA for quantitative PCR assays.

2.8 Quantitative (real time)-PCR

Real time PCR (RT-PCR) was performed using a LightCycler 480 instrument (Roche, Burgess Hill, UK). A primer and probe technique was used in the PCR detection system. Probes were from the Universal Probe Library (Roche, Burgess Hill, UK) and when incorporated into a PCR product the 5' conjugated fluorescein molecule emits light of 518nm wavelength. RT-PCR assays were designed through the Roche Universal Probes Library Assay Design Centre. This online tool assists *in-silico* assay design. The primers and the corresponding probes used in these assays are listed in Table 2.6.

Target	L Primer	R Primer	Probe	Amplicon
IFN-γ	ATC-TGG-AGG AAC-TGG-CAA-AA	TTC-AAG-ACT-TCA-AAG-AGT-CTG-AGG-TA	#21	89
IL-1β	TTG-ACG-GAC-CCC-AAA-AGA-T	GAA-GCT-GGA-TGC-TCT-CAT-CTG	#26	75
TNF-α	TCT-TCT-CAT-TCC-TGC-TTG-TGG	GGT-CTG-GGC-CAT-AGA-ACT-GA	#49	128
IL6	GCT-ACC-AAA-CTG-GAT-ATA-ATC-AGG-A	CCA-GGT-AGC-TAT-GGT-ACT-CCA-GAA	#6	78
IL14	GAG-AAG-CTG-GCT-GCA-CTG-T	TCA-TCT-GCT-TCT-GCG-AGT-TC	#11	73
TRAIL	GCT-CCT-GCA-GGC-TGT-GTC	CCA-ATT-TTG-GAG-TAA-TTG-TCC-TG	#76	87
Casp12	TGA-TGC-TTT-TTA-TGT-CCA-GGA-GT	TGG-ATC-TCT-TTC-ATG-TGT-CCT-C	#76	67
BAK	GGA-ATG-CCT-ACG-AAC-TCT-TCA	CCA-GCT-GAT-GCC-ACT-CTT-AAA	#19	62
FAS-L	ACC-GGT-GGT-ATT-TTT-CAT-GG	AGG-CTT-TGG-TTG-GTG-AAC-TC	#21	117
FAS	TGC-AGA-CAT-GCT-GTG-GAT-CT	CTT-AAC-TGT-GAG-CCA-GCA-AGC	#34	60
P53	ATG-CCC-ATG-CTA-CAG-AGG-AG	AGA-CTG-GCC-CTT-CTT-GGT-CT	#78	74
c-IAP2	GGG-GAC-GAT-TTA-AAG-GTA-TCG	TCG-GTT-TTA-CTG-CTA-GGC-TGA	#5	139
XIAP	GCT-TGC-AAG-AGC-TGG-ATT-TT	TGG-CTT-CCA-ATC-CGT-GAG	#25	88
BCL2	GTA-CCT-GAA-CCG-GCA-TCT-G	GGG-GCC-ATA-TAG-TTC-CAC-AA	#75	76
BCL-XL	TGA-CCA-CCT-AGA-GCC-TTG-GA	TGT-TCC-CGT-AGA-GAT-CCA-CAA	#2	68
GAPDH	GGG-TTC-CTA-TAA-ATA-CGG-ACT-GC	CCA-TTT-TGT-CTA-CGG-GAC-GA	#52	112

Table 2.6: Details of primers and probes used for the target genes in RT-PCR.

20µl final volume reactions were used throughout all assays. Initially, primers and probes were aliquoted into plates in a volume of 5µl per reaction to give 0.4µM final concentration of primer and 0.2µM of probe in 20µl reactions as described in Table 2.7. The 96 well plate was arrange in such way to complete the 10 selected apoptosis regulating genes or the 6 selected proinflammatory genes in triplicate for each mouse sample in a single plate. This resulted in 64 and 12 loaded (primers and probes mix) 96 well plates for small intestinal and colonic samples for apoptosis regulating genes and proinflammatory genes assays respectively. LightCycler 480 Probes Master mix (Roche, Burgess Hill, UK) was used in these assays. A working

mix of master mix and of PCR grade water cDNA was prepared to be sufficient for all primer and probe mixes in triplicate across a single PCR plate. The constituents of this mix are described in Table 2.8. Assays were designed to function with an annealing temperature of 60°C and hence functioned under standard PCR conditions as described in Table 2.9. Following each PCR detection run, crossing point values (cp) were determined by Roche LightCycler software release 1.5.0 using the maximal second derivative mathematical model. This algorithm is superior to threshold values as it excludes any bias derived from human selection of threshold levels. The efficiency of each PCR assay was also determined by generating standard curves. Crossing point data and efficiency values were exported to GenEx 5.3.4 (MultiD Software). Crossing point data were then normalised to GAPDH and represented as relative quantities compared to untreated wild type mice. Data were then scaled to Log2, transforming exponentially distributed data into normally distributed data representing fold increases before being statistically analysed.

Constituents	Stock concentration	Volume added per reaction	Resultant final concentration per reaction
Primer	20µM	0.4µL	0.4µM
Probe	10µM	0.4µL	0.2µM
PCR grade water	-	4.2µL	-
Total Volume		5µL	

Table 2.7: Primer and probe mix constituents per 20µL PCR reaction.

Constituents	Volume per 20µl reaction
LightCycler480 Probes Master	10µL
PCR grade water	4.4
Template cDNA	0.56
Primer and probe mix (already loaded in plate)	5µL
Total volume	20µL

Table 2.8: Master mix constituents for 20µL real-time PCR assays.

Cycle description	Temperature (°C)	Duration (seconds)	Cycles
Pre-incubation	95	600	1
Amplification	95	10	45
	60	30	
	72	1	
Cooling	40	30	1

Table 2.9: Cycling conditions for real-time PCR assays.

2.9 Statistical analysis

Data sets consisting of multiple groups with one variable (genotype) and found to be both normally distributed (using the Shapiro-Wilk W test) and of equal variance were analysed using one-way analysis of variance (ANOVA), followed by Dunnet's multiple comparison test (where all groups were compared to the control group). Data sets consisting of multiple groups with one variable and found to be either non-normally distributed or showing unequal variance were analysed using non-parametric one-way (Kruskal-Wallis) ANOVA followed by Dunn's multiple comparison test . Data sets consisting of only two groups were assessed by student's *t*-test (two-tailed, assuming unequal variance). The modified median test was used to assess significant differences at individual cell positions between groups of mice during the scoring of histology slides as described by Potten *et al* (291). PCR data which consisted of multiple groups with two variables (genotype and irradiation or DSS treatment) were analysed using two-way ANOVA with Bonferroni post-hoc tests. All statistical analysis was performed using GraphPad PRISM for Widows v4 software. In the one-way ANOVA with Dunnet's multiple comparison test, Kruskal-Wallis with Dunn's multiple comparison test, two-way ANOVA with Bonferroni post-hoc tests and student's *t*-test, differences were considered significant when $p < 0.05$. All data presented within this thesis are expressed as mean ± standard deviation unless otherwise stated.

3 Importance of specific members of the NFκB family of transcription factors in regulating intestinal epithelial apoptosis and proliferation

3.1 Introduction

The link between the activation of NFκB signalling and intestinal cancer and inflammation has been previously demonstrated in humans and animal models of disease. Several mechanisms are likely to be involved including modulation of the key cellular processes of proliferation, apoptosis and inflammation. NFκB is an important player in regulating cell survival and apoptosis in a cell type and stimulus dependent manner. Improper regulation of the cell cycle and apoptotic process following DNA damage is believed to contribute to cancer development and progression (177). Apoptosis is an important physiological process for the removal of unnecessary, aged or damaged cells. Abnormal inhibition of apoptosis can lead to the development of autoimmune diseases or cancer due to the persistence of unwanted cells (292). According to the established carcinogenesis hypothesis proposed by Vogelstein's work in colorectal cancer, evasion of apoptosis results in the retention of mutations in stem cells, enhancing the progression toward carcinogenesis (293). Therefore, NFκB may promote carcinogenesis when its activation enhances cell survival and inhibit carcinogenesis when its activation leads to cell death.

Various transgenic mouse models have clarified the importance of NFκB family members in regulating apoptosis and proliferation. One of these transgenic mouse

models is the RelA-null mouse which died at embryonic day 15 as a result of extensive liver apoptosis (224). Abrogation of classical pathway NFκB signalling by selective intestinal deletion of IKKβ has demonstrated that IKKβ activation (classical NFκB activation pathway) protects the intestinal epithelium from apoptosis as well as systemic inflammation following ischemia-reperfusion injury (249). This type of NFκB classical pathway disruption has also been shown to enhance γ-irradiation induced intestinal apoptosis (251). In a mouse model, germline deletion of NFκB1 has similarly been shown to increase the amount of small intestinal apoptosis following γ-irradiation relative to wild-type small intestine. In the same study, NFκB was shown to be activated in murine intestinal epithelial cells following whole body γ-irradiation in a dose dependent manner (229). Additionally, NFκB1-null mice have previously been shown to demonstrate longer colonic crypts and increased colonic crypt proliferation (230). *In vitro* investigations of the role of NFκB in apoptosis and proliferation in a range of lymphoma cell lines have shown that NFκB1 and NFκB2 promote cell survival and proliferation in these cell types (294). It has also previously been shown that knockdown of NFκB2 expression in U-2 OS human osteosarcoma cells resulted in a significant decrease in cell proliferation (218).

However, the role of the alternative pathway or the specific roles of other NFκB family members in regulating intestinal epithelial apoptosis and proliferation have not been well defined to date. Therefore we have investigated small intestinal and colonic crypt epithelial apoptosis and proliferation in wild-type mice and those with specific germline deletions of c-Rel, NFκB1 and NFκB2 both at baseline and following the induction of acute epithelial apoptosis by various types of DNA

damage inducing stimuli. Due to lack of access to a mouse with a germline deletion of RelB and for further evaluation of the importance of alternative pathway in regulating intestinal apoptosis, an *in vitro* model has also been used. This was achieved by knocking down the expression of RelB and NFκB2 in human colon adenocarcinoma cells (HCT116) using the siRNA technique. Hence, the roles of RelB and NFκB2 in HCT116 cell proliferation and apoptosis have been investigated.

3.2 Aims

1. In the *in vivo* study, to assess whether there are any alterations in the amounts of small intestinal and colonic crypt epithelial apoptosis and mitosis in mice with specific germline deletions of c-Rel, NFκB1 and NFκB2 compared to their wild-type counterparts both at baseline and following the induction of acute epithelial apoptosis by whole-body γ-irradiation or irinotecan adminstration. Additionally to investigate the molecular mechanisms responsible for any altered phenotypes observed.

2. In the *in vitro* study, to determine whether RelB or NFκB2 suppression in the human colon adenocarcinoma cell line HCT116 alters its proliferation and apoptosis in both the unstimulated state and following Etoposide treatment.

3.3 The effects of deleting various NFκB family members on small intestinal and colonic crypt epithelial cell turnover

To assess the specific roles of each individual NFκB family member in regulating intestinal crypt epithelial cell turnover, groups of 6 male 10-12 weeks old mice were investigated. H and E sections were prepared from formalin fixed small intestine and distal half of the colon. Crypt cell number, apoptosis and mitosis were assessed on a cell positional basis as described in section 2.4.1.

3.3.1 Untreated mice with NFκB deletions show small intestinal and colonic crypt hyperplasia

NFκB1-null and NFκB2-null mice showed significant small intestinal crypt hyperplasia (C57BL/6 18.1 ± 1 mean number of cells per hemi-crypt ± standard deviation; c-Rel-null 18.2 ± 1.2; NFκB1-null 19.8± 0.6; NFκB2-null 20 ± 1.2) (Figure 3.1). Significant distal colon crypt hyperplasia was observed in c-Rel null and NFκB1-null mice (C57BL/6 24.4 ± 1.9 mean number of cells per hemi-crypt ± standard deviation; c-Rel-null 29 ± 1.9; NFκB1-null 30.6 ± 0.5; NFκB2-null 26 ± 1.6). Although the number of cells per hemi-crypt was increased in the distal colon of NFκB2-null mice compared with C57BL/6 mice, this was not statistically significant (Figure 3.1).

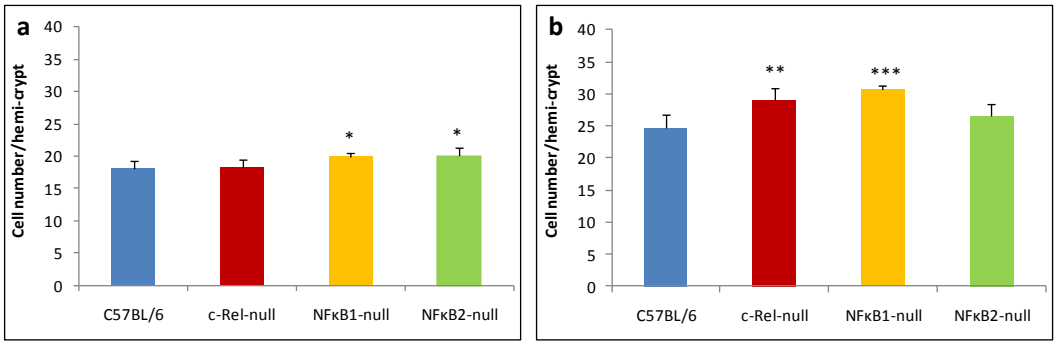

Figure 3.1: Number of cells per hemi-crypt in untreated animals. Small intestine (a) and distal colon (b) mean cell number per hemi-crypt ± standard deviation in C57BL/6, c-Rel-null, NFκB1-null and NFκB2-null mice. Statistical differences were assessed by one way ANOVA and Dunnett's multiple comparison tests (*p<0.05, **p<0.01 ***p<0.001 compared to C57BL/6) (n=6 per genotype group).

3.3.2 No alteration in basal levels of small intestinal and colonic crypt mitosis in mice with disrupted NFκB signalling

The amounts of small intestinal and colonic crypt mitosis from untreated C57BL/6, c-Rel-null, NFκB1-null and NFκB2-null mice were assessed on a cell positional basis using H and E stained sections. Because of the differences in the mean number of cells per hemi-crypt observed between the strains of mice and documented above, we also calculated the mean number of mitotic events per hemi-crypt.

In the small intestine of wild-type C57BL/6 mice, 3.8% of cells showed features of mitosis whilst in the colon, 1.6% of cells were mitotic by morphological criteria. No significant differences in baseline mitosis within the small intestine and distal colon were observed between any of the 4 groups of mice. The amount of distal colonic crypt mitosis was however lower than the amount of basal small intestinal crypt mitosis in all cases (Figure 3.2). When plotted on a cell positional basis, wild-type C57BL/6 mice showed maximal numbers of mitotic events at cell position 6 in the small intestine and 5 in the distal colon. c-Rel-null, NFκB1-null and NFκB2-null mice

showed no differences in these distributions either in the small intestine or colon by the modified median test (Figure 3.2).

3.3.3 NFκB2-null mice show elevated levels of small intestinal spontaneous apoptosis

The amounts of apoptosis in the small intestinal and distal colonic crypts of untreated C57BL/6, c-Rel-null, NFκB1-null and NFκB2-null mice were also assessed on a cell positional basis using H and E stained sections. Because of differences in the crypt lengths observed between the strains of mice as mentioned previously, we also calculated the mean number of apoptotic bodies per hemi-crypt. Untreated wild-type mice showed predictably low epithelial apoptotic indices in the intestine; in the small intestine 0.1% of cells had features of apoptosis, whilst in the distal colon 0.05% of cells were morphologically apoptotic. In the small intestine of these mice, apoptotic bodies were distributed at a low frequency between cell positions 3 to 18 (Figure 3.3). NFκB1-null mice displayed a small increase in spontaneous small intestinal apoptosis, but this was not statistically significant relative to C57BL/6 mice. A significant fourfold increase in mean apoptotic index and average number of apoptotic bodies per hemi-crypt was however found in the untreated small intestinal crypts of NFκB2-null mice compared to C57BL/6 mice. No significant differences were seen in apoptosis distribution in comparison to the wild-type mice. Levels of spontaneous apoptosis in distal colonic crypts were very low and barely detectable and no significant differences were detected between any of the strains of mice tested (Figure 3.3).

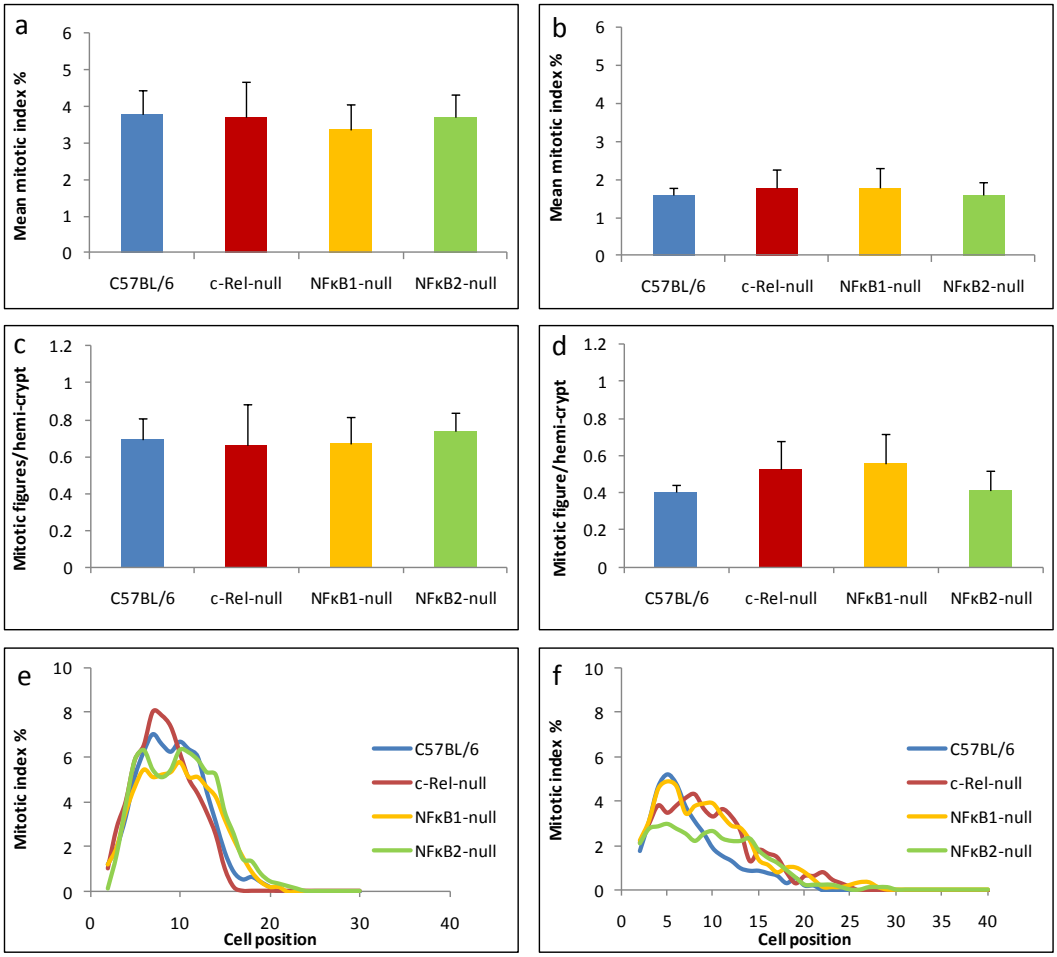

Figure 3.2: Quantitative analysis of intestinal crypt epithelial mitosis in untreated mice. Small intestinal (a) and distal colon (b) mean mitotic index ± standard deviation separated by genotype. Small intestinal (c) and distal colon (d) mean number of mitotic figures per hemi-crypt ± standard deviation separated by genotype. Cell positional distribution of baseline mitosis in small intestine (e) and distal colon (f) separated by genotype. Statistical differences were assessed by Kruskal–Wallis test followed by Dunn's multiple comparison tests in (a), (b), (c) and (d). Statistical differences were assessed by modified median test in (e) and (f). (n=6 per genotype group).

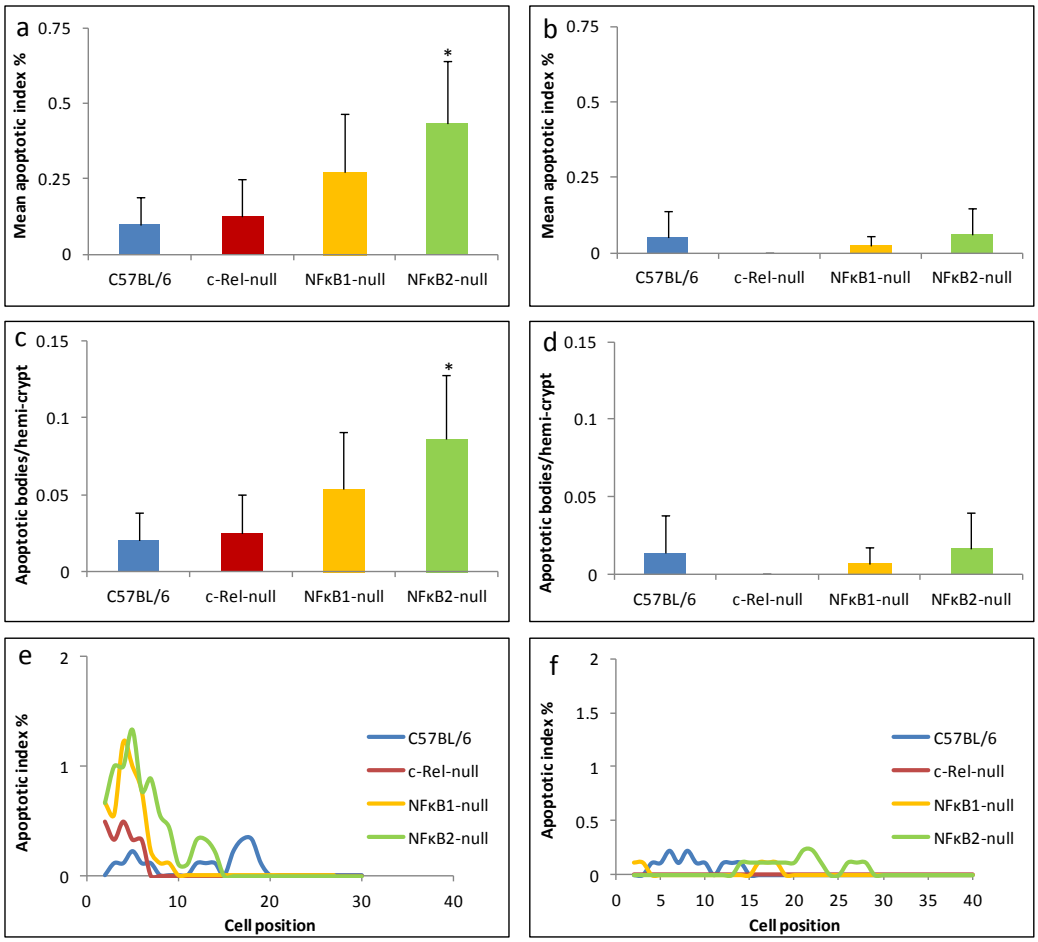

Figure 3.3: Quantitative analysis of intestinal crypt epithelial apoptosis in untreated mice. Small intestinal (a) and distal colon (b) mean apoptotoc index ± standard deviation separated by genotype. Small intestinal (c) and distal colon (d) mean number of apoptotic bodies per hemi-crypt ± standard deviation separated by genotype. Cell positional plot demonstrating baseline small intestinal (e) and distal colon (f) apoptosis separated by genotype. Statistical differences were assessed by Kruskal–Wallis test followed by Dunn's multiple comparison tests in (a), (b), (c) and (d) (*$p<0.05$ compared to C57BL/6). Statistical differences were assessed by modified median test in (e) and (f) (n=6 per genotype group).

3.4 The effects of deleting various NFκB family members on small intestinal and colonic crypt epithelial cell proliferation and apoptosis following γ-irradiation

To investigate the specific roles of each individual member of the NFκB family of transcription factors in regulating intestinal epithelial cell proliferation and apoptosis following DNA damage inducing stimuli, these parameters were assessed in mice with various NFκB family member deletions following whole body γ-irradiation. Previous studies have established that a dose of 8Gy whole body γ-irradiation for 4.5 hours induces maximal differences in intestinal apoptosis between different groups of mice. Hence, 6 mice per genotype were subjected to 8Gy whole body γ-irradiation and culled 4.5 hours later. Apoptosis and mitosis were quantified by cell positional scoring from H&E stained sections of both small intestine and distal colon as described in section 2.4.1.

3.4.1 No alteration in small intestinal and colonic crypt mitosis in mice with disrupted NFκB signalling following γ-irradiation

Mitosis was barely detectable in the small intestinal crypts of C57BL/6 and NFκB1-null mice and was completely suppressed in c-Rel-null and NFκB2-null small intestine 4.5 hours after 8Gy γ-irradiation. In the distal colon, mitosis was completely absent in most strains of mice and only persisted in NFκB1-null mice at a very low level. However, no significant differences were seen between any of the genotypes of mice (Figure 3.4).

3.4.2 NFκB1-null and NFκB2-null small intestine and colon demonstrate increased epithelial apoptosis in response to γ-irradiation

In the small intestine of wild-type mice, 12% of crypt epithelial cells were apoptotic following irradiation and these were predominantly located at the base of crypts with maximum apoptotic events occurring at cell position 5. In the distal colon of these mice, 12.6% of epithelial cells were morphologically apoptotic and these were mainly seen at the crypt base with the maximum frequency of apoptosis being observed at cell positions 1 and 2 (Figure 3.5). These positions of maximal apoptotic frequency are similar to the cell positions of the putative stem cell zone in the small intestine and colon.

In the small intestine, irradiation-induced crypt epithelial apoptosis was significantly increased by 3-fold and 2-fold in NFκB1-null and NFκB2-null mice respectively compared to C57BL/6 mice. Significant differences in the cell positional distributions of apoptotic scores were observed between cell positions 2 to 14 in NFκB1-null mice and 3 to 15 in NFκB2-null mice compared to wild-type mice following the same treatment using the modified median test. c-Rel-null small intestine did not show any significant alteration in the amount of irradiation-induced apoptosis or in the cell positional distribution of apoptotic events relative to wild-type mice (Figure 3.5).

In the distal colon, there was also a significant increase in both mean apoptotic indices and average number of apoptotic bodies per hemi-crypt in NFκB2-null mice compared to wild-type mice following the same treatment. As result of colonic crypt hyperplasia, NFκB1-null distal colon showed only a significant increase in

average number of apoptotic bodies per hemi-crypt compared to C57BL/6 mice following the same treatment. NFκB1-null and NFκB2-null distal colon showed significantly increased apoptotic scores at cell position 4 to 5 and 2 to 10 respectively relative to wild-type mice. Although c-Rel-null distal colon did not demonstrate any alteration in the amount of irradiation-induced epithelial apoptosis, a significant increase in apoptotic scores was observed at cell positions 10 to 14 compared to wild-type mice using the modified median test (Figure 3.5).

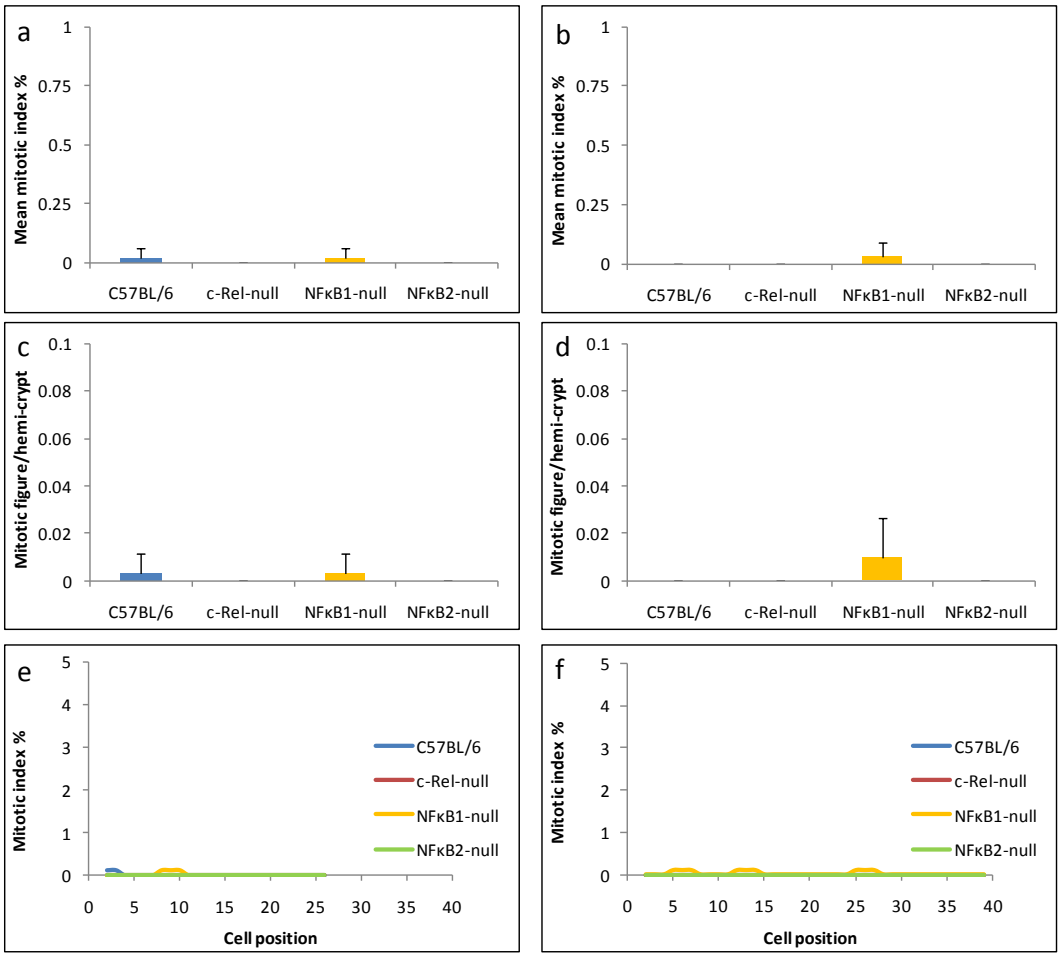

Figure 3.4: Quantitative analysis of intestinal crypt epithelial mitosis 4.5 hours after 8Gy γ-irradiation. Small intestinal (a) and distal colon (b) mean mitotic index ± standard deviation separated by genotype. Small intestinal (c) and distal colon (d) mean number of mitotic figures per hemi-crypt ± standard deviation separated by genotype. Cell positional distribution of mitosis in small intestine (e) and distal colon (f) separated by genotype. Statistical differences were assessed by Kruskal–Wallis test followed by Dunn's multiple comparison tests in (a), (b), (c) and (d). Statistical differences were assessed by modified median test in (e) and (f). (n=6 per genotype group).

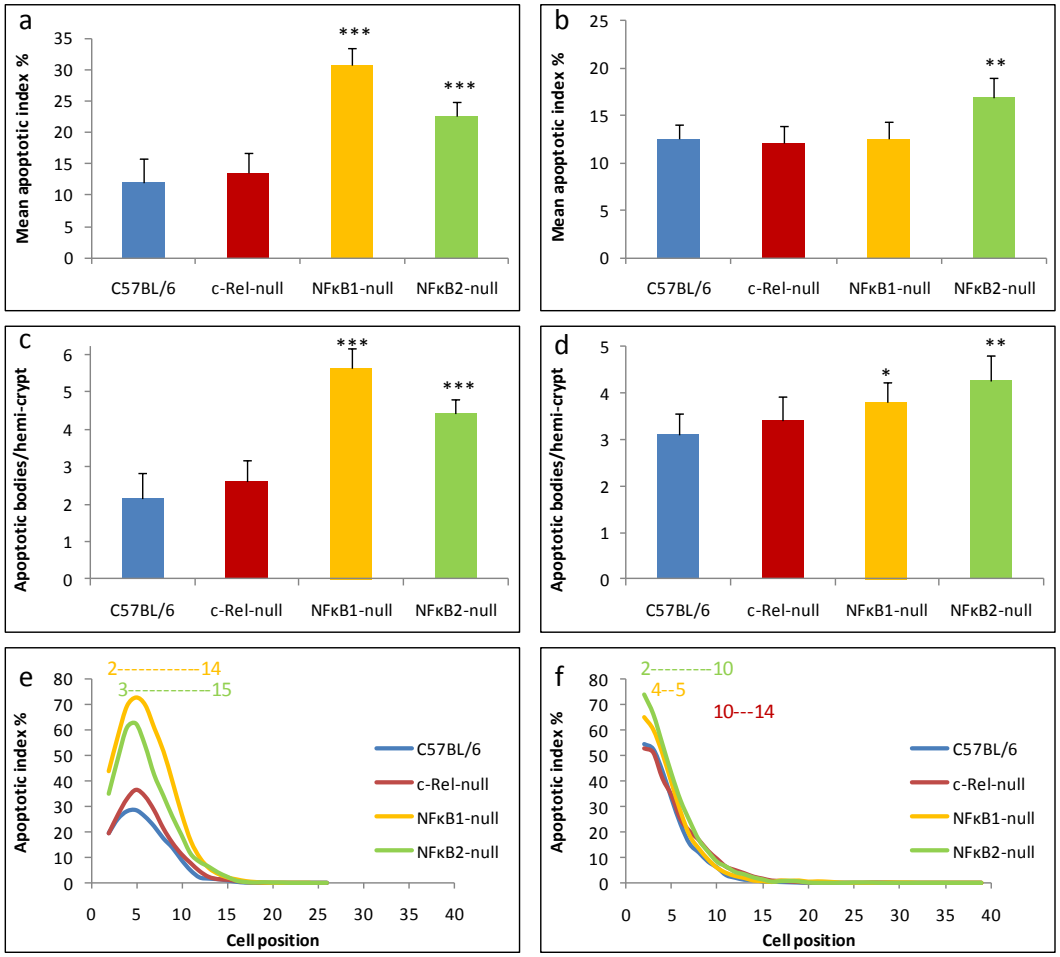

Figure 3.5: Quantitative analysis of intestinal crypt epithelial apoptosis 4.5 hours after 8Gy γ-irradiation. Small intestinal (a) and distal colon (b) mean apoptotic index ± standard deviation separated by genotype. Small intestinal (c) and distal colon (d) mean number of apoptotic bodies per hemi-crypt ± standard deviation separated by genotype. Cell positional plot demonstrating small intestinal (e) and distal colon (f) apoptosis separated by genotype. Statistical differences were assessed by one way ANOVA and Dunnett's multiple comparison tests in (a), (b), (c) and (d) (*p<0.05, **p<0.01, ***p<0.001 compared to C57BL/6). Statistical differences were assessed by modified median test in (e) and (f). Dashed line denotes cell positions over which there was a significant difference in apoptotic scores compared to wild-type. Colour of dashed line denotes comparison genotype. (n=6 per genotype).

3.5 The effects of deleting various NFκB family members on small intestinal and colonic crypt epithelial cell proliferation and apoptosis following irinotecan treatment

3.5.1 Intestinal damage and mitotic and apoptotic indices in wild-type mice following irinotecan time course

Although it has been shown that intestinal apoptosis is induced following irinotecan administration, we could find no validated protocol in the literature describing the use of irinotecan as a stimulus to induce murine intestinal apoptosis. In view of a previous study that showed the extent of intestinal damage and mortality of mice following a dose of 280mg/kg irinotecan (295), the consequences of a single dose of 250mg/kg irinotecan were assessed in C57BL/6 wild-type mice (5 mice per group) as described in section 2.2.1.2.

3.5.1.1 Reduction in crypt length in the small intestine and colon of C57BL/6 mice following irinotecan administration

A single dose of 250mg/kg irinotecan was injected (i.p.) into C57BL/6 mice and the number of epithelial cells per hemi-crypt in the small intestine and the colon was assessed after 0, 6, 12, 24, 48, 72 and 96 hours. In the small intestine, irinotecan resulted in a significant decrease in the number of epithelial cells per hemi-crypt at 24 and 48 hours and the maximum reduction was observed at 48 hours. In response to irinotecan damage, a significant compensatory increase in the number of epithelial cells per hemi-crypt in the small intestine was observed at 96 hours

(Figure 3.6). In the colon, a significant reduction in the number of crypt epithelial cells was also observed at 24 and 48 hours following irinotecan administration (Figure 3.6). However the effect of irinotecan on the number of crypt epithelial cells was more pronounced in the small intestine than the colon.

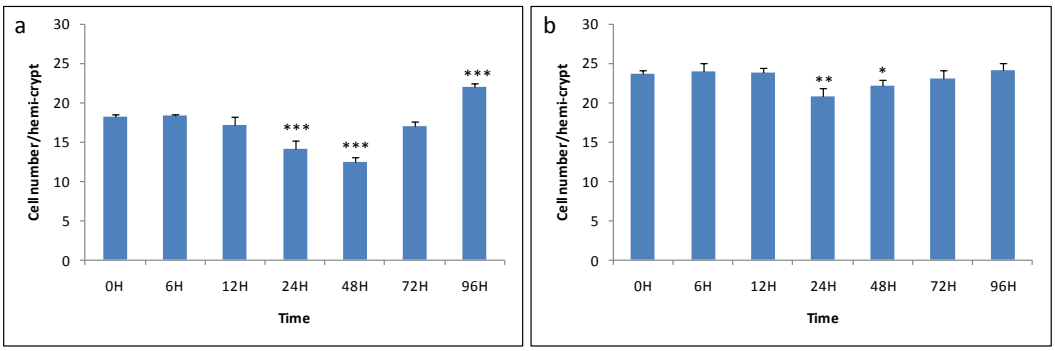

Figure 3.6: Intestinal epithelial cell number per hemi-crypt in wild-type mice following irinotecan time course. Small intestine (a) and distal colon (b) mean cell number per hemi-crypt ± standard deviation in C57BL/6 mice at 0, 6, 12, 24, 48, 72 and 96 hours following administration (i.p.) of a single dose of 250mg/kg irinotecan. Statistical differences were assessed by one way ANOVA and Dunnett's multiple comparison test (*p<0.05, **p<0.01, ***p<0.001 compared to untreated C57BL/6) (n=5 per group).

3.5.1.2 Mitosis is suppressed and apoptosis is induced in murine crypt intestinal epithelia following irinotecan treatment

A single dose of 250mg/kg of irinotecan was administrated (i.p.) to C57BL/6 mice, and crypt intestinal mitosis and apoptosis were quantified on a cell positional basis from H and E stained sections after 0, 6, 12, 24, 48, 72 and 96 hours. In the small intestine, a significant suppression of mitosis was found at the 6, 12, 24 and 48 hour time points. This was followed by a sharp increase in mitosis in the small intestine at 72 hours when the amount of mitosis returned to the basal levels seen in untreated small intestine. Small intestinal mitosis was significantly and rapidly increased by 3-fold at the 96 hour time point compared to untreated small intestine and this mitosis was predominantly observed in the lower half of intestinal crypts (Figure 3.7). This increase in the mitosis of crypt epithelial cells in response to irinotecan damage correlated with the significant increase observed in the number of crypt cells in the small intestine at the 96 hour time point as mentioned above (Figure 3.6). In the distal colon, a significant suppression of mitosis was also observed at the 6, 12, 24, 48 and 72 hours time points and this mitosis was mainly observed in the lower half of colonic crypts. At 96 hours, the amount of mitosis returned to the basal levels observed in untreated colon (Figure 3.7).

In the small intestine, a significant increase in irinotecan-induced small intestinal apoptosis was observed at 6, 12, 24, 48, 72, and 96 hours. The maximum amounts of apoptosis were observed at the 6 and 12 hour time points. Apoptosis then gradually decreased over time, but remained at significantly higher levels than untreated small intestine until the 48 hour time point (Figure 3.8). In the distal

colon, a significant and maximum increase in irinotecan-induced distal colonic apoptosis was observed at 12 and 24 hours. Apoptosis then gradually decreased over time but remained at higher than baseline levels at 48, 72 and 96 hours, athough this was not statistically significant. Colonic crypt cell apoptosis was mainly located at the crypt base (Figure 3.8).

According to these findings, 6 hours after irinotecan administration was chosen as an early time point which showed an increase in apoptosis induction and mitosis suppression and 48 hours was chosen as a late time point that demonstrated maximum intestinal damage. Therefore 6 hour and 48 hour time points were chosen for further studies of irinotecan-induced apoptosis and intestinal damage in transgenic mice.

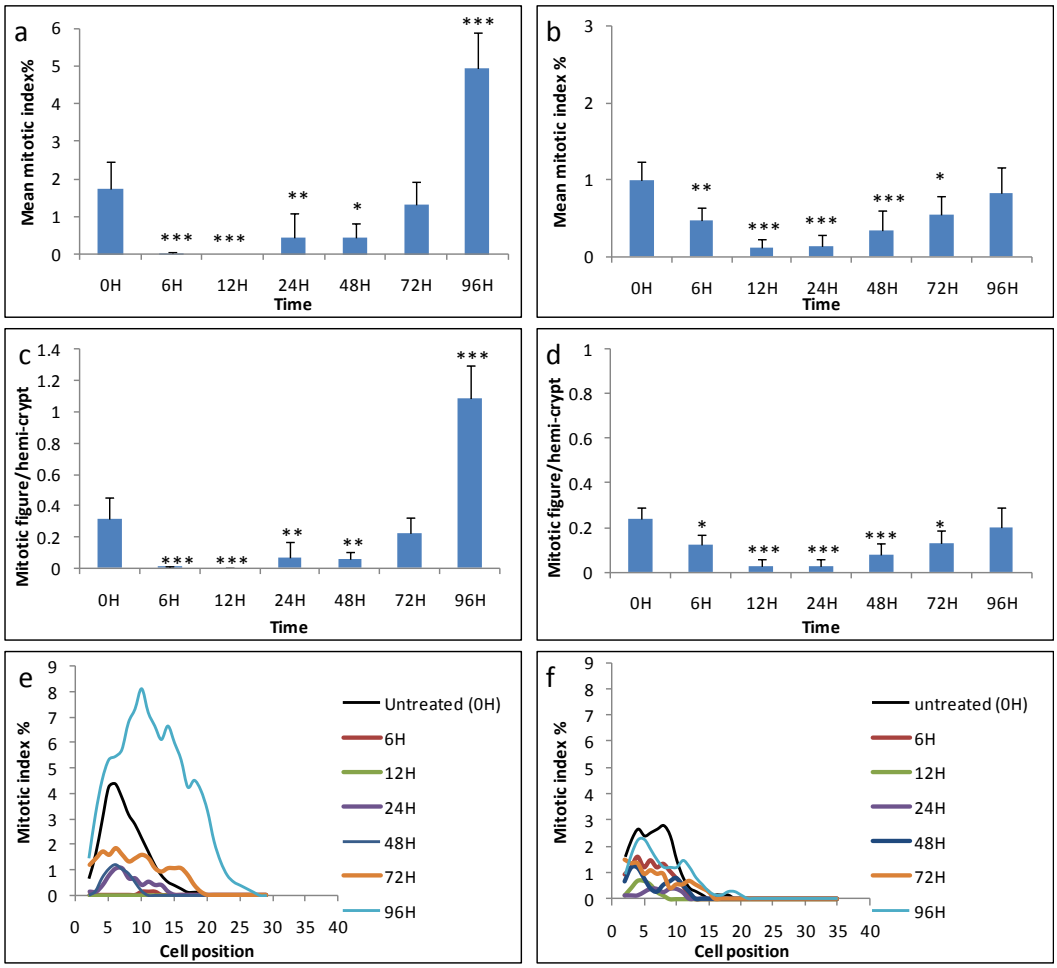

Figure 3.7: Quantitative analysis of intestinal crypt epithelial mitosis in wild-type mice at 0, 6, 12, 24, 48, 72 and 96 hours following administration (i.p.) of a single dose of 250mg/kg irinotecan. Small intestinal (a) and distal colon (b) mean mitotic index ± standard deviation separated by time. Small intestinal (c) and distal colon (d) mean number of mitotic figures per hemi-crypt ± standard deviation separated by time. Cell positional distribution of small intestinal (e) and distal colon (f) mitosis separated by time. Statistical differences were assessed by one way ANOVA and Dunnett's multiple comparison tests in (a), (b), (c) and (d) (*p<0.05, **p<0.01, ***p<0.001 compared to untreated C57BL/6) (n=5 per group).

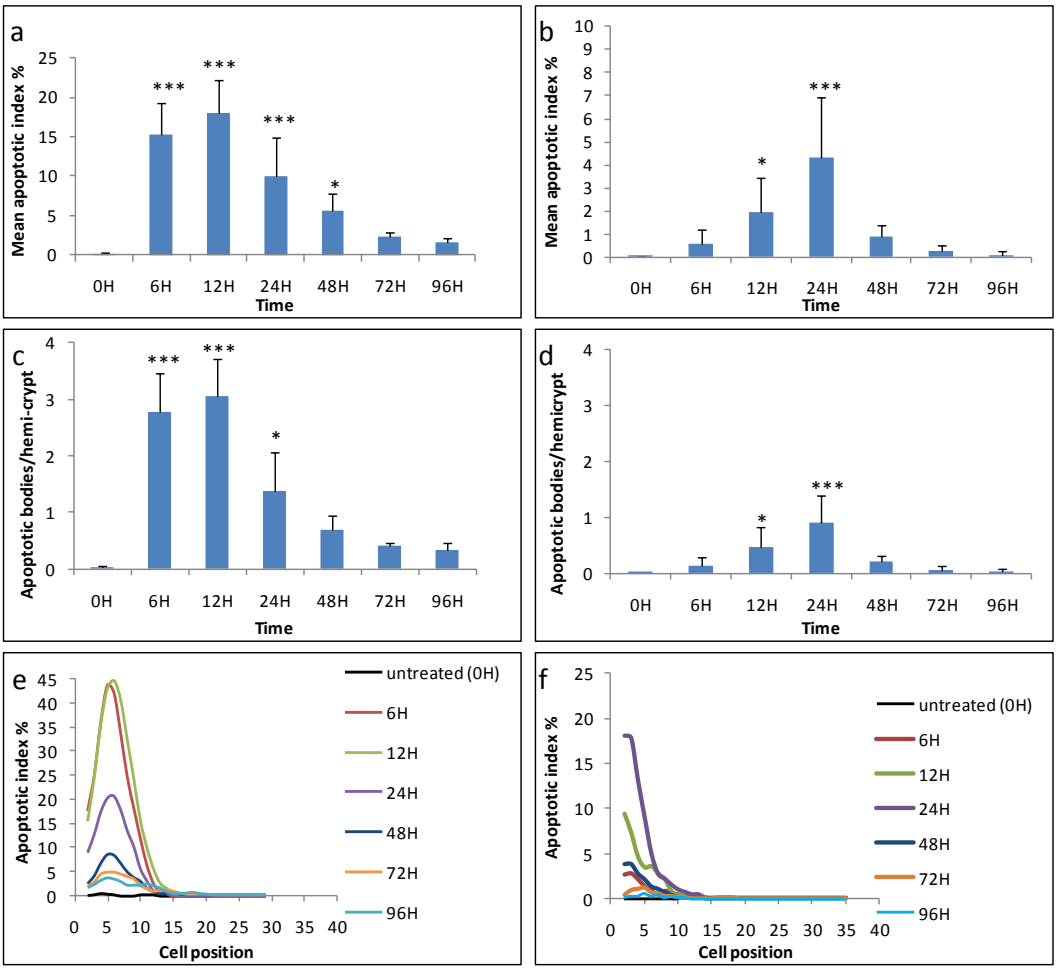

Figure 3.8: Quantitative analysis of intestinal crypt epithelial apoptosis in wild-type mice at 0, 6, 12, 24, 48, 72 and 96 hours following administration (i.p.) of a single dose of 250mg/kg irinotecan. Small intestinal (a) and distal colon (b) mean apoptotic index ± standard deviation separated by time. Small intestinal (c) and distal colon (d) mean number of apoptotic bodies per hemi-crypt ± standard deviation separated by time. Cell positional distribution of small intestinal (e) and distal colon (f) apoptosis separated by time. Statistical differences were assessed by one way ANOVA and Dunnett's multiple comparison tests in (a), (b), (c) and (d) (*p<0.05, ***p<0.001 compared to untreated C57BL/6). (n=5 per group).

3.5.2 c-Rel-null and NFκB1-null mice continue to show elongated colonic crypts 48 hours following irinotecan administration

In keeping with crypt length in untreated mice as shown earlier in Figure 3.1, NFκB1-null mice continued to show elongated small intestinal crypts 6 hours after irinotecan administration, with a mean crypt length of 19.5 cells per hemi-crypt compared to 18.0 cells per hemi-crypt in similarly treated wild-type mice. This difference in small intestinal crypt length was not however observed at 48 hours following irinotecan treatment compared to similarly treated wild-type mice (Figure 3.9 a and c).

A similar pattern of crypt elongation was observed in the distal colon of NFκB1-null mice both at 6 and 48 hours following irinotecan administration, with mean crypt lengths of 32.6 and 26.5 cells per hemi-crypt compared to 24.6 and 22.1 cells per hemi-crypt in wild-type mice at the 6 and 48 hours time points respectively. c-Rel-null mice also continued to show significantly longer colonic crypts at the 48 hour time point, with 25.4 cells per hemi-crypt compared to 22.1 cells per hemi-crypt in wild-type mice (Figure 3.9 b and d).

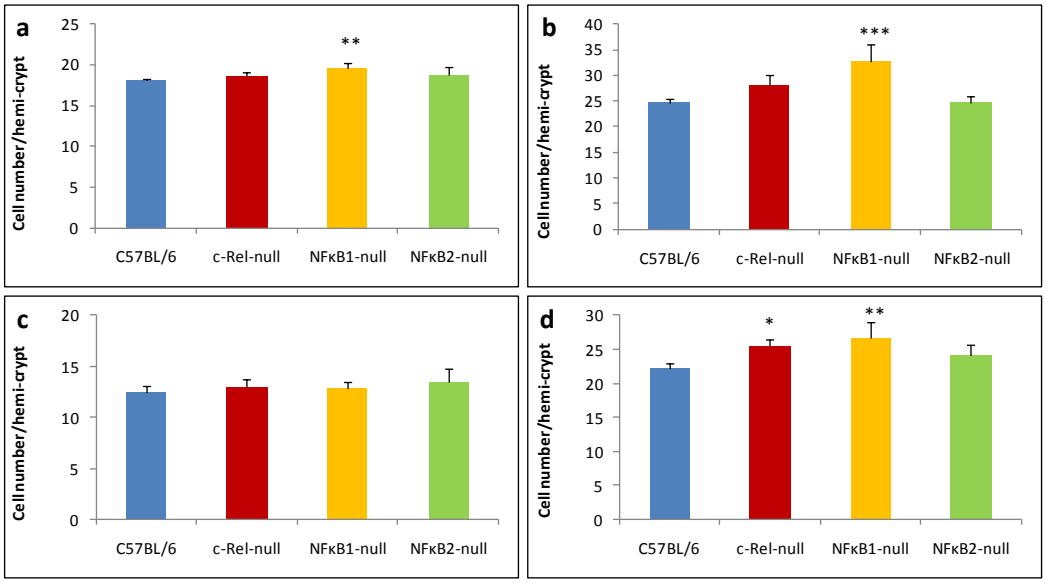

Figure 3.9: Number of intestinal epithelial cells per hemi-crypt in mice 6 hours and 48 hours following administration (i.p.) of a single dose of 250mg/kg irinotecan. Small intestine (a) and distal colon (b) mean cell number per hemi-crypt ± standard deviation in C57BL/6, c-Rel-null, NFκB1-null and NFκB2-null mice 6 hours following irinotecan. Small intestine (c) and distal colon (d) mean cell number per hemi-crypt ± standard deviation in C57BL/6, c-Rel-null, NFκB1-null and NFκB2-null mice 48 hours following irinotecan. Statistical differences were assessed by one way ANOVA and Dunnett's multiple comparison test (*$p<0.05$, **$p<0.01$ ***$p<0.001$ compared to similarly treated C57BL/6) (n=5 per genotype group).

3.5.3 Intestinal epithelial mitosis is suppressed following irinotecan administration

Following administration of 250mg/kg irinotecan to C57BL/6, c-Rel-null, NFκB1-null and NFκB2-null mice, small intestines and colons were harvested after 6 and 48 hours (5 mice per group). The amounts of mitosis and apoptosis were quantified using H and E stained sections. In comparison to untreated animals (Figure 3.2 a and c), mitosis was suppressed and barely detectable in C57BL/6 small intestine and completely suppressed in c-Rel-null and NFκB2-null small intestine 6 hours following irinotecan. However, this mitosis suppression in c-Rel-null, NFκB1-null and NFκB2-null small intestine was not statistically significant compared to C57BL/6 small intestine (Figure 3.10 a and c). Mitosis in the small intestine 48 hours following irinotecan was suppressed in all groups of mice but to a lesser extent than that which observed at the 6 hour time point and no significant alterations were observed between transgenic mice compared to wild-type mice (Figure 3.10 b and d).

Although colonic epithelial mitosis was reduced at greater extent in transgenic mice 6 hours following irinotecan administration relative to similarly treated wild-type mice, this was not statistically significant. This mitosis suppression remained until 48 hours relative to untreated mice (as previously shown in Figure 3.2 b and d), there were also no significant alterations between transgenic mice and wild-type mice following the same treatment and duration. Mitosis continued to occur in the lower quarter of colonic crypts at both the 6 hour and 48 hour time points (Figure 3.11).

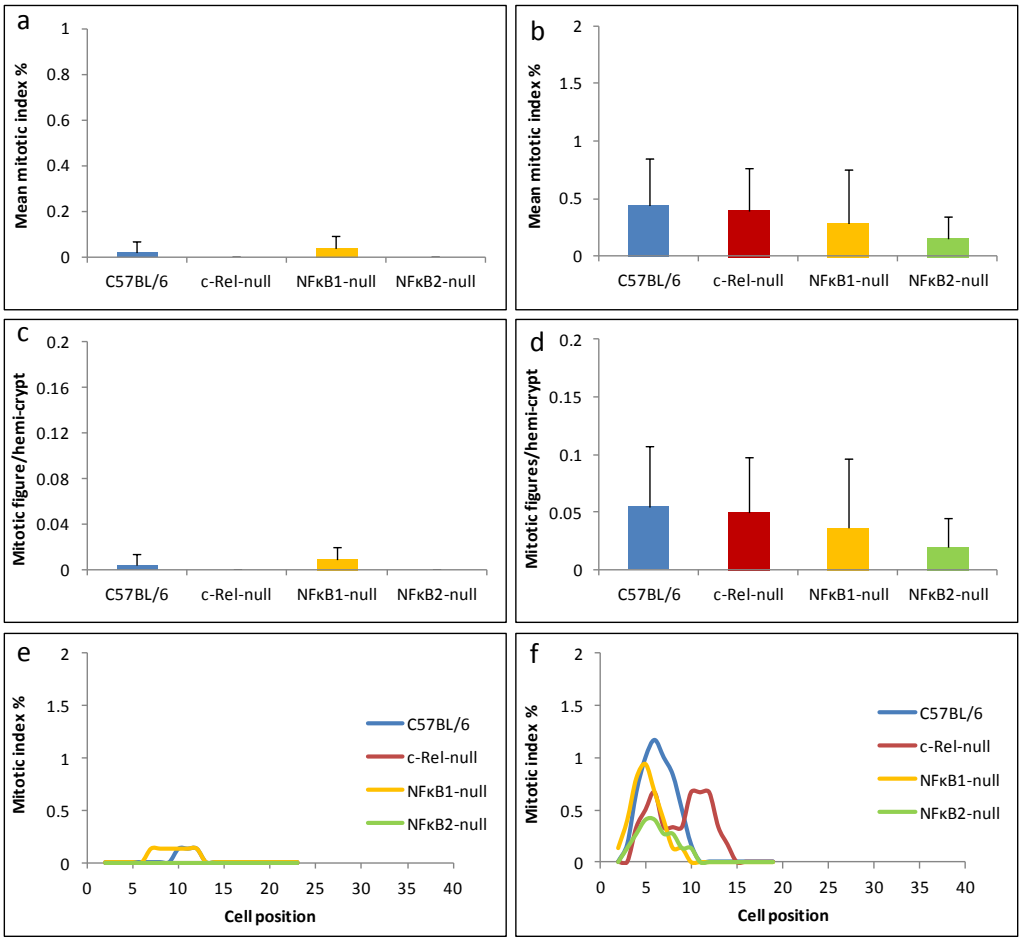

Figure 3.10: Quantitative analysis of small intestinal crypt epithelial mitosis 6 and 48 hours after administration (i.p.) of a single dose of 250mg/kg irinotecan. Mean mitotic index ± standard deviation 6 hours (a) and 48 hours (b) following irinotecan in small intestine separated by genotype. Mean number of mitotic figures per hemi-crypt ± standard deviation 6 hours (c) and 48 hours (d) following irinotecan in small intestine separated by genotype. Cell positional distribution of small intestinal crypt epithelial mitosis 6 hours (e) and 48 hours (f) following Irinotecan separated by genotype. Statistical differences were assessed by Kruskal–Wallis test followed by Dunn's multiple comparison tests in (a), (b), (c) and (d) compared to similarly treated C57BL/6. Statistical differences were assessed by modified median test in (e) and (f). (n=5 per genotype group).

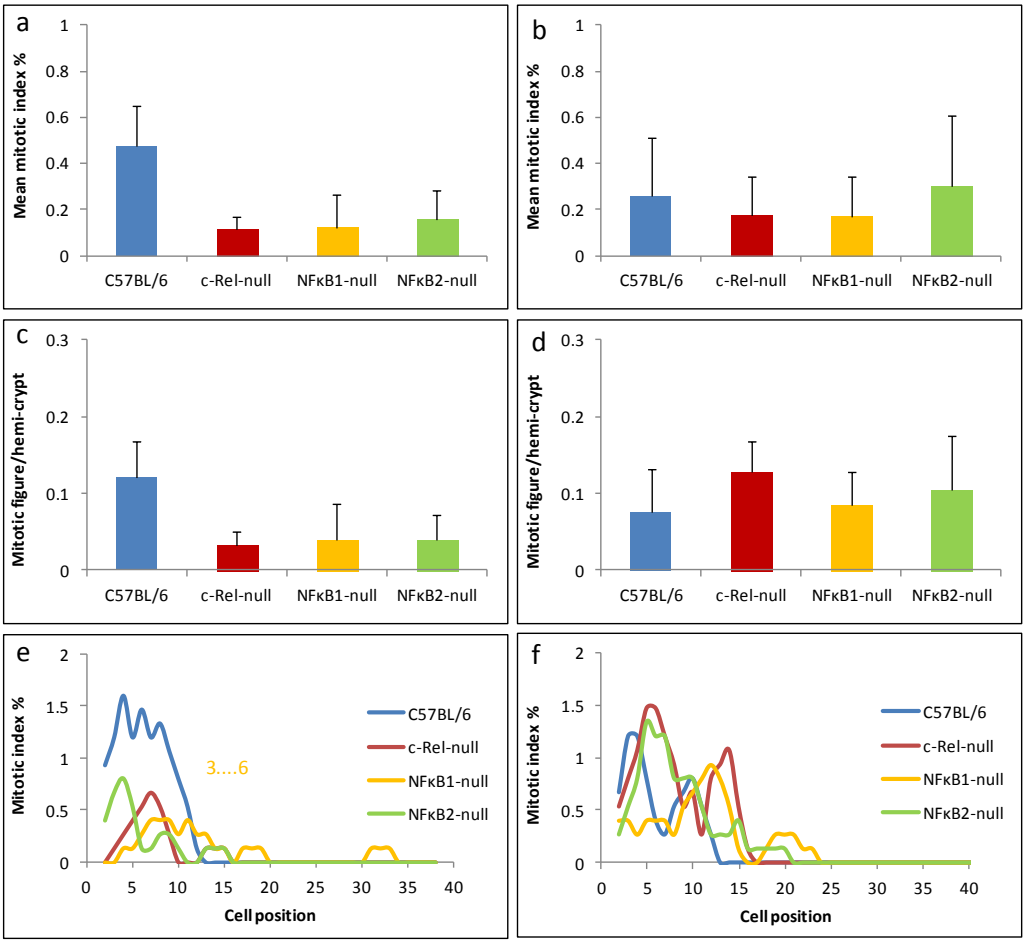

Figure 3.11: Quantitative analysis of distal colonic crypt epithelial mitosis 6 and 48 hours after administration (i.p.) of a single dose of 250mg/kg irinotecan. Mean mitotic index ± standard deviation 6 hours (a) and 48 hours (b) following irinotecan in distal colon separated by genotype. Mean number of mitotic figures per hemi-crypt ± standard deviation 6 hours (c) and 48 hours (d) following Irinotecan in distal colon separated by genotype. Cell positional distribution of distal colonic crypt epithelial mitosis 6 hours (e) and 48 hours (f) following irinotecan separated by genotype. Statistical differences were assessed by Kruskal–Wallis test followed by Dunn's multiple comparison tests in (a), (b), (c) and (d). Statistical differences were assessed by modified median test in (e) and (f). Dotted line denotes cell positions over which there was a significant difference from wild-type. Colour of dotted line denotes comparison genotype. (n=5 per genotype group).

3.5.4 NFκB1-null and NFκB2-null mice showed an increase in both small intestinal and colonic epithelial apoptosis at both 6 and 48 hours following irinotecan treatment

Intestines were obtained 6 and 48 hours after mice being subjected to a single dose of 250mg/kg irinotecan (5 mice per group). Amounts of apoptosis were quantified from H and E stained sections. In the small intestine of wild-type mice, 15.2% and 4.1% of the crypt epithelial cells were morphologically apoptotic 6 and 48 hours following irinotecan treatment respectively. This irinotecan induced apoptosis was predominantly located at the base of crypts and maximum apoptotic events occurred at cell position 5 following irinotecan adminstration (Figure 3.12). In the distal colon of these mice, apoptosis was also induced by irinotecan treatment, but to a lesser extent than that observed in the small intestine. According to morphological criteria, 0.57% and 0.97% of colonic crypt epithelial cells were apoptotic 6 and 48 hours following irinotecan administration respectively and apoptosis was mainly seen at the crypt base. The maximum frequency of irinotecan induced colonic crypt epithelial apoptosis was observed at cell position 2 (Figure 3.13). These positions of maximal apoptotic frequency of irinotecan induced apoptosis both in the small intestine and colon are similar to the cell positions of the proposed stem cell zone in these tissues.

In the small intestine, deletion of either NFκB1 or NFκB2 resulted in a significant increase in crypt epithelial apoptosis 6 hours following irinotecan (by 2-fold relative to similarly treated C57BL/6 mice). Significant differences in the cell positional distributions of apoptotic scores were observed between cell positions 10 to 15, 3

to 16 and 3 to 17 in c-Rel-null, NFκB1-null and NFκB2-null mice respectively compared to similarly treated wild-type mice using the modified median test (Figure 3.12 a, c and e). A similar pattern was seen at the 48 hour time point, where approximately 2-fold and 3-fold increases in irinotecan induced small intestinal crypt epithelial apoptosis were observed in NFκB1-null and NFκB2-null mice respectively relative to C57BL/6 mice following the same treatment. Significant differences in the distribution of apoptotic events were observed between cell positions 8 to 13 in NFκB1-null mice and 3 to 15 in NFκB2-null mice respectively using the modified median test (Figure 3.12 b, d and f). Maximum small intestinal crypt apoptosis was observed at cell position 5 in all strains of mice at both 6 and 48 hours following irinotecan.

In the distal colon, there was also a significant increase in the number of apoptotic events observed in NFκB1 null (6.8-fold increase) and NFκB2 null (6.8-fold increase) mice 6 hours following irinotecan administration compared to C57BL/6 mice following the same treatment. This correlated with significantly increased apoptotic scores between cell positions 3 to 17 in NFκB1-null mice and 2 to 8 in NFκB2-null mice using the modified median test (Figure 3.13 a, c and e). 48 hours after irinotecan administration, mice with germline deletions of either NFκB1 or NFκB2 continued to show significantly elevated apoptotic scores in the distal colon in comparison to similarly treated wild-type mice, with 2.5- fold and 2-fold increases in apoptosis being observed respectively. These transgenic mice (NFκB1-null and NFκB2-null) demonstrated significant increases in apoptotic scores at cell positions 3 to 12 and 3 to 5 respectively compared to similarly treated wild-type mice (Figure

3.13 b, d and f). Comparisons between wild-type and c-Rel-null mice at the 6 and 48 hour time points demonstrated no significant differences in apoptosis scores in either the small intestine or distal colon.

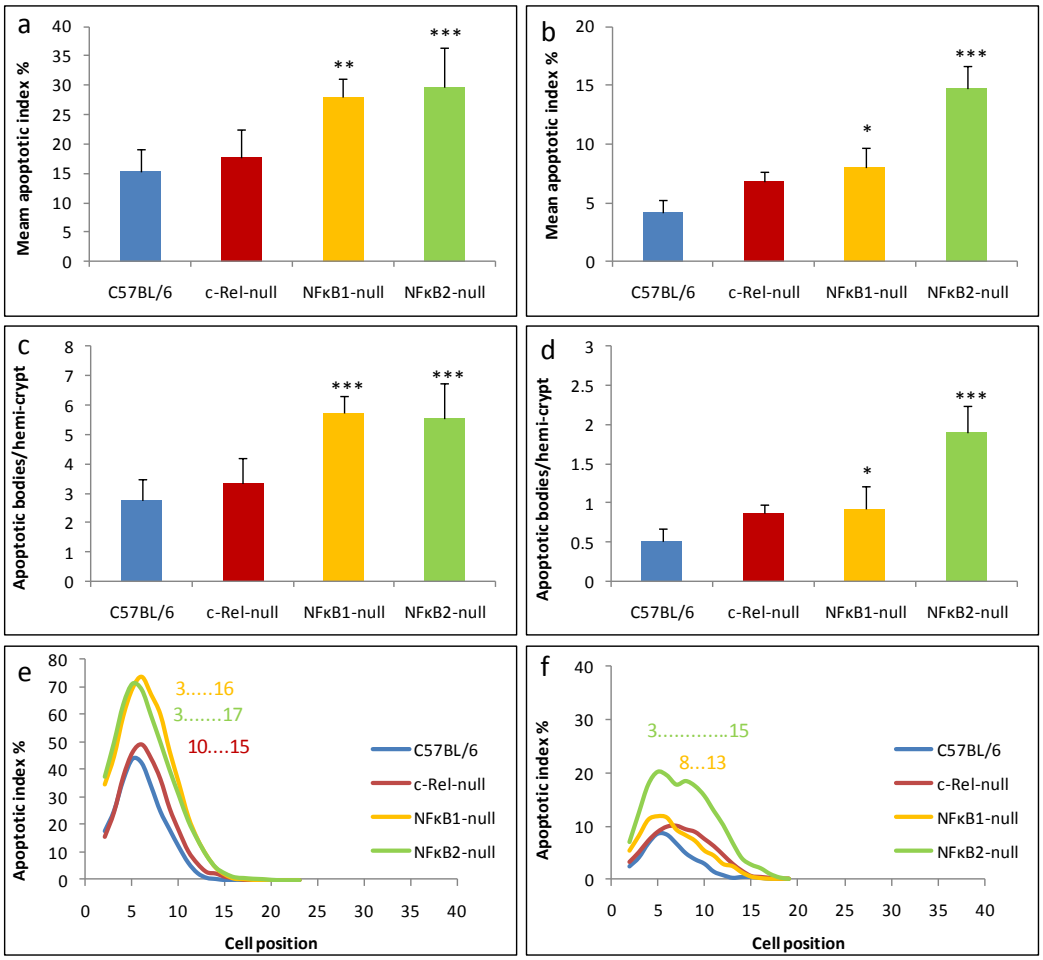

Figure 3.12: Quantitative analysis of small intestinal crypt epithelial apoptosis 6 and 48 hours after administration (i.p.) of a single dose of 250mg/kg irinotecan. Mean apoptotic index 6 hours (a) and 48 hours (b) following irinotecan in small intestine separated by genotype. Mean number of apoptotic scores per hemi-crypt ± standard deviation 6 hours (c) and 48 hours (d) following irinotecan in small intestine separated by genotype. Cell positional distribution of small intestinal crypt epithelial apoptosis 6 hours (e) and 48 hours (f) following irinotecan separated by genotype. Statistical differences were assessed by one way ANOVA and Dunnett's multiple comparison tests in (a), (b), (c) and (d) (*p<0.05,**p<0.01, ***p<0.001 compared to C57BL/6). Statistical differences were assessed by modified median test in (e) and (f). Dashed line denotes cell positions over which there was a significant difference in apoptotic scores compared to wild-type. Colour of dashed line denotes comparison genotype. (n=5 per genotype group).

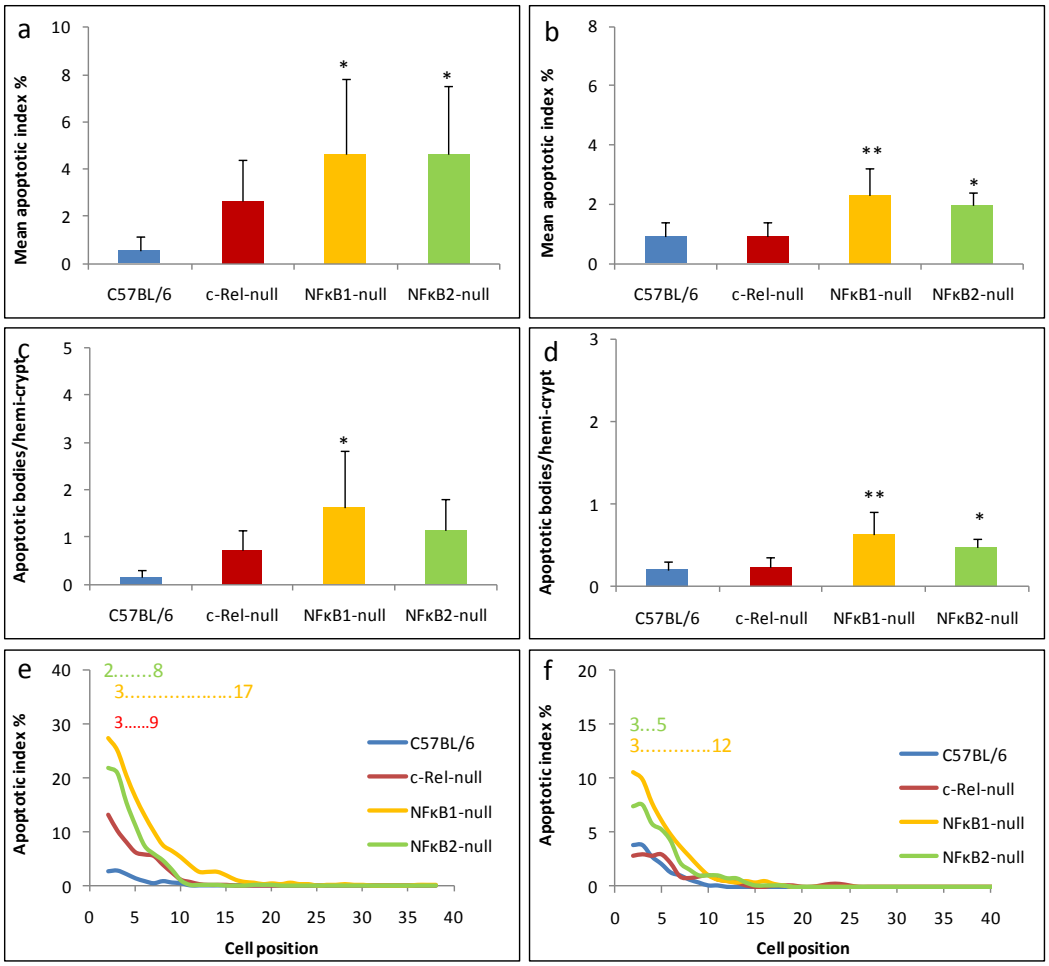

Figure 3.13: Quantitative analysis of distal colonic crypt epithelial apoptosis 6 and 48 hours after administration (i.p.) of a single dose of 250mg/kg Irinotecan. Mean apoptotic index ± standard deviation 6 hours (a) and 48 hours (b) following Irinotecan in distal colon separated by genotype. Mean number of apoptotic scores per hemi-crypt ± standard deviation 6 hours (c) and 48 hours (d) following Irinotecan in distal colon separated by genotype. Cell positional distribution of distal colonic crypt epithelial apoptosis 6 hours (e) and 48 hours (f) following Irinotecan separated by genotype. Statistical differences were assessed by one way ANOVA and Dunnett's multiple comparison tests in (a), (b), (c) and (d) (*$p<0.05$,**$p<0.01$ compared to C57BL/6). Statistical differences were assessed by modified median test in (e) and (f). Dashed line denotes cell positions over which there was a significant difference in apoptotic scores compared to wild-type. Colour of dashed line denotes comparison genotype. (n=5 per genotype group).

3.6 Expression of apoptosis regulating genes in untreated and irradiated mice with disrupted NFκB signalling

To investigate the molecular mechanisms responsible for the increased irradiation induced apoptosis observed in small intestine and colon of NFκB1-null and NFκB2-null mice, the mRNA expression of 10 key apoptosis regulating genes was assessed in the small intestinal and colonic epithelia of untreated and treated mice by real time PCR. 8 of these 10 genes were known NFκB-regulated genes. 2 novel genes (TRAIL and caspase 12) were also included, due to preliminary observations that showed that they were up-regulated on an apoptosis pathway specific microarray in NFκB2-null colon following azoxymethane treatment (A. Hanedi, MRes project 2008). Depending on function, 6 of these genes were pro-apoptotic namely TRAIL, Caspase12, BAK, FAS-L, FAS and p53 and the remaining 4 genes were anti-apoptotic namely BCL2, BCL-XL, c-IAP2 and XIAP. Adult male c-Rel-null, NFκB1-null and NFκB2-null mice and their wild-type (C57BL/6) counterparts (4 mice per genotype) were subjected to 8Gy γ-irradiation and mice were culled 4.5 hours later. Corresponding untreated mice of the same age and genotype were also culled as control animals (4 mice per genotype). RNA samples were extracted from small intestinal and colonic epithelia before being reverse transcribed to cDNA and quantified by real-time PCR. Values of relative mRNA expression in transgenic mice were compared to similarly treated wild-type (C57BL/6) mice.

In untreated groups, NFκB1-null and NFκB2-null mice showed reduced relative mRNA expressions of the anti-apoptotic genes BCL2, BCL-XL, c-IAP2 and XIAP in the small intestine compared to untreated wild-type mice (Figure 3.15). These

molecular changes might explain the increased susceptibility to small intestinal spontaneous apoptosis observed in these strains particularly in NFκB2-null mice where it reached statistical significance. In untreated distal colon, changes in the relative mRNA expression of apoptosis regulating genes were also observed in transgenic mice compared to wild-type mice. In particular NFκB1-null and NFκB2-null distal colon showed reduction in the relative mRNA expression of the anti-apoptotic genes c-IAP2 and XIAP (Figure 3.17). Untreated c-Rel-null mice showed increased expression of BCL2 and reduced expression of XIAP in the small intestine (Figure 3.15), while untreated c-Rel-null colon showed increased expression of BAK (Figure 3.16) and reduced expression c-IAP2 (Figure 3.17). However, these slight alterations in the expression of apoptosis regulating genes were not associated with changes in baseline apoptosis in the distal colon of these transgenic mice as shown earlier (Figure 3.3).

Following irradiation, NFκB1-null mice showed significant increases in the expression of the pro-apoptotic genes TRAIL and Caspase12 in the small intestine (Figure 3.14). Irradiated NFκB1-null colon also showed a significant increase in the expression of the pro-apoptotic gene TRAIL and reduced expression of the anti-apoptotic gene c-IAP2 compared to irradiated wild-type mice (Figure 3.16 and Figure 3.17). Irradiated NFκB2-null mice also demonstrated significant increases in the expression of the pro-apoptotic genes Caspase12, BAK, p53 and FAS-L in the small intestine (Figure 3.14) and TRAIL, Caspase12 and FAS-L in the colon relative to irradiated wild-type mice (Figure 3.16). Strikingly, a huge increase in relative mRNA expressions of FAS-L by 15-fold in the small intestine and 40-fold in the colon was

observed only in NFκB2-null mice following irradiation compared to similarly treated wild-type mice. This suggests that NFκB2 plays a crucial role in the transcriptional regulation FAS-L expression in the intestine. These increases in the mRNA expression of pro-apoptotic genes in NFκB2-null small intestine were associated with modest increases in the expression of the anti-apoptotic genes BCL-XL, c-IAP2 and XIAP following irradiation compared to wild-type mice (Figure 3.15). The increased expressions of pro-apoptotic genes which were observed in both the small intestine and colon of irradiated NFκB1-null and NFκB2-null mice may be the mechanisms responsible for the increased irradiation induced apoptosis observed in these animals.

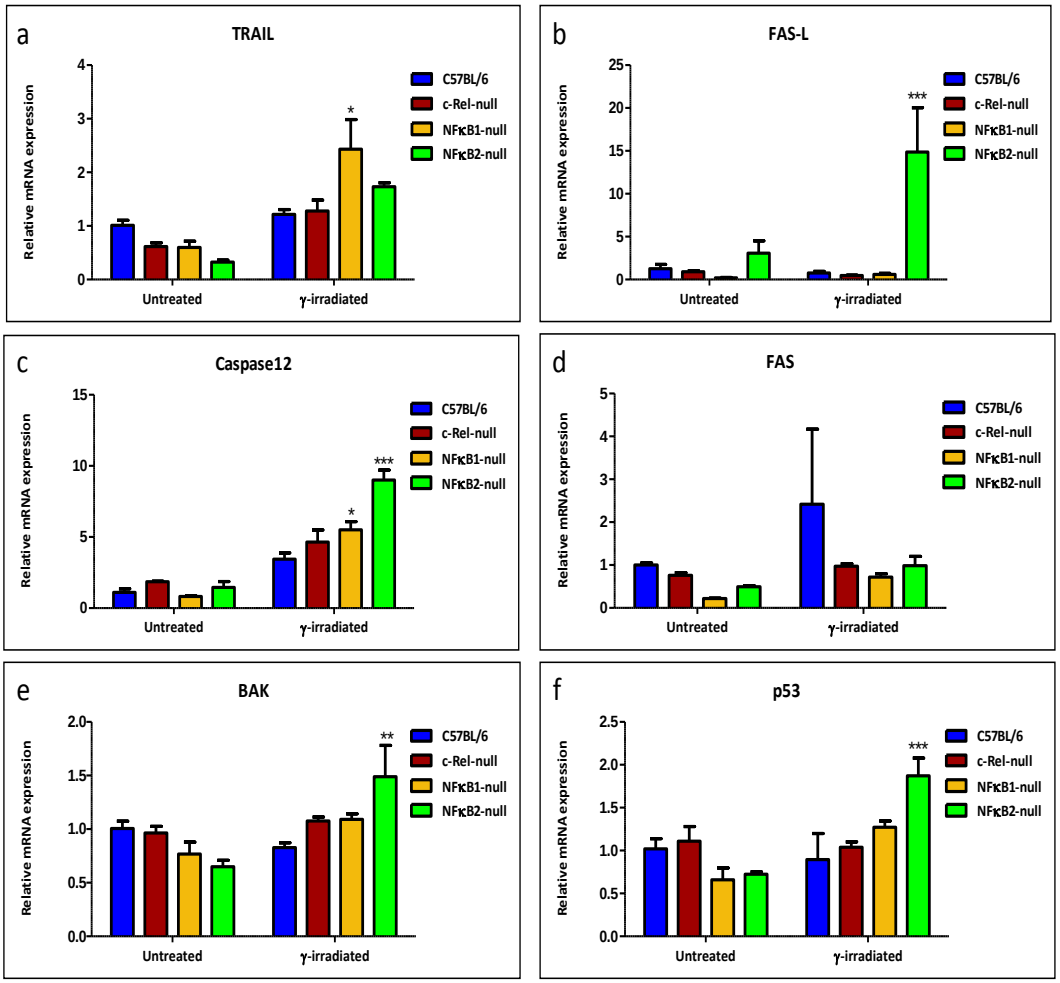

Figure 3.14: Quantification of relative mRNA expression of pro-apoptotic genes in the small intestinal epithelia of untreated mice and mice 4.5 hours following 8Gy whole body γ-irradiation. Relative mRNA expression of TRAIL (a), FAS-L (b), Caspase12 (c), FAS (d), BAK (e) and p53 (f) were assessed by real-time PCR in the small intestinal epithelial cells from untreated and irradiated strains of mice as indicated above using real-time PCR. Statistical analysis was performed by 2-way ANOVA with Bonferroni post-hoc tests (*p<0.05, **p<0.01, ***p<0.001 compared to similarly treated C57BL/6) (n=4 mice per genotype group).

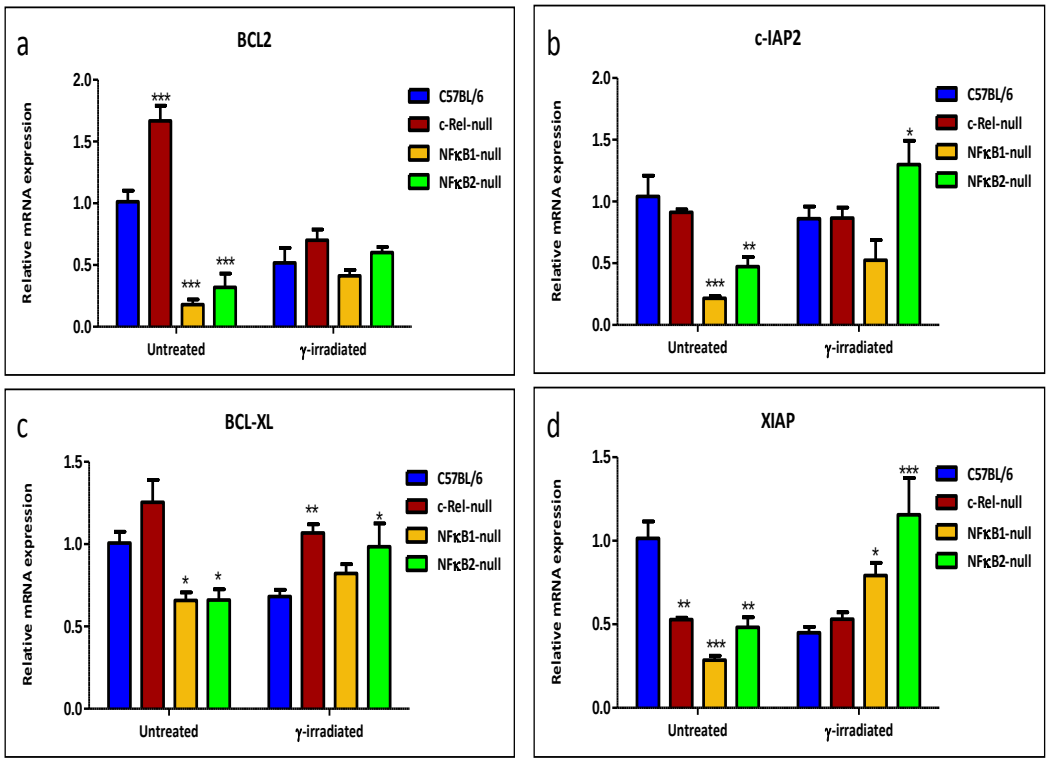

Figure 3.15: Quantification of relative mRNA expression of anti-apoptotic genes in the small intestinal epithelia of untreated mice and mice 4.5 hours following 8Gy whole body γ-irradiation. Relative mRNA expressions of BCL2 (a), c-IAP2 (b), BCL-XL (c) and XIAP (d) were assessed in the small intestinal epithelial cells from untreated and irradiated strains of mice as indicated above using real-time PCR. Statistical analysis was performed by 2-way ANOVA and with Bonferroni post-hoc tests (*p<0.05, **p<0.01, ***p<0.001 compared to similarly treated C57BL/6) (n=4 mice per genotype group).

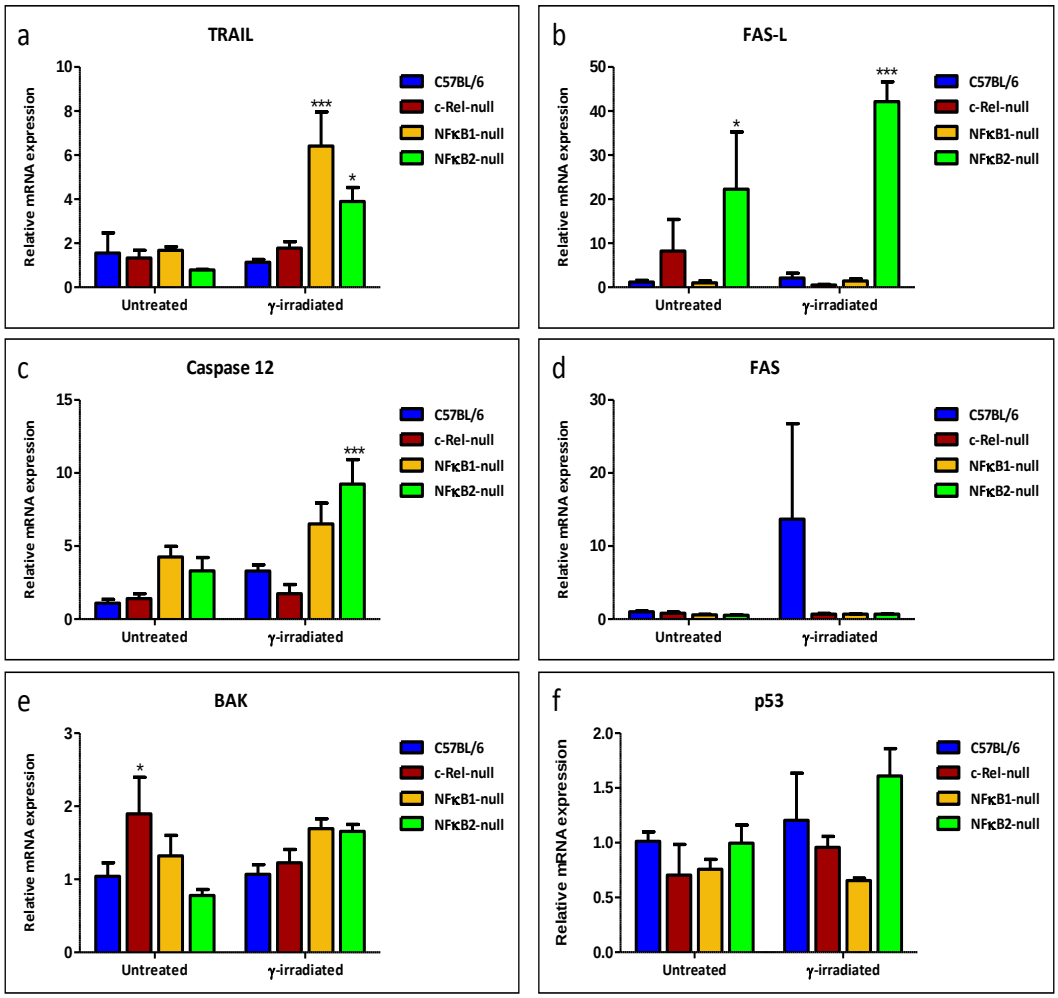

Figure 3.16: Quantification of relative mRNA expression of pro-apoptotic genes in the colonic epithelia of untreated mice and mice 4.5 hours following 8Gy whole body γ-irradiation. Relative mRNA expressions of TRAIL (a), FAS-L (b), Caspase12 (c), FAS (d), BAK (e) and p53 (f) were assessed in the colonic epithelial cells from untreated and irradiated strains of mice as indicated above using real-time PCR. Statistical analysis was performed by 2-way ANOVA with Bonferroni post-hoc tests (*$p<0.05$, ***$p<0.001$ compared to similarly treated C57BL/6) (n=4 mice per genotype group).

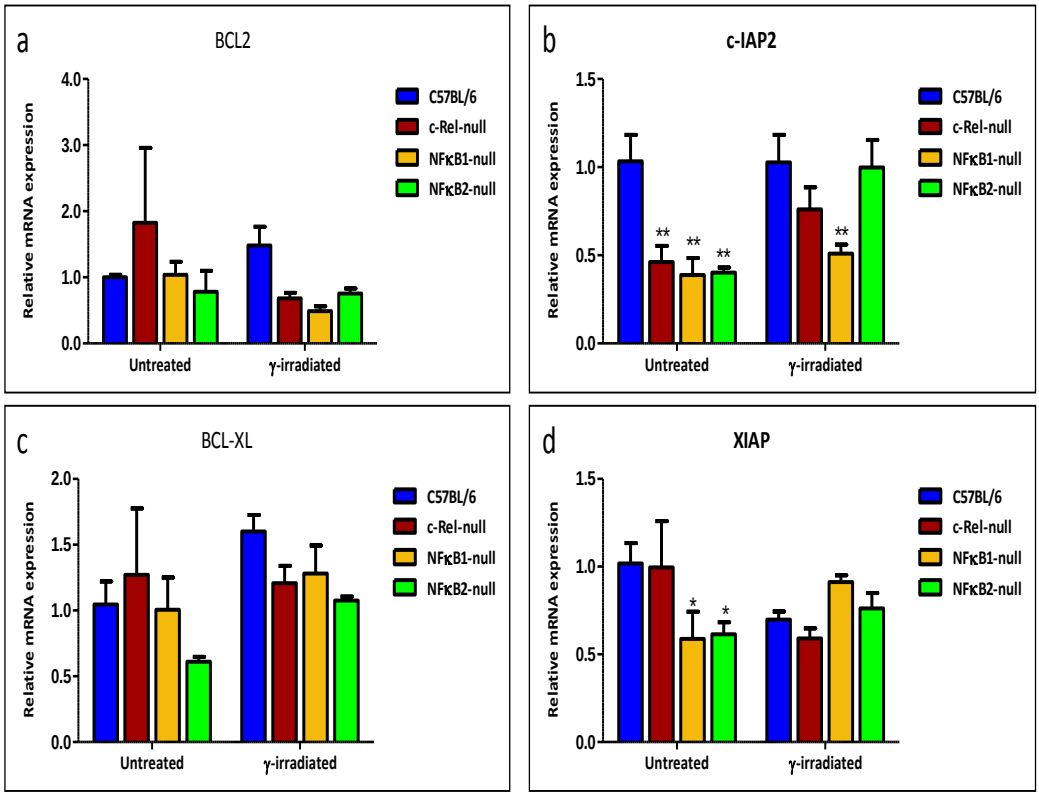

Figure 3.17: Quantification of relative mRNA expression of anti-apoptotic genes in the colonic epithelia of untreated mice and mice 4.5 hours following 8Gy whole body γ-irradiation. Relative mRNA expressions of BCL2 (a), c-IAP2 (b), BCL-XL (c) and XIAP (d) were assessed in the colonic epithelial cells from untreated and irradiated strains of mice as indicated above using real-time PCR. Statistical analysis was performed by 2-way ANOVA and with Bonferroni post-hoc tests (*$p<0.05$, **$p<0.01$ compared to similarly treated C57BL/6) (n=4 mice per genotype group).

3.7 Investigating the effect of NFκB2 and RelB suppression upon HCT116 cell proliferation and apoptosis *in vitro*

Due to lack of access to RelB-null mice and to further characterise the role of alternative pathway of NFκB signalling in regulating intestinal epithelial apoptosis and proliferation, *in vitro* assessment of the effects of suppression of RelB and NFκB2 expression on these cellular processes was performed.

3.7.1 Assessment of NFκB2 expression in various colon cancer cell lines using three NFκB2 antibodies from different suppliers

In order to identify a suitable cell line for the *in vitro* study, a number of different colon cancer cell lines were tested to investigate the expression of NFκB2. These cell lines include Caco2, DLD-1, HCT116, HT29 and LS1747. Alongside these cells, Raji (human Burkitt's lymphoma cell line) and AGS (human gastric cancer cell lines) were also used as positive controls. Western blotting was performed upon the protein extracted from these cell lines using NFκB2 antibodies from three suppliers (Dr Caamano's antibody, Abcam and Santa Cruz) as described in section 2.6. NFκB2 was expressed in all cell lines. HCT116 cells showed the strongest expression and clearly showed the two bands of NFκB2 (the precursor p100 and the processed form p52). Not the all antibodies clearly detected the two bands of NFκB2. However, the NFκB2 antibody which was provided by Dr. Caamano appeared to generate the clearest image (Figure 3.18). Therefore, HCT116 cells and Dr Caamano's anti-NFκB2 antibody were used for further studies.

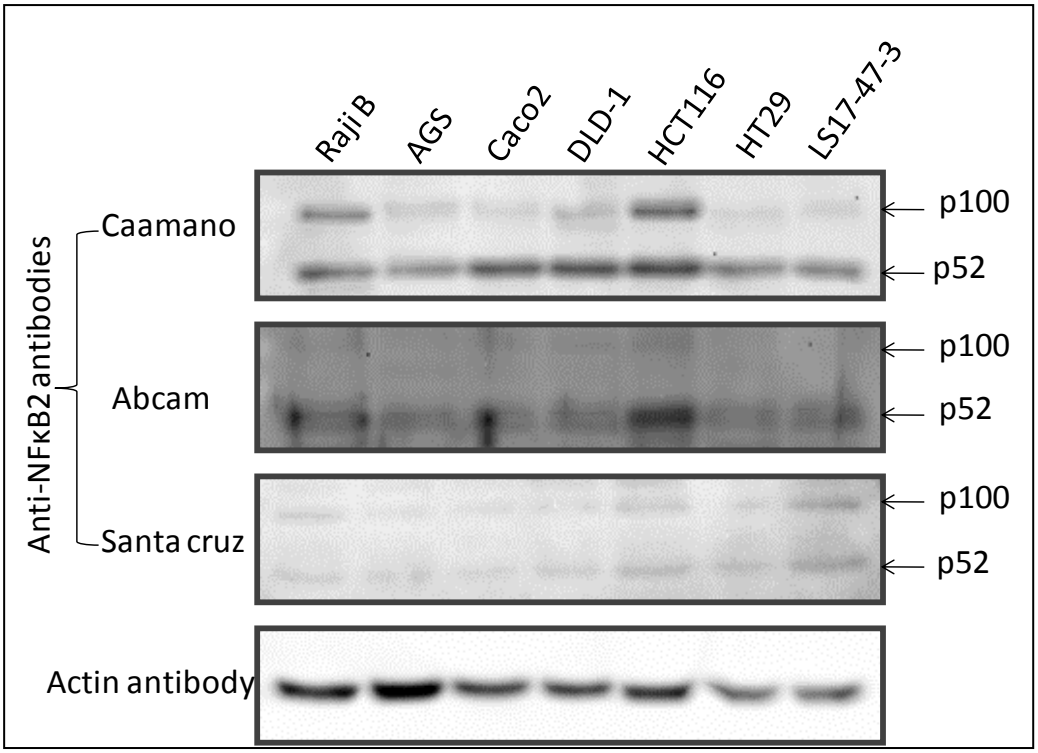

Figure 3.18: Immunoblotting of protein samples obtained from Raji B and AGS (as positive controls), Caco2, DLD-1, HCT116, HT29, and LS1747-3 (colon cancer cells) using anti-NFκB2 antibodies from three different suppliers (Dr Caamano, Abcam and Santa Cruz) and an anti-actin antibody.

3.7.2 Time course of NFκB2 siRNA transfection in HCT116 cells

In order to evaluate the time required for knockdown of the expression of NFκB2, a time course following NFκB2 siRNA transfection was performed. Protein expression of NFκB2 was assessed 24, 48 and 72 hours following transfection using Western blot. All time points showed reduced expression of the precursor form of NFκB2 (p100), but no change was seen in the abundance of the processed form (p52). Changes were observed only in target siRNA transfected cells (Figure 3.19). The percentage of knockdown was approximately 45% at all the time points tested in one experiment, as assessed by protein densitometry. Unaltered protein expression

of the processed form (p52) of NFκB2 during this time course may be due to a longer half life of this protein (thus slowing the rate of turnover). Hence, it may take longer for p52 protein stores to be depleted to allow actual knockdown to be observed. Therefore, a longer time course was also performed. p100 and p52 protein expressions were analysed 5 and 6 days after NFκB2 siRNA transfection. Although the percentage knockdown of p100 was more than 80% at these longer time points, as assessed by protein densitometry, no change was observed in the abundance of the processed form (p52) as shown in Figure 3.20.

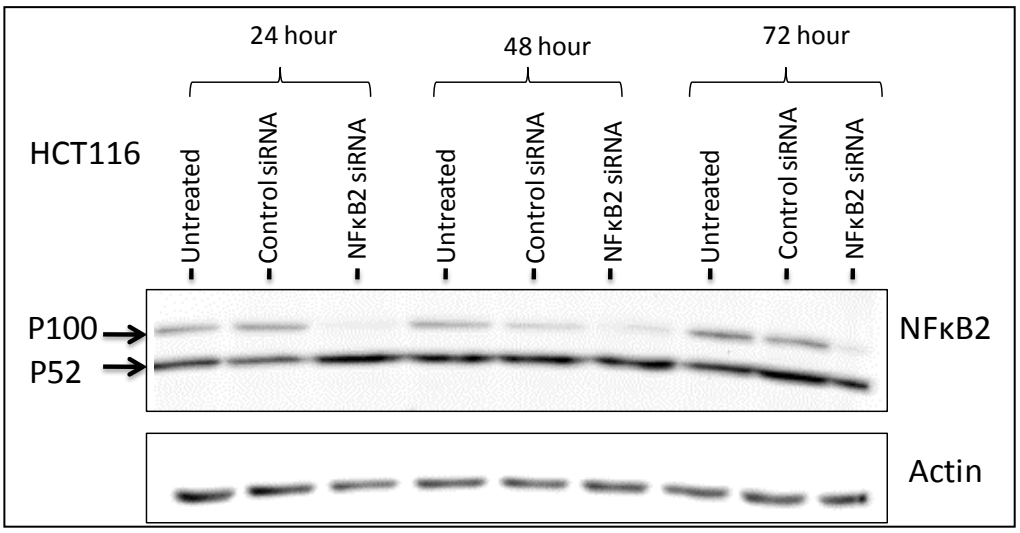

Figure 3.19: Western blot to assess NFκB2 protein expression 24, 48 and 72 hours following NFκB2 siRNA transfection of HCT116 cells. Knockdown of the p100 but not the p52 form of NFκB2 was observed at all the time points tested.

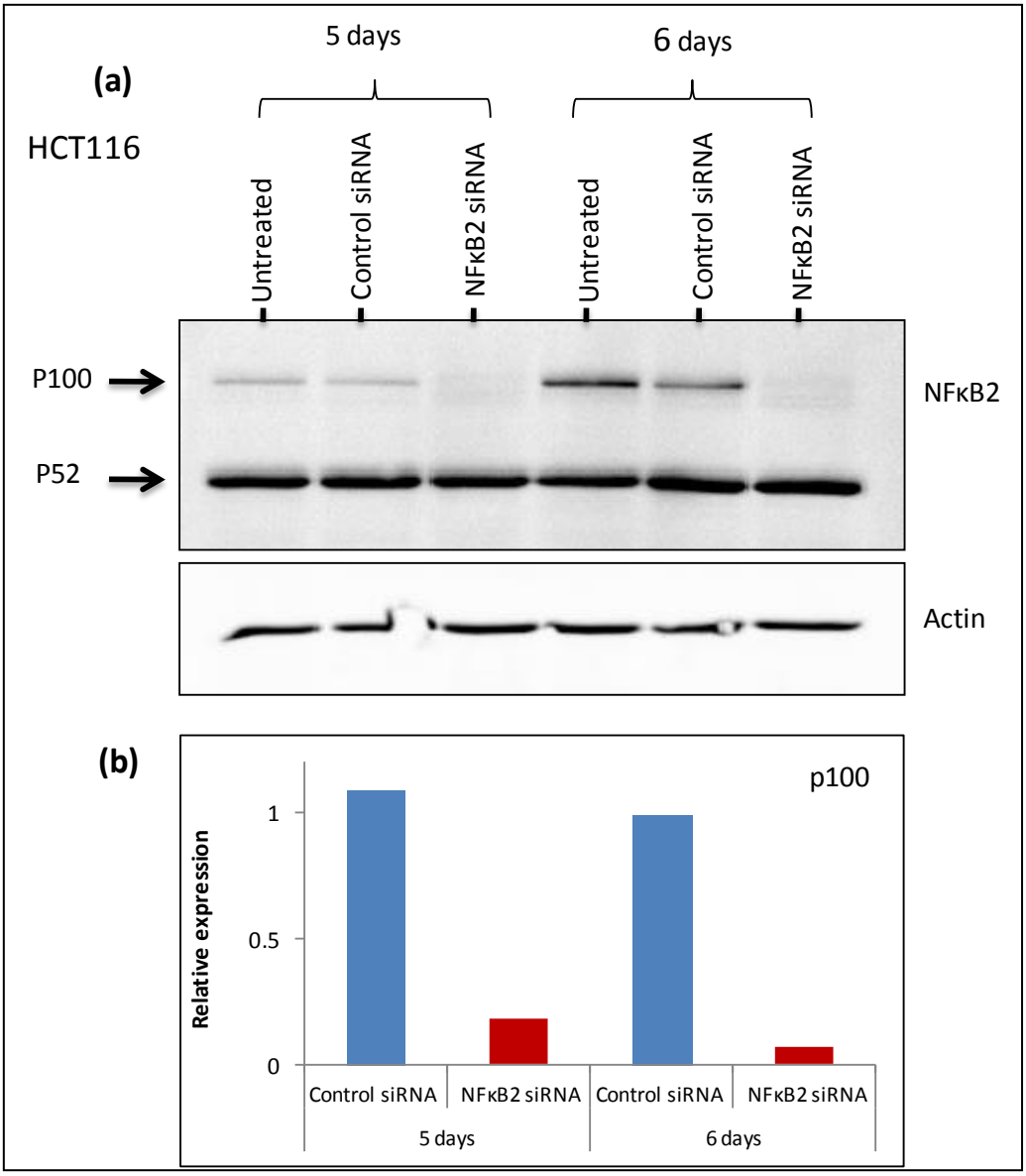

Figure 3.20: Western blot to assess NFκB2 protein expression 5 and 6 days following NFκB2 siRNA transfection of HCT116 cells. (a) Western blotting of protein samples obtained from HCT116 cells following 5 and 6 days of siRNA transfection as indicated above. Knockdown of the p100 but not the p52 form of NFκB2 was observed at all the time points tested. Anti-actin antibody was used as a loading control. (b) Relative expression of p100 compared to its expression in control siRNA transfected cells. NFκB2 siRNA treatment resulted in reduced expression of the p100 but not the p52 form of NFκB2 by 83% and 90% at the 5 and 6 day time points respectively compared to control siRNA at the same time points. This figure demonstrates the findings from one representative experiment.

3.7.3 Effect of NFκB2 suppression upon cell proliferation and apoptosis with and without Etoposide treatment

24 hours following seeding of HCT116 cells, they were transfected with NFκB2 siRNA or control siRNA. 24 hours after this siRNA transfection, Etoposide treatment was performed. Etoposide, which is a chemotherapeutic agent that inhibits topoisomerase II was used to induce apoptosis (at a final concentration of 20μM). Etoposide treated and untreated cells were incubated for a further 24 hours. Floating cells (as a measure of apoptosis) and attached cells (as a measure of cell proliferation) were then counted as outlined in Figure 3.21 a. Because there was a difference between the number of attached cells in the control and NFκB2 siRNA treated cells, apoptosis was calculated as a percentage of apoptotic cells to total cells [number of floating cells/number of (floating cells + attached cells) x100%]. The percentage of apoptotic cells in NFκB2 siRNA treated cells compared to the percentage of apoptotic cells in control siRNA treated cells was then calculated. The percentage of attached cells following NFκB2 siRNA treatment was also compared to the percentage of attached cells following control siRNA treatment.

In Etoposide-untreated HCT116 cells, knocking down NFκB2 protein expression using siRNA resulted in a significant decrease in the percentage of attached cells compared with control siRNA treated cells ($p<0.05$, student's *t*-test) (Figure 3.21 b). Knockdown of NFκB2 protein expression however did not alter the percentage of apoptotic cells compared to control siRNA (Figure 3.21 d).

Etoposide treatment resulted in a reduction in attached cells by 33% and 30% following control siRNA and NFκB2 siRNA treatments respectively compared with

Etoposide-untreated cells of corresponding siRNA treatments. Also, Etoposide resulted in increases of 33% and 46% respectively in apoptosis in control siRNA and NFκB2 siRNA transfected cells, compared with Etoposide-untreated cells of corresponding siRNA treatment.

In Etoposide treated HCT116 cells, there was again a significant decrease in the percentage of attached cells following NFκB2 siRNA treatment compared with control siRNA treated cells ($p<0.05$, student's *t*-test) (Figure 3.21 c). Also, a significant increase in the percentage of apoptotic cells was observed in NFκB2 siRNA transfected cells compared to control siRNA transfected cells following Etoposide treatment ($p<0.05$, student's *t*-test) (Figure 3.21 e).

Therefore, these data demonstrated that reducing the protein expression of the precursor form of NFκB2 (p100) decreased HCT116 cell proliferation both with and without Etoposide treatment and also increased apoptosis following Etoposide treatment.

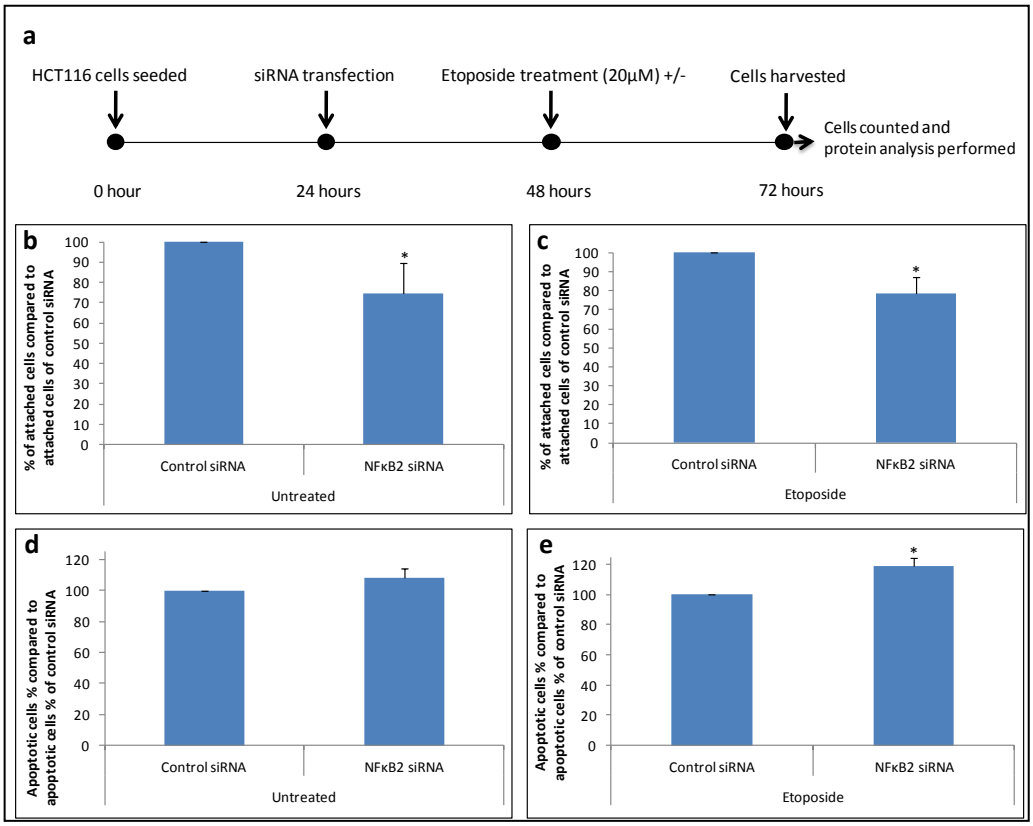

Figure 3.21: Effects of NFκB2 suppression using siRNA technique on HCT116 cell proliferation and apoptosis in either untreated or Etoposide treated cells. (a) Schematic diagram showing siRNA transfection and Etoposide treatment protocol in HCT116 cells. % of attached cells compared to control siRNA transfected cells (± standard deviation) in untreated (b) and Etoposide treated (c) cells respectively. % of apoptotic cells compared to control siRNA transfected cells (± standard deviation) in untreated (d) and Etoposide treated (e) cells respectively (± standard deviation) (*p<0.05 by student's *t*-test). The data are from 3 independent experiment (n=3).

3.7.4 Effect of NFκB2 suppression on the expression of proteins that regulate cell proliferation, differentiation and apoptosis

To investigate the mechanisms by which NFκB2 regulates HCT 116 cell proliferation and apoptosis, the expression of key proteins that are known to regulate proliferation and apoptosis was assessed following siRNA treatment using Western blot. These proteins included p53 and its target genes cyclin D1 and p21 that are involved in regulating cell proliferation. The protein expression of an NFκB2 regulated anti-apoptotic target gene BCL-2 was also assessed.

Etoposide treatment resulted in a significant increase in the expression of NFκB2, p53 and its target gene p21 in both control siRNA and NFκB2 siRNA transfected cells compared to Etoposide-untreated cells. However, no change in the expression of p53, p21, cyclin D1 or BCL2 was observed in NFκB2 siRNA transfected cells compared to control siRNA transfected cells either before or after Etoposide treatment (Figure 3.22).

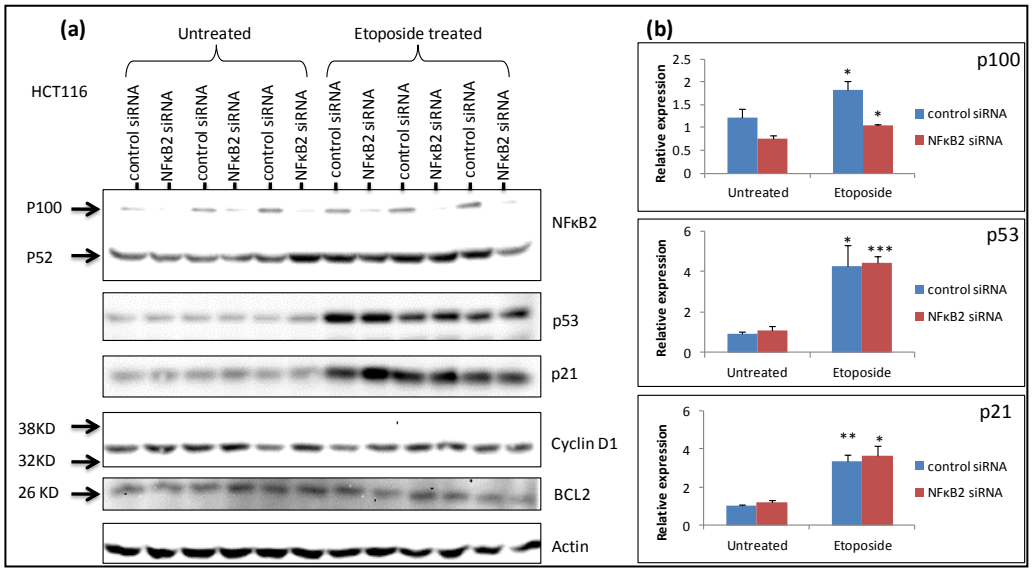

Figure 3.22: Protein expression of NFκB2 and other key genes that regulate proliferation and apoptosis in HCT116 cells following NFκB2 siRNA and Etoposide treatment. (a) Western blotting of protein samples obtained from HCT116 cells following siRNA transfection and then Etoposide treatment using anti-NFκB2, p53, cyclin D1, p21 and BCL-2 antibodies. Anti-actin antibody was also used as a loading control. (b) Relative expression of p100, p53 and p21 compared to their expression in control siRNA and Etoposide-untreated cells (± standard deviation). NFκB2 siRNA treatment resulted in reduced expression of the p100 but not the p52 form of NFκB2 by 45% compared to control siRNA. Etoposide treatment caused a significant increase in the expression of NFκB2, p53 and p21 (*p<0.05, **p<0.01, ***p<0.001 by student's *t*-test). This figure demonstrates the findings from triplicate samples.

3.7.5 Time course of RelB siRNA transfection in HCT116 cells

To determine the optimal time point required for efficient knockdown of RelB expression, a time course following RelB siRNA transfection was performed using HCT116 cells. Protein expression of RelB was assessed 24, 48 and 72 hours following transfection using Western blot. All time points showed reduced expression of RelB. Changes were observed only in target siRNA transfected cells (Figure 3.23). The percentage of knockdown was approximately 60%, 75% and 75% at the 24, 48 and 72 hour time points respectively as assessed by protein densitometry. Therefore, the 48 hour time point was chosen for subsequent studies.

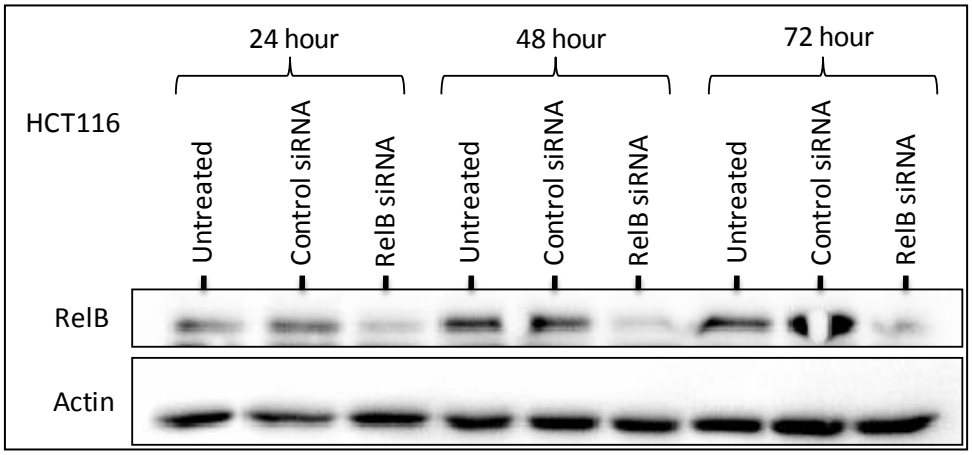

Figure 3.23: Western blot to assess RelB protein expression 24, 48 and 72 hours following RelB siRNA transfection of HCT116 cells. Knockdown of RelB was observed at all the time points tested.

3.7.6 Effect of RelB suppression upon cell proliferation and apoptosis with and without Etoposide treatment

24 hours following seeding of HCT116 cells, they were transfected with RelB siRNA or control siRNA. 24 hours after this siRNA transfection, Etoposide was added and Etoposide treated and untreated cells were incubated for a further 24 hours. Floating cells (as a measure of apoptosis) and attached cells (as a measure of cell proliferation) were then counted as outlined in Figure 3.24 a. To avoid the effect of any possible differences between the number of attached cells in the control and in the RelB siRNA treated cells as shown above in NFκB2 siRNA transfection, apoptosis was calculated as a percentage of apoptotic cells to total cells [number of floating cells/number of (floating cells + attached cells) x100%]. The percentage of apoptotic cells in RelB siRNA treated cells was then compared to the percentage of apoptotic cells in control siRNA treated cells. The percentage of attached cells following RelB siRNA treatment was also compared to the percentage of attached cells following control siRNA treatment.

In Etoposide-untreated HCT116 cells, knocking down RelB protein expression using siRNA did not cause any alterations in the percentage of attached cells or apoptotic cells compared to control siRNA. In Etoposide treated HCT116 cells, RelB suppression by siRNA also did not result in change in the percentage of attached cells or apoptotic cells compared to control siRNA (Figure 3.24).

Although the RelB suppression did not affect HCT116 proliferation and apoptosis, the molecular consequences of RelB suppression on these cellular processes were further evaluated by assessing the expression of key proteins that are known to

regulate proliferation and apoptosis following RelB siRNA treatment. These proteins were p53 and its target genes cyclin D1 and p21 that are involved in regulating cell proliferation and differentiation along with the pro-apoptotic protein BAX and the anti-apoptotic protein BCL2. Etoposide treatment resulted in an increase in the expression of p53 and its target gene p21 in both control siRNA and RelB siRNA transfected cells compared to Etoposide-untreated cells. No changes in the expression of p53, p21, cyclin D1, Bax or BCL2 were observed in RelB siRNA transfected cells compared to control siRNA transfected cells either before or after Etoposide treatment (Figure 3.25).

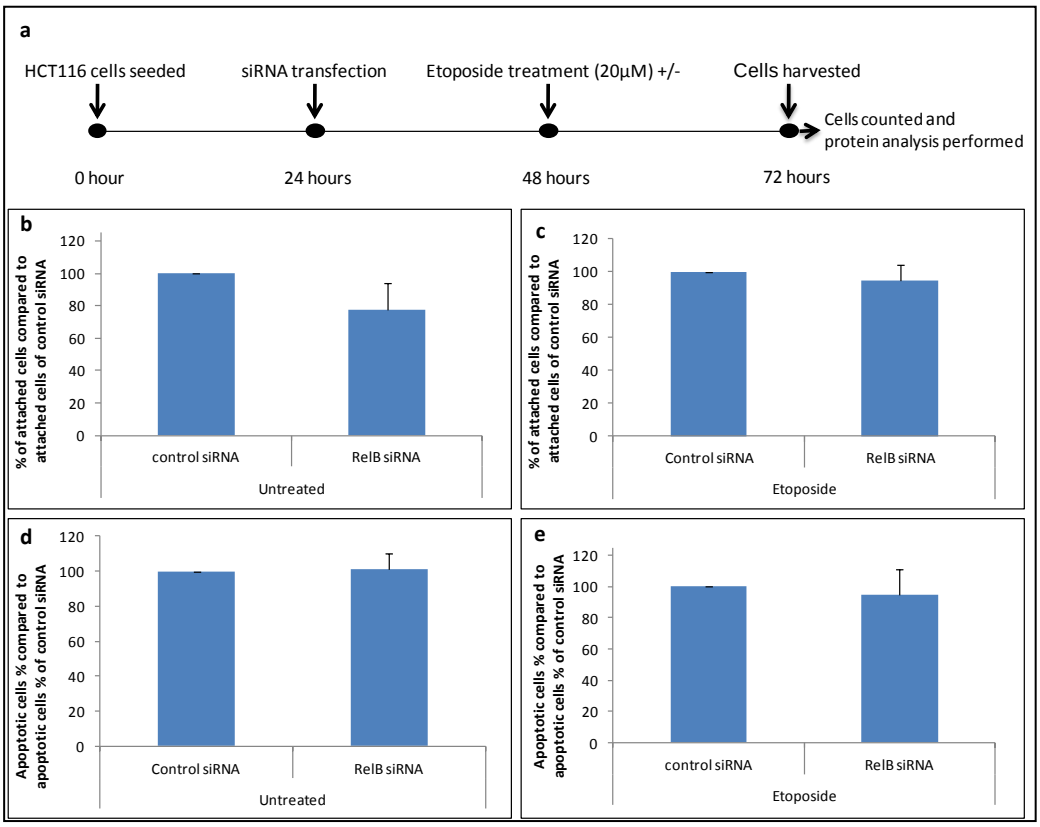

Figure 3.24: Effects of RelB suppression using siRNA technique on HCT116 cell proliferation and apoptosis in either untreated or Etoposide treated cells. (a) Schematic diagram showing siRNA transfection and Etoposide treatment protocol in HCT116 cells. % of attached cells compared to control siRNA transfected cells (± standard deviation) in untreated (b) and Etoposide treated (c) cells respectively. % of apoptotic cells compared to control siRNA transfected cells (± standard deviation) in untreated (d) and Etoposide treated (e) cells respectively (± standard deviation). Statistical analysis was performed by student's *t*-test. The data are from 3 independent experiment (n=3).

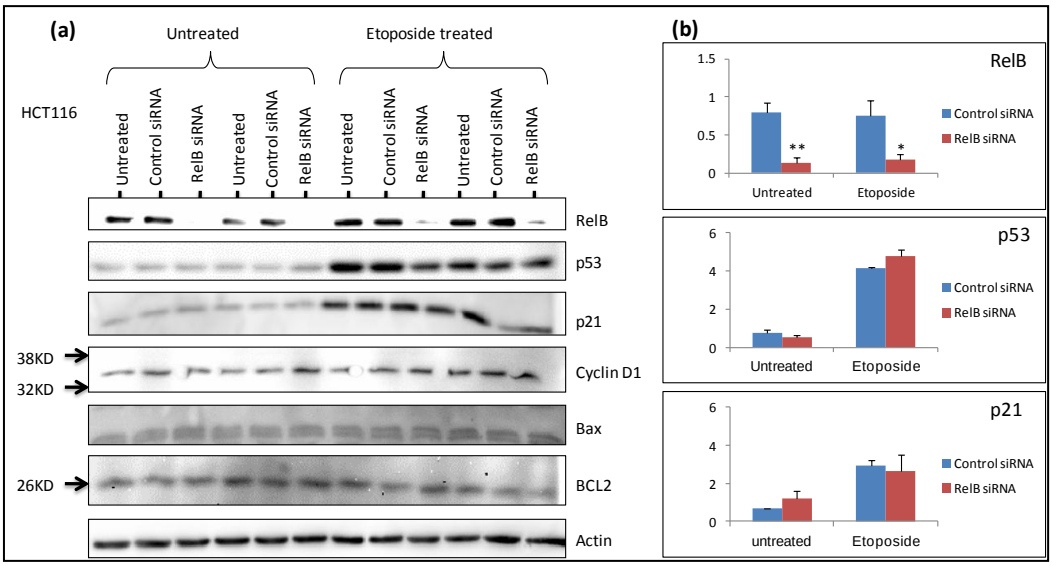

Figure 3.25: Protein expression of RelB and other key genes that regulate proliferation and apoptosis in HCT116 cells following RelB siRNA and Etoposide treatment. Western blotting of protein samples obtained from HCT116 cells following siRNA transfection and then Etoposide treatment using anti-RelB, p53, cyclin D1, p21, Bax and BCL-2 antibodies. Anti-actin antibody was also used as a loading control. (b) Relative expression of RelB, p53 and p21 compared to their expression in control siRNA and Etoposide-untreated cells (± standard deviation). RelB siRNA treatment resulted in reduced expression of RelB by approximately 80% compared to control siRNA. Etoposide treatment caused a significant increase in the expression of RelB and also resulted in an increase in expression of p53 and p21 (* $p<0.05$, ** $p<0.01$ by student's t-test). RelB protein densitometry is the average of 3 independent experiments. p53 and p21 protein densitometry is the average of readings from duplicate samples in one experiment.

3.8 Discussion

NFκB has been shown to regulate cell proliferation and apoptosis in a number of cell types and has been found to both promote and inhibit apoptosis in different contexts. The role of NFκB in regulating apoptosis appears to be dependent on both the cell type and the nature of the death-triggering stimulus (241, 242, 296, 297).

In the current study, disruption of the classical pathway of NFκB activation by deletions of c-Rel or NFκB1 altered murine small intestinal and colonic crypt lengths as measured by cell number per hemi-crypt. Longer small intestinal and colonic crypts were found in NFκB1-null mice and longer colonic crypts were seen in c-Rel-null mice compared to wild-type counterparts. This is consistent with a previous study by Inan *et al* who demonstrated that NFκB1-null mice had longer colonic crypts and a more extensive proliferative zone (as determined by proliferating cell nuclear antigen staining and *in vivo* bromodeoxyuridine labeling) than their wild-type counterparts (230). In our present study the elongations of intestinal crypts observed in c-Rel-null and NFκB1-null mice were not associated with changes in crypt epithelial proliferation as determined by mitotic indices. However the number of mitotic figures with defining morphological criteria is far fewer than the number of proliferating cells determined by proliferating cell nuclear antigen (PCNA) staining or *in vivo* bromodeoxyuridine (BrdU) labelling. This might partially explain our inability to detect any changes in proliferation by mitotic indices in the intestinal epithelia of either c-Rel-null or NFκB1-null mice. In contrast to previous studies using cell culture which have revealed that NFκB promotes cell proliferation and inhibits apoptosis (298, 299), these observations in untreated mice suggest that the

classical NFκB activation pathway plays a complex role in whole intestinal tissue, where all cell types are present. Taken as a whole, these finding suggest that the classical NFκB activation pathway via both c-Rel and NFκB1 plays a role in maintaining intestinal homeostasis. Real time PCR data from untreated animals showed alterations in the expression of some apoptosis regulating genes. NFκB1-null mice showed reduced relative mRNA expression of the anti-apoptotic genes BCL2, BCL-XL, c-IAP2 and XIAP in the small intestine and c-IAP2 and XIAP in the colon compared to wild-type mice. However, the increase in small intestinal spontaneous epithelial apoptosis seen in NFκB1-null mice was not statistically significant and no alteration in basal epithelial apoptosis was found in NFκB1-null colon.

The influence of the alternative NFκB activation pathway in regulating intestinal epithelial turnover has not previously been studied in detail. Disruption of this pathway by deleting NFκB2 resulted in elongation of small intestinal crypts and an increase in epithelial apoptosis in the small intestine, but not in the colon compared with wild-type mice. In keeping with this, NFκB2-null mice showed reduced relative mRNA expression of the anti-apoptotic genes BCL2, BCL-XL, c-IAP2 and XIAP in the small intestine and down regulation of c-IAP2 and XIAP in the distal colon compared to untreated wild-type mice. No alterations in mitotic indices were observed in either the small intestine or colon of NFκB2-null mice relative to wild-type mice. Ishikawa *et al* have previously shown that a mouse model with deleted ankyrin repeats at the C-terminus of p100 (the precursor form of NFκB2) leading to

constitutive activation of p52 (the active form of NFκB2) showed marked gastric hyperplasia (300).

Activation of NFκB is considered to be one of the important physiological responses of cells to external stresses such γ-irradiation. DNA damage induced by 8Gy γ-irradiation has been shown to cause a 219-fold increase in small intestinal epithelial NFκB activity in wild-type mice and this activation mainly consisted of p50/RelA heterodimers (229) . However, ablation of the p50 (NFκB1) gene in mice resulted only in a 43-fold increase in small intestinal epithelial NFκB activity, consisting mainly of p52/RelA heterodimers, following the same treatment. NFκB1-null small intestinal epithelia have also been reported to show a significant increase in apoptosis 24 hours following 8Gy γ-irradiation (229). These findings suggest that although activation of the classical pathway of NFκB signalling appears to predominately occur in the small intestine following DNA damage, the alternative pathway is also implicated in regulating the small intestinal response to injury. In a previous study, abrogation of the classical NFκB activation pathway by selective intestinal deletion of IKKβ resulted in an increase in small intestinal epithelial apoptosis following γ-irradiation compared to similarly treated wild-type mice (251). With the exception of NFκB1 in the small intestine, the specific roles of other individual NFκB family members, particularly those involved in the alternative activation pathway in regulating DNA damage induced apoptosis in small intestinal and colonic epithelia have not previously been assessed. Additionally, the molecular changes associated with either perturbed classical or alternative NFκB activation pathways have not previously been investigated. In this current study, consistent

with previous studies, NFκB1-null mice demonstrated a significant increase in small intestinal crypt epithelial apoptosis 4.5 hours following 8Gy γ-irradiation relative to similarly treated wild-type mice. Although NFκB has not previously been shown to be activated in colonic epithelia following γ-irradiation (229), NFκB1-null mice also showed a significant increase colonic epithelial apoptosis following 8Gy γ-irradiation relative to wild-type animals. However, disruption of the same NFκB activation pathway (classical) by deleting c-Rel did not cause any alteration in the amount of epithelial apoptosis observed in either the small intestine or colon following γ-irradiation compared to wild-type mice. This suggests that the role of the classical NFκB signalling pathway in limiting intestinal epithelial apoptosis after DNA damage is mediated through NFκB1-dependent but c-Rel-independent mechanisms. We provide the first evidence that alternative NFκB pathway signalling plays a role in the regulation of radiation induced intestinal epithelial apoptosis, as we observed increased irradiation induced epithelial apoptosis in both the small intestine and colon of NFκB2-null mice.

For further evaluation of the specific roles of c-Rel, NFκB1 and NFκB2 in regulating DNA damage induced intestinal apoptosis, a chemical method of apoptosis induction was also investigated. Our findings showed that the small intestine was more susceptible to damage, apoptosis induction and mitosis suppression than the distal colon following administration of the chemotherapeutic agent irinotecan to wild-type mice. These differences in extent of tissue damage between the small intestine and the colon have previously been attributed to the finding that the *in vivo* intestinal concentration of irinotecan is highest in the ileum and lowest in the

colon (77). In comparison with untreated mice, c-Rel-null and NFκB1-null mice continued to show elongated colonic crypts 48 hours following irinotecan administration. In keeping with observations in previous irradiation studies, NFκB1-null mice were more susceptible to irinotecan induced intestinal epithelial apoptosis in both the small intestine and colon and at both the 6 and 48 hour time points. Similar to the phenotype observed following irradiation, c-Rel-null mice did not show any altered apoptosis in the small intestine or in colon at both the 6 and 48 hour time points following irinotecan administration compared to similarly treated wild-type mice. NFκB2-null mice, which were more susceptible to irradiation induced intestinal apoptosis, were also more susceptible to irinotecan induced apoptosis in both the small intestine and colon and at both the 6 and 48 hour time points compared to similarly treated wild-type animals. These observations at 6 and 48 hours post irinotecan treatment at two sites within the intestine therefore reinforce our previous findings at 4.5 hours following 8Gy γ-irradiation. This suggests that classical NFκB pathway signalling via NFκB1, but not through c-Rel regulates the susceptibility of intestinal epithelia to apoptosis following two different types of DNA damage inducing stimuli. Additionally we provide evidence for major participation of the alternative NFκB activation pathway in regulating intestinal epithelial apoptosis following administration of two different types of injury.

For the first time, the molecular mechanisms responsible for these altered responses have been investigated using quantitative PCR assays. In agreement with the observed increase in irradiation induced apoptosis observed in the intestinal

epithelia of NFκB1-null mice relative to their wild-type counterparts, NFκB1-null mice showed significant increases in the expression of the pro-apoptotic genes TRAIL and Caspase12 in the small intestine and TRAIL in the colon following irradiation compared to wild-type mice after the same treatment. Following irradiation, c-Rel-null mice did not show major alterations in the expression of the apoptosis regulating genes that were assessed either in the small intestine or colon relative to wild-type mice, with only a modest increase in the expression of anti-apoptotic BCL-XL being observed in the small intestine.

The increased susceptibility to irradiation-induced intestinal epithelial apoptosis observed in NFκB2-null mice was associated with significant increases in the expression of the pro-apoptotic genes Caspase12, BAK, p53 and FAS-L in the small intestine and Caspase12, TRAIL, and FAS-L in the colon. Noticeably, the increase in the transcriptional expression of FAS-L was substantial in both the small intestine (19-fold) and colon (21-fold) of NFκB2-null mice following irradiation relative to similarly treated wild-type mice. Thus, FAS-L may play a major role in the increased susceptibility to irradiation-induced intestinal epithelial apoptosis observed in NFκB2-null mice. It has previously been shown that TRAIL can induce apoptosis in normal colonic epithelial cells and that irinotecan can increase the susceptibility of these cells to TRAIL-induced apoptosis (301). TRAIL has not previously been shown to be a downstream target gene of NFκB in intestinal epithelia. In a previous study however it has been demonstrated that NEMO/IKKγ-dependent NFκB activation was required for the up-regulation of TRAIL in T cells (302). However, our data suggest that NFκB1-dependent classical activation pathway signalling in intestinal

epithelia leads to down-regulation of TRAIL. Although Caspase12 belongs to the inflammatory group of Caspases including Caspases 1, 4, 5 and 11 (303), it has been demonstrated that Caspase12 is processed in many pro-apoptotic conditions and thus it has been proposed that Caspase12 influences the apoptotic process (304). Caspase12 has not previously been shown to be a target gene of NFκB in the published literature. In this study, we provide strong evidence for a transcriptional regulation of Caspase12 expression by NFκB, as we demonstrate up-regulation of Caspase12 at two sites within the intestine (the small intestine and colon) and in both NFκB1-null and NFκB2-null strains of mice.

It is important to bear in mind certain limitations that can influence the interpretation of our quantitative PCR results. For example, post transcriptional effects such as post-transcriptional decay of mRNAs may not lead to altered protein translation. Additionally, protein function can be affected by post translational modifications that do not directly depend on transcriptional regulation. However as the pathway under investigation relies on a transcription factor system, quantifying transcriptional levels can potentially determine the apparent functions of this pathway. For more robust analysis, our findings of the altered transcriptional expression of apoptosis regulating genes in these transgenic mice require further confirmation at the protein level either by immunohistochemical staining or Western blotting.

Mitosis (as proliferation index) was suppressed in both the small intestine and colon of all groups of mice following irradiation, hence no significant alterations were observed between any strains of mice following this stimulus. Although c-Rel-null

and NFκB1-null mice continued to show elongated colonic crypts 48 hours following irinotecan treatment, no significant alterations in mitosis suppression were observed in either of these strains of mice at this time point. Similar to a study performed by Inan *et al* (230), we demonstrated that abrogation of the classical NFκB activation pathway either by deleting c-Rel or NFκB1 resulted in significant increases in distal colonic crypts lengths. However, this elongation of colonic crypts in c-Rel-null and NFκB1-null mice was not associated with any observed increase in cell proliferation (as determined by mitotic indices). In the cell cycle, the duration of the mitosis phase is relatively shorter than the S phase which marked by PCNA staining or *in vivo* BrdU labelling. Thus, the absolute numbers of mitotic figures are much less than the numbers of proliferating cells determined by PCNA staining or *in vivo* BrdU labelling. This may have been responsible for our inability to detect any significant alteration in proliferation. Moreover, as colonic crypt length is determined by the balance between the rates of cell input (proliferation) and output (apoptosis and cell shedding), other mechanisms may be responsible for the elongated colonic crypts that we observed in mice with an abrogated classical NFκB activation pathway. Future work is needed to assess intestinal epithelial proliferation in these animals using techniques such as immunohistochemical staining for PCNA or Ki67. Additionally, investigating intestinal epithelial shedding rates would be helpful to better characterise the role of NFκB in regulating intestinal epithelial homeostasis.

In vitro studies involving NFκB2 siRNA transfection for a short period of time (up to 3 days) resulted in reduction of the protein expression of the precursor form of

NFκB2 (p100), but not the processed form (p52) by approximately 45% at all-time points tested. The unchanged expression of p52 might be due to the stability and longer half-life of this protein. Therefore a longer time course was performed. Despite a greater reduction in the expression of the precursor form of NFκB2 (p100) (more than 80%) at 5 and 6 day time points, the expression of the processed form of NFκB2 (p52) was still not altered at all these longer time points. Although a similar pattern of increased protein abundance of p52 and p100 was observed following Etoposide (a chemotherapeutic agent) treatment, non-specific binding of the antibody to another similar sized protein to p52 cannot be excluded. However, suppression of NFκB2 expression (at least of its precursor form p100) in HCT116 cells resulted in a significant reduction in cell proliferation in the un-stimulated condition and following administration of a DNA damage inducing stimulus (Etoposide). It has previously been shown that knockdown of NFκB2 expression in U-2 OS human osteosarcoma cells resulted in a significant decrease in cell proliferation and this was associated with downregulation of Cyclin D1. However, examination of cell cycle distribution of these NFκB2 siRNA treated cells, suggested that decreased Cyclin D1 expression could not account for all the effects on proliferation observed following NFκB2 (p52/p100) suppression. Therefore, a Cyclin D1-independent role of NFκB2 in regulating cell proliferation has been suggested (218). This might explain at least in part our findings that p100 suppression resulted in a decrease in HCT116 cell proliferation, without causing any change in Cyclin D1 protein abundance. Our findings also indicate that NFκB2 inhibits the apoptosis of HCT116 cells following treatment with apoptosis inducing stimuli. This is consistent with previous findings which showed that lymphoma cell lines with constitutive

activation of NFκB were resistant to apoptosis induction and that suppression of p100 using siRNA resulted in a 2- to 3-fold increase in apoptosis following Etoposide treatment (294). The increased susceptibility to Etoposide-induced apoptosis following NFκB2 suppression in HCT116 cells was not associated with any changes in the protein expression of any of the assessed apoptosis regulating genes. However, this *in vitro* study was performed before the investigations of transcriptional expressions of 10 apoptosis regulating genes in the intestinal epithelia of NFκB2-null mice. It would therefore now be helpful to assess the protein expressions of those apoptosis regulating genes (such as TRAIL, Caspase12, FAS-L which showed altered expression in NFκB2-null mice *in vivo*) in HCT116 cells following NFκB2 siRNA treatment. However, time was not available to conduct these additional studies during my PhD.

On the other hand, suppression of RelB protein expression by approximately 70% did not result in any alteration in HCT116 cell proliferation or apoptosis either with or without Etoposide treatment. Suppression of RelB protein expression was also not associated with any changes in the abundance of any of the assessed proliferation and apoptosis regulating proteins. In contrast to our findings in transformed intestinal epithelial cells, RelB has previously been shown to promote proliferation and inhibit apoptosis in transformed lymphocytes and breast cancer cells (305, 306). Our *in vitro* findings therefore suggest that NFκB2 but not RelB promotes colon cancer cell proliferation and similar to our *in vivo* observations in normal intestinal epithelial cells, NFκB2 inhibits apoptosis following DNA damage inducing stimuli.

Further work is required to further characterise the roles of both the classical and alternative NFκB activation pathways in regulating intestinal epithelial turnover. For example, studying DNA binding activity of specific NFκB proteins using electrophoretic mobility shift assays (EMSA) would provide a clearer picture of gene regulation by these proteins. It would also be interesting to assess transgenic mice with germline deletions of RelB, particularly their intestinal epithelial apoptotic responses in order to dissect the importance of individual components of the alternative NFκB activation pathway in regulating intestinal epithelial turnover. As NFκB can modulate both immune and intestinal epithelial cells responses, selective tissue deletions of various NFκB family members in either murine intestinal epithelial or immune cells could also help to determine the precise mechanisms involved in regulating intestinal epithelial turnover. This could be accomplished through either bone marrow chimaeras or transgenic technology.

In summary, consistent with previous studies, we have shown that the classical NFκB activation pathway is implicated in regulating intestinal homeostasis and protects intestinal epithelia from apoptosis induced by two different types of DNA damage inducing stimuli. Our data suggest that this is mainly mediated by NFκB1-dependent mechanisms. We also provide the first evidence that alternative NFκB pathway signalling via NFκB2 plays a major role in regulating intestinal epithelial apoptosis *in vivo* and *in vitro*. The increased susceptibility to intestinal apoptosis resulting from deletion of NFκB1 or NFκB2 may occur as a result of altered expression of a number of known NFκB dependent apoptosis regulating genes as well as the novel genes TRAIL and caspase12. NFκB1 and NFκB2 may therefore also

play important roles in regulating the susceptibility of intestinal epithelia to the consequences of DNA damage such as cancer.

4 The impact of deletion of various NFκB family of members on intestinal inflammatory responses

4.1 Introduction

NFκB is known to play crucial roles in regulating gastrointestinal inflammation. In particular, NFκB signalling has been implicated in the pathogenesis of inflammatory bowel disease (IBD). This has been mainly attributed to the pro-inflammatory function of NFκB through its transcriptional regulation of several genes which encode proteins that are involved in inflammation, including pro-inflammatory cytokines, cell surface receptors and adhesion molecules (264). However, several recent murine studies have also demonstrated an anti-inflammatory role for classical NFκB activation pathway in the intestine. This anti-inflammatory role has been attributed to the ability of NFκB to protect intestinal epithelial cells from apoptosis and necrosis, thus protecting tissue from damage and helping to maintain the intestinal barrier following injury. Therefore, NFκB can act indirectly in an anti-inflammatory fashion (268). Similarly in previous studies, researchers have shown that specific intestinal deletion of IKKγ or both IKKα and IKKβ subunits, spontaneously resulted in the development of severe chronic intestinal inflammation in mice and impaired the expression of antimicrobial peptides and the translocation of bacteria into the mucosa (252). However, selective intestinal deletion of IKKβ or IKKα alone did not spontaneously induce colitis (249-251). This might be due to a compensatory mechanism exerted by either IKKα or IKKβ in the absence of the other subunit. The role of the alternative NFκB activation pathway or the specific roles of individual NFκB family members in modulating intestinal

inflammation have not previously investigated. In fact, there is only one previous study and this investigated the intestinal responses to a helminth parasite (*Trichuris muris)*. In this study, unlike c-Rel deficient mice, NFκB1 and NFκB2 deficient mice were both unable to clear infection with this parasite, but only chronically infected NFκB1-null mice developed destructive colitis-like pathology (272).

These recent studies have raised a concern about the potential of using NFκB inhibitors to treat IBD. A role of the alternative (via NFκB2) and the classical NFκB pathways (mainly mediated by NFκB1) in protecting intestinal epithelial cells from apoptosis following two types of stimuli was demonstrated in chapter 3. This suggests that the alternative activation pathway might also be implicated in modulating intestinal inflammatory responses. Therefore, the impact of deleting specific NFκB family members on intestinal inflammatory responses was investigated in this chapter. This was achieved utilising an established murine model of DSS-induced colitis.

4.2 Aims

To investigate the susceptibility of mice deficient in various NFκB family members to DSS-induced colitis and the molecular mechanisms responsible for any altered susceptibility.

4.3 Effects of deleting various NFκB family members on clinical parameters of DSS-induced colitis

The clinical signs that developing following exposure to DSS for 5 days have been documented in several previous studies. These clinical signs are loss of body weight, loose faeces/watery diarrhoea and faecal blood/rectal bleeding (111).

4.3.1 c-Rel-null and NFκB1-null mice showed significantly more body weight loss whereas NFκB2-null mice showed significantly less body weight loss following dextran sulphate sodium treatment

C57BL/6, c-Rel-null, NFκB1-null and NFκB2-null mice (10 mice per strain) were administrated 2% DSS in their drinking water for 5 days to induce colitis. This was followed by one day of DSS-free water before they were sacrificed on day 6 after the start of the experiment. The body weight of these mice was recorded daily to monitor the percentage of body weight change as shown in Figure 4.1. Strikingly, NFκB2-null mice only lost 2.2% and 3.5% of their starting body weight on days 5 and 6 respectively. This was significantly less than C57BL/6 mice which lost 8% and 14.6% of their starting body weight on days 5 and 6 respectively from the start of the experiment. However, c-Rel-null and NFκB1-null mice both showed a significant 2-fold increase in the percentage of body weight loss compared to wild-type mice on days 5 and 6. c-Rel-null mice showed 14% and 23% weight loss while NFκB1-null mice showed 14.7% and 23% weight loss on days 5 and 6 respectively (Figure 4.1).

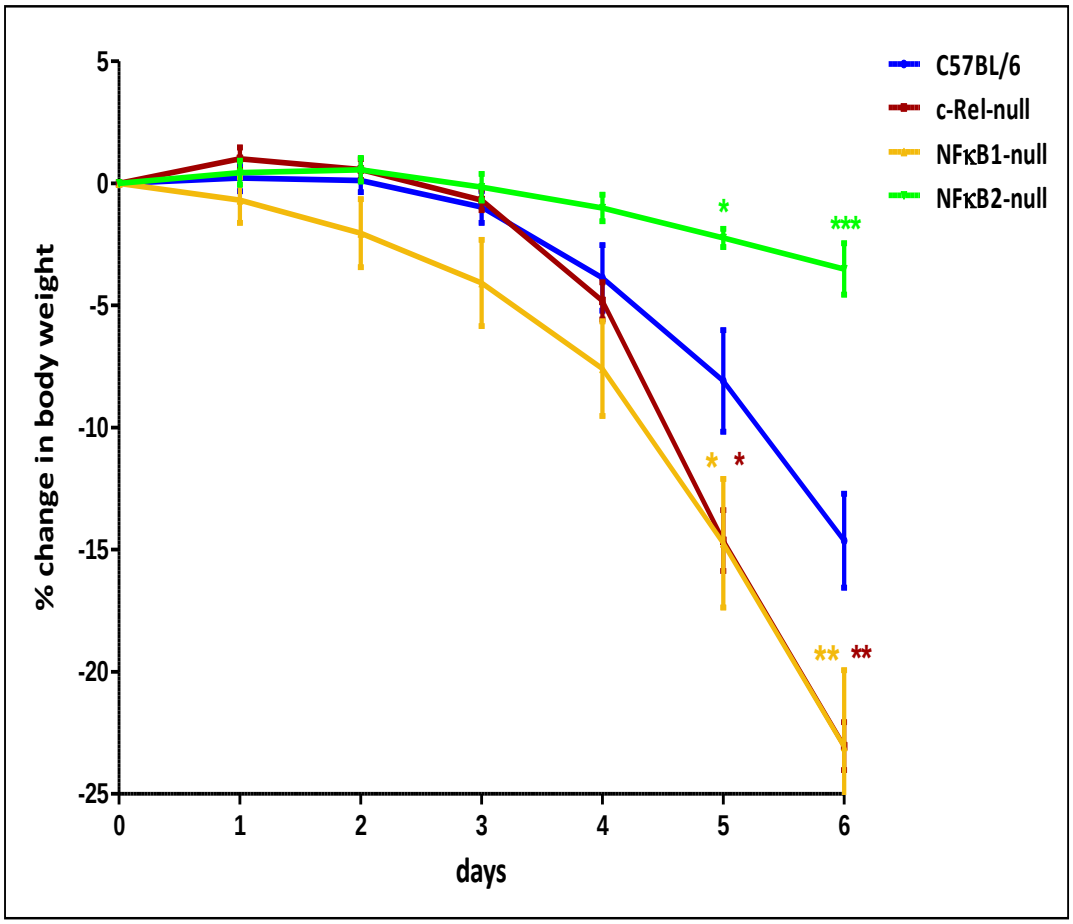

Figure 4.1: Percentage weight change observed in mice during the course of dextran sulphate sodium induced colitis. 2% DSS was orally administered for 5 days and mice were sacrificed on day 6. Percentage body weight change was recorded daily for C57BL/6 (blue), c-Rel-null (red), NFκB1-null (yellow) and NFκB2-null mice (green). Data are presented as mean ± standard error of the mean. Statistical differences were assessed by one way ANOVA and Dunnett's multiple comparison test (*p<0.05, **p<0.01, ***p<0.001 compared to C57BL/6). (n=10 male mice per genotype).

4.3.2 c-Rel-null and NFκB1-null mice showed significantly higher disease activity indices whereas NFκB2-null mice showed a significantly lower disease activity index following dextran sulphate sodium treatment

To evaluate the general condition of mice, a disease activity index (DAI) ranging from 0 to 4 was calculated on daily basis. This was based on the following clinical parameters: weight loss, stool consistency and presence of rectal bleeding. Exposure of mice to DSS in their drinking water profoundly affected the general health of most strains of mice with the exception of the NFκB2-null strain and resulted in the development of weight loss and the production of loose, bloody stools. The disease activity index markedly increased from day 4 to day 6 at which point the mice were sacrificed. NFκB1-null mice showed an earlier onset of increased severity of the disease, which was significant at day 2 (Figure 4.2). The DAI was higher in c-Rel-null and NFκB1-null mice than C57BL/6 mice and this was significant at day 4 in c-Rel-null mice, and on days 2 and 3 in NFκB1-null mice. Consistent with the weight loss changes, NFκB2-null mice showed a lower DAI and this was significant on days 5 and 6 compared to wild-type mice (Figure 4.2).

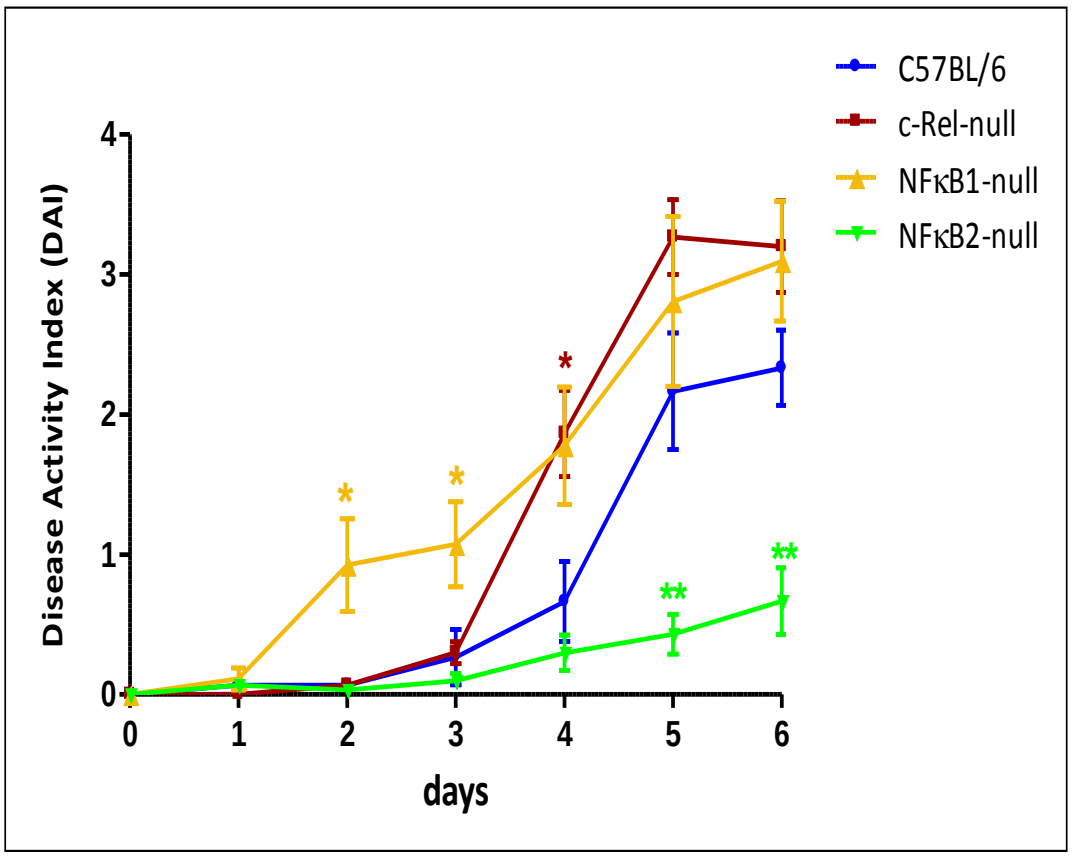

Figure 4.2: Changes in disease activity index (DAI) (clinical score) during the course of dextran sulphate sodium induced colitis. 2% DSS was orally administered for 5 days and mice were sacrificed on day 6. DAI was daily determined for C57BL/6 (blue), c-Rel-null (red), NFκB1-null (yellow) and NFκB2-null mice (green). Data are presented as mean ± standard error of the mean. Statistical differences were assessed by Kruskal–Wallis test followed by Dunn's multiple comparison tests (*$p<0.05$, **$p<0.01$ compared to C57BL/6). (n=10 male mice per genotype).

4.4 Effects of deleting various NFκB family members on severity of histopathological changes in DSS-induced colitis

Several previous studies have reported that the colon shortens during colitis induction and this has been proven to be a useful indicator of colitis severity (110, 307, 308). Histological changes and inflammatory responses are typical microscopic features of colitis. Therefore, H and E stained colonic sections were examined under the light microscope to assess histological and inflammatory changes.

4.4.1 c-Rel-null and NFκB1-null mice showed a significantly shorter colon whereas NFκB2-null mice showed a significantly longer colon following dextran sulphate sodium administration

Mice were given 2% DSS in their drinking water for 5 days and were sacrificed on day 6. The colon was dissected and the entire colon length was measured to assess the colon shortening due to inflammation, scarring and damage. Colons from c-Rel-null and NFκB1-null mice were significantly shorter and colons from NFκB2-null mice were significantly longer than those from C57BL/6 mice (Figure 4.3).

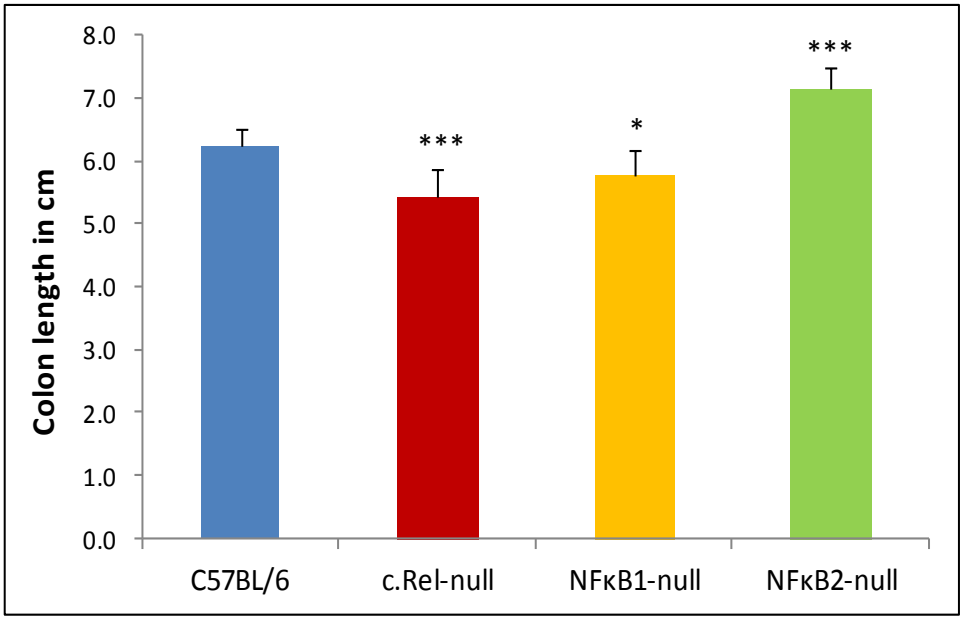

Figure 4.3: Colon lengths in mice subjected to DSS-induced colitis. 2% DSS was orally administered for 5 days and mice were sacrificed on day 6. Length of colon from C57BL/6 (blue), c-Rel-null (red), NFκB1-null (yellow) and NFκB2-null mice (green) was measured. Data are presented as mean ± standard deviation. Statistical differences were assessed by one way ANOVA and Dunnett's multiple comparison test (*p<0.05, ***p<0.001 compared to C57BL/6). (n=10 male mice per genotype).

4.4.2 NFκB2-null mice displayed less colonic inflammation following dextran sulphate sodium administration

Following dissection, colons were divided into 3 segments, fixed, sectioned and stained with H and E for histological analysis. Distal colon from all untreated strains of mice had similar histological findings showing normal crypts without any noticeable inflammation (Figure 4.4 a, c, e and g). Histological assessment of DSS treated animals revealed severely damaged and inflamed distal colons from C57BL/6, c-Rel-null and NFκB1-null mice. The epithelial layer was completely destroyed and submucosal oedema was prominent. Neutrophils were the main type

of inflammatory cell infiltrate which was intense and present throughout the colon wall (Figure 4.4 b, d and f). A marked reduction in the severity of these histological changes was observed in the distal colon of NFκB2-null mice compared to all other strains of mice. Crypts maintained a normal morphological appearance with only mild histological damage observed. This was associated with only a mild inflammatory cell infiltrate that was predominantly confined to the mucosa and no oedema was observed in the submucosal layer (Figure 4.4 h).

In order to translate the previous histological findings to a quantifiable measure of inflammation, a histological score was performed. This histological score, which has been described and validated previously, is based on the severity of inflammation and tissue damage (287). The severity of inflammation which was observed in the distal colon from DSS treated C57BL/6, c-Rel-null and NFκB1-null mice was matched by a higher histological score in these strains of mice. In agreement with previous observations, NFκB2-null mice displayed a significant lower score compared to their wild-type counterparts (Figure 4.5).

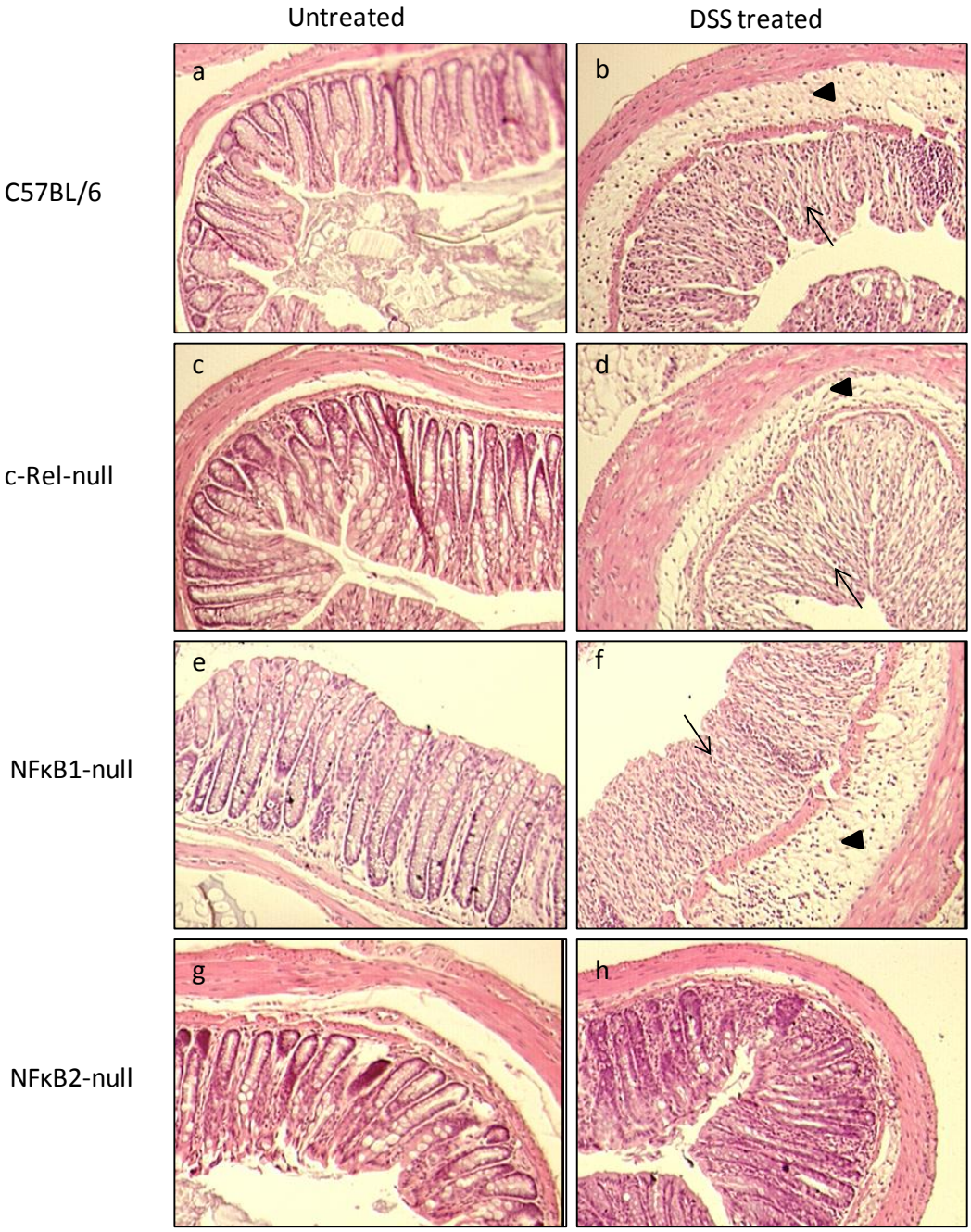

Figure 4.4: Microscopic examination of H/E stained distal colonic sections from untreated and 2% DSS treated mice. Histology (H/E) of distal colonic sections which were taken from C57BL/6 (a, b), c-Rel-null (c, d), NFκB1-null (e, f) and NFκB2-null (g, h) mice receiving either water (control) (a, c, e, g) or 2% DSS for 5 days and sacrificed on day 6 (b, d f, h). (Arrows indicate damaged crypts with inflammatory cell infiltrate, triangles indicate the submucosal layer with oedema and inflammatory cell infiltrate).

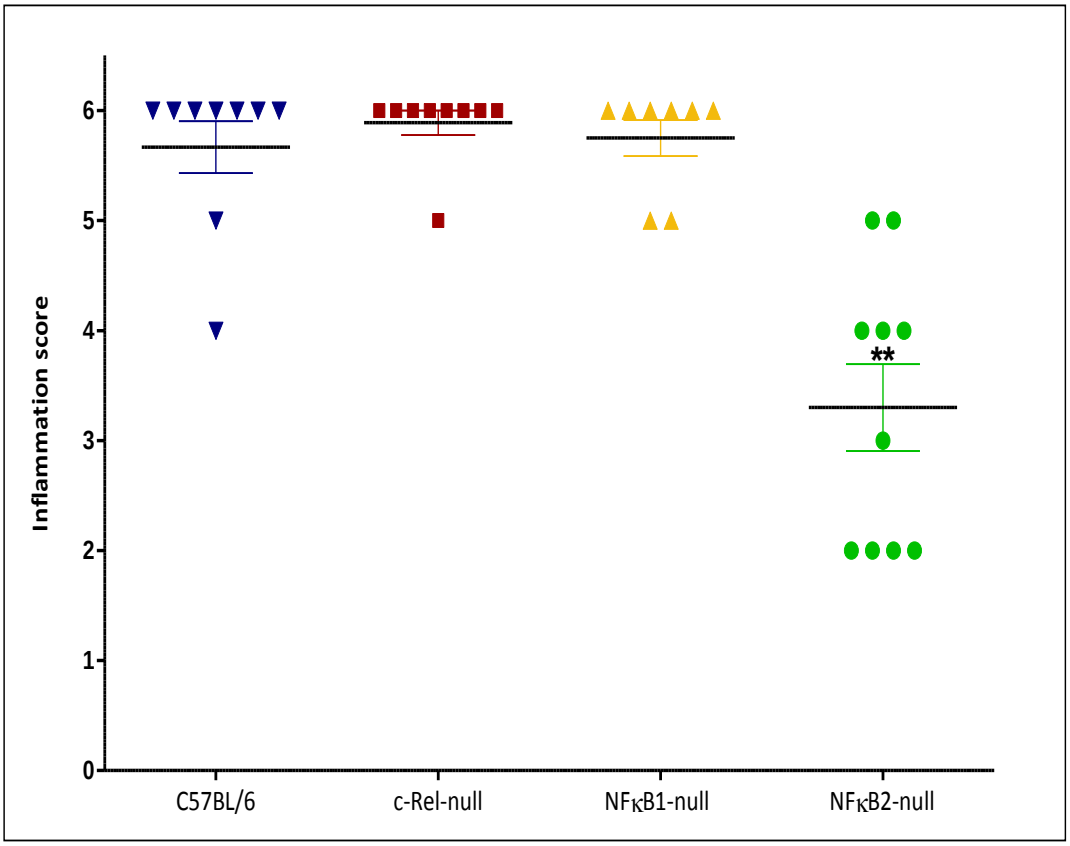

Figure 4.5: Histological (inflammation) scores of DSS-induced colitis in mice. Inflammation score of distal colon taken from C57BL/6 (blue), c-Rel-null (red), NFκB1-null (yellow) and NFκB2-null mice (green) which received 2% DSS for 5 days and were sacrificed on day 6. (Each dot represents a score from one mouse and data are presented as mean ± standard error of the mean, **p<0.01 by Kruskal–Wallis test followed by multiple comparison Dunn's test).

4.5 Intestinal expression of cytokine-encoding genes in DSS-induced colitis in mice deficient in various NFκB family members

To investigate the mechanisms responsible for the differences in the susceptibility to DSS-induced colitis observed in mice lacking specific NFκB proteins, real-time PCR for several key cytokines was performed. Colitis was induced in adult male mice by oral 2% DSS administration for 5 days and mice were euthanased on day 6 (n=4 per group). Untreated mice of the same age were also sacrificed at the same time as control animals. The small intestine and colon were removed and processed for RNA extraction and subsequent cDNA quantification by real-time PCR as described in sections 2.7 and 2.8.

The small intestine is not the target organ of DSS treatment and therefore these cytokines were assesses in the small intestine of only the untreated groups of mice. This allowed us to evaluate the effect of deleting specific NFκB family members on the small intestinal mRNA expression of these cytokines namely TNF-α, IL-β, IFN-γ, IL-4, IL-6 and IL-14. All the transgenic strains assessed did not show any significant alteration in the small intestinal mRNA expression of the assessed cytokines compared to wild-type mice with the exception of significant increases in IL-14 and IFN-γ in the small intestinal samples from NFκB1-null and NFκB2-null mice respectively relative to wild-type mice (Figure 4.6).

Generally, the abundance of the assessed cytokines was low in the colons of untreated mice. In C57BL/6 mice, all the assessed cytokines showed massive dynamic changes in the distal colon in response to DSS treatment. DSS treatment caused huge increases in the abundance of most of the assessed cytokines which

reached approximately a 600-fold increase in some cases compared to untreated wild-type distal colon (Figure 4.7).

The colon of untreated NFκB1-null mice demonstrated small increases in the mRNA levels of TNF-α and IL-14 but these did not reach statistical significance when compared to untreated wild-type mice. Consistent with the clinical and histological findings described above, the relative mRNA expressions of IL-1β and IL-6 were significantly increased in colonic samples from NFκB1-null mice following DSS administration relative to wild-type mice following the same treatment (Figure 4.7).

The relative mRNA expressions of the assessed cytokines in untreated c-Rel-null mouse colon were similar to those in untreated wild-type colon. Following DSS administration however, c-Rel-null mice also showed a similar pattern of dynamic changes in the assessed cytokines compared to wild-type mice. Despite the increased clinical severity of colitis observed in c-Rel-null mice following 2% DSS treatment, the transcriptional expression of colonic TNF-α was significantly less in DSS-treated c-Rel-null mice than in DSS treated wild-type mice.

The transcriptional expression of the pro-inflammatory cytokine IFN-γ was reduced in all transgenic mice relative to C57BL/6 mice (Figure 4.7). Hence, it is unlikely that IFN-γ contributes to the differences in colitis susceptibility which were seen between the different transgenic mice.

No significant alterations were observed in the mRNA expression of the assessed cytokines in the colons of untreated NFκB2-null mice compared to wild-type mice. In agreement with the clinical and histological observations described above, we observed a significant suppression of the relative mRNA expression of the pro-

inflammatory cytokine TNF-α and a significant increase in the transcriptional expression of the anti-inflammatory cytokine IL-4 in colonic tissue from DSS-treated NFκB2-null mice compared to wild-type mice following the same treatment. This increase in the transcriptional expression of IL-4 in the colon of NFκB2-null mice following 2% DSS was approximately 400-fold relative to wild-type mice following the same treatment. Additionally, the mRNA abundance of the other assessed pro-inflammatory cytokines was generally less in NFκB2-null colon than wild-type mice following DSS administration, but these differences were not statistically significant with the exception of IFN-γ as mentioned above (Figure 4.7).

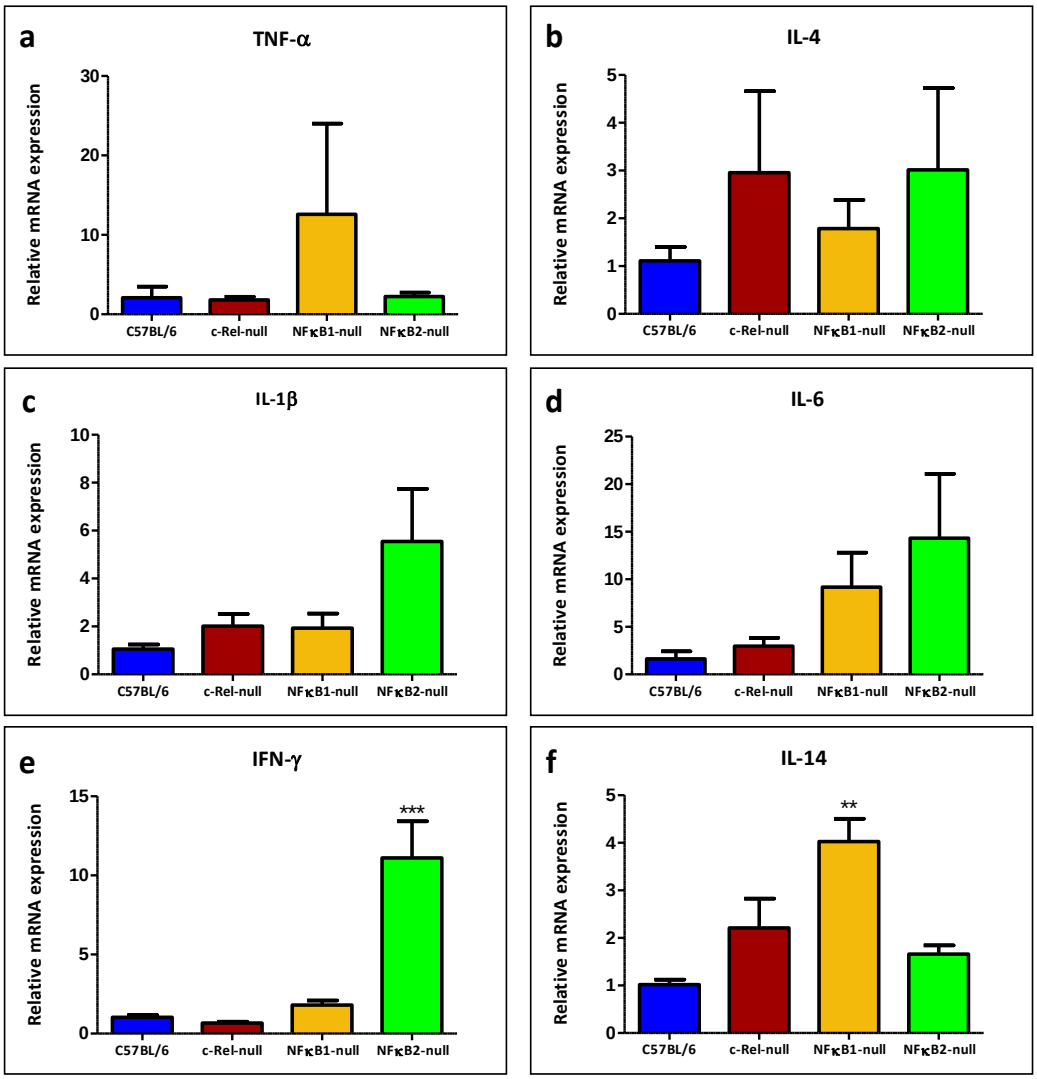

Figure 4.6: Quantification of relative mRNA expression of several cytokines in the small intestine of untreated mice. Relative mRNA expression of TNF-α (a), IL-4 (b), IL-1β (c), IL-6 (d), IFN-γ (e) and IL-14 (f) in small intestinal epithelial cells from untreated strains of mice as indicated above using real-time PCR. Data are presented as mean ± standard error of the mean. Statistical analysis was performed by 1-way ANOVA with Bonferroni post-hoc tests (**p<0.01, ***p<0.001 compared C57BL/6) (n=4 mice per genotype group).

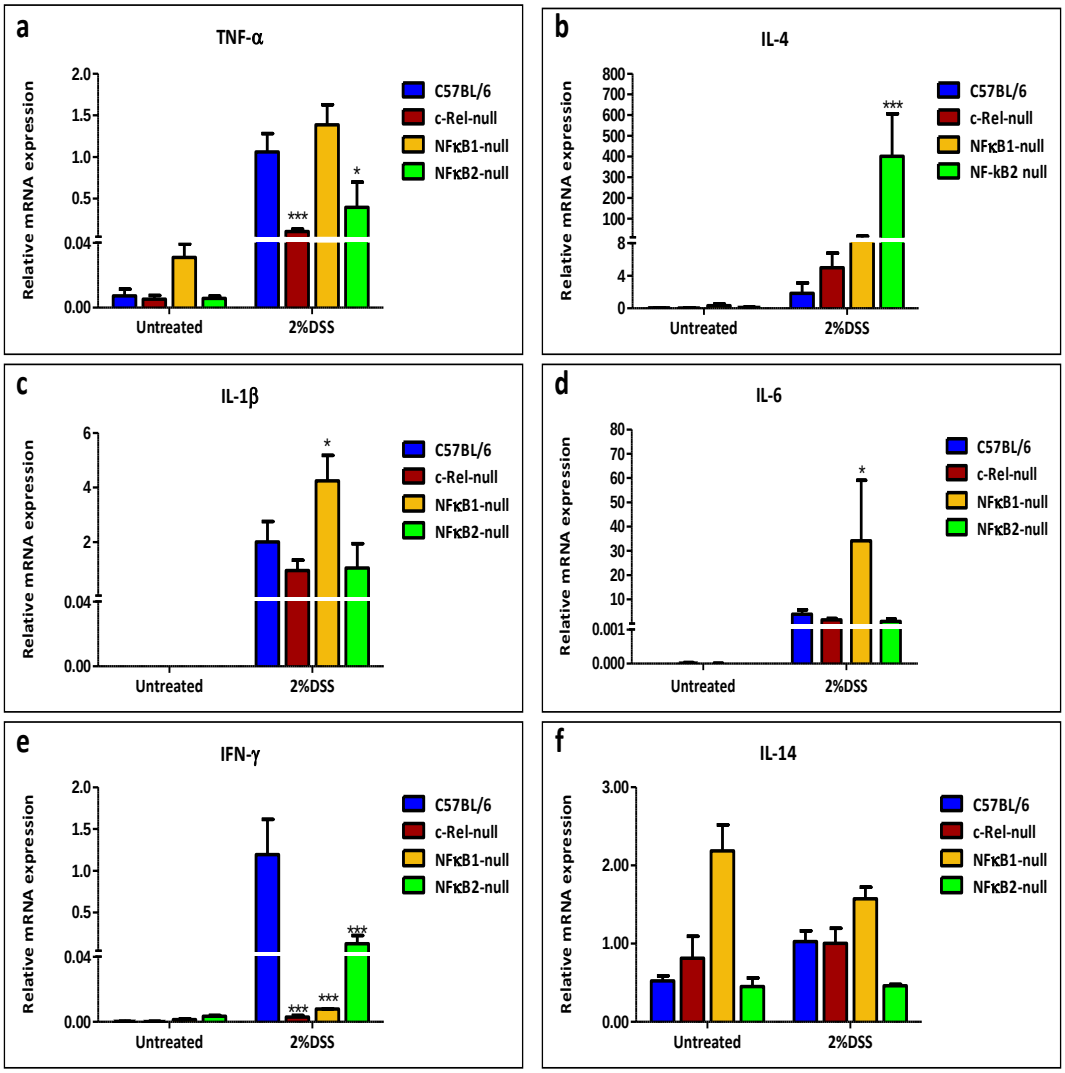

Figure 4.7: Quantification of relative mRNA expression of several cytokines in the colon of untreated and 2% DSS treated mice. Relative mRNA expression of TNF-α (a), IL-4 (b), IL-1β (c), IL-6 (d), IFN-γ (e) and IL-14 (f) in the colon of untreated animals and 5 days following 2% DSS treatment in the strains of mice indicated above using real-time PCR. Data are presented as mean ± standard error of the mean. Statistical analysis was performed by 2-way ANOVA with Bonferroni post-hoc tests (*$p<0.05$, ***$p<0.001$ compared to similarly treated C57BL/6) (n=4 mice per genotype group).

4.6 Discussion

In this chapter, mice deficient in various NFκB family members were used to dissect the importance of specific NFκB family members in the development of experimental colitis. DSS-induced colitis in mice is a recognised model for human ulcerative colitis and shares similar manifestations. However, the mechanism by which DSS induces colitis remains unclear. Several mechanisms have been proposed such as direct toxic effects on colonic epithelial cells, by altering the microbiota and by activation of macrophage inflammatory responses (110). Like human IBD, DSS-induced colitis in mice is manifested by clinical signs such as body weight loss, rectal bleeding and diarrhoea. Additionally colitis in this model has histological similarities to those observed in humans (309). To increase the accuracy of this study, colitis was therefore assessed on the basis of both clinical and histological manifestations.

Data in this chapter clearly demonstrate the importance of both the classical and alternative pathways of NFκB signalling in regulating acute colonic intestinal inflammatory responses. Disrupting the classical NFκB activation pathway by deleting c-Rel or NFκB1 resulted in increased susceptibility of mice to developing DSS-induced colitis. Both c-Rel-null and NFκB1-null mice showed more weight loss than wild-type mice at days 5 and 6 following DSS administration. The disease activity index was also significantly higher in c-Rel-null and NFκB1-null mice than wild-type mice. In addition, the colons from mice with either c-Rel or NFκB1 deletions were significantly shorter than those from their wild-type counterparts. Finally microscopic examination revealed extensive damage and increased inflammatory cell infiltration in wild-type, c-Rel-null and NFκB1-null mice. However,

this technique did not allow detection of differences in inflammatory scores between these strains of mice. These findings suggest that the classical activation pathway of NFκB signalling plays an anti-inflammatory role in the colon. NFκB has long been thought the prototypical pro-inflammatory signalling pathway that is implicated in the pathogenesis of IBD. This is demonstrated for example by its activation by pro-inflammatory cytokines and by its role in the transcriptional regulation of these cytokines (205). In keeping with this, genetic manipulations that result in increased NFκB activity have been shown to cause inflammation-related pathologies (310). Additionally, it has been shown that *in vivo* suppression of NFκB activity in certain tissues resulted in attenuation of inflammatory responses (250, 311). In the colon, it has been demonstrated that inhibition of NFκB by an antisense oligonucleotide for RelA (P65) (266) or by a small-molecule inhibitor of IKKβ (267) resulted in attenuation of inflammation in a murine model of colitis. However, several recent murine studies unexpectedly demonstrated that specific deletion of IKKγ in intestinal epithelial cells resulted in the development of a spontaneous colitis (252) and deletion of IKKβ from intestinal epithelial cells resulted in increased inflammation in the DSS-induced colitis model (250, 268). This implies that classical NFκB pathway signalling in non-immune, epithelial cells might play an anti-inflammatory role. This anti-inflammatory function has been attributed to the ability of NFκB to promote epithelial cell survival and maintenance of tissue integrity (243). In a recent study, the mechanisms responsible for the anti-inflammatory role of classical NFκB pathway signalling in intestinal epithelial cells were investigated. Selective deletion of IKKβ in murine intestinal epithelia was associated with more severe mucosal inflammation 16 days after a course of 5 days

of DSS in drinking water. To exclude the possibility that the increased inflammation observed in these mice was due to increased early damage induced by increased apoptosis in IKKβ deficient enterocytes (250), wild-type mice were treated with a highly specific IKKβ inhibitor (ML120B) following completion of DSS treatment, and histological examination was performed on day 10 after the start of DSS administration. Similar to enterocyte specific IKKβ genetic deletion, pharmacological inhibition of IKKβ resulted in more severe mucosal inflammation relative to vehicle-treated controls. These results indicate that the anti-inflammatory function of IKKβ in intestinal epithelial cells is independent of the initial damage (268). Furthermore, as described in a previous study, NFκB has a pro-apoptotic role in neutophils during inflammation, which might represent an additional anti-inflammatory mechanism played by NFκB during the development of acute inflammation (2, 312, 313). In agreement with these studies, data in this chapter have shown that c-Rel and NFκB1, which are both involved in the classical NFκB activation pathway have an overall anti-inflammatory role in the colon. Similarly, in a recent study conducted by Steinbrecher *et al*, selective intestinal deletion of RelA was shown to increase intestinal epithelial apoptosis and aggravate acute intestinal inflammation in a murine model of DSS-induced colitis (271).

In humans, a previous study has identified a polymorphism within the NFκB1 promoter (termed -94ins/delATTG) and the variant allele with a 4-bp deletion (-94delATTG) has been shown to be associated with decreased promoter activity (314). Several recent studies have investigated the association of this functional polymorphism of NFκB1 with IBD. Some of these studies have found an association

between this polymorphism and IBD (315, 316). However, other studies have not detected any association between this polymorphism and IBD (317-319). Genome-wide association studies have recently identified 99 susceptibility loci/genes that are significantly associated with ulcerative colitis and/or Crohn's disease. *Rel* gene which encodes c-Rel is one of these genes which have been shown to confer susceptibility to both colitis and Crohn's disease (82, 320, 321).

As we showed in chapter 3, NFκB1 deletion caused increased intestinal epithelial apoptosis following administration of two different stimuli. This loss of barrier function could lead to increased exposure of mucosal immune cells to luminal contents and trigger a more severe inflammatory response. Thus, disruption of the intestinal epithelial barrier might be a plausible explanation for the increased clinical severity of colitis which was observed in NFκB1-null mice. Although c-Rel-null mice did not show an increase in intestinal epithelial apoptosis following γ-irradiation or irinotecan treatment compared to wild-type mice, c-Rel deletion also sensitised mice to DSS-induced colitis. This supports the notion that the classical NFκB activation pathway has an additional function in intestinal epithelia beyond protection against apoptosis and its anti-inflammatory function is also mediated by other mechanisms which are independent of the initial damage (268).

Given the importance of cytokines in regulating inflammation, the mRNA expression of several cytokines was assessed to investigate the molecular mechanisms responsible for the increased colitis susceptibility observed in c-Rel-null and NFκB1-null mice. Pro-inflammatory cytokines have previously been shown to play a vital role in the pathogenesis of inflammatory bowel diseases. It has been reported that

inflammatory bowel disease is associated with up-regulation of several pro-inflammatory cytokines such as TNF-α, IL-1β and IL-6 (322, 323). As expected, the quantification of the transcriptional expression of several key cytokines namely TNF-α, IL-1β, IFN-γ, IL-4, IL-6 and IL-14 in this study, revealed dynamic changes in response to DSS treatment. Consistent with the increased severity of colitis observed in NFκB1-null mice, the relative mRNA expressions of IL-1β and IL-6 were significantly increased in colonic samples from NFκB1-null mice following DSS administration relative to similarly treated wild-type mice. Moreover, NFκB1-null distal colon also demonstrated small increases in the mRNA expression of the pro-inflammatory cytokines TNF-α and IL-14, but these increases were not statistically significant. It has been shown that IL-1β expression is increased in the colorectal mucosa in patients with ulcerative colitis during the acute phase of the disease (324-326). It has also been demonstrated that administration of an anti-murine IL-1β antibody reduced the weight loss and shortening of colon in a model of experimental colitis induced by DSS treatment (327). The importance of IL-6 in colonic inflammation has come from various studies which have shown up-regulation of tissue and circulating IL-6 and sIL-6R abundance in patients with acute Crohn's disease and ulcerative colitis (328-330). Additionally, it has been shown that treatment of mice with an anti-IL-6 receptor antibody ameliorated intestinal inflammation in murine models of experimental colitis. Recent studies have also demonstrated that mice deficient in IL-6 were partially protected from development of TNBS-induced (331) and DSS-induced (332) acute experimental colitis. Hence, the more severe colitis observed in NFκB1-null mice might be explained by a significant transcriptional up-regulation of IL-1β and IL-6 in colonic

samples from DSS-treated NFκB1-null mice compared to similarly treated wild-type mice. However, the increased susceptibility of c-Rel mice to DSS-induced colitis was associated with a significant decrease in the mRNA expression of TNF-α and was not associated with any increase in the mRNA expression of the other assessed cytokines relative to similarly treated wild-type mice. It has been shown that c-Rel is transcriptional activator for TNF-α in the peritoneal macrophages and in c-Rel deficient mice, these cells were shown to secrete lower amounts of TNF-α than wild-type cells following their stimulation (333). This suggests that the assessed cytokines are unlikely to be involved in determining the increased susceptibility of c-Rel-null mice to DSS-induced colitis and thus the mechanism responsible for increased colitis severity in c-Rel-null mice is different from NFκB1-null mice. Given that the severity of colonic inflammation depends on the overall changes of all cytokines, other cytokines that were not assessed in this study could be involved.

In contrast to the findings in NFκB1-null and c-Rel-null mice, NFκB2 deletion (disrupting the alternative NFκB activation pathway) resulted in resistance of mice to developing colitis. This was manifested by measurement of both clinical and histological parameters. Although, the colons of NFκB2-null mice were more susceptible to epithelial apoptosis following two different types of damage inducing stimuli (as shown in the chapter 3), they showed significantly less inflammation and damage following DSS administration compared to wild-type mice. For the first time therefore, we have shown an important role of the alternative NFκB activation pathway in regulating colonic inflammatory responses. Genetic manipulation of the two major components of the alternative pathway RelB and NFκB2, has previously

demonstrated a vital role of this pathway in lymphoid organogenesis (204). Moreover, studies of RelB and NFκB2 deficient mice have demonstrated important roles for these proteins in regulating dendritic cell function and in the generation of cellular immunity (232, 334). For example, RelB-null mice demonstrated T cell mediated inflammation in multiple organs and showed impaired cell-mediated immunity (233). However, the role of these components of the alternative pathway in regulating intestinal inflammation has not been previously studied *in vivo.* Here for the first time, we have demonstrated that disruption of the alternative pathway by deleting NFκB2 resulted in protection of mice from developing the severe colitis which was observed in wild-type animals. To investigate the underlying mechanisms responsible for the reduced colonic inflammation observed in NFκB2-null mice, the mRNA abundance of several cytokines were assessed by real-time PCR. NFκB2-null mice showed a significant reduction in the transcriptional expression of the pro-inflammatory cytokine TNF-α and a significant increase in the transcriptional expression of the anti-inflammatory cytokine IL-4 following DSS treatment, compared to similarly treated wild-type mice.

Nenci *et al* demonstrated that TNF-α was involved in the pathogenesis of colitis observed in IKKγ-null mice (252). It has been suggested that TNF-α orchestrated the inflammatory response in IKKγ-null colon by enhancing stromal, endothelial and immune cells to up-regulate the expression of pro-inflammatory cytokines and chemokines leading to the subsequent recruitment and activation of inflammatory cells. Alternatively, TNF-α might act on intestinal epithelial cells to induce epithelial apoptosis and facilitate bacterial translocation to induce a high inflammatory

response (270). TNF-α is a potent pro-inflammatory cytokine and its inhibition in human patients by targeted therapy is an effective treatment for IBD (270, 335, 336).

IL-4 is considered to be an anti-inflammatory cytokine. It inhibits the secretion of the pro-inflammatory cytokines TNF-α, IL-1β and IL-6 by monocytes for prolonged periods of time (337). This inhibition by IL-4 has been shown to be impaired in IBD. The IL-4-mediated suppression of secretion of these pro-inflammatory cytokines has been thought to be a crucial inflammation limiting function (338). A study conducted by Togawa *et al* illustrated that lactoferrin (Natural immunomodulator) exerted an anti-inflammatory effect in rats subjected to TNBS-induced colitis via induction of IL-4 and IL-10 secretion (339). A previous study conducted by Melgar *et al*, also showed very low protein levels of IL-4 in the colon following induction of DSS-induced colitis (7). However, there are also a limited number of studies that have revealed a pro-inflammatory role of IL-4 in intestinal inflammation (340, 341). Taken together, the substantial attenuation of DSS-induced colitis observed in NFκB2-null mice might be mediated by the significant down-regulation of the pro-inflammatory cytokine TNF-α and by up-regulation of anti-inflammatory IL-4.

Collectively, this chapter demonstrates that disruption of the classical NFκB signalling pathway by deleting NFκB1 or c-Rel exacerbated colonic inflammation and damage during the development of acute intestinal inflammatory conditions. Consistent with previous studies, the classical pathway therefore appears to play an overall anti-inflammatory function in the colon. The increased susceptibility of NFκB1-null, but not c-Rel-null mice to DSS-induced colitis might be mediated by up-

regulation of IL-1β and IL-6. This therefore has negative implications for the potential therapeutic use of classical NFκB pathway inhibitors in IBD. However, disruption of the alternative pathway by deleting NFκB2 substantially protected murine colon from developing acute inflammation following DSS administration and this was associated with reduced transcriptional expression of the pro-inflammatory cytokine TNF-α and increased transcriptional expression of the anti-inflammatory cytokine IL-4. Thus, this study provides the first evidence of a major role of the alternative NFκB activation pathway in regulating colonic inflammation. In contrast to the classical activation pathway, the NFκB2-dependent alternative NFκB activation pathway appears to play an overall pro-inflammatory function in the colon. This finding raises the potential of specific inhibition of NFκB2 as a therapy for IBD treatment. However current conclusions have been based on an acute colitis model. Thus, further studies in a DSS-induced chronic colitis model are required to assess the outcome of deletion of NFκB2 or other NFκB family members on chronic colitis. This will be described in the next chapter by exposing mice to repeated cycles of a lower DSS concentration to avoid the death of mice before the end of the experiment.

Given that NFκB can modulate intestinal inflammatory responses by acting on both immune and intestinal epithelial cells, our current experiments have not yet distinguished which compartment plays the dominant role. Therefore, selective tissue deletion of specific NFκB family members either in epithelial or immune cells could help to determine the exact cellular mechanisms responsible for the altered susceptibility to DSS-induced colitis observed in transgenic mice. This could be performed by utilising either bone morrow chimaeras or transgenic technology.

Investigating the susceptibility to DSS-induced colitis in mice with a germline deletion of RelB would also help to characterise of the role of individual members of the alternative NFκB activation pathway in regulating intestinal inflammation. Since the increased susceptibility to colitis in NFκB1-null mice and the reduced severity of colitis in NFκB2-null mice were associated with particular cytokine responses, it would be also useful to investigate the outcome of using pharmacological or transgenic methods to manipulate these responses. For example, it would be interesting to assess whether administering an anti-IL-6 receptor antibody to NFκB1-null mice rescued these animals from developing an increased severity of colitis following DSS treatment.

5 The impact of deletion of specific NFκB family members on inflammation associated colonic carcinogenesis

5.1 Introduction

The contribution of NFκB signalling to cancer promotion and progression has been well documented in several recent studies. Hanahan and Weinberg suggested that tumourigenesis requires six essential alterations to normal cell physiology that collectively lead to neoplastic growth: self-sufficiency in growth signals, insensitivity to growth-inhibitory (antigrowth) signals, evasion of programmed cell death (apoptosis), limitless replicative potential, sustained angiogenesis, and tissue invasion and metastasis (177). NFκB is a key regulator of cell survival and apoptosis in a cell type and stimulus dependent manner. Dysregulation of the cell cycle and apoptotic process following DNA damage is believed to contribute to cancer development and progression (177). Therefore, NFκB may promote carcinogenesis when its activation enhances cell survival and inhibit carcinogenesis when its activation leads to cell death. Chronic inflammation sometimes occurs after the development of colorectal cancer, which is initially caused without any obvious inflammation (276). Although NFκB activation has been observed in many inflammation related cancers, it has been suggested that inflammation is not involved in tumour promotion in all cases of cancer (342). It was shown in chapter 3 that both NFκB1 and NFκB2 have a strong anti-apoptotic role in intestinal epithelia and that they protect intestinal epithelial cells from apoptosis following two types of DNA damage inducing stimuli. This suggests that these NFκB family members may have important roles in regulating colonic carcinogenesis. Given that NFκB's

functions depend on tissue context, these roles should be specifically investigated in the setting of inflammation associated colonic carcinogenesis.

In addition to the central role of NFκB in promoting cancer cell survival, it also functions in a paracrine manner to enhance cancer cell growth. Several recent studies have suggested that the inflammatory process is mainly mediated by activation of the NFκB pathway (236). Persistent activation of NFκB in epithelial cells has been linked to the development of inflammation-associated cancer as demonstrated in colitis-associated cancer (CAC). This suggests that persistent NFκB activation in epithelial cells in response to chronic inflammation is a key factor in the process of intestinal carcinogenesis (250, 343). This is illustrated by several mouse models of inflammation-associated cancer (241, 250). Mouse models of CAC provide direct evidence that classical NFκB signalling (IKKβ-dependent classical NFκB activation) links inflammation and cancer. In one model of CAC, deleting IKKβ selectively in intestinal epithelial cells resulted in a reduction in tumour incidence and this effect was attributed to increased apoptosis of IKKβ deficient-epithelial cells. However, deleting IKKβ specifically in myeloid cells reduced tumour number and size without affecting apoptosis. This decrease in tumour size resulted from reduced expression of pro-inflammtory cytokines which are required for tumour growth (250). The expression of major inflammatory factors such as TNFα, IL-1, IL-6, IL-8 is regulated by NFκB and these cytokines in turn activate NFκB expression. This therefore represents a positive feedback loop whereby cellular and DNA damage promote cell proliferation and transformation, ultimately leading to the initiation, promotion and progression of cancer (175, 273, 275). However, the role of the

alternative pathway and the specific roles of NFκB family members in inflammation associated colon cancer have not previously been investigated. In chapters 3 and 4 of this thesis, it was shown that specific NFκB family members belonging to either the classical or alternative activation pathways differentially regulate intestinal epithelial cell survival and colonic inflammation. This suggests that specific NFκB family members from both pathways may differentially regulate the development of inflammation related colon cancer. Therefore, this hypothesis was investigated using a murine model of colitis associated cancer.

5.2 Aims

To investigate the susceptibility of mice deficient in various NFκB family members to inflammation associated colonic carcinogenesis using a murine model of colitis associated colon cancer.

To investigate the cellular mechanisms responsible for any altered susceptibility to colitis associated colon cancer in mice deficient in various NFκB family members by assessing the amount of intestinal epithelial proliferation and apoptosis in response to the pro-carcinogen azoxymethane (AOM).

5.3 Effects of deleting specific NFκB family members on susceptibility to inflammation associated colon tumours

To evaluate the role of specific NFκB family members in intestinal carcinogenesis, the susceptibility of mice deficient in various NFκB family members to initiating intestinal solid tumour formation particularly inflammatory driven colonic tumours was assessed using a murine model of colitis associated cancer.

5.3.1 Finding the optimal DSS concentrations for the colitis associated tumour experiment (AOM/DSS regimen)

As demonstrated in chapter 4, 2% DSS administration for 5 days resulted in a dramatic loss of body weight (more than 20%) and severe toxicity at day 6 particularly in c-Rel-null and NFκB1-null strains of mice. Hence, it was necessary to optimise the DSS concentration for the repeated cycles of DSS administration which were required for colitis associated tumour induction, in order to avoid the death of mice before the end of the experiment. Therefore the effects of various lower DSS concentrations on the body weight of the susceptible animal strains (c-Rel-null and NFκB1-null mice) were assessed for 10 days following the start of DSS administration (Figure 5.1). Groups of mice (3 to 5 mice per group from c-Rel-null and NFκB1-null strains) received a particular DSS concentration (1.5%, 1%, 0.75% or 0.5% DSS) in their drinking water for 5 days and were sacrificed on day 10. Body weight loss was assessed throughout the whole experiment. All mice that received 1.5% DSS became severely ill and showed a substantial loss of weight before dying between days 5 and 8 (Figure 5.1 a). Two mice which received 1% DSS lost more than 20% of their body weight before dying between days 6 and 9. The remaining

two mice treated with 1% DSS survived until day 10, but one was very ill and lost 27.9% of its body weight and did not show any signs of recovery (Figure 5.1b). Groups of mice that received either 0.75% or 0.5% DSS lost weight which was more profound in the 0.75% DSS group but they were able to survive and recover (and regain weight) before being sacrificed at day 10, with the exception of one mouse from the 0.75% DSS group which died before day 9 (Figure 5.1 c and d). Therefore 0.5% and 0.75% DSS concentrations were chosen as the doses for subsequent cycles of AOM/DSS administration in the following experiments.

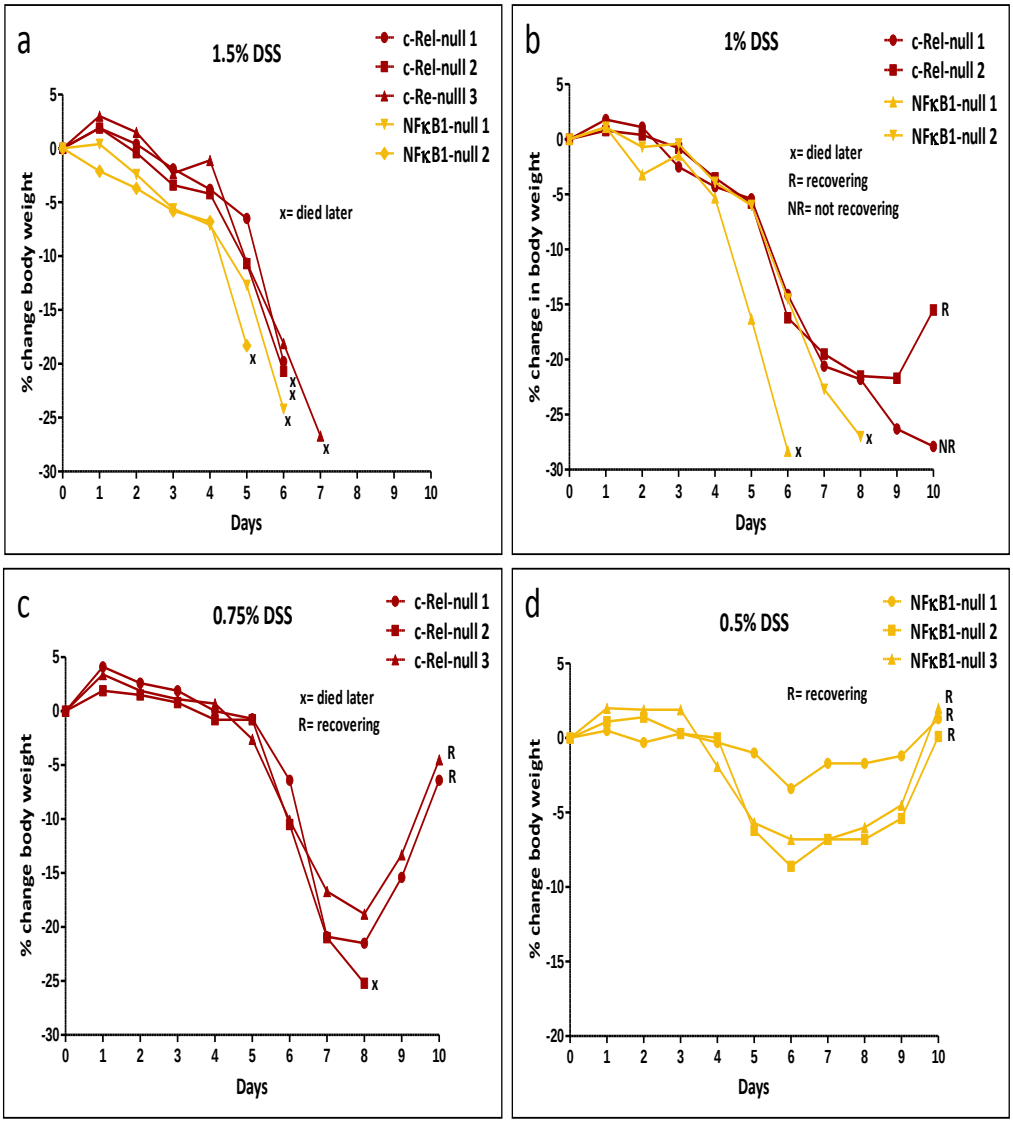

Figure 5.1: Percentage weight change observed in mice following different concentrations of dextran sulphate sodium administration. 1.5% (a), 1% (b), 0.75% (c) and 0.5% DSS (d) was orally administered to groups of mice from c-rel-null and NFκB1-null strains as indicated for 5 days and mice were sacrificed on day 10. Percentage body weight change was daily recorded.

5.3.2 c-Rel-null and NFκB1-null mice showed a significant increase and NFκB2-null mice a substantial decrease in weight loss following AOM/DSS regime

In order to evaluate the severity of colitis in mice deficient in various NFκB family members during the course of tumour induction, mice were weighed daily and % body weight loss was determined as an indicator of the severity of colitis. 5 days following a single dose of 12.5mg/kg AOM (pro-carcinogen), DSS was orally administrated to mice for 5 days and this was followed by 16 days of DSS-free water. This cycle was repeated twice and mice were sacrificed 12 days after the last DSS cycle. 0.5% DSS was used in the first cycle and because this was very well tolerated the dose was increased to 0.75% DSS for the second and third cycles as illustrated in Figure 5.2 a.

Similar to the observations from mice which were treated with DSS alone as shown in chapter 4, c-Rel-null and NFκB1-null mice treated with AOM/DSS appeared to be more susceptible to developing colitis (as determined by weight loss during the DSS cycles) particularly during the 0.75% DSS cycles. During the second cycle of DSS, % body weight loss in both c-Rel-null and NFκB1-null mice was significantly increased (maximum approximately 11%) compared to wild-type mice (maximum approximately 3%). This increased susceptibility to DSS-induced colitis was even more pronounced in c-Rel-null mice in the last DSS cycle where they lost more than 20% of their body weight compared to 7.8% and 7% body weight loss seen in NFκB1-null and wild-type mice respectively (Figure 5.2 b). Consistent with the observations following 2% DSS treatment shown in chapter 4, NFκB2-null mice lost less weight than wild-type mice particularly during the third DSS cycle and this was

statistically significant (Figure 5.2 b). These observations along with previous findings in chapter 4 suggest that deletion of the classical NFκB family member c-Rel or NFκB1 sensitised mice to DSS-induced colitis whereas deleting the alternative NFκB family member NFκB2 resulted in resistance to developing DSS-induced colitis. Body weight loss is a characteristic clinical feature of DSS-induced colitis and positively correlates with the activity of the disease. Hence, c-Rel-null and NFκB1-null mice may have more colonic inflammation, while NFκB2-null mice may have less colonic inflammation compared to their wild-type counterparts during the course of tumour induction. However, the increased body weight loss seen in c-Rel-null mice may also have resulted from increased colon tumour load rather than due to increased severity of DSS-induced colitis.

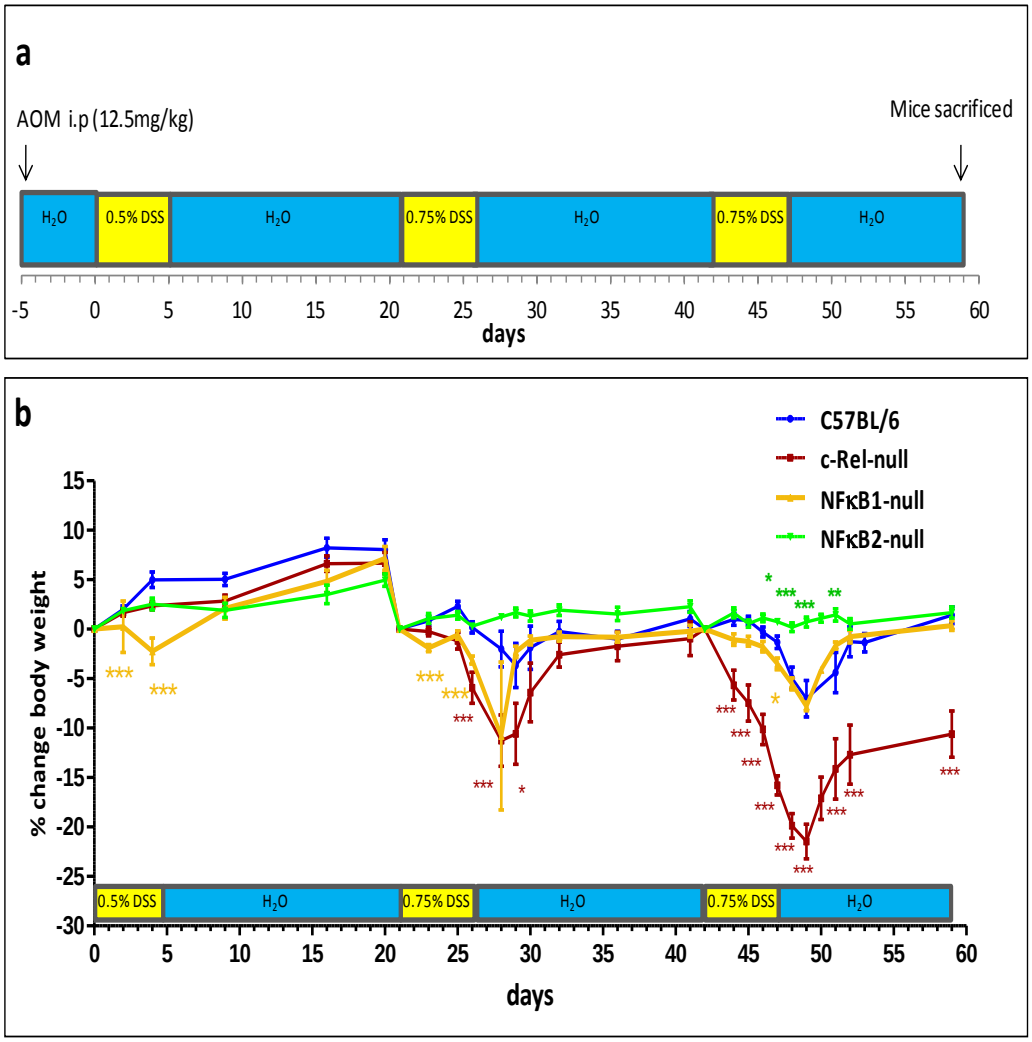

Figure 5.2: Colitis-associated cancer model and percentage of weight change observed in mice during the course of AOM/DSS treatment. 5 days following a single dose of 12.5mg/kg AOM (pro-carcinogen), DSS was orally administrated to mice for 5 days and this was followed by 16 days of DSS-free water. This cycle was repeated twice and mice were sacrificed 12 days after the last DSS cycle (a). Percentage of body weight change was recorded for C57BL/6 (blue), c-Rel-null (red), NFκB1-null (yellow) and NFκB2-null mice (green) throughout the AOM/DSS course (b). Data are presented as mean ± standard error of the mean. Statistical differences were assessed by one way ANOVA and Dunnett's multiple comparison test (*p<0.05, **p<0.01, ***p<0.001 compared to C57BL/6). (n=10 male mice per genotype).

5.3.3 Deleting c-Rel increased colitis associated tumour incidence whereas deleting NFκB2 greatly reduced colitis associated tumour incidence

Mice were administered a single dose of 12.5mg/kg AOM (pro-carcinogen) followed by three cycles of DSS as illustrated in Figure 5.2 a. Repeated DSS exposure induces chronic inflammation in the colon that resembles human IBD. This in turn greatly increases the incidence of AOM-induced tumours in the colon (108). In this study, all mice from the different genotypes that underwent AOM/DSS treatment developed colonic tumours with the exception of 40% of the NFκB2-null mice which did not develop any detectable tumours. Tumours were mainly located within the distal and middle thirds of the colon as shown in Figure 5.3. This tumour location correlates with the parts of the colon that show severe inflammatory changes following DSS administration (110). c-Rel deficient mice which were more susceptible to colitis showed a larger number of AOM/DSS-induced tumours. These tumours coalesced together and only minimal normal intervening colonic mucosa was apparent. In contrast, the tumours which developed in wild-type mice were more scattered in the colon and were separated by larger areas of normal colonic mucosa. On the other hand, NFκB2-null mice, which more resistant to developing colitis either did not develop tumours or only a few small polyps were seen (Figure 5.3). Microscopic examination of H and E stained colonic sections showed that, these tumours were mainly broad-based adenomas and they did not penetrate the muscularis mucosa in any genotype group (Figure 5.4).

Figure 5.3: Macroscopic view of longitudinally open colon from mice following tumour induction by AOM/DSS treatment as illustrated in Figure 5.2 a. After washing the longitudinally open colon with saline, images were taken. A scaled ruler was used to measure the size of the formed tumours. Tumour load was markedly increased in c-Rel-null colon and substantially reduced or absent in NFκB2-null colon compared to C57BL/6 (wild-type) colon (green arrows indicate visible tumours).

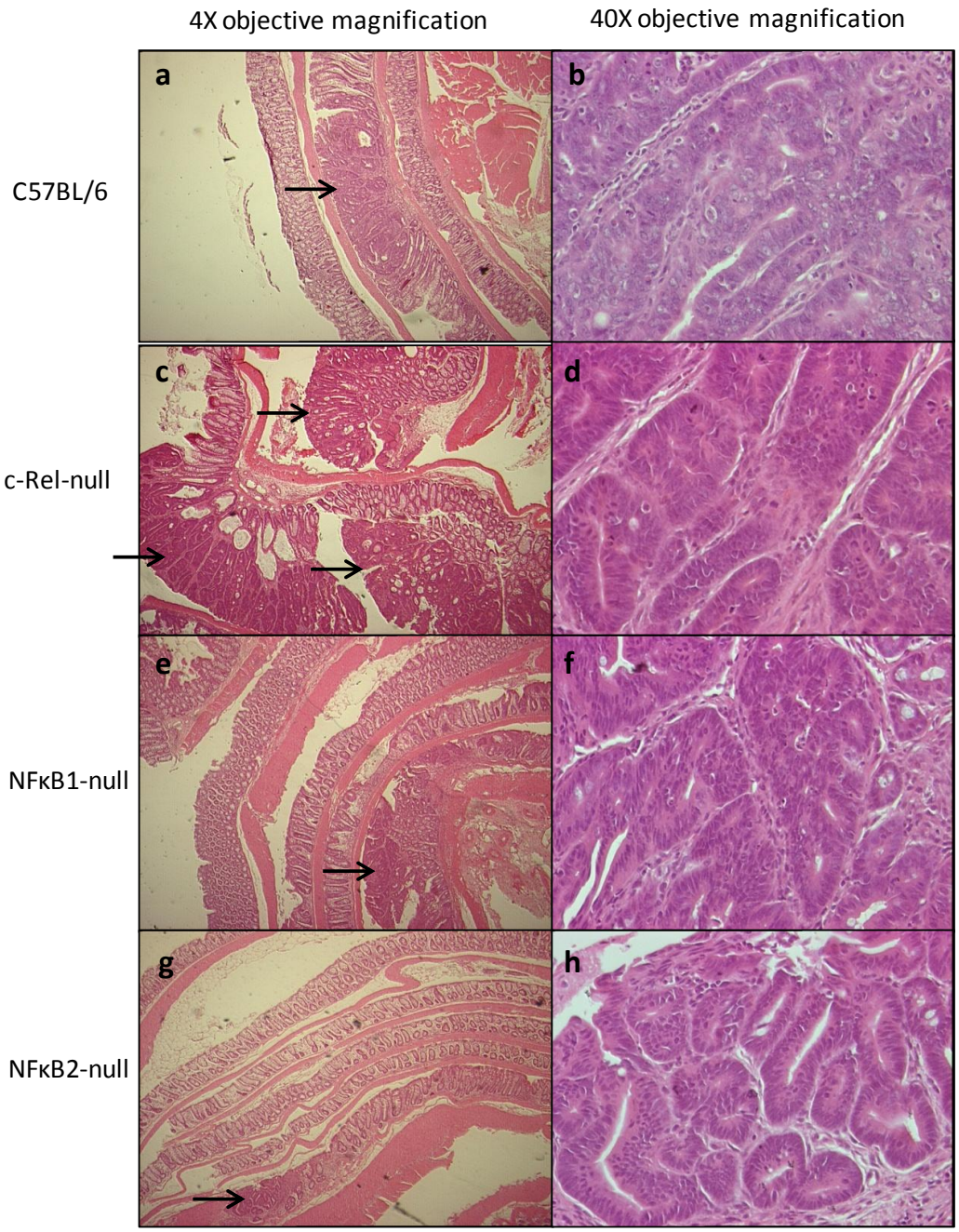

Figure 5.4: Photomicrographs of representative H and E stained colonic sections from mice following tumour induction by AOM/DSS treatment. Histology (H/E) of colonic tumours in sections (Swiss roll) from C57BL/6 (a, b), c-Rel-null (c, d), NFκB1-null (e, f) and NFκB2-null (g, h) mice following AOM/DSS treatment at 4x objective magnification (a, c, e, g) and 40x objective magnification (b, d f, h). (Arrows indicate the formed polyps).

Following careful macroscopic inspection, the number and size of colonic tumours was determined. c-Rel-null mice showed a significant 3.5-fold increase in the number of colonic tumours relative to wild-type mice (Figure 5.5). These tumours were also larger in size than those observed in C57BL/6 animals (Figure 5.6). However, NFκB1-null mice which were also more sensitive to colitis development did not show any increase in the number or size of colonic tumours relative to wild-type mice as shown in Figure 5.5 and Figure 5.6. On the other hand, disruption of the alternative pathway by deleting NFκB2 resulted in a decrease of 77% in the number of tumours compared to wild-type mice (Figure 5.5). The colonic tumours which developed in NFκB2-null mice were also smaller than those seen in wild-type mice (Figure 5.6). Additionally, 40% of NFκB2-null mice did not develop any colonic tumours. This substantial decrease in tumour incidence and size seen in NFκB2-null mice correlated with the reduced severity of colitis that was also observed in this strain of mice following administration of either DSS alone or AOM/DSS.

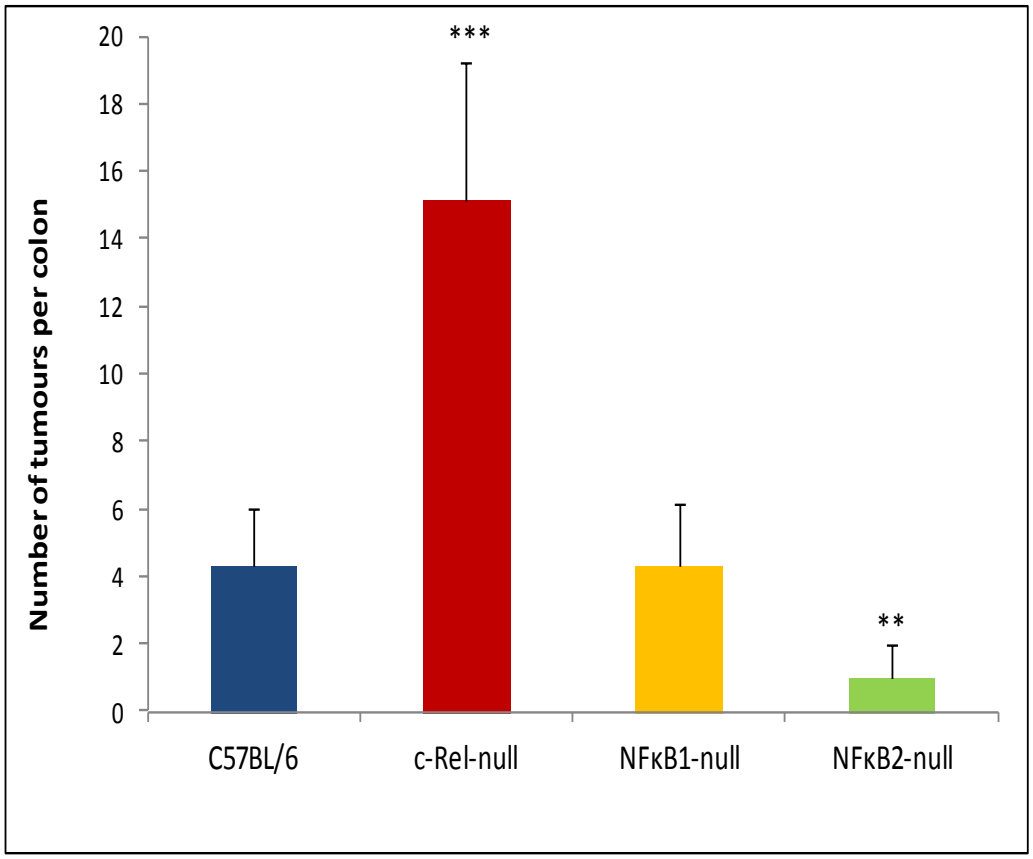

Figure 5.5: Tumour incidence in mice following colitis associated tumour induction using AOM/DSS. Number of visible colonic tumours per mouse in C57BL/6 (blue), c-Rel-null (red), NFκB1-null (yellow) and NFκB2-null (green) genotypes was determined following AOM/DSS administration (as illustrated in Figure 5.2). Statistical differences were assessed by one way ANOVA and Dunnett's multiple comparison test (**p<0.01, ***p<0.001 compared to C57BL/6). (n=10 male mice per genotype).

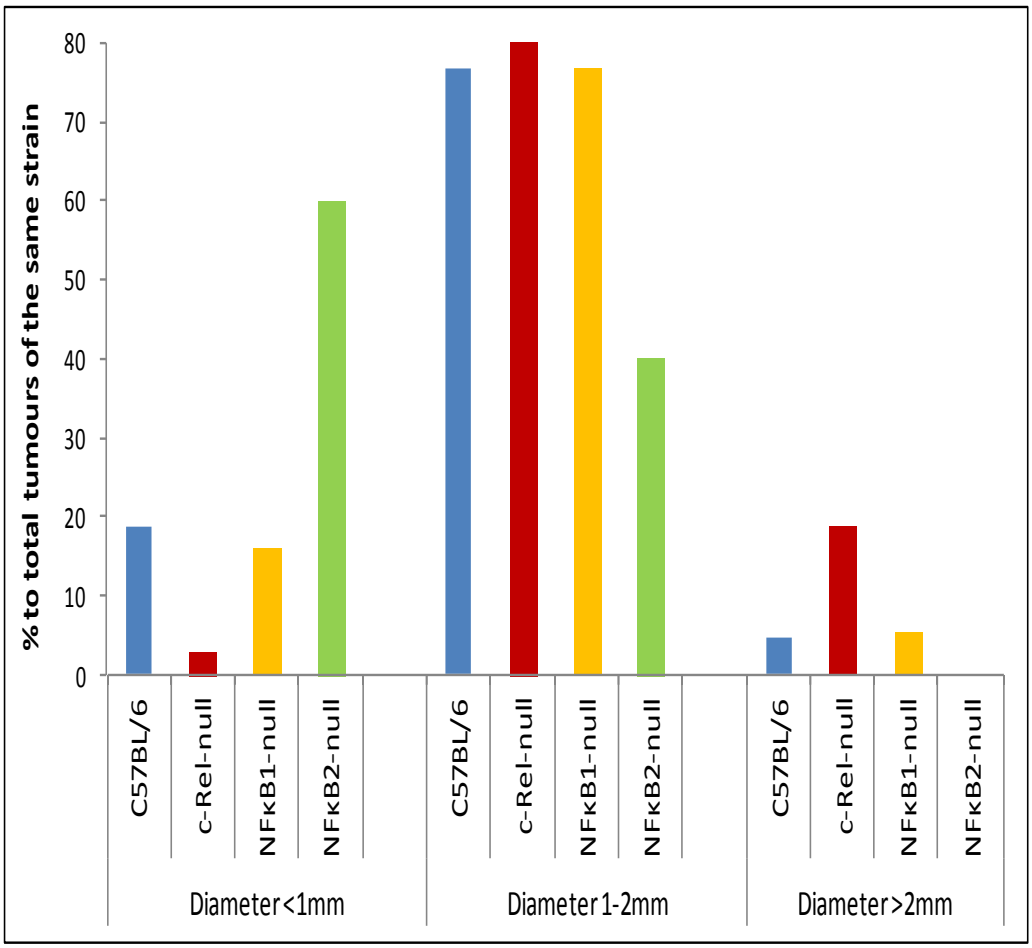

Figure 5.6: Size distribution of AOM/DSS induced colonic tumours in mice. Following tumour induction by AOM/DSS treatment as illustrated in Figure 5.2 a, the diameter of visible colonic tumours in C57BL/6 (blue), c-Rel-null (red), NFκB1-null (yellow) and NFκB2-null (green) animals was measured using a ruler. Percentages of tumours with a diameter <1mm, 1-2mm or >2mm to total tumours in the same strain of mice were determined as shown above.

5.3.4 Deleting c-Rel significantly increased the proliferation rate of colonic tumour cells induced by AOM/DSS treatment

Given that proliferation is an important cellular process for tumour growth, the differences in tumour size which were observed between the different genotypes of mice might have arisen due to differences in the proliferation rates of neoplastic cells within polyps. Therefore, a proliferation (Ki67) index was determined in these tumours by counting the number of Ki67 positive neoplastic cells per 0.25mm^2 area in the tumour section which showed the highest Ki67 staining for each mouse as described in section 2.4.5. In addition to this quantitative measure, the grade of dysplasia of AOM/DSS induced tumours was reported by a qualified veterinary pathologist (Jonathon Williams) blinded to the genotype of mice. Consistent with the increased incidence and increased proportion of larger tumours observed in c-Rel-null mice, the tumours in these animals showed a significantly increased proliferation index and a greater percentage of these tumours also showed high-grade dysplasia compared to their wild-type counterparts (Figure 5.7,Figure 5.8 and Figure 5.9). Although, NFκB2-null mice showed a greater percentage of tumours measuring <1mm diameter and with low-grade dysplasia compared to wild-type mice, no differences in tumour proliferation indices were observed in this genotype of mice compared to wild-type animals. Tumours from NFκB1-null mice exhibited no alteration in proliferation index or in degree of dysplasia compared to wild-type mice as shown in Figure 5.7, Figure 5.8 and Figure 5.9.

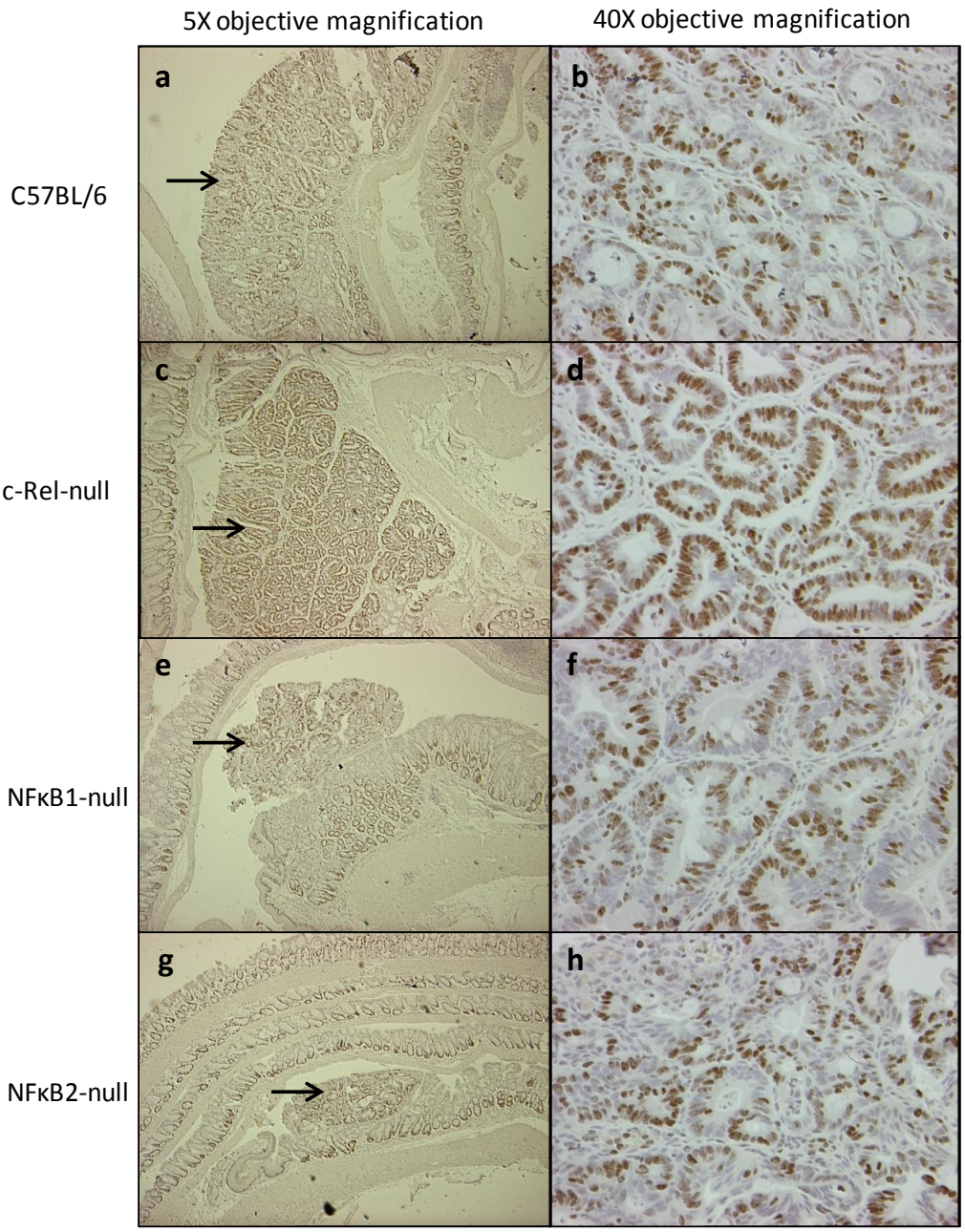

Figure 5.7: Photomicrographs of Ki67 immunohistochemistry of representative colonic sections from mice following tumour induction by AOM/DSS. Ki67 positive cells are shown in colonic sections (Swiss roll) from C57BL/6 (a), c-Rel-null (c), NFκB1-null (e) and NFκB2-null (g) mice following AOM/DSS treatment (as illustrated in Figure 5.2) at 5x objective magnification (tumours are indicated by arrows). b, d f and h shows Ki67 positive cells in these tumours (marked by arrows) at 40x objective magnification.

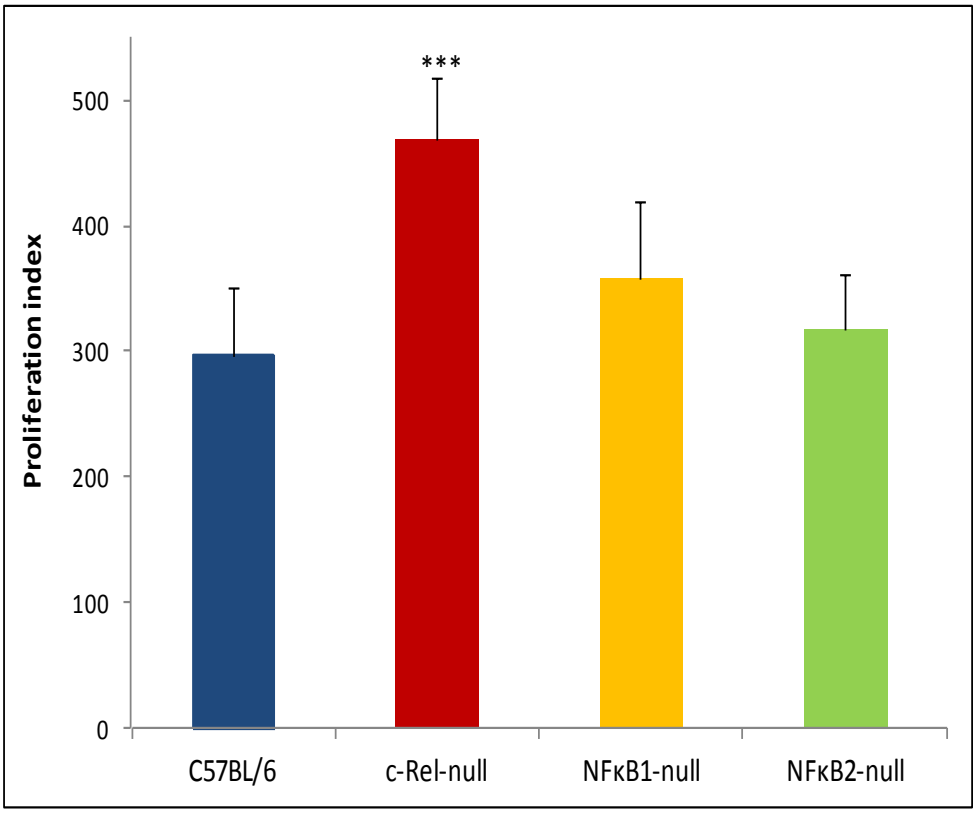

Figure 5.8: Proliferation index of colonic tumours in mice subjected to colitis associated cancer regimen. Following AOM/DSS administration, colonic sections were subjected to Ki67 immunohistochemical staining. A proliferation index was then determined by counting the number of Ki67 positive cells per 0.25mm^2 area of the tumour which showed the highest Ki67 staining in each mouse. Statistical differences were assessed by one way ANOVA and Dunnett's multiple comparison test (***$p<0.001$ compared to C57BL/6). (n=5-9 male mice per genotype as 4 NFκB2-null mice did not develop colonic tumours and some of the colonic sections particularly from this strain did not include any tumour tissue.

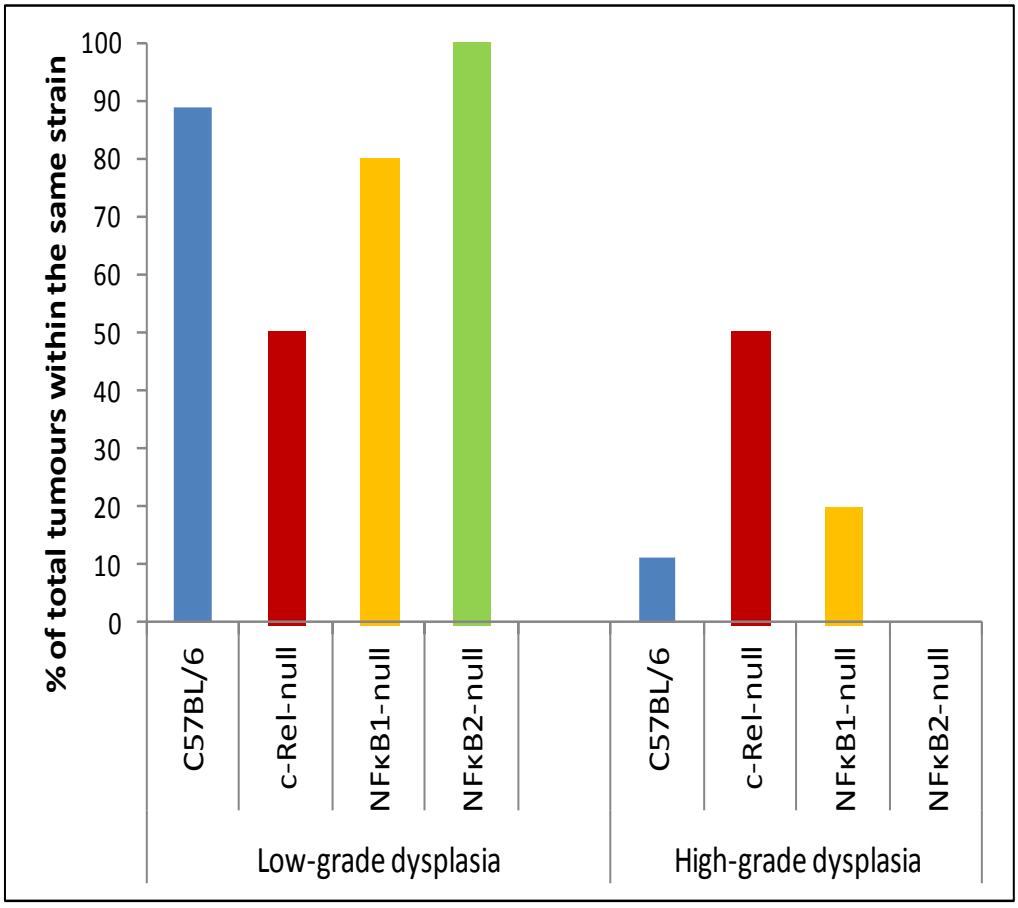

Figure 5.9: Degree of dysplasia in AOM/DSS induced colonic tumours in mice. Degree of dysplasia (either low-grade or high-grade) of AOM/DSS induced colonic tumours was reported by a veterinary pathologist blinded to genotype of mice. Percentage of tumours with either low-grade or high-grade dysplasia relative to total tumours in the same strain of mice is shown.

5.4 Effects of deleting specific NFκB family members on intestinal crypt regeneration

Impairment of the regulation of cell proliferation following injury is considered to be a potential trigger of carcinogenesis. Thus, investigating the role of specific NFκB family members in regulating intestinal epithelial cell proliferation following injury may help to reveal the cellular mechanisms responsible for the differential susceptibility to colitis associated tumourigenesis observed in c-Rel-null and NFκB2-null mice. Therefore, the effect of deleting specific NFκB family members on intestinal crypt regeneration following whole body γ-irradiation was assessed. Mice deficient in various NFκB family members along with wild-type mice (5 mice per genotype group) were subjected to a single dose of 12Gy γ-irradiation and then sacrificed 96 hours later. Regenerating crypts were scored from H and E stained small intestinal and colonic sections. NFκB2-null mice demonstrated a significant reduction in small intestinal crypt regeneration compared with wild-type mice, but no significant alterations in small intestinal crypt regeneration were observed in either c-Rel-null or NFκB1-null mice as shown in Figure 5.10 and Figure 5.12 a. However in the colon, c-Rel-null mice showed a significant increase in colonic crypt regeneration while NFκB1-null and NFκB2-null mice did not demonstrate any significant change in colonic crypt regeneration as shown in Figure 5.11 and Figure 5.12 b. These findings suggest that NFκB2 deletion suppresses epithelial crypt regeneration (proliferation) in the small intestine and that c-Rel deletion increases epithelial regeneration in the colon following injury.

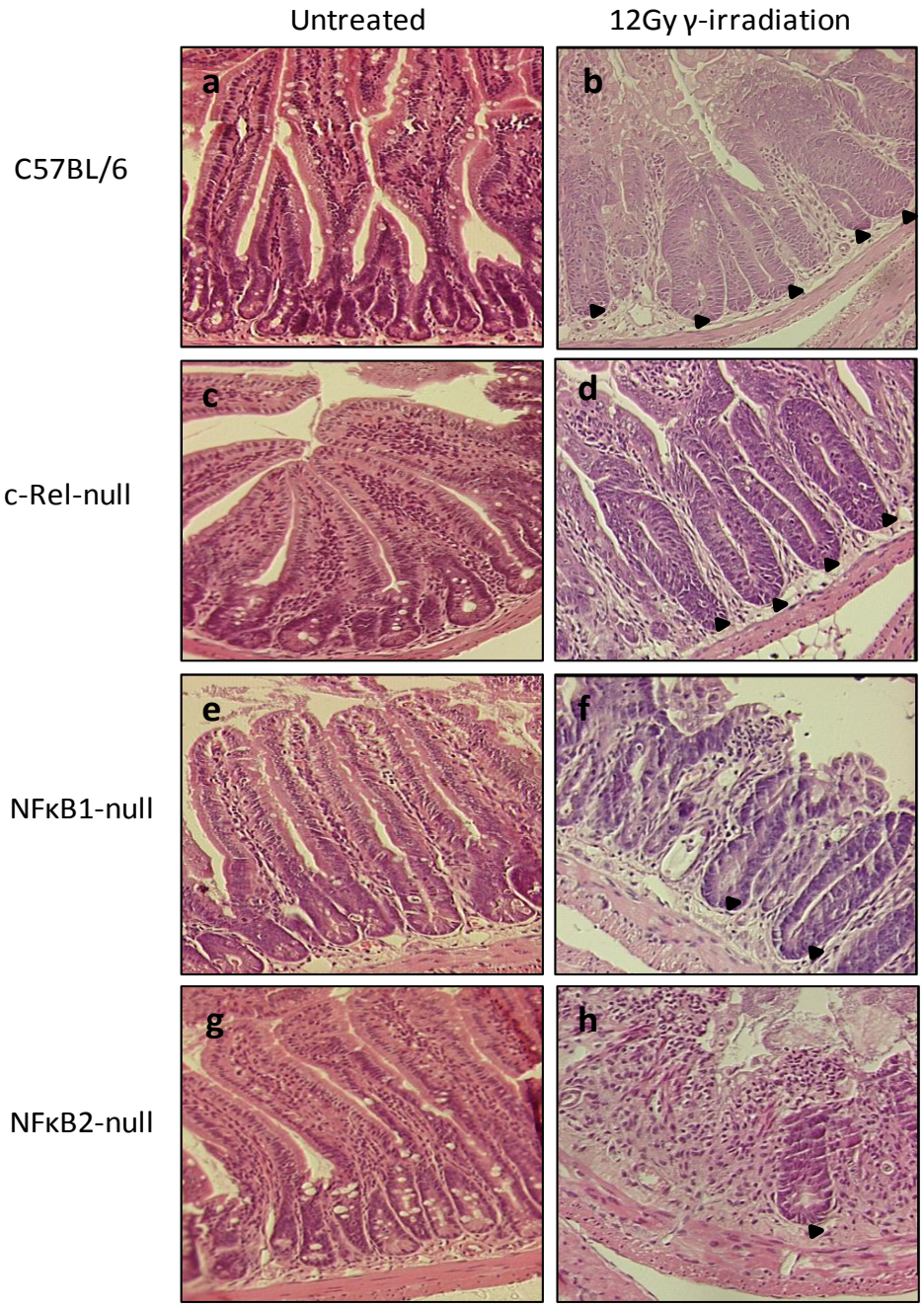

Figure 5.10: Representative photomicrographs showing small intestinal crypt regeneration in mice subjected to 12Gy γ-irradition and killed 96 hours later along with untreated mice. Histological assessment (H/E) of small intestinal sections taken from C57BL/6 (a, b), C-Rel-null (c, d), NFκB1-null (e, f) and NFκB2-null (g, h) mice. Mice were either untreated (a, c, e, g) or subjected to 12 Gy γ-irradition and sacrificed 96 hours later (b, d, f, h). Regenerating small intestinal crypts in irradiated mice are indicated by arrowheads.

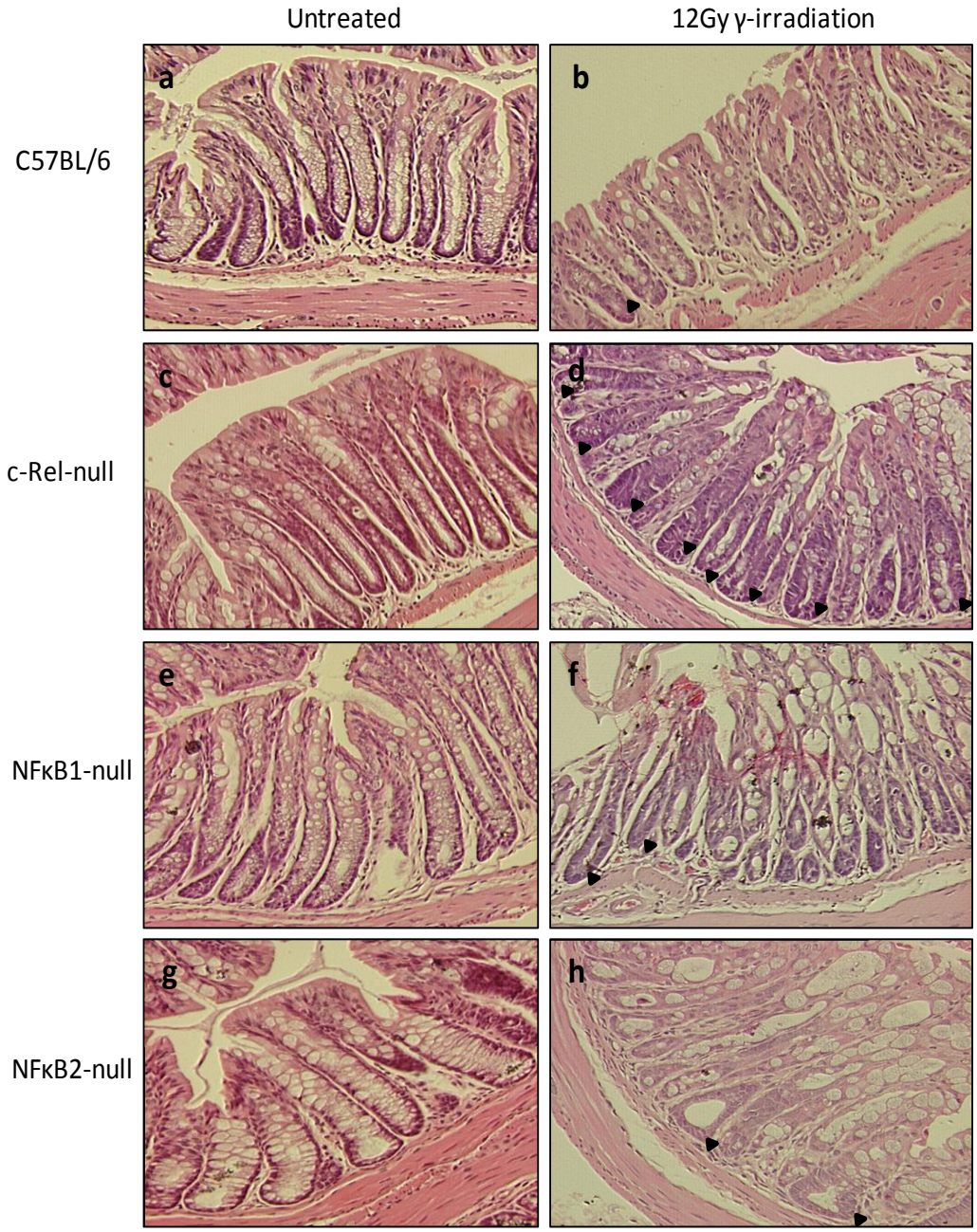

Figure 5.11: Representative photomicrographs showing colonic crypt regeneration in mice subjected to 12Gy γ-irradition and killed 96 hours later along with untreated mice. Histological assessment (H/E) of colonic sections taken from C57BL/6 (a, b), C-Rel-null (c, d), NFκB1-null (e, f) and NFκB2-null (g, h) mice. Mice were either untreated (a, c, e, g) or subjected to 12 Gy γ-irradition and sacrificed 96 hours later (b, d, f, h). Regenerating colonic crypts in irradiated mice are indicated by arrowheads.

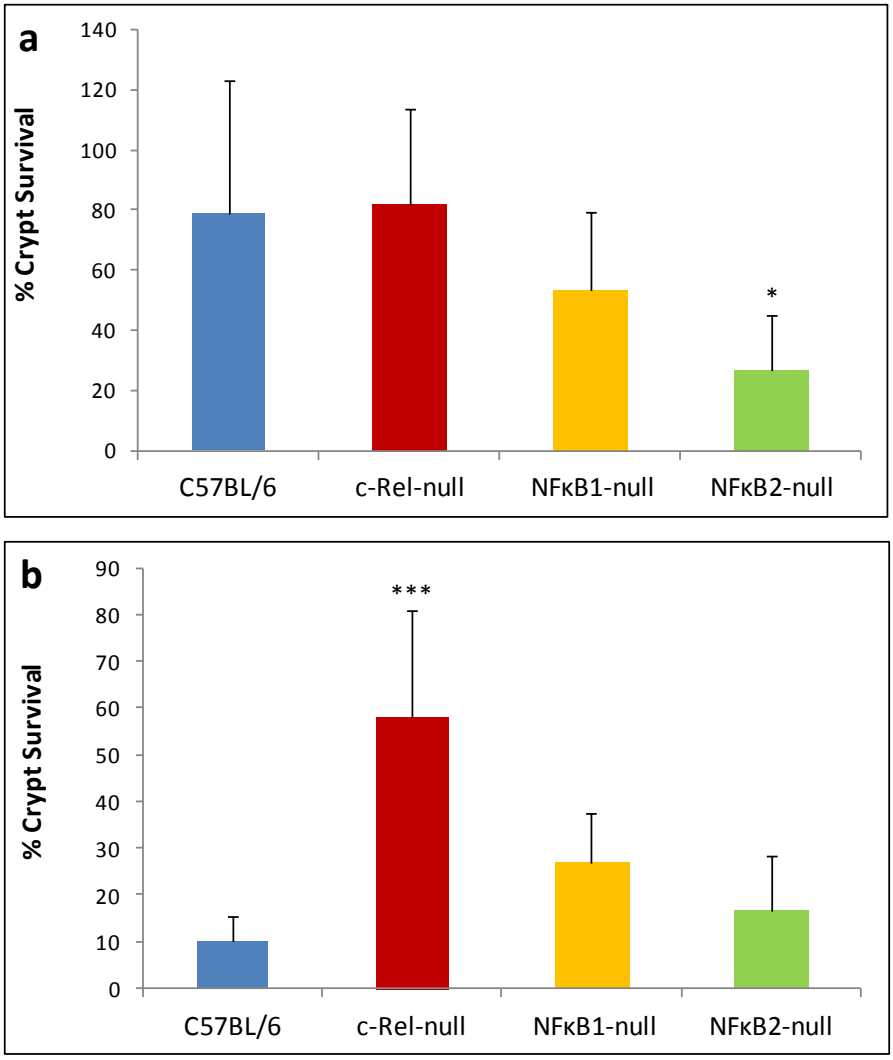

Figure 5.12: Small intestinal and colonic crypt survival in mice 96 hours after 12Gy γ-irradiation. Small intestinal crypt survival (a) and colonic crypt survival (b) in different genotypes of mice as indicated above 96 hours following 12 Gy of γ-irradiation. Statistical differences assessed by one way ANOVA and Dunnett's multiple comparison test (*$p<0.05$, ***$p<0.001$ compared to C57BL/6). (n=5 male mice per genotype).

5.5 Effects of deleting specific NFκB family members on intestinal epithelial mitosis and apoptosis 8 and 24 hours following carcinogen (azoxymethane) administration

Given the importance of apoptosis and proliferation in carcinogenesis, intestinal epithelial apoptosis and mitosis were assessed at 8 and 24 hours following administration of the carcinogen azoxymethane (AOM). These initial responses of intestinal epithelial cells to the carcinogen at two different time points might reveal the principal cellular mechanisms responsible for the altered susceptibility to colitis associated carcinogenesis observed in mice deficient in various NFκB family members. This possibility is supported by the observations from NFκB1-null and NFκB2-null mice shown in chapter 3. We demonstrated increased susceptibility to intestinal epithelial apoptosis in these genotypes of mice following γ-irradiation and irinotecan. Therefore, a single dose of 10mg/kg carcinogen (AOM) was injected intraperitoneally into all groups of mice. Small intestinal and colonic epithelial mitosis and apoptosis were assessed 8 and 24 hours following (6 male mice per genotype group at each time point).

5.5.1 NFκB2-null mice were more susceptible to small intestinal epithelial apoptosis at both 8 and 24 hours following AOM treatment

Small intestinal crypt epithelial apoptosis and mitosis were quantified from H and E stained small intestinal sections from mice killed either at 8 or 24 hours after 10mg/kg AOM. Mitosis was observed mainly in the lower 2/3 of small intestinal crypts and was suppressed in all strains of mice 8 and 24 hours following AOM treatment (see the basal levels of small intestinal mitosis in chapter 3). No

significant differences were observed between any of the genotypes of mice (Figure 5.13). Small intestinal crypt epithelial apoptosis was induced in all strains of mice at both 8 and 24 hours following AOM (see the basal levels of small intestinal apoptosis in chapter 3) and maximum apoptosis were observed at cell position 5. Only NFκB2-null mice showed a significant increase in the amount of small intestinal crypt apoptosis and this was observed at both 8 and 24 hours following AOM compared to similarly treated C57BL/6 mice. Significant differences in apoptotic scores were observed at cell positions 2 to 14 and 3 to 17 at the 8 and 24 hour time points respectively in NFκB2-null small intestine relative to wild-type mice following the same treatment by the modified median test (Figure 5.14).

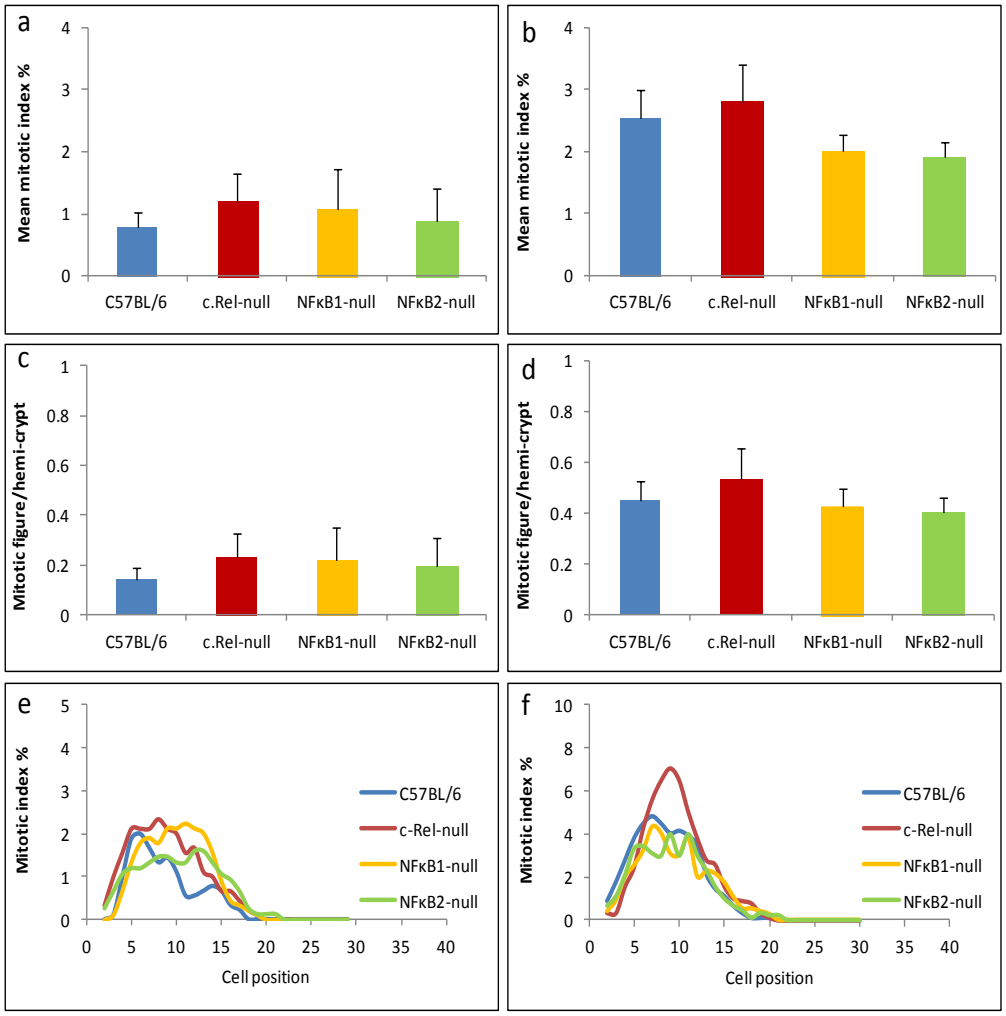

Figure 5.13: Quantitative analysis of small intestinal crypt epithelial mitosis 8 and 24 hours after 10mg/kg AOM (i.p). Mean mitotic index 8 hours (a) and 24 hours (b) following 10mg/kg AOM in small intestine separated by genotype as indicated above. Mean number of mitotic figures per hemi-crypt 8 hours (c) and 24 hours (d) following 10mg/kg AOM in small intestine separated by genotype as indicated above. Cell positional distribution of mitotic scores 8 hours (e) and 24 hours (f) following 10mg/kg AOM in small intestine separated by genotype as indicated above. Statistical differences were assessed by Kruskal–Wallis test followed by Dunn's multiple comparison tests in (a), (b), (c) and (d). Statistical differences were assessed by modified median test in (e) and (f). (n=6 per genotype group).

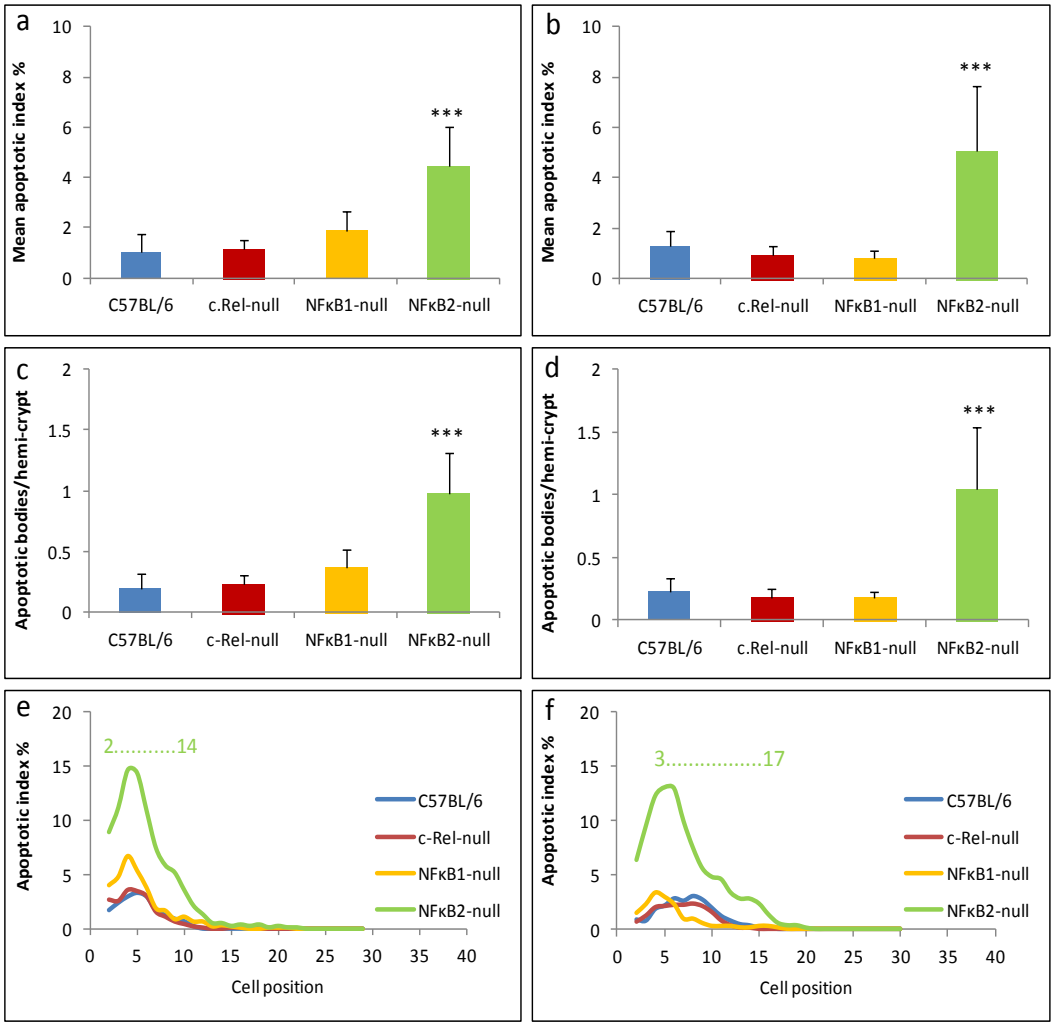

Figure 5.14: Quantitative analysis of small intestinal crypt epithelial apoptosis 8 and 24 hours after 10mg/kg AOM (i.p). Mean apoptotic index 8 hours (a) and 24 hours (b) following 10mg/kg AOM in small intestine separated by genotype as indicated above. Mean number of apoptotic events per hemi-crypt 8 hours (c) and 24 hours (d) following 10mg/kg AOM in small intestine separated by genotype as indicated above. Cell positional distribution of apoptotic scores 8 hours (e) and 24 hours (f) following 10mg/kg AOM in small intestine separated by genotype as indicated above. Statistical differences were assessed by one way ANOVA and Dunnett's multiple comparison tests in (a), (b), (c) and (d) (**p<0.01, ***p<0.001 compared to C57BL/6). Statistical differences were assessed by modified median test in (e) and (f). Dashed line denotes cell positions over which there was a significant difference in apoptotic scores compared to wild-type. Colour of dashed line denotes comparison genotype (n=6 per genotype group).

5.5.2 c-Rel-null mice showed persistent colonic epithelial mitosis and NFκB2-null mice showed increased colonic epithelial apoptosis at 8 and 24 hours following AOM treatment

Following administration of 10mg/kg AOM to C57BL/6, c-Rel-null, NFκB1-null and NFκB2-null mice, distal colons were harvested after either 8 or 24 hours. The amounts of colonic crypt epithelial mitosis and apoptosis were again quantified using H and E stained sections. Mitosis was suppressed in all strains of mice at both time points compared to the corresponding untreated similar strain of mice (see the basal colonic mitosis in chapter 3) and mitosis was mainly observed in the lower half of colonic crypts. However, colonic epithelial mitosis was suppressed to a lesser extent in c-Rel-null mice and remained significantly higher than similarly treated C57BL/6 mice by 4- fold at the 8 hour time point and 2.5-fold at the 24 hour time point. The significant differences in mitotic scores in c-Rel-null colon were observed at cell positions 10 to 12 at the 8 hour time point and 5 to 10 at the 24 hour time point using the modified median test (Figure 5.15). These findings of persistent elevated mitosis observed in c-Rel-null colon at two different time points following AOM administration are compatible with the increased colonic crypt regeneration observed in c-Rel-null mice following irradiation compared to similarly treated wild-type mice. Both NFκB1-null and NFκB2-null mice did not show any changes in colonic epithelial mitosis at 8 and 24 hours following AOM compared to wild-type mice following the same treatment (Figure 5.15).

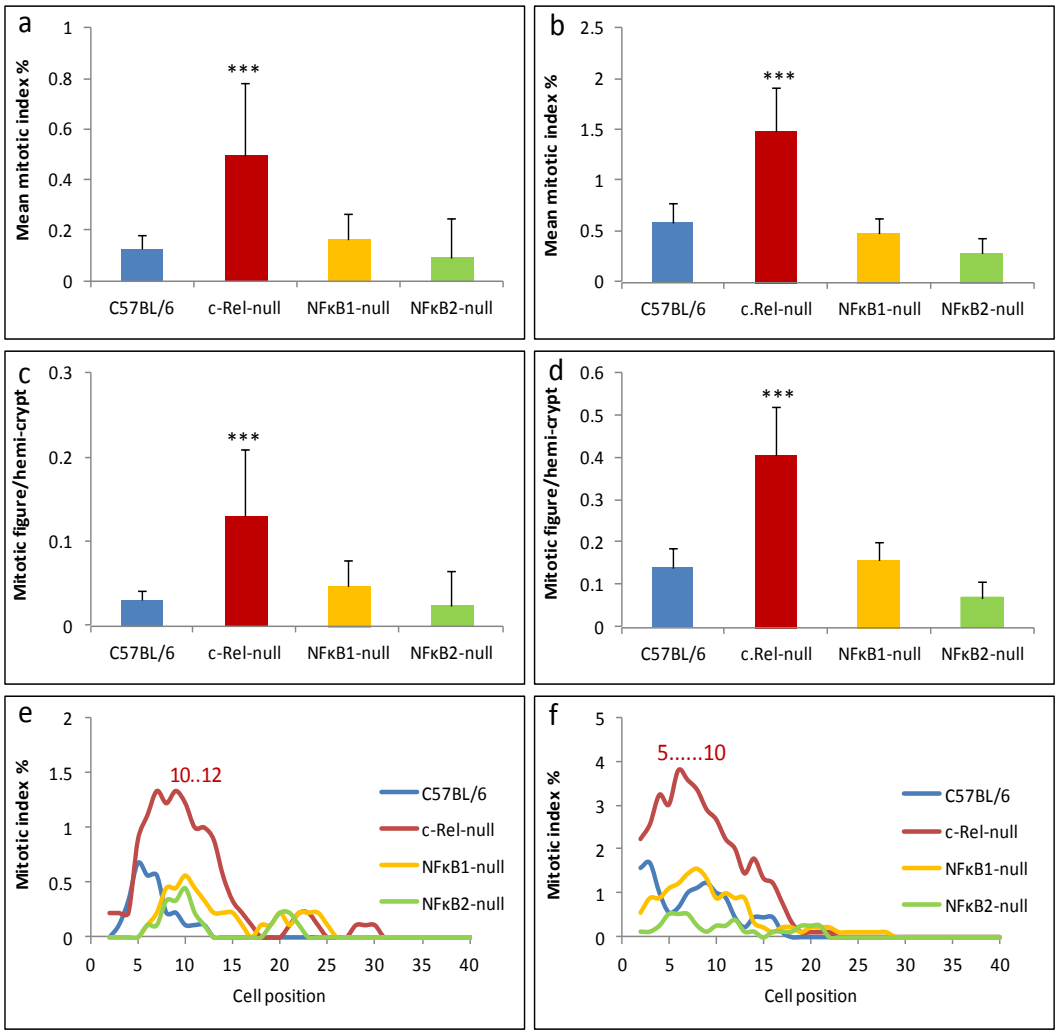

Figure 5.15: Quantitative analysis of colonic crypt epithelial mitosis 8 and 24 hours after 10mg/kg AOM (i.p). Mean mitotic index 8 hours (a) and 24 hours (b) following 10mg/kg AOM in the colon separated by genotype as indicated above. Mean number of mitotic figures per hemi-crypt 8 hours (c) and 24 hours (d) following 10mg/kg AOM in the colon separated by genotype as indicated above. Cell positional distribution of mitotic scores 8 hours (e) and 24 hours (f) following 10mg/kg AOM in the colon separated by genotype as indicated above. Statistical differences were assessed by one way ANOVA and Dunnett's multiple comparison tests in (a), (b), (c) and (d) (*$p<0.05$, ***$p<0.001$ compared to C57BL/6). Statistical differences were assessed by modified median test in (e) and (f). Dashed line denotes cell positions over which there was a significant difference in mitotic figures compared to wild-type. Colour of dashed line denotes comparison genotype (n=6 per genotype group).

AOM-induced colonic crypt epithelial apoptosis occurred predominantly at the crypt base in all strains of mice. Similar to observations in the small intestine, NFκB2-null mice also showed a significant increase in susceptibility to colonic apoptosis at both 8 (as determined by increased mean apoptotic events per hemi-crypt) and 24 hour time points following AOM relative to their wild-type counterparts following the same treatment. Significant differences in apoptotic scores were also observed at cell positions 5 to 9 at 8 hours following AOM in NFκB2-null colon relative to wild-type mice using the modified median test (Figure 5.16). However, disruption of the classical NFκB activation pathway by deleting c-Rel but not NFκB1 resulted in a significant decrease in colonic crypt apoptosis at 24 hours following AOM compared to similarly treated wild-type mice (Figure 5.16).

In summary therefore, c-Rel deletion was associated with increased colonic epithelial mitosis at the 8 hour and 24 hour time points and decreased colonic epithelial apoptosis at the 24 hour time point following carcinogen (AOM) administration. NFκB2 deletion was associated with increased small intestinal and colonic epithelial apoptosis at both 8 and 24 hour time points following AOM administration.

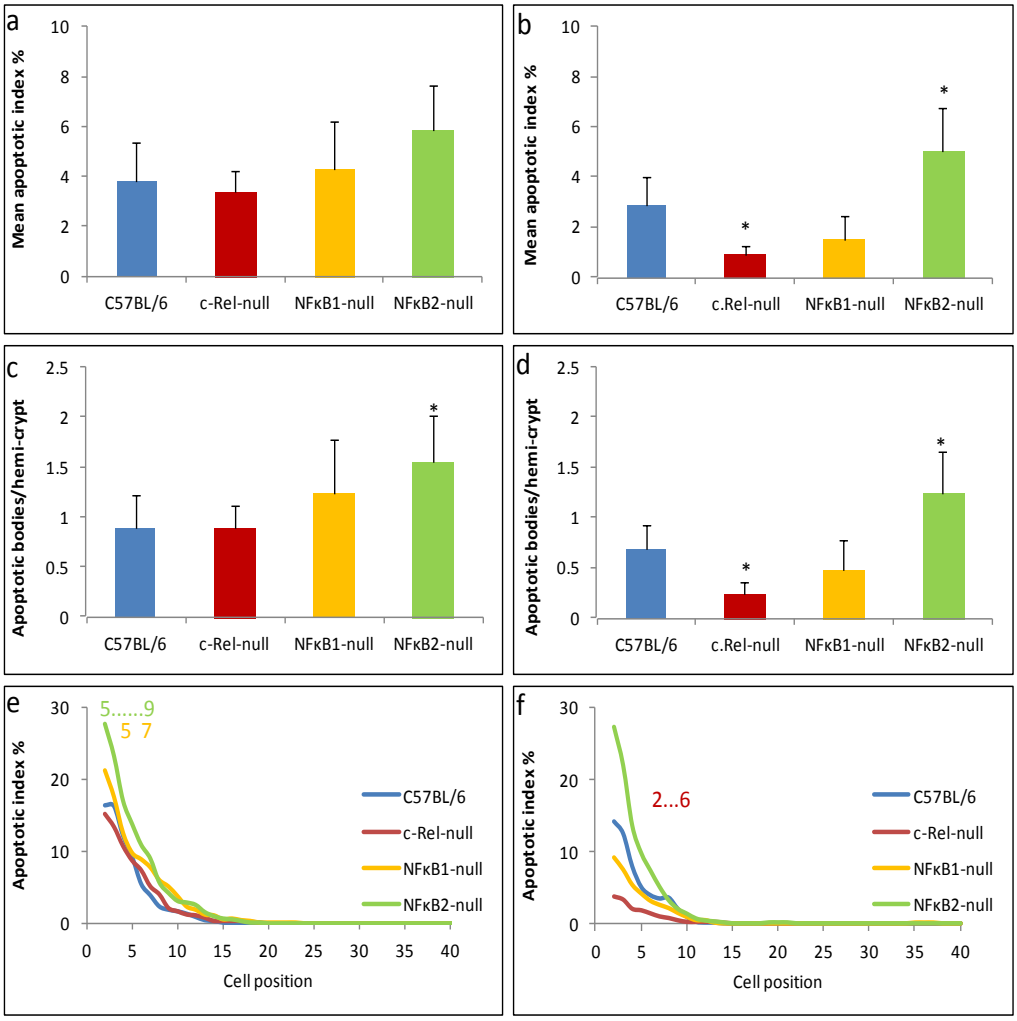

Figure 5.16: Quantitative analysis of colonic crypt epithelial apoptosis 8 and 24 hours after 10mg/kg AOM (i.p). Mean apoptotic index 8 hours (a) and 24 hours (b) following 10mg/kg AOM in the colon separated by genotype as indicated above. Mean number of apoptotic scores per hemi-crypt 8 hours (c) and 24 hours (d) following 10mg/kg AOM in the colon separated by genotype as indicated above. Cell positional distribution of apoptotic scores 8 hours (e) and 24 hours (f) following 10mg/kg AOM in the colon separated by genotype as indicated above. Statistical differences were assessed by one way ANOVA and Dunnett's multiple comparison tests in (a), (b), (c) and (d) (*$p<0.05$ compared to C57BL/6). Statistical differences were assessed by modified median test in (e) and (f). Dashed line denotes cell positions over which there was a significant difference in apoptotic scores compared to wild-type. Colour of dashed line denotes comparison genotype (n=6 per genotype group).

5.6 Discussion

The findings in this chapter have shown that deleting either c-Rel or NFκB1 from the germline of mice was associated with increased severity of colitis following DSS administration. However, only deletion of c-Rel was associated with a significant increase in the number of colonic tumours and these were also larger than those observed in wild-type mice following administration of the colitis associated tumour regimen. On the other hand, NFκB2 deletion resulted in a marked reduction in the severity of colitis and an associated decrease in both the number and size of colonic tumours compared to wild-type mice following administration of the same colitis associated tumour regimen. Nowadays, a positive correlation between inflammation and cancer in many tissues is widely accepted. This relationship is particularly evident in the human gastrointestinal tract where ulcerative colitis and Crohn's disease are both associated with an increased risk for developing colon cancer (153, 344, 345). This positive relationship between IBD and colon cancer has also been demonstrated in animal models of colitis associated colon cancer (346-348). Consistent with these observations, the marked decrease in the severity of DSS-induced colitis observed in NFκB2-null mice was associated with a substantial reduction in tumour load, and the increased severity of colitis observed in c-Rel-null mice was associated with an increased colonic tumour load.

Several previous reports have described a pro-inflammatory role for NFκB in the intestine (267, 349). However, several recent studies have also demonstrated an anti-inflammatory function of NFκB in the colon. For instance, it has been demonstrated that selective disruption of the classical NFκB activation pathway by

deleting IKK-β specifically in intestinal epithelial cells resulted in increased severity of DSS-induced colitis (268). Moreover, Greten *et al* (250) showed that selective deletion of IKK-β (resulting in disruption of the classical NFκB activation pathway) in either intestinal epithelial or myeloid cells exacerbated the severity of DSS-induced colitis and resulted in a marked reduction in tumour incidence in a mouse model of colitis associated cancer. In relation to the role of classical NFκB activation pathway in regulating intestinal inflammation, the results of these studies correlate with our findings that have shown increased colitis severity following administration of DSS alone (as described in chapter 4) or AOM plus DSS in both c-Rel-null and NFκB1-null mice. In contrast to the decreased susceptibility to colitis associated cancer observed in animals with either IKK-β deficiency in intestinal epithelial or myeloid cells as described by Greten *et al* (250), we have demonstrated that disruption of the classical NFκB activation pathway by germline deletion of c-Rel but not NFκB1 was associated with an increased susceptibility to colitis associated carcinogenesis.

Colorectal carcinogenesis can be divided into three stages: tumour initiation, tumour promotion and tumour progression. At tumour initiation, cellular DNA is mutated, resulting in activation of proto-oncogenes and inhibition of tumour suppressor genes. This initiated cell then enters into a tumour promotion phase which is characterised by increased cell proliferation and/or decreased apoptosis. The third stage of carcinogenesis is tumour progression which involves invasion, metastasis and an increase in tumour size (177, 348). It has been shown that inflammation may affect all these stages of tumourigenesis in various ways. Several pro-inflammatory cytokines such as TNF-α, IL-1 and IL-6, whose transcriptional

expressions are regulated by the classical NFκB activation pathway, have been shown to contribute to tumour development (350). Several previous studies which have used various murine models of inflammation associated cancer have shown that NFκB's ability to enhance tumour growth can also be attributed to its role in modulating the tumour microenvironment via the transcriptional induction of inflammatory mediators such as pro-inflammatory cytokines (175, 351).

The study of inflammation associated cancer conducted by Greten *et al* (250) and discussed above suggested that the IKK-β-dependent NFκB activation pathway links inflammation to cancer in the colon, and also explored the mechanisms by which inflammation enhances tumour promotion and progression. The authors of this paper demonstrated that IKK-β-dependent NFκB activation in the epithelium promoted carcinogenesis by inhibiting apoptosis in chemically induced premalignant cells. However, IKK-β-dependent NFκB activation in myeloid cells enhanced the production of pro-inflammatory cytokines (such as IL-1β and IL-6) in order to influence tumour promotion in colitis associated cancer. Our findings show that global disruption of the classical NFκB activation pathway by germline deletion of c-Rel but not NFκB1 resulted in a significant increase in the number and size of colonic tumours in a murine model of colitis associated cancer. Consistent with this increased tumour incidence, c-Rel-null mice also demonstrated increased severity of colitis. We investigated whether this was related to altered tumour cell proliferation and detected a significant increase in proliferation (Ki67) index in tumours from c-Rel-null mice compared to those from their wild-type counterparts.

IKK-β is an upstream component of the classical NFκB activation pathway compared to the NFκB family members c-Rel and NFκB1. Therefore, IKK-β deletion can globally affect all downstream components of the classical NFκB activation pathway. This may partially explain the differences between the effects of deleting IKK-β and deleting the classical NFκB family members c-Rel and NFκB1 during colitis associated carcinogenesis.

On the other hand, disrupting the alternative NFκB activation pathway by deleting NFκB2 resulted in a substantial reduction in the severity of colitis and in the number and size of colonic tumours compared to wild-type mice following administration of the colitis associated tumour regimen. This finding represents the first direct evidence for an important role for the alternative NFκB activation pathway in regulating inflammation associated carcinogenesis in the colon. This finding of reduced susceptibility to the effects of AOM/DSS is consistent with our observations in the acute experimental colitis model following administration of DSS alone as described in chapter 4. Additionally, we detected reduced transcriptional expression of the pro-inflammatory cytokine TNF-α and increased transcriptional expression of the anti-inflammatory cytokine IL-4 in NFκB2-deficent colon 6 days following 2% DSS administration. In a recent study, in addition to its role in colitis, TNF-α has been shown to be directly implicated in the development of colitis associated carcinogenesis (343). Given the importance of inflammation and the direct role of the pro-inflammatory cytokine TNF-α in colitis associated carcinogenesis, the reduced colonic tumour number and size observed in NFκB2-null mice following AOM/DSS administration may possibly result from impaired

production of TNF-α and overproduction of IL-4. This hypothesis could be further investigated by assessing the mRNA and/or protein expression of these along with other cytokines in all strains of mice following AOM/DSS administration.

A previous study that explored the anti-inflammatory role of NLR family pyrin domain containing 12 (Nlrp12) protein in the colon conducted by Zaki *et al*. The researchers in this study showed that the increased colonic inflammation and tumour burden observed in Nlrp12-deficient mice was associated with increased activity of the classical NFκB activation pathway (352). These observations were also confirmed in a recent publication by Allen *et al* (353). However, in agreement with our observations, this study also showed that the increased colonic inflammation and tumour burden observed in *Nlrp12*-deficient mice was associated with increased activation of the alternative NFκB pathway (353). The authors suggested that Nlrp12, through its interaction with NIK and subsequent interference with the processing of the precursor form of NFκB2 (p100) to generate the active form p52, represents a robust negative regulator of the alternative NFκB activation pathway, and that the modest in increase in classical NFκB signalling following Nlrp12 loss may be mediated by the fact that the alternative NFκB activation pathway can influence the classical NFκB activation pathway via IKK-α and TRAF3-dependent mechanisms (353-355).

Enhanced cell proliferation and escape from apoptosis are the key features of neo-plastic transformed cells during the tumour promotion phase. Indeed the chemopreventive properties of several drugs are mainly based on their ability to induce apoptosis during the tumour promotion stage. As already discussed, the

NFκB family of transcription factors are considered to be major regulators of apoptosis and cell cycle progression (241, 356). Therefore, it appears that in addition to its crucial role in inflammation induced tumour promotion, NFκB plays an important role in tumour promotion by regulating cell apoptosis and proliferation. We firstly used a crypt regeneration assay as a tool to measure crypt intestinal epithelial cell proliferation in different strains of mice. NFκB2 deficient mice showed reduced crypt regeneration in the small intestine while c-Rel deficient mice demonstrated a marked increase in crypt regeneration in the colon 96 hours following 12Gy γ-irradiation. This suggests that NFκB2 loss suppresses epithelial cell proliferation in the small intestine whereas c-Rel loss enhances epithelial cell proliferation in the colon following injury. Thus the increased tumour incidence in c-Rel-null mice may be caused by enhanced colonic epithelial cell proliferation following exposure of these animals to the AOM/DSS regimen.

Thus, we also measured intestinal crypt epithelial mitosis and apoptosis at two different time points following carcinogen (AOM) administration. In the small intestine, no alterations in mitotic indices were observed between any genotype of mice at either 8 or 24 hour time points following AOM administration. However in the colon, c-Rel-null mice showed a marked increase in epithelial mitosis at both 8 and 24 hour time points and an associated inhibition of colonic epithelial apoptosis 24 hours following carcinogen (AOM) administration relative to their wild-type counterparts. These findings suggest that the increased tumour load observed in c-Rel-null mice may also be mediated by the increased proliferation and suppressed apoptosis of epithelial cells following initiation by the carcinogen. Therefore, the

increased susceptibility of c-Rel-null mice to colitis associated carcinogenesis may be mediated by two mechanisms. The first is related to the ability of c-Rel to suppress proliferation and induce apoptosis of pre-neoplastic cells initiated by the carcinogen and to its suppression to proliferation within AOM/DSS induced tumours. The second mechanism is attributed to the ability of c-Rel to suppress inflammation which subsequently inhibits tumour promotion and progression.

NFκB2-null mice showed significant increases in small intestinal and colonic crypt epithelial apoptosis at both 8 and 24 hours following AOM compared to similarly treated C57BL/6 mice. In addition to the reduced severity of colitis observed in NFκB2-null mice, these findings provide an additional mechanism which may contributed to the reduced tumour incidence observed in NFκB2-null mice. During colorectal carcinogenesis, deleting DNA-damaged cells by apoptosis represents a key mechanism for reducing the load of mutated cells and this subsequently reduces the risk of neoplastic transformation and cancer formation (357, 358). Various published studies have suggested that non-steroidal anti-inflammatory drugs (NSAID) reduce the risk of colon cancer via various mechanisms. One of these is by induction of cell apoptosis (282, 342, 359-361). This supports our suggestion that the increased AOM-induced apoptosis observed in the intestinal epithelia of NFκB2-null mice is a second cellular mechanism which contributes to the reduced tumour incidence observed in this genotype of mice.

Taken together, the results presented in this chapter suggest that disruption of the classical NFκB activation pathway particularly by deleting c-Rel increases susceptibility to developing colitis and colitis associated carcinogenesis. Along with

our observations in chapter 4, this provides additional evidence for an anti-inflammatory function of the classical NFκB activation pathway in the colon. In addition to increased colonic inflammation, enhanced proliferation and suppressed apoptosis of tumour initiated cells are likely to be cellular mechanisms which contribute to the increased tumour number and size which was observed in c-Rel-null animals. Together, these studies clearly indicate that inhibition of the classical NFκB activation pathway in the colon might lead to serious consequences and that classical NFκB activation pathway inhibitors as a therapy for IBD are unlikely to be helpful. Conversely, abrogation of the alternative NFκB activation pathway by deleting NFκB2 dramatically protected animals from developing colitis and colitis associated carcinogenesis following AOM/DSS administration. The reduced number and size of tumours observed in the colon of NFκB2-null mice might be explained by the increased apoptosis of tumour initiated cells and reduced severity of colonic inflammation observed in these animals following AOM and DSS administrations respectively. Hence, we suggest that specific inhibition of NFκB2 may be a promising therapeutic strategy for treating IBD and might also reduce the risk of cancer development in such patients. It would however first be useful to determine the individual contributions of epithelial and immune cells towards the altered susceptibility to colitis associated carcinogenesis observed in c-Rel-null and NFκB2-null mice. Bone marrow chimaeras and transgenic technology are possible methods for investigating these mechanisms. This might help to determine the optimal approach for NFκB2 inhibition as a therapy for IBD and as a chemopreventive agent for colitis associated cancer. This may avoid unnecessary inhibition of NFκB2 in other cell types where NFκB2 activity may be protective against inflammation

rather than having a pro-inflammatory function. Although alterations in cell proliferation and survival have been identified as cellular mechanisms likely to be responsible for the altered susceptibilities to colitis associated carcinogenesis observed in c-Rel-null and NFκB2-null animals, the precise molecular mechanisms have not yet been investigated. It would therefore also be interesting to assess the expression of various cell cycle and apoptosis regulating genes in these genotypes of mice following carcinogen (AOM) administration as previously described in chapters 3 and 4 following administration of γ-irradiation and DSS.

6 Discussion

6.1 Main findings and subsequent concepts

It is now widely accepted that the NFκB family of transcription factors is a major regulator of various physiological and pathological processes such as proliferation, apoptosis, inflammation and carcinogenesis (202, 362, 363). Evidence from numerous studies has indicated that the pro-inflammatory role, particularly of the classical NFκB activation pathway is implicated in the pathogenesis of inflammatory bowel diseases. However, several recent studies which have investigated the effects of disrupting upstream components of this pathway have provided compelling evidence for a new paradigm of contradictory cytoprotective and pro-inflammatory functions of classical NFκB signalling in the intestine. However, the specific role of the alternative NFκB activation pathway and the functions of individual members of the NFκB family in regulating the susceptibility of the intestine to apoptosis, inflammation and carcinogenesis have not been well defined to date. We therefore aimed to investigate the specific roles of individual members of NFκB family of transcription factors in regulating intestinal epithelial cell turnover at baseline and in response to two types of injury *in vivo* and one type of cellular injury *in vitro*. Given that epithelial cell survival and proliferation are critical processes that influence intestinal inflammation and colorectal carcinogenesis, the roles of individual members of NFκB family in regulating intestinal inflammation and its associated carcinogenesis were also assessed. Most of the aims of this thesis were addressed using various mice that were deficient in individual NFκB family members.

6.1.1 Effects of deleting specific NFκB family members of the classical activation pathway

Deleting the classical NFκB family member NFκB1 resulted in elongation of murine small intestinal and colonic crypts, while deleting c-Rel resulted only in elongation of colonic crypts under baseline physiological conditions. These findings are in keeping with a previous study by Inan *et al* who demonstrated that NFκB1-null mice had longer colonic crypts and a more extensive proliferative zone than their wild-type counterparts (230). Although this thesis showed reduced relative mRNA expression of several anti-apoptotic genes in the intestinal epithelia of untreated NFκB1-null mice, I was not able to detect any changes in basal amounts of apoptosis in these genotypes of animals relative to their wild-type counterparts.

8Gy γ-irradiation has previously been shown to cause a 219-fold increase in NFκB activity in the small intestinal epithelia of wild-type mice and this activation occurs mainly through classical NFκB pathway signalling, which is dominated by p50/RelA heterodimers (229). Disruption of this pathway by deleting either NFκB1 (229) or IKKβ (251) sensitised the small intestinal epithelia of these animal to irradiation-induced apoptosis compared to similarly treated wild-type mice. In agreement, the small intestinal epithelial cells of NFκB1-null mice in this thesis were highly susceptible to undergoing apoptosis 4.5 hours following 8Gy γ-irradiation relative to similarly treated wild-type mice. Although NFκB activation has not previously been quantified in colonic epithelia following γ-irradiation (229), we also showed that deleting NFκB1 sensitised colonic epithelia to irradiation-induced apoptosis. In keeping with these observations from irradiation experiments, NFκB1-null mice

were also more susceptible than wild-type mice to irinotecan induced intestinal epithelial apoptosis in both the small intestine and colon and at both the 6 and 48 hour time points. However, disruption of the classical NFκB activation pathway by deleting c-Rel did not cause any alterations in the amount of epithelial apoptosis observed in either the small intestine or colon following either γ-irradiation or irinotecan administration compared to wild-type mice. We also observed increases in the expression of the pro-apoptotic genes TRAIL and Caspase12 in the small intestine and TRAIL in the colon of NFκB1-null mice following irradiation compared to wild-type mice after the same treatment. This provides evidence for a possible molecular mechanism by which increased susceptibility to intestinal epithelial apoptosis is induced in NFκB1-null mice following irradiation and suggests that these observations of increased susceptibility to intestinal epithelial apoptosis seen in NFκB1-null mice are due to specific effects of the NFκB1 subunit and not due to general classical pathway disruption effects.

In the context of acute inflammation, deleting either NFκB1 or c-Rel resulted in a significant increase in the severity of DSS-induced colitis. This was evident using both clinical and histological criteria. At the molecular level, NFκB1-null mice showed significant up-regulation in the transcriptional expression of the pro-inflammatory cytokines IL-1β and IL-6 in the colon following DSS administration relative to similarly treated wild-type mice. The early onset of increased severity of colitis that was observed in NFκB1-null mice correlates with the hypersusceptibility of intestinal epithelial cells to undergoing apoptosis following induction of cellular injury in this strain of mice as discussed above. Thus, disruption of the intestinal

epithelial barrier by increased intestinal epithelial apoptosis as an initial response to DSS and the consequent increase in exposure of mucosal immune cells to the luminal contents of the colon and enhanced cytokine production might be plausible explanations for the increased clinical severity of colitis which was observed in NFκB1-null mice. In agreement with our observations from mice with abrogated classical NFκB signalling, it has previously been shown that specific IKKβ deletion in intestinal epithelial cells resulted in increased inflammation in the DSS-induced colitis model (250, 268). Similarly, Greten *et al* (312) showed that selective IKK-β deletion in myeloid cells or its specific pharmacological inhibition enhanced LPS toxicity and mortality. Despite reduced mRNA expression of IL-1β 4 hours following LPS administration in IKK-β deficient macrophages, increased secretion of IL-1β into the plasma by these macrophages was due to the enhanced processing of pro-IL-1β to IL-1β and a subsequent increase in the secretion of IL-1β. This mechanism appears to be different from the mechanism responsible for the increased mRNA expression of IL-1β in NFκB1-null colon following DSS treatment.

Unlike NFκB1-null mice, c-Rel-null mice showed a relatively late onset of increased severity of colitis and they did not show any altered susceptibility toward irradiation or irinotecan induced intestinal epithelial apoptosis. Hence, the molecular mechanisms responsible for increased susceptibility of c-Rel deficient mice to DSS-induced colitis may be different from those observed in NFκB1-null mice. In addition to maintaining intestinal barrier integrity as an anti-inflammatory function, there is evidence that NFκB activity can contribute to the resolution of an inflammatory response. Inhibition of this late stage of NFκB activity has been shown to inhibit the

apoptosis of infiltrating immune cells and prolong the inflammatory response (313, 363). Based on the observations that (a) c-Rel is mainly expressed at high levels in hematopoietic cells and only at low levels in epithelial cells (364), (b) c-Rel deletion did not increase the susceptibility of intestinal epithelial cells to undergo apoptosis following two types of injury, and (c) the relatively late onset of increased severity of DSS induced colitis that was observed in c-Rel-null mice relative to NFκB1-null mice, we suggest that the increased susceptibility of c-Rel deficient mice to DSS-induced colitis may be immune-cell mediated rather than due to the initial intestinal epithelial damage response to DSS. In the skin, loss of NFκB dependent c-Rel and RelA activation has also been shown to result in the development of several inflammatory skin lesions (365). In humans, several recent studies have reported associations between REL (82, 320, 321) (the human gene which encodes c-Rel) and NFκB1 polymorphisms (315, 316) and IBD. However, it is not clear whether the IBD associated with these SNPs is caused by either altered expression or function of the c-Rel and NFκB1 proteins (364).

In the AOM/DSS murine model of inflammation related colonic carcinogenesis, our data clearly showed that deleting the classical NFκB family members c-Rel or NFκB1 resulted in an increase in the severity of colitis, and this was more profound in the case of c-Rel loss. These results reinforce our findings in the acute DSS-induced colitis model and suggest anti-inflammatory roles for c-Rel and NFκB1 subunits in the intestine. However, c-Rel-null but not NFκB1-null mice also showed a marked increase in the number and size of colonic tumours following administration of AOM/DSS. Congruent with the increased tumour number and size which was

observed in c-Rel-null mice, c-Rel deficient colonic tumours showed higher proliferation indices and a greater percentage of these tumours showed high-grade dysplasia compared to those arising in their wild-type counterparts. c-Rel-null colon also showed enhanced epithelial proliferation and reduced epithelial apoptosis following carcinogen (AOM) administration. In addition colonic crypt regeneration was significantly increased in c-Rel-null colon following γ-irradiation. These altered cellular responses following c-Rel deletion might explain the enhanced inflammation associated colorectal carcinogenesis that we observed in c-Rel-null but not NFκB1-null mice. Conversely, it has previously been shown that deleting an upstream component of the classical NFκB activation pathway (IKK-β) selectively in either intestinal epithelial or immune cells resulted in a marked reduction in tumour load following administration of the AOM/DSS regimen despite more severe colitis being observed following administration of high doses of DSS. This reduction in tumour load was attributed to increased apoptosis of IKK-β deficient enterocytes and reduced colonic expression of several cytokines in the case of IKK-β deletion from immune cells (250). These observations from either IKK-β deficient or NFκB1 deficient mice indicate that the increased susceptibility of c-Rel-null mice to inflammation associated colorectal carcinogenesis is due to specific and unique effects of the c-Rel subunit rather than to generic effects of disrupting the classical NFκB activation pathway.

6.1.2 Effects of deleting a NFκB family member of the alternative activation pathway

For the first time, this thesis has provided evidence for major role of the alternative NFκB activation pathway in regulating intestinal turnover. In addition to showing elongated small intestinal crypts, NFκB2-null small intestine showed a significant increase in the amounts of epithelial apoptosis in physiological conditions. This increased spontaneous apoptosis might be due to the reduced relative mRNA expression of the anti-apoptotic genes BCL2, BCL-XL, c-IAP2 and XIAP which we observed in NFκB2-null small intestine. For the first time, we have also provided evidence that alternative NFκB pathway signalling plays a crucial role in regulating DNA damage induced intestinal apoptosis following two different methods of cellular injury (physical and chemical). We showed increased susceptibility to both irradiation and irinotecan induced epithelial apoptosis in both the small intestine and colon of NFκB2-null mice. Similar to these *in vivo* observations in normal intestinal epithelial cells, *in vitro* findings also demonstrated that NFκB2 but not RelB inhibited apoptosis following a DNA damage inducing stimulus and promoted colon cancer cell proliferation. Significant increases in the expression of the pro-apoptotic genes Caspase12, BAK, p53 and FAS-L were found in the small intestine and Caspase12, TRAIL, and FAS-L in the colon of NFκB2-null mice following irradiation relative to similarly treated wild-type mice. These may therefore be some of the molecular mechanisms responsible for the increased susceptibility to irradiation induced epithelial apoptosis observed in NFκB2-null mice. The transcriptional regulation of Caspase12 expression by the NFκB family of transcription factors is a novel finding and is strongly supported by the observations

of up-regulated Caspase12 expression at two sites within the intestine (the small intestine and colon) and in both NFκB1-null and NFκB2-null strains of mice.

Although deleting either NFκB2 or NFκB1 were associated with a dramatic increase in intestinal epithelial apoptosis following two types of injury as discussed above, intriguingly deleting NFκB2, but not c-Rel or NFκB1 protected mice from developing colitis following DSS administration. This suggests that the anti-inflammatory effect of deleting NFκB2 may be mediated by mechanisms independent of initial intestinal epithelial damage. The reduced severity of colonic inflammation found in NFκB2-null mice following 2% DSS administration correlated with observations of reduced transcriptional expression of the pro-inflammatory cytokine TNF-α and increased transcriptional expression of the anti-inflammatory cytokine IL-4. Additionally, we have provided the first direct evidence for a crucial role of the alternative NFκB activation pathway in regulating inflammation associated carcinogenesis in the colon. We found a great reduction in the number and size of colonic tumours in NFκB2-null mice compared to their wild-type counterparts following administration of the AOM/DSS regimen. Data from a recently published study indirectly support our observation that activation of the alternative NFκB pathway promotes colonic inflammation and its associated colorectal carcinogenesis. This study showed that the increased colonic inflammation and tumour load that was observed in mice deficient in the anti-inflammatory protein Nlrp12 was associated with a marked increase in the activation of the alternative NFκB signalling pathway (353). Hence, we suggest that loss of the pro-inflammatory function of the alternative NFκB family protein NFκB2 is a plausible mechanism responsible for the reduced colonic

inflammation and protection against colitis associated colonic carcinogenesis that was observed in NFκB2-null mice.

In addition to the influence of inflammation, impaired apoptosis is an important cellular mechanism that contributes to carcinogenesis (47, 357). Thus, the increased intestinal epithelial apoptosis that was observed at both 8 and 24 hours in NFκB2-null mice following administration of the carcinogen AOM could be a second cellular mechanism that contributes to the reduced incidence of AOM/DSS induced colonic tumours. However, the molecular mechanisms responsible for this have not yet been fully identified. It has been shown that binding of membrane bound FAS-L to FAS (CD95) induces apoptosis (366, 367). A recent study (368) showed that the alternative NFκB activation pathway is a negative regulator of FAS expression and FAS-L induces apoptosis and inhibits the growth of various types of tumours specifically through the FAS receptor *in vitro*. Additionally, mice deficient in FAS have been shown to be more susceptible to developing 3-methylcholanthrene (MCA)-induced sarcoma and AOM/DSS-induced colorectal carcinoma (368). Our observations of marked increases in the relative mRNA expressions of FAS-L in the small intestine and colon of NFκB2-null mice following irradiation provide evidence that the alternative NFκB activation pathway is a negative regulator of the physiological ligand of FAS (FAS-L) *in vivo*. Hence, up-regulated intestinal expression of FAS-L may be one of the possible causes of the enhanced epithelial apoptosis and reduced tumour incidence that was seen in NFκB2-null mice following AOM/DSS administration.

6.2 Potential medical implications

Current anti-inflammatory drugs that are used to manage IBD such as steroids have multiple endocrine and metabolic side effects. Indeed, there is a large body of evidence which supports the notion that inhibition of NFκB can be a therapeutic target for treating IBD (349). For example the anti-inflammatory effects of many available general anti-inflammatory drugs such as glucocorticoids (369), aspirin (370), gold salts (371) and mesalazine (372) have been at least in part attributed to their ability to inhibit NFκB activity. However, recent studies have also shown that NFκB is protective in intestinal inflammatory conditions and its inhibition may therefore exacerbate these diseases (252, 268). To provide a more rational approach, it is essential to dissect the roles of specific NFκB family members in regulating the development of inflammation and inflammation associated carcinogenesis in the colon. The data in this thesis have for the first time shown differential and unique functions of individual NFκB family members in murine models of colitis and colitis associated colon cancer. Our results suggest that specific inhibition of NFκB2 may be a promising novel strategy to manage IBD and reduce the risk of cancer development in these patients. Once specific NFκB2 inhibitors have been developed, an ideal approach would be to target NFκB2 inhibition selectively in intestinal cells where NFκB2 appears to exert its major role in promoting intestinal inflammation and inflammation associated colorectal carcinogenesis. Such specific cell type administration of NFκB2 inhibitors may be possible in the future using nanotechnology approaches.

6.3 Limitations of presented studies and potential future approaches to resolve them

6.3.1 Limitations related to the animal models used

Germline deletion of specific NFκB family proteins in mice is a viable method for studying the various functions of these proteins in the complete organism. However, the presence of these deletions in all cell types in the animal from embryonic development does not permit assessment of the functions of individual members of NFκB family in specific cell types or at selected times. It is therefore not currently clear whether the decreased susceptibility to colitis observed in NFκB2-null mice or the increased susceptibility to colitis observed in c-Rel-null and NFκB1-null mice following DSS administration are due to epithelial and/or immune cell effects. Assessing the expression of c-Rel, NFκB1 and NFκB2 in murine colonic epithelia or immune cells following DSS treatment could help in identifying the responsible cellular mechanisms. Due to a lack of specificity of all commercially available anti-NFκB2 antibodies tested to date using immunohistochemistry and Western blotting in mice (M. Burkitt, unpublished data), we suggest that the EMSA technique may be required for assessing NFκB family member activation in nuclear preparations from whole colonic tissue, purified colonic epithelial cells and lymphocytes (sorted by flow cytometry). As discussed in previous chapters, selective tissue deletion of NFκB proteins either in intestinal epithelial or immune cells using transgenic technology or bone marrow transplantation chimaeras could also be utilised to address these important research questions. Additionally, inducible gene knockouts (108) could be utilised to define the roles of individual members of the NFκB family in intestinal epithelia at selected times of adulthood

and under selected physiological and pathophysiological conditions. For example, inducing NFκB2 gene disruption in adult murine intestinal epithelia might help to determine whether the reduced colorectal carcinogenesis observed in NFκB2-null mice is due to effects of NFκB2 deletion during the prenatal or postnatal period.

DSS-induced colitis in C57BL/6 mice has previously been validated as a relevant model to translate findings to human diseases and as such it is a useful model to identify and validate new therapies for treatment of IBD (109). The AOM/DSS model has also been shown to be a relevant model for colitis associated cancer in humans and has been described as a valuable and practical tool for investigating the pathogenesis of colitis associated colon cancer (194). However, the duration required for developing colitis and colitis associated cancer is relatively short in both these models. This appears to be a limiting factor for the relevance of these animal models to human disease. Development of colon cancer in IBD patients is thought to require a long period of chronic inflammation that results in accumulating epigenetic and genetic alterations to key proto-oncogenes and tumour suppressor genes (373). IL10-null mice which spontaneously develop colitis followed by cancer (374) could be a useful tool to study the consequences of a longer period colonic inflammation in a setting which may be closer to that observed in IBD patients. Thus, the current studies of colonic inflammation and its associated cancer could further extended by crossing our transgenic mice (c-Rel-null, NFκB1-null and NFκB2-null mice) with IL10-null mice. Given the importance of micrbiota in the pathogenesis of DSS induced colitis, the differences in susceptibility to DSS observed between the transgenic mice used in this thesis might be (at least

partially) due to the effects of deletion of specific NFκB proteins on gut micrbiota. Hence, future work should also study the consequences of deleting various NFκB family members on gut micrbiota.

6.3.2 Limitations related to the techniques employed

Mitotic index is a cheap, simple and relatively consistent way to measure a proliferation rate. Mitosis represents the shortest phase of the cell cycle, but it may not be possible to detect the early and late stages of this process using a light microscope. As a result, the absolute numbers of mitotic figures are much less than the numbers of proliferating cells determined by other methods such as immunohistochemical staining for Ki67 which marks all stages of a cycling cell (active proliferating cell) (375). It has also been reported that the duration of the mitotic phase is variable and therefore the correlation between mitosis and proliferation rate may not be linear (341, 376). These considerations might potentially explain our inability to detect any significant increases in proliferation as determined by mitotic figure counts in the elongated intestinal crypts of c-Rel-null and NFκB1-null mice relative to wild-type mice. It would therefore be helpful to perform immunohistochemical staining for Ki67 to investigate this further.

The HCT116 cell line originates from colonic epithelial cells and represents several biological aspects of normal colonic epithelial cells. In addition to the non-physiological conditions of the culture media in which these cells were maintained, this *in vitro* model also has the disadvantage that these cells have undergone several mutations in order to permit unlimited growth in culture. This is likely to have changed the biology and biochemical characteristics of the cells. This may

therefore affect the interpretation of any analysis. Unfortunately however, it is not currently possible to maintain long term cultures of non-transformed human colonic epithelial cells.

Assessing mRNA expression can give valuable information about possible molecular mechanisms that are involved in different processes. However, protein expression and ultimately protein function are also affected by post transcriptional and post translational modifications. Given that the proteins under investigation in this thesis belong to the transcriptional system, assessing mRNA can provide evidence for apparent functions of these transcriptional factors. However, it would also be interesting to further assess protein expression particularly of those genes which showed altered transcriptional expression in our studies.

6.4 Future research plans

Several potential future plans have already been discussed above and performing these experiments could help to answer several important research questions and elucidate the molecular mechanisms responsible for the different intestinal responses to injury that were observed between animals with specific deletions of individual NFκB proteins. Data in this thesis have demonstrated that NFκB signalling via NFκB2 is essential for the development of colitis and colitis associated cancer. Thus, it would be interesting to investigate the effect of administering antisense oligonucleotides for NFκB2 on the development of DSS induced colitis and AOM/DSS induced colon cancer using C57BL/6 mice.

The ultimate aim of our studies was to improve understanding of pathogenesis of inflammatory bowel disease and its associated colon cancer in humans. Therefore,

it is now necessary to extend these studies into humans. Several antibodies have been established and can be used to detect specific NFκB proteins in human cells. Such antibodies could therefore be utilised to quantify the activity of individual NFκB family proteins in colonic mucosal biopsy samples taken from patients with IBD or colonic tumour biopsies obtained from patients with colitis associated cancer using techniques such as EMSA. Real time PCR could also be used to assess mRNA expression of individual members of the NFκB family in these biopsy samples.

6.5 Conclusions

Findings from this thesis have demonstrated that individual members of the NFκB family of proteins play specific roles in regulating intestinal homeostasis and intestinal responses to various types of injury. NFκB1-dependent classical NFκB signalling is involved in the regulation of epithelial susceptibility to DNA damage induced apoptosis, whereas c-Rel appears to be redundant in this process. In the setting of inflammation, deleting either c-Rel or NFκB1 exacerbated the severity of experimental acute and chronic colitis in mice. However, c-Rel but not NFκB1 deletion resulted in increased inflammation associated colorectal carcinogenesis induced by AOM/DSS as summarised in Table 6.1. These findings suggest that classical NFκB pathway inhibitors may be paradoxically harmful in IBD.

Data in this thesis also provide evidence that alternative pathway NFκB signalling via NFκB2 plays a major role in regulating intestinal epithelial apoptosis *in vitro* and *in vivo*. The increased susceptibility to irradiation induced intestinal epithelia apoptosis resulting from deletion of NFκB1 and NFκB2 may be mediated by modulating expression of a number of known NFκB dependent apoptosis regulating

genes as well as the novel gene caspase12. Although deletion of NFκB2 sensitised mice to intestinal epithelial apoptosis, conversely and intriguingly, NFκB2 loss also protected mice from developing colitis and colitis associated colon cancer as summarised in Table 6.1. This suggests that the alternative NFκB2 activation pathway is essential for the development of colonic inflammation and its associated colorectal cancer. Pharmacological inhibition of NFκB2 signalling may therefore be a promising novel therapeutic strategy for treating IBD and preventing cancer development in such patients. Whether these specific roles of individual members of NFκB family are due to epithelial and/or immune cell mediated effects currently remains to be established.

Response	**Tissue**	**c-Rel-null mice**	**NFκB1-null mice**	**NFκB2-null mice**
Irradiation-induced apoptosis	Small intestine	↔	↑	↑
	Colon	↔	↑	↑
mRNA expression of pro-apoptotic genes following irradiation	Small intestine	↔	↑ TRAIL, Caspase12	↑TRAIL, Caspase12, BAK, P53 and FAS-L
	Colon	↔	↑ TRAIL	↑Caspase12, BAK and FAS-L
Irinotecan-induced apoptosis (6 and 48 hours)	Small intestine	↔	↑	↑
	Colon	↔	↑	↑
Severity of DSS-induced colitis	Colon	↑	↑	↓
mRNA expression of cytokines encoding genes in DSS-induced colitis	Colon	↓ TNF-α	↑ IL-1β, IL-6	↓TNF-α , ↑ IL-4
Incidence and size of AOM/DSS induced tumours	Colon	↑	↔	↓
Proliferation index of AOM/DSS induced tumours	Colon	↑	↔	↔
Initial colonic epithelial responses to the carcinogen AOM	Colon	↑ mitosis ↓ apoptosis	↔	↑ apoptosis

Table 6.1: Summary of the main observations from transgenic mice following irradiation, irinotecan, DSS or AOM/DSS administration compared to wild-type mice.

7 References

1. Abreu, M.T. *Toll-like receptor signalling in the intestinal epithelium: how bacterial recognition shapes intestinal function.* Nat Rev Immunol, 2010. **10**(2): p. 131-44.

2. Lawrence, T. *The nuclear factor NF-kappaB pathway in inflammation.* Cold Spring Harb Perspect Biol, 2009. **1**(6): p. a001651.

3. Karrasch, T. and C. Jobin. *NF-kappaB and the intestine: friend or foe?* Inflamm Bowel Dis, 2008. **14**(1): p. 114-24.

4. Barker, N., M. van de Wetering and H. Clevers. *The intestinal stem cell.* Genes Dev, 2008. **22**(14): p. 1856-64.

5. Potten, C.S., L. Kovacs and E. Hamilton. *Continuous labelling studies on mouse skin and intestine.* Cell Tissue Kinet, 1974. **7**(3): p. 271-83.

6. Potten, C.S. *Extreme sensitivity of some intestinal crypt cells to X and gamma irradiation.* Nature, 1977. **269**(5628): p. 518-21.

7. Cheng, H. and C.P. Leblond. *Origin, differentiation and renewal of the four main epithelial cell types in the mouse small intestine. V. Unitarian Theory of the origin of the four epithelial cell types.* Am J Anat, 1974. **141**(4): p. 537-61.

8. Stappenbeck, T.S., J.C. Mills and J.I. Gordon. *Molecular features of adult mouse small intestinal epithelial progenitors.* Proc Natl Acad Sci U S A, 2003. **100**(3): p. 1004-9.

9. Bjerknes, M. and H. Cheng. *The stem-cell zone of the small intestinal epithelium. I. Evidence from Paneth cells in the adult mouse.* Am J Anat, 1981. **160**(1): p. 51-63.

10. Bjerknes, M. and H. Cheng. *Clonal analysis of mouse intestinal epithelial progenitors.* Gastroenterology, 1999. **116**(1): p. 7-14.

11. Samuel, S., R. Walsh, J. Webb, A. Robins, C. Potten and Y.R. Mahida. *Characterization of putative stem cells in isolated human colonic crypt epithelial cells and their interactions with myofibroblasts.* Am J Physiol Cell Physiol, 2009. **296**(2): p. C296-305.

12. Marshman, E., C. Booth and C.S. Potten. *The intestinal epithelial stem cell.* Bioessays, 2002. **24**(1): p. 91-8.

13. Potten, C.S., R. Gandara, Y.R. Mahida, M. Loeffler and N.A. Wright. *The stem cells of small intestinal crypts: where are they?* Cell Prolif, 2009. **42**(6): p. 731-50.

14. Nishimura, S., N. Wakabayashi, K. Toyoda, K. Kashima and S. Mitsufuji. *Expression of Musashi-1 in human normal colon crypt cells: a possible stem cell marker of human colon epithelium.* Dig Dis Sci, 2003. **48**(8): p. 1523-9.

15. Ricci-Vitiani, L., E. Fabrizi, E. Palio and R. De Maria. *Colon cancer stem cells.* J Mol Med (Berl), 2009. **87**(11): p. 1097-104.

16. Cunliffe, R.N., F.R. Rose, J. Keyte, L. Abberley, W.C. Chan and Y.R. Mahida. *Human defensin 5 is stored in precursor form in normal Paneth cells and is expressed by some villous epithelial cells and by metaplastic Paneth cells in the colon in inflammatory bowel disease.* Gut, 2001. **48**(2): p. 176-85.

17. Paterson, J.C. and S.H. Watson. *Paneth cell metaplasia in ulcerative colitis.* Am J Pathol, 1961. **38**: p. 243-9.

18. Lin, S.A. and N. Barker. *Gastrointestinal stem cells in self-renewal and cancer.* J Gastroenterol, 2011. **46**(9): p. 1039-55.

19. Barker, N., J.H. van Es, J. Kuipers, P. Kujala, M. van den Born, M. Cozijnsen, A. Haegebarth, J. Korving, H. Begthel, P.J. Peters and H. Clevers. *Identification of stem cells in small intestine and colon by marker gene Lgr5.* Nature, 2007. **449**(7165): p. 1003-7.

20. Garrison, A.P., M.A. Helmrath and C.M. Dekaney. *Intestinal stem cells.* J Pediatr Gastroenterol Nutr, 2009. **49**(1): p. 2-7.

21. Sangiorgi, E. and M.R. Capecchi. *Bmi1 is expressed in vivo in intestinal stem cells.* Nat Genet, 2008. **40**(7): p. 915-20.

22. Potten, C.S., C. Booth, G.L. Tudor, D. Booth, G. Brady, P. Hurley, G. Ashton, R. Clarke, S. Sakakibara and H. Okano. *Identification of a putative intestinal stem cell and early lineage marker; musashi-1.* Differentiation, 2003. **71**(1): p. 28-41.

23. van der Flier, L.G. and H. Clevers. *Stem cells, self-renewal, and differentiation in the intestinal epithelium.* Annu Rev Physiol, 2009. **71**: p. 241-60.

24. Potten, C.S. *Stem cells in gastrointestinal epithelium: numbers, characteristics and death.* Philos Trans R Soc Lond B Biol Sci, 1998. **353**(1370): p. 821-30.

25. Cai, W.B., S.A. Roberts and C.S. Potten. *The number of clonogenic cells in crypts in three regions of murine large intestine.* Int J Radiat Biol, 1997. **71**(5): p. 573-9.

26. Pinto, D. and H. Clevers. *Wnt control of stem cells and differentiation in the intestinal epithelium.* Exp Cell Res, 2005. **306**(2): p. 357-63.

27. Garabedian, E.M., L.J. Roberts, M.S. McNevin and J.I. Gordon. *Examining the role of Paneth cells in the small intestine by lineage ablation in transgenic mice.* J Biol Chem, 1997. **272**(38): p. 23729-40.

28. Booth, D. and C.S. Potten. *Protection against mucosal injury by growth factors and cytokines.* J Natl Cancer Inst Monogr, 2001(29): p. 16-20.

29. Pinto, D., A. Gregorieff, H. Begthel and H. Clevers. *Canonical Wnt signals are essential for homeostasis of the intestinal epithelium.* Genes Dev, 2003. **17**(14): p. 1709-13.

30. Kuhnert, F., C.R. Davis, H.T. Wang, P. Chu, M. Lee, J. Yuan, R. Nusse and C.J. Kuo. *Essential requirement for Wnt signaling in proliferation of adult small intestine and colon revealed by adenoviral expression of Dickkopf-1.* Proc Natl Acad Sci U S A, 2004. **101**(1): p. 266-71.

31. van de Wetering, M., E. Sancho, C. Verweij, W. de Lau, I. Oving, A. Hurlstone, K. van der Horn, E. Batlle, D. Coudreuse, A.P. Haramis, M. Tjon-Pon-Fong, P. Moerer, M. van den Born, G. Soete, S. Pals, M. Eilers, R. Medema and H. Clevers. *The beta-catenin/TCF-4 complex imposes a crypt progenitor phenotype on colorectal cancer cells.* Cell, 2002. **111**(2): p. 241-50.

32. Nakamura, T., K. Tsuchiya and M. Watanabe. *Crosstalk between Wnt and Notch signaling in intestinal epithelial cell fate decision.* J Gastroenterol, 2007. **42**(9): p. 705-10.

33. Furriols, M. and S. Bray. *A model Notch response element detects Suppressor of Hairless-dependent molecular switch.* Curr Biol, 2001. **11**(1): p. 60-4.

34. Artavanis-Tsakonas, S., M.D. Rand and R.J. Lake. *Notch signaling: cell fate control and signal integration in development.* Science, 1999. **284**(5415): p. 770-6.

35. Zecchini, V., R. Domaschenz, D. Winton and P. Jones. *Notch signaling regulates the differentiation of post-mitotic intestinal epithelial cells.* Genes Dev, 2005. **19**(14): p. 1686-91.

36. van Es, J.H., M.E. van Gijn, O. Riccio, M. van den Born, M. Vooijs, H. Begthel, M. Cozijnsen, S. Robine, D.J. Winton, F. Radtke and H. Clevers. *Notch/gamma-secretase inhibition turns proliferative cells in intestinal crypts and adenomas into goblet cells.* Nature, 2005. **435**(7044): p. 959-63.

37. van Es, J.H. and H. Clevers. *Notch and Wnt inhibitors as potential new drugs for intestinal neoplastic disease.* Trends Mol Med, 2005. **11**(11): p. 496-502.

38. Crosnier, C., N. Vargesson, S. Gschmeissner, L. Ariza-McNaughton, A. Morrison and J. Lewis. *Delta-Notch signalling controls commitment to a secretory fate in the zebrafish intestine.* Development, 2005. **132**(5): p. 1093-104.

39. Jensen, J., E.E. Pedersen, P. Galante, J. Hald, R.S. Heller, M. Ishibashi, R. Kageyama, F. Guillemot, P. Serup and O.D. Madsen. *Control of endodermal endocrine development by Hes-1.* Nat Genet, 2000. **24**(1): p. 36-44.

40. Yang, Q., N.A. Bermingham, M.J. Finegold and H.Y. Zoghbi. *Requirement of Math1 for secretory cell lineage commitment in the mouse intestine.* Science, 2001. **294**(5549): p. 2155-8.

41. Shroyer, N.F., D. Wallis, K.J. Venken, H.J. Bellen and H.Y. Zoghbi. *Gfi1 functions downstream of Math1 to control intestinal secretory cell subtype allocation and differentiation.* Genes Dev, 2005. **19**(20): p. 2412-7.

42. Jenny, M., C. Uhl, C. Roche, I. Duluc, V. Guillermin, F. Guillemot, J. Jensen, M. Kedinger and G. Gradwohl. *Neurogenin3 is differentially required for endocrine cell fate specification in the intestinal and gastric epithelium.* EMBO J, 2002. **21**(23): p. 6338-47.

43. Katz, J.P., N. Perreault, B.G. Goldstein, C.S. Lee, P.A. Labosky, V.W. Yang and K.H. Kaestner. *The zinc-finger transcription factor Klf4 is required for terminal differentiation of goblet cells in the colon.* Development, 2002. **129**(11): p. 2619-28.

44. Bastide, P., C. Darido, J. Pannequin, R. Kist, S. Robine, C. Marty-Double, F. Bibeau, G. Scherer, D. Joubert, F. Hollande, P. Blache and P. Jay. *Sox9 regulates cell proliferation and is required for Paneth cell differentiation in the intestinal epithelium.* J Cell Biol, 2007. **178**(4): p. 635-48.

45. Glick, D., S. Barth and K.F. Macleod. *Autophagy: cellular and molecular mechanisms.* J Pathol, 2010. **221**(1): p. 3-12.

46. Watson, A.J. and D.M. Pritchard. *Lessons from genetically engineered animal models. VII. Apoptosis in intestinal epithelium: lessons from transgenic and knockout mice.* Am J Physiol Gastrointest Liver Physiol, 2000. **278**(1): p. G1-5.

47. Butler, L.M., P.J. Hewett, R.A. Fitridge and P.A. Cowled. *Deregulation of apoptosis in colorectal carcinoma: theoretical and therapeutic implications.* Aust N Z J Surg, 1999. **69**(2): p. 88-94.

48. Ashkenazi, A. *Targeting death and decoy receptors of the tumour-necrosis factor superfamily.* Nat Rev Cancer, 2002. **2**(6): p. 420-30.

49. Fulda, S. and K.M. Debatin. *Extrinsic versus intrinsic apoptosis pathways in anticancer chemotherapy.* Oncogene, 2006. **25**(34): p. 4798-811.

50. Ravi, R., A.J. Jain, R.D. Schulick, V. Pham, T.S. Prouser, H. Allen, E.G. Mayer, H. Yu, D.M. Pardoll, A. Ashkenazi and A. Bedi. *Elimination of hepatic metastases of colon cancer cells via p53-independent cross-talk between irinotecan and Apo2 ligand/TRAIL.* Cancer Res, 2004. **64**(24): p. 9105-14.

51. Reed, J.C. *Bcl-2 family proteins.* Oncogene, 1998. **17**(25): p. 3225-36.

52. Henry-Mowatt, J., C. Dive, J.C. Martinou and D. James. *Role of mitochondrial membrane permeabilization in apoptosis and cancer.* Oncogene, 2004. **23**(16): p. 2850-60.

53. Srinivasula, S.M., P. Datta, X.J. Fan, T. Fernandes-Alnemri, Z. Huang and E.S. Alnemri. *Molecular determinants of the caspase-promoting activity of Smac/DIABLO and its role in the death receptor pathway.* J Biol Chem, 2000. **275**(46): p. 36152-7.

54. Jones, B.A. and G.J. Gores. *Physiology and pathophysiology of apoptosis in epithelial cells of the liver, pancreas, and intestine.* Am J Physiol, 1997. **273**(6 Pt 1): p. G1174-88.

55. Potten, C.S. *Epithelial cell growth and differentiation. II. Intestinal apoptosis.* Am J Physiol, 1997. **273**(2 Pt 1): p. G253-7.

56. Potten, C.S. *What is an apoptotic index measuring? A commentary.* Br J Cancer, 1996. **74**(11): p. 1743-8.

57. Potten, C.S. *The significance of spontaneous and induced apoptosis in the gastrointestinal tract of mice.* Cancer Metastasis Rev, 1992. **11**(2): p. 179-95.

58. Potten, C.S. and M. Loeffler. *Stem cells: attributes, cycles, spirals, pitfalls and uncertainties. Lessons for and from the crypt.* Development, 1990. **110**(4): p. 1001-20.

59. Potten, C.S., J.W. Wilson and C. Booth. *Regulation and significance of apoptosis in the stem cells of the gastrointestinal epithelium.* Stem Cells, 1997. **15**(2): p. 82-93.

60. Merritt, A.J., C.S. Potten, C.J. Kemp, J.A. Hickman, A. Balmain, D.P. Lane and P.A. Hall. *The role of p53 in spontaneous and radiation-induced apoptosis in the gastrointestinal tract of normal and p53-deficient mice.* Cancer Res, 1994. **54**(3): p. 614-7.

61. Merritt, A.J., C.S. Potten, A.J. Watson, D.Y. Loh, K. Nakayama and J.A. Hickman. *Differential expression of bcl-2 in intestinal epithelia. Correlation with attenuation of apoptosis in colonic crypts and the incidence of colonic neoplasia.* J Cell Sci, 1995. **108 (Pt 6)**: p. 2261-71.

62. Hall, P.A., P.J. Coates, B. Ansari and D. Hopwood. *Regulation of cell number in the mammalian gastrointestinal tract: the importance of apoptosis.* J Cell Sci, 1994. **107 (Pt 12)**: p. 3569-77.

63. Nakayama, K., I. Negishi, K. Kuida, H. Sawa and D.Y. Loh. *Targeted disruption of Bcl-2 alpha beta in mice: occurrence of gray hair, polycystic kidney*

disease, and lymphocytopenia. Proc Natl Acad Sci U S A, 1994. **91**(9): p. 3700-4.

64. Pritchard, D.M., C.S. Potten, S.J. Korsmeyer, S. Roberts and J.A. Hickman. *Damage-induced apoptosis in intestinal epithelia from bcl-2-null and bax-null mice: investigations of the mechanistic determinants of epithelial apoptosis in vivo.* Oncogene, 1999. **18**(51): p. 7287-93.

65. Krajewski, S., M. Krajewska, A. Shabaik, T. Miyashita, H.G. Wang and J.C. Reed. *Immunohistochemical determination of in vivo distribution of Bax, a dominant inhibitor of Bcl-2.* Am J Pathol, 1994. **145**(6): p. 1323-36.

66. Pritchard, D.M., C. Print, L. O'Reilly, J.M. Adams, C.S. Potten and J.A. Hickman. *Bcl-w is an important determinant of damage-induced apoptosis in epithelia of small and large intestine.* Oncogene, 2000. **19**(34): p. 3955-9.

67. Duckworth, C.A. and D.M. Pritchard. *Suppression of apoptosis, crypt hyperplasia, and altered differentiation in the colonic epithelia of bak-null mice.* Gastroenterology, 2009. **136**(3): p. 943-52.

68. Clarke, A.R., S. Gledhill, M.L. Hooper, C.C. Bird and A.H. Wyllie. *p53 dependence of early apoptotic and proliferative responses within the mouse intestinal epithelium following gamma-irradiation.* Oncogene, 1994. **9**(6): p. 1767-73.

69. Sansom, O.J., J. Zabkiewicz, S.M. Bishop, J. Guy, A. Bird and A.R. Clarke. *MBD4 deficiency reduces the apoptotic response to DNA-damaging agents in the murine small intestine.* Oncogene, 2003. **22**(46): p. 7130-6.

70. Ijiri, K. and C.S. Potten. *Response of intestinal cells of differing topographical and hierarchical status to ten cytotoxic drugs and five sources of radiation.* Br J Cancer, 1983. **47**(2): p. 175-85.

71. Ijiri, K. and C.S. Potten. *Further studies on the response of intestinal crypt cells of different hierarchical status to eighteen different cytotoxic agents.* Br J Cancer, 1987. **55**(2): p. 113-23.

72. Li, Y.Q., C.Y. Fan, P.J. O'Connor, D.J. Winton and C.S. Potten. *Target cells for the cytotoxic effects of carcinogens in the murine small bowel.* Carcinogenesis, 1992. **13**(3): p. 361-8.

73. Potten, C.S., Y.Q. Li, P.J. O'Connor and D.J. Winton. *A possible explanation for the differential cancer incidence in the intestine, based on distribution of the cytotoxic effects of carcinogens in the murine large bowel.* Carcinogenesis, 1992. **13**(12): p. 2305-12.

74. Kunimoto, T., K. Nitta, T. Tanaka, N. Uehara, H. Baba, M. Takeuchi, T. Yokokura, S. Sawada, T. Miyasaka and M. Mutai. *Antitumor activity of 7-ethyl-10-[4-(1-piperidino)-1-piperidino]carbonyloxy-camptothec in, a novel*

water-soluble derivative of camptothecin, against murine tumors. Cancer Res, 1987. **47**(22): p. 5944-7.

75. Andoh, T., K. Ishii, Y. Suzuki, Y. Ikegami, Y. Kusunoki, Y. Takemoto and K. Okada. *Characterization of a mammalian mutant with a camptothecin-resistant DNA topoisomerase I.* Proc Natl Acad Sci U S A, 1987. **84**(16): p. 5565-9.

76. Solary, E., R. Bertrand, K.W. Kohn and Y. Pommier. *Differential induction of apoptosis in undifferentiated and differentiated HL-60 cells by DNA topoisomerase I and II inhibitors.* Blood, 1993. **81**(5): p. 1359-68.

77. Ikuno, N., H. Soda, M. Watanabe and M. Oka. *Irinotecan (CPT-11) and characteristic mucosal changes in the mouse ileum and cecum.* J Natl Cancer Inst, 1995. **87**(24): p. 1876-83.

78. Hanauer, S.B. *Inflammatory bowel disease: epidemiology, pathogenesis, and therapeutic opportunities.* Inflamm Bowel Dis, 2006. **12 Suppl 1**: p. S3-9.

79. Van Limbergen, J., D.C. Wilson and J. Satsangi. *The genetics of Crohn's disease.* Annu Rev Genomics Hum Genet, 2009. **10**: p. 89-116.

80. Sokol, H. and P. Seksik. *The intestinal microbiota in inflammatory bowel diseases: time to connect with the host.* Curr Opin Gastroenterol, 2010. **26**(4): p. 327-31.

81. Salim, S.Y. and J.D. Soderholm. *Importance of disrupted intestinal barrier in inflammatory bowel diseases.* Inflamm Bowel Dis, 2011. **17**(1): p. 362-81.

82. Cho, J.H. and S.R. Brant. *Recent insights into the genetics of inflammatory bowel disease.* Gastroenterology, 2011. **140**(6): p. 1704-12.

83. Barrett, J.C., S. Hansoul, D.L. Nicolae, J.H. Cho, R.H. Duerr, J.D. Rioux, S.R. Brant, M.S. Silverberg, K.D. Taylor, M.M. Barmada, A. Bitton, T. Dassopoulos, L.W. Datta, T. Green, A.M. Griffiths, E.O. Kistner, M.T. Murtha, M.D. Regueiro, J.I. Rotter, L.P. Schumm, A.H. Steinhart, S.R. Targan, R.J. Xavier, N.I.G. Consortium, C. Libioulle, C. Sandor, M. Lathrop, J. Belaiche, O. Dewit, I. Gut, S. Heath, D. Laukens, M. Mni, P. Rutgeerts, A. Van Gossum, D. Zelenika, D. Franchimont, J.P. Hugot, M. de Vos, S. Vermeire, E. Louis, I.B.D.C. Belgian-French, C. Wellcome Trust Case Control, L.R. Cardon, C.A. Anderson, H. Drummond, E. Nimmo, T. Ahmad, N.J. Prescott, C.M. Onnie, S.A. Fisher, J. Marchini, J. Ghori, S. Bumpstead, R. Gwilliam, M. Tremelling, P. Deloukas, J. Mansfield, D. Jewell, J. Satsangi, C.G. Mathew, M. Parkes, M. Georges and M.J. Daly. *Genome-wide association defines more than 30 distinct susceptibility loci for Crohn's disease.* Nat Genet, 2008. **40**(8): p. 955-62.

84. Ogura, Y., D.K. Bonen, N. Inohara, D.L. Nicolae, F.F. Chen, R. Ramos, H. Britton, T. Moran, R. Karaliuskas, R.H. Duerr, J.P. Achkar, S.R. Brant, T.M. Bayless, B.S. Kirschner, S.B. Hanauer, G. Nunez and J.H. Cho. *A frameshift*

mutation in NOD2 associated with susceptibility to Crohn's disease. Nature, 2001. **411**(6837): p. 603-6.

85. Hampe, J., A. Franke, P. Rosenstiel, A. Till, M. Teuber, K. Huse, M. Albrecht, G. Mayr, F.M. De La Vega, J. Briggs, S. Gunther, N.J. Prescott, C.M. Onnie, R. Hasler, B. Sipos, U.R. Folsch, T. Lengauer, M. Platzer, C.G. Mathew, M. Krawczak and S. Schreiber. *A genome-wide association scan of nonsynonymous SNPs identifies a susceptibility variant for Crohn disease in ATG16L1.* Nat Genet, 2007. **39**(2): p. 207-11.

86. Parkes, M., J.C. Barrett, N.J. Prescott, M. Tremelling, C.A. Anderson, S.A. Fisher, R.G. Roberts, E.R. Nimmo, F.R. Cummings, D. Soars, H. Drummond, C.W. Lees, S.A. Khawaja, R. Bagnall, D.A. Burke, C.E. Todhunter, T. Ahmad, C.M. Onnie, W. McArdle, D. Strachan, G. Bethel, C. Bryan, C.M. Lewis, P. Deloukas, A. Forbes, J. Sanderson, D.P. Jewell, J. Satsangi, J.C. Mansfield, C. Wellcome Trust Case Control, L. Cardon and C.G. Mathew. *Sequence variants in the autophagy gene IRGM and multiple other replicating loci contribute to Crohn's disease susceptibility.* Nat Genet, 2007. **39**(7): p. 830-2.

87. Abraham, C. and J.H. Cho. *Functional consequences of NOD2 (CARD15) mutations.* Inflamm Bowel Dis, 2006. **12**(7): p. 641-50.

88. Levine, B. and V. Deretic. *Unveiling the roles of autophagy in innate and adaptive immunity.* Nat Rev Immunol, 2007. **7**(10): p. 767-77.

89. Kuballa, P., A. Huett, J.D. Rioux, M.J. Daly and R.J. Xavier. *Impaired autophagy of an intracellular pathogen induced by a Crohn's disease associated ATG16L1 variant.* PLoS One, 2008. **3**(10): p. e3391.

90. Travassos, L.H., L.A. Carneiro, S. Girardin and D.J. Philpott. *Nod proteins link bacterial sensing and autophagy.* Autophagy, 2010. **6**(3): p. 409-11.

91. Bjarnason, I., A. MacPherson and D. Hollander. *Intestinal permeability: an overview.* Gastroenterology, 1995. **108**(5): p. 1566-81.

92. Ukabam, S.O., J.R. Clamp and B.T. Cooper. *Abnormal small intestinal permeability to sugars in patients with Crohn's disease of the terminal ileum and colon.* Digestion, 1983. **27**(2): p. 70-4.

93. Artis, D. *Epithelial-cell recognition of commensal bacteria and maintenance of immune homeostasis in the gut.* Nat Rev Immunol, 2008. **8**(6): p. 411-20.

94. Umesaki, Y. and H. Setoyama. *Structure of the intestinal flora responsible for development of the gut immune system in a rodent model.* Microbes Infect, 2000. **2**(11): p. 1343-51.

95. Guarner, F. *What is the role of the enteric commensal flora in IBD?* Inflamm Bowel Dis, 2008. **14 Suppl 2**: p. S83-4.

96. Manichanh, C., N. Borruel, F. Casellas and F. Guarner. *The gut microbiota in IBD.* Nat Rev Gastroenterol Hepatol, 2012.

97. De Filippo, C., D. Cavalieri, M. Di Paola, M. Ramazzotti, J.B. Poullet, S. Massart, S. Collini, G. Pieraccini and P. Lionetti. *Impact of diet in shaping gut microbiota revealed by a comparative study in children from Europe and rural Africa.* Proc Natl Acad Sci U S A, 2010. **107**(33): p. 14691-6.

98. Asquith, M. and F. Powrie. *An innately dangerous balancing act: intestinal homeostasis, inflammation, and colitis-associated cancer.* J Exp Med, 2010. **207**(8): p. 1573-7.

99. Neurath, M., I. Fuss and W. Strober. *TNBS-colitis.* Int Rev Immunol, 2000. **19**(1): p. 51-62.

100. Wirtz, S. and M.F. Neurath. *Mouse models of inflammatory bowel disease.* Adv Drug Deliv Rev, 2007. **59**(11): p. 1073-83.

101. Wirtz, S., C. Neufert, B. Weigmann and M.F. Neurath. *Chemically induced mouse models of intestinal inflammation.* Nat Protoc, 2007. **2**(3): p. 541-6.

102. Cong, Y., S.L. Brandwein, R.P. McCabe, A. Lazenby, E.H. Birkenmeier, J.P. Sundberg and C.O. Elson. *CD4+ T cells reactive to enteric bacterial antigens in spontaneously colitic C3H/HeJBir mice: increased T helper cell type 1 response and ability to transfer disease.* J Exp Med, 1998. **187**(6): p. 855-64.

103. Rivera-Nieves, J., G. Bamias, A. Vidrich, M. Marini, T.T. Pizarro, M.J. McDuffie, C.A. Moskaluk, S.M. Cohn and F. Cominelli. *Emergence of perianal fistulizing disease in the SAMP1/YitFc mouse, a spontaneous model of chronic ileitis.* Gastroenterology, 2003. **124**(4): p. 972-82.

104. Watanabe, M., Y. Ueno, T. Yajima, S. Okamoto, T. Hayashi, M. Yamazaki, Y. Iwao, H. Ishii, S. Habu, M. Uehira, H. Nishimoto, H. Ishikawa, J. Hata and T. Hibi. *Interleukin 7 transgenic mice develop chronic colitis with decreased interleukin 7 protein accumulation in the colonic mucosa.* J Exp Med, 1998. **187**(3): p. 389-402.

105. Kuhn, R., J. Lohler, D. Rennick, K. Rajewsky and W. Muller. *Interleukin-10-deficient mice develop chronic enterocolitis.* Cell, 1993. **75**(2): p. 263-74.

106. Powrie, F., M.W. Leach, S. Mauze, L.B. Caddle and R.L. Coffman. *Phenotypically distinct subsets of CD4+ T cells induce or protect from chronic intestinal inflammation in C. B-17 scid mice.* Int Immunol, 1993. **5**(11): p. 1461-71.

107. Wirtz, S. and M.F. Neurath. *Animal models of intestinal inflammation: new insights into the molecular pathogenesis and immunotherapy of inflammatory bowel disease.* Int J Colorectal Dis, 2000. **15**(3): p. 144-60.

108. Okayasu, I., T. Ohkusa, K. Kajiura, J. Kanno and S. Sakamoto. *Promotion of colorectal neoplasia in experimental murine ulcerative colitis.* Gut, 1996. **39**(1): p. 87-92.

109. Melgar, S., L. Karlsson, E. Rehnstrom, A. Karlsson, H. Utkovic, L. Jansson and E. Michaelsson. *Validation of murine dextran sulfate sodium-induced colitis using four therapeutic agents for human inflammatory bowel disease.* Int Immunopharmacol, 2008. **8**(6): p. 836-44.

110. Okayasu, I., S. Hatakeyama, M. Yamada, T. Ohkusa, Y. Inagaki and R. Nakaya. *A novel method in the induction of reliable experimental acute and chronic ulcerative colitis in mice.* Gastroenterology, 1990. **98**(3): p. 694-702.

111. Melgar, S., A. Karlsson and E. Michaelsson. *Acute colitis induced by dextran sulfate sodium progresses to chronicity in C57BL/6 but not in BALB/c mice: correlation between symptoms and inflammation.* Am J Physiol Gastrointest Liver Physiol, 2005. **288**(6): p. G1328-38.

112. Fredin, M.F., L. Hultin, G. Hyberg, E. Rehnstrom, E. Hultgren Hornquist, S. Melgar and L. Jansson. *Predicting and monitoring colitis development in mice by micro-computed tomography.* Inflamm Bowel Dis, 2008. **14**(4): p. 491-9.

113. Kitajima, S., S. Takuma and M. Morimoto. *Histological analysis of murine colitis induced by dextran sulfate sodium of different molecular weights.* Exp Anim, 2000. **49**(1): p. 9-15.

114. Hirono, I., K. Kuhara, T. Yamaji, S. Hosaka and L. Golberg. *Carcinogenicity of dextran sulfate sodium in relation to its molecular weight.* Cancer Lett, 1983. **18**(1): p. 29-34.

115. Perse, M. and A. Cerar. *Dextran sodium sulphate colitis mouse model: traps and tricks.* J Biomed Biotechnol, 2012. **2012**: p. 718617.

116. Nell, S., S. Suerbaum and C. Josenhans. *The impact of the microbiota on the pathogenesis of IBD: lessons from mouse infection models.* Nat Rev Microbiol, 2010. **8**(8): p. 564-77.

117. Mennigen, R., K. Nolte, E. Rijcken, M. Utech, B. Loeffler, N. Senninger and M. Bruewer. *Probiotic mixture VSL#3 protects the epithelial barrier by maintaining tight junction protein expression and preventing apoptosis in a murine model of colitis.* Am J Physiol Gastrointest Liver Physiol, 2009. **296**(5): p. G1140-9.

118. Araki, Y., K. Mukaisyo, H. Sugihara, Y. Fujiyama and T. Hattori. *Increased apoptosis and decreased proliferation of colonic epithelium in dextran sulfate sodium-induced colitis in mice.* Oncol Rep, 2010. **24**(4): p. 869-74.

119. Dieleman, L.A., M.J. Palmen, H. Akol, E. Bloemena, A.S. Pena, S.G. Meuwissen and E.P. Van Rees. *Chronic experimental colitis induced by*

dextran sulphate sodium (DSS) is characterized by Th1 and Th2 cytokines. Clin Exp Immunol, 1998. **114**(3): p. 385-91.

120. Elson, C.O., R.B. Sartor, G.S. Tennyson and R.H. Riddell. *Experimental models of inflammatory bowel disease.* Gastroenterology, 1995. **109**(4): p. 1344-67.

121. Higa, A., N. Ishikawa, T. Eto and Y. Nawa. *Evaluation of the role of mast cells in the progression of acetic acid-induced colitis in mice.* Scand J Gastroenterol, 1996. **31**(8): p. 774-7.

122. Jagtap, A.G., S.S. Shirke and A.S. Phadke. *Effect of polyherbal formulation on experimental models of inflammatory bowel diseases.* J Ethnopharmacol, 2004. **90**(2-3): p. 195-204.

123. Mizoguchi, A., E. Mizoguchi and A.K. Bhan. *Immune networks in animal models of inflammatory bowel disease.* Inflamm Bowel Dis, 2003. **9**(4): p. 246-59.

124. Hibi, T., H. Ogata and A. Sakuraba. *Animal models of inflammatory bowel disease.* J Gastroenterol, 2002. **37**(6): p. 409-17.

125. Boirivant, M., I.J. Fuss, A. Chu and W. Strober. *Oxazolone colitis: A murine model of T helper cell type 2 colitis treatable with antibodies to interleukin 4.* J Exp Med, 1998. **188**(10): p. 1929-39.

126. Hoffmann, J.C., N.N. Pawlowski, A.A. Kuhl, W. Hohne and M. Zeitz. *Animal models of inflammatory bowel disease: an overview.* Pathobiology, 2002. **70**(3): p. 121-30.

127. Sackett, D.L. *Bias in analytic research.* J Chronic Dis, 1979. **32**(1-2): p. 51-63.

128. Whelan, G. *Ulcerative colitis--what is the risk of developing colorectal cancer?* Aust N Z J Med, 1991. **21**(1): p. 71-7.

129. Hardy, R.G., S.J. Meltzer and J.A. Jankowski. *ABC of colorectal cancer. Molecular basis for risk factors.* BMJ, 2000. **321**(7265): p. 886-9.

130. Eaden, J.A., K.R. Abrams and J.F. Mayberry. *The risk of colorectal cancer in ulcerative colitis: a meta-analysis.* Gut, 2001. **48**(4): p. 526-35.

131. Canavan, C., K.R. Abrams and J. Mayberry. *Meta-analysis: colorectal and small bowel cancer risk in patients with Crohn's disease.* Aliment Pharmacol Ther, 2006. **23**(8): p. 1097-104.

132. Rutter, M., B. Saunders, K. Wilkinson, S. Rumbles, G. Schofield, M. Kamm, C. Williams, A. Price, I. Talbot and A. Forbes. *Severity of inflammation is a risk factor for colorectal neoplasia in ulcerative colitis.* Gastroenterology, 2004. **126**(2): p. 451-9.

133. Triantafillidis, J.K., G. Nasioulas and P.A. Kosmidis. *Colorectal cancer and inflammatory bowel disease: epidemiology, risk factors, mechanisms of carcinogenesis and prevention strategies.* Anticancer Res, 2009. **29**(7): p. 2727-37.

134. Pinczowski, D., A. Ekbom, J. Baron, J. Yuen and H.O. Adami. *Risk factors for colorectal cancer in patients with ulcerative colitis: a case-control study.* Gastroenterology, 1994. **107**(1): p. 117-20.

135. Roessner, A., D. Kuester, P. Malfertheiner and R. Schneider-Stock. *Oxidative stress in ulcerative colitis-associated carcinogenesis.* Pathol Res Pract, 2008. **204**(7): p. 511-24.

136. Fantini, M.C. and F. Pallone. *Cytokines: from gut inflammation to colorectal cancer.* Curr Drug Targets, 2008. **9**(5): p. 375-80.

137. Jemal, A., R. Siegel, E. Ward, T. Murray, J. Xu and M.J. Thun. *Cancer statistics, 2007.* CA Cancer J Clin, 2007. **57**(1): p. 43-66.

138. Ferlay, J., D.M. Parkin and E. Steliarova-Foucher. *Estimates of cancer incidence and mortality in Europe in 2008.* Eur J Cancer, 2010. **46**(4): p. 765-81.

139. Lee, B.B., E.J. Lee, E.H. Jung, H.K. Chun, D.K. Chang, S.Y. Song, J. Park and D.H. Kim. *Aberrant methylation of APC, MGMT, RASSF2A, and Wif-1 genes in plasma as a biomarker for early detection of colorectal cancer.* Clin Cancer Res, 2009. **15**(19): p. 6185-91.

140. Fodde, R. *The APC gene in colorectal cancer.* Eur J Cancer, 2002. **38**(7): p. 867-71.

141. Taylor, D.P., R.W. Burt, M.S. Williams, P.J. Haug and L.A. Cannon-Albright. *Population-based family history-specific risks for colorectal cancer: a constellation approach.* Gastroenterology, 2010. **138**(3): p. 877-85.

142. Fearnhead, N.S., J.L. Wilding and W.F. Bodmer. *Genetics of colorectal cancer: hereditary aspects and overview of colorectal tumorigenesis.* Br Med Bull, 2002. **64**: p. 27-43.

143. Weitz, J., M. Koch, J. Debus, T. Hohler, P.R. Galle and M.W. Buchler. *Colorectal cancer.* Lancet, 2005. **365**(9454): p. 153-65.

144. Win, A.K., R.J. Macinnis, J.L. Hopper and M.A. Jenkins. *Risk prediction models for colorectal cancer: a review.* Cancer Epidemiol Biomarkers Prev, 2012. **21**(3): p. 398-410.

145. Luchtenborg, M., M.P. Weijenberg, G.M. Roemen, A.P. de Bruine, P.A. van den Brandt, M.H. Lentjes, M. Brink, M. van Engeland, R.A. Goldbohm and

A.F. de Goeij. *APC mutations in sporadic colorectal carcinomas from The Netherlands Cohort Study.* Carcinogenesis, 2004. **25**(7): p. 1219-26.

146. Takayama, T., K. Miyanishi, T. Hayashi, Y. Sato and Y. Niitsu. *Colorectal cancer: genetics of development and metastasis.* J Gastroenterol, 2006. **41**(3): p. 185-92.

147. Benito, M. and E. Diaz-Rubio. *Molecular biology in colorectal cancer.* Clin Transl Oncol, 2006. **8**(6): p. 391-8.

148. Saletti, P., I.D. Edwin, K. Pack, F. Cavalli and W.S. Atkin. *Microsatellite instability: application in hereditary non-polyposis colorectal cancer.* Ann Oncol, 2001. **12**(2): p. 151-60.

149. Lynch, H.T. and A. de la Chapelle. *Hereditary colorectal cancer.* N Engl J Med, 2003. **348**(10): p. 919-32.

150. Gryfe, R., C. Swallow, B. Bapat, M. Redston, S. Gallinger and J. Couture. *Molecular biology of colorectal cancer.* Curr Probl Cancer, 1997. **21**(5): p. 233-300.

151. Su, L.K., K.W. Kinzler, B. Vogelstein, A.C. Preisinger, A.R. Moser, C. Luongo, K.A. Gould and W.F. Dove. *Multiple intestinal neoplasia caused by a mutation in the murine homolog of the APC gene.* Science, 1992. **256**(5057): p. 668-70.

152. Thibodeau, S.N., G. Bren and D. Schaid. *Microsatellite instability in cancer of the proximal colon.* Science, 1993. **260**(5109): p. 816-9.

153. Lakatos, P.L. and L. Lakatos. *Risk for colorectal cancer in ulcerative colitis: changes, causes and management strategies.* World J Gastroenterol, 2008. **14**(25): p. 3937-47.

154. Winther, K.V., T. Jess, E. Langholz, P. Munkholm and V. Binder. *Long-term risk of cancer in ulcerative colitis: a population-based cohort study from Copenhagen County.* Clin Gastroenterol Hepatol, 2004. **2**(12): p. 1088-95.

155. Jess, T., E.V. Loftus, Jr., F.S. Velayos, W.S. Harmsen, A.R. Zinsmeister, T.C. Smyrk, C.D. Schleck, W.J. Tremaine, L.J. Melton, 3rd, P. Munkholm and W.J. Sandborn. *Risk of intestinal cancer in inflammatory bowel disease: a population-based study from olmsted county, Minnesota.* Gastroenterology, 2006. **130**(4): p. 1039-46.

156. Fodde, R., J. Kuipers, C. Rosenberg, R. Smits, M. Kielman, C. Gaspar, J.H. van Es, C. Breukel, J. Wiegant, R.H. Giles and H. Clevers. *Mutations in the APC tumour suppressor gene cause chromosomal instability.* Nat Cell Biol, 2001. **3**(4): p. 433-8.

157. Grady, W.M., A. Rajput, L. Myeroff, D.F. Liu, K. Kwon, J. Willis and S. Markowitz. *Mutation of the type II transforming growth factor-beta receptor is coincident with the transformation of human colon adenomas to malignant carcinomas.* Cancer Res, 1998. **58**(14): p. 3101-4.

158. Shih, I.M., W. Zhou, S.N. Goodman, C. Lengauer, K.W. Kinzler and B. Vogelstein. *Evidence that genetic instability occurs at an early stage of colorectal tumorigenesis.* Cancer Res, 2001. **61**(3): p. 818-22.

159. Aust, D.E., R.F. Willenbucher, J.P. Terdiman, L.D. Ferrell, C.G. Chang, D.H. Moore, 2nd, A. Molinaro-Clark, G.B. Baretton, U. Loehrs and F.M. Waldman. *Chromosomal alterations in ulcerative colitis-related and sporadic colorectal cancers by comparative genomic hybridization.* Hum Pathol, 2000. **31**(1): p. 109-14.

160. Grady, W.M. *Genomic instability and colon cancer.* Cancer Metastasis Rev, 2004. **23**(1-2): p. 11-27.

161. Boland, C.R., S.N. Thibodeau, S.R. Hamilton, D. Sidransky, J.R. Eshleman, R.W. Burt, S.J. Meltzer, M.A. Rodriguez-Bigas, R. Fodde, G.N. Ranzani and S. Srivastava. *A National Cancer Institute Workshop on Microsatellite Instability for cancer detection and familial predisposition: development of international criteria for the determination of microsatellite instability in colorectal cancer.* Cancer Res, 1998. **58**(22): p. 5248-57.

162. Soreide, K., E.A. Janssen, H. Soiland, H. Korner and J.P. Baak. *Microsatellite instability in colorectal cancer.* Br J Surg, 2006. **93**(4): p. 395-406.

163. Bronner, C.E., S.M. Baker, P.T. Morrison, G. Warren, L.G. Smith, M.K. Lescoe, M. Kane, C. Earabino, J. Lipford, A. Lindblom and et al. *Mutation in the DNA mismatch repair gene homologue hMLH1 is associated with hereditary non-polyposis colon cancer.* Nature, 1994. **368**(6468): p. 258-61.

164. Svrcek, M., J. El-Bchiri, A. Chalastanis, E. Capel, S. Dumont, O. Buhard, C. Oliveira, R. Seruca, C. Bossard, J.F. Mosnier, F. Berger, E. Leteurtre, A. Lavergne-Slove, M.P. Chenard, R. Hamelin, J. Cosnes, L. Beaugerie, E. Tiret, A. Duval and J.F. Flejou. *Specific clinical and biological features characterize inflammatory bowel disease associated colorectal cancers showing microsatellite instability.* J Clin Oncol, 2007. **25**(27): p. 4231-8.

165. Vogelstein, B., E.R. Fearon, S.R. Hamilton, S.E. Kern, A.C. Preisinger, M. Leppert, Y. Nakamura, R. White, A.M. Smits and J.L. Bos. *Genetic alterations during colorectal-tumor development.* N Engl J Med, 1988. **319**(9): p. 525-32.

166. Nakayama, T., T. Morishita and T. Kamiya. *Adenomatous polyposis coli gene as a gatekeeper.* Rev Gastroenterol Peru, 2002. **22**(2): p. 164-7.

167. Janssen, K.P., P. Alberici, H. Fsihi, C. Gaspar, C. Breukel, P. Franken, C. Rosty, M. Abal, F. El Marjou, R. Smits, D. Louvard, R. Fodde and S. Robine. *APC and*

oncogenic KRAS are synergistic in enhancing Wnt signaling in intestinal tumor formation and progression. Gastroenterology, 2006. **131**(4): p. 1096-109.

168. Neufeld, K.L. *Nuclear APC.* Adv Exp Med Biol, 2009. **656**: p. 13-29.

169. Terzic, J., S. Grivennikov, E. Karin and M. Karin. *Inflammation and colon cancer.* Gastroenterology, 2010. **138**(6): p. 2101-2114 e5.

170. Xie, J. and S.H. Itzkowitz. *Cancer in inflammatory bowel disease.* World J Gastroenterol, 2008. **14**(3): p. 378-89.

171. Atreya, I. and M.F. Neurath. *Immune cells in colorectal cancer: prognostic relevance and therapeutic strategies.* Expert Rev Anticancer Ther, 2008. **8**(4): p. 561-72.

172. Atreya, I., R. Atreya and M.F. Neurath. *NF-kappaB in inflammatory bowel disease.* J Intern Med, 2008. **263**(6): p. 591-6.

173. Waldner, M.J. and M.F. Neurath. *Cytokines in colitis associated cancer: potential drug targets?* Inflamm Allergy Drug Targets, 2008. **7**(3): p. 187-94.

174. Kundu, J.K. and Y.J. Surh. *Inflammation: gearing the journey to cancer.* Mutat Res, 2008. **659**(1-2): p. 15-30.

175. Pikarsky, E., R.M. Porat, I. Stein, R. Abramovitch, S. Amit, S. Kasem, E. Gutkovich-Pyest, S. Urieli-Shoval, E. Galun and Y. Ben-Neriah. *NF-kappaB functions as a tumour promoter in inflammation-associated cancer.* Nature, 2004. **431**(7007): p. 461-6.

176. Lin, W.W. and M. Karin. *A cytokine-mediated link between innate immunity, inflammation, and cancer.* J Clin Invest, 2007. **117**(5): p. 1175-83.

177. Hanahan, D. and R.A. Weinberg. *The hallmarks of cancer.* Cell, 2000. **100**(1): p. 57-70.

178. Surh, Y.J. and J.K. Kundu. *Cancer preventive phytochemicals as speed breakers in inflammatory signaling involved in aberrant COX-2 expression.* Curr Cancer Drug Targets, 2007. **7**(5): p. 447-58.

179. Jaiswal, M., N.F. LaRusso and G.J. Gores. *Nitric oxide in gastrointestinal epithelial cell carcinogenesis: linking inflammation to oncogenesis.* Am J Physiol Gastrointest Liver Physiol, 2001. **281**(3): p. G626-34.

180. Seidelin, J.B. and O.H. Nielsen. *Continuous cytokine exposure of colonic epithelial cells induces DNA damage.* Eur J Gastroenterol Hepatol, 2005. **17**(3): p. 363-9.

181. Cooke, M.S., M.D. Evans, M. Dizdaroglu and J. Lunec. *Oxidative DNA damage: mechanisms, mutation, and disease.* FASEB J, 2003. **17**(10): p. 1195-214.

182. Thorsteinsdottir, S., T. Gudjonsson, O.H. Nielsen, B. Vainer and J.B. Seidelin. *Pathogenesis and biomarkers of carcinogenesis in ulcerative colitis.* Nat Rev Gastroenterol Hepatol, 2011. **8**(7): p. 395-404.

183. Ben-Porath, I. and R.A. Weinberg. *The signals and pathways activating cellular senescence.* Int J Biochem Cell Biol, 2005. **37**(5): p. 961-76.

184. Coppe, J.P., P.Y. Desprez, A. Krtolica and J. Campisi. *The senescence-associated secretory phenotype: the dark side of tumor suppression.* Annu Rev Pathol, 2010. **5**: p. 99-118.

185. Shattuck-Brandt, R.L., G.W. Varilek, A. Radhika, F. Yang, M.K. Washington and R.N. DuBois. *Cyclooxygenase 2 expression is increased in the stroma of colon carcinomas from IL-10(-/-) mice.* Gastroenterology, 2000. **118**(2): p. 337-45.

186. Sohn, K.J., S.A. Shah, S. Reid, M. Choi, J. Carrier, M. Comiskey, C. Terhorst and Y.I. Kim. *Molecular genetics of ulcerative colitis-associated colon cancer in the interleukin 2- and beta(2)-microglobulin-deficient mouse.* Cancer Res, 2001. **61**(18): p. 6912-7.

187. Erdman, S.E., T. Poutahidis, M. Tomczak, A.B. Rogers, K. Cormier, B. Plank, B.H. Horwitz and J.G. Fox. *CD4+ CD25+ regulatory T lymphocytes inhibit microbially induced colon cancer in Rag2-deficient mice.* Am J Pathol, 2003. **162**(2): p. 691-702.

188. Velcich, A., W. Yang, J. Heyer, A. Fragale, C. Nicholas, S. Viani, R. Kucherlapati, M. Lipkin, K. Yang and L. Augenlicht. *Colorectal cancer in mice genetically deficient in the mucin Muc2.* Science, 2002. **295**(5560): p. 1726-9.

189. Okayasu, I., M. Yamada, T. Mikami, T. Yoshida, J. Kanno and T. Ohkusa. *Dysplasia and carcinoma development in a repeated dextran sulfate sodium-induced colitis model.* J Gastroenterol Hepatol, 2002. **17**(10): p. 1078-83.

190. Tanaka, T., H. Kohno, R. Suzuki, Y. Yamada, S. Sugie and H. Mori. *A novel inflammation-related mouse colon carcinogenesis model induced by azoxymethane and dextran sodium sulfate.* Cancer Sci, 2003. **94**(11): p. 965-73.

191. Sugimura, T., M. Nagao and K. Wakabayashi. *How we should deal with unavoidable exposure of man to environmental mutagens: cooked food mutagen discovery, facts and lessons for cancer prevention.* Mutat Res, 2000. **447**(1): p. 15-25.

192. Suzuki, R., S. Miyamoto, Y. Yasui, S. Sugie and T. Tanaka. *Global gene expression analysis of the mouse colonic mucosa treated with azoxymethane and dextran sodium sulfate.* BMC Cancer, 2007. **7**: p. 84.

193. Takahashi, M. and K. Wakabayashi. *Gene mutations and altered gene expression in azoxymethane-induced colon carcinogenesis in rodents.* Cancer Sci, 2004. **95**(6): p. 475-80.

194. De Robertis, M., E. Massi, M.L. Poeta, S. Carotti, S. Morini, L. Cecchetelli, E. Signori and V.M. Fazio. *The AOM/DSS murine model for the study of colon carcinogenesis: From pathways to diagnosis and therapy studies.* J Carcinog, 2011. **10**: p. 9.

195. Gerondakis, S., R. Grumont, R. Gugasyan, L. Wong, I. Isomura, W. Ho and A. Banerjee. *Unravelling the complexities of the NF-kappaB signalling pathway using mouse knockout and transgenic models.* Oncogene, 2006. **25**(51): p. 6781-99.

196. Hoffmann, A., G. Natoli and G. Ghosh. *Transcriptional regulation via the NF-kappaB signaling module.* Oncogene, 2006. **25**(51): p. 6706-16.

197. Vallabhapurapu, S. and M. Karin. *Regulation and function of NF-kappaB transcription factors in the immune system.* Annu Rev Immunol, 2009. **27**: p. 693-733.

198. Senftleben, U., Y. Cao, G. Xiao, F.R. Greten, G. Krahn, G. Bonizzi, Y. Chen, Y. Hu, A. Fong, S.C. Sun and M. Karin. *Activation by IKKalpha of a second, evolutionary conserved, NF-kappa B signaling pathway.* Science, 2001. **293**(5534): p. 1495-9.

199. Yilmaz, Z.B., D.S. Weih, V. Sivakumar and F. Weih. *RelB is required for Peyer's patch development: differential regulation of p52-RelB by lymphotoxin and TNF.* EMBO J, 2003. **22**(1): p. 121-30.

200. Dobrzanski, P., R.P. Ryseck and R. Bravo. *Specific inhibition of RelB/p52 transcriptional activity by the C-terminal domain of p100.* Oncogene, 1995. **10**(5): p. 1003-7.

201. Hayden, M.S. and S. Ghosh. *Shared principles in NF-kappaB signaling.* Cell, 2008. **132**(3): p. 344-62.

202. Gilmore, T.D. *Introduction to NF-kappaB: players, pathways, perspectives.* Oncogene, 2006. **25**(51): p. 6680-4.

203. Ghosh, S. and M.S. Hayden. *New regulators of NF-kappaB in inflammation.* Nat Rev Immunol, 2008. **8**(11): p. 837-48.

204. Bonizzi, G. and M. Karin. *The two NF-kappaB activation pathways and their role in innate and adaptive immunity.* Trends Immunol, 2004. **25**(6): p. 280-8.

205. Ghosh, S. and M. Karin. *Missing pieces in the NF-kappaB puzzle.* Cell, 2002. **109 Suppl**: p. S81-96.

206. Karin, M. and Y. Ben-Neriah. *Phosphorylation meets ubiquitination: the control of NF-[kappa]B activity.* Annu Rev Immunol, 2000. **18**: p. 621-63.

207. Scheidereit, C. *IkappaB kinase complexes: gateways to NF-kappaB activation and transcription.* Oncogene, 2006. **25**(51): p. 6685-705.

208. Hacker, H. and M. Karin. *Regulation and function of IKK and IKK-related kinases.* Sci STKE, 2006. **2006**(357): p. re13.

209. Coope, H.J., P.G. Atkinson, B. Huhse, M. Belich, J. Janzen, M.J. Holman, G.G. Klaus, L.H. Johnston and S.C. Ley. *CD40 regulates the processing of NF-kappaB2 p100 to p52.* EMBO J, 2002. **21**(20): p. 5375-85.

210. Xiao, G., E.W. Harhaj and S.C. Sun. *NF-kappaB-inducing kinase regulates the processing of NF-kappaB2 p100.* Mol Cell, 2001. **7**(2): p. 401-9.

211. Liang, C., M. Zhang and S.C. Sun. *beta-TrCP binding and processing of NF-kappaB2/p100 involve its phosphorylation at serines 866 and 870.* Cell Signal, 2006. **18**(8): p. 1309-17.

212. Beinke, S. and S.C. Ley. *Functions of NF-kappaB1 and NF-kappaB2 in immune cell biology.* Biochem J, 2004. **382**(Pt 2): p. 393-409.

213. Gilmore, T. *Rel/NF-kB transcription factors*. 2011.

214. Singh, N.P., M. Nagarkatti and P.S. Nagarkatti. *Role of dioxin response element and nuclear factor-kappaB motifs in 2,3,7,8-tetrachlorodibenzo-p-dioxin-mediated regulation of Fas and Fas ligand expression.* Mol Pharmacol, 2007. **71**(1): p. 145-57.

215. Catz, S.D. and J.L. Johnson. *Transcriptional regulation of bcl-2 by nuclear factor kappa B and its significance in prostate cancer.* Oncogene, 2001. **20**(50): p. 7342-51.

216. Lee, R.M., G. Gillet, J. Burnside, S.J. Thomas and P. Neiman. *Role of Nr13 in regulation of programmed cell death in the bursa of Fabricius.* Genes Dev, 1999. **13**(6): p. 718-28.

217. Iwanaga, R., E. Ozono, J. Fujisawa, M.A. Ikeda, N. Okamura, Y. Huang and K. Ohtani. *Activation of the cyclin D2 and cdk6 genes through NF-kappaB is critical for cell-cycle progression induced by HTLV-I Tax.* Oncogene, 2008. **27**(42): p. 5635-42.

218. Schumm, K., S. Rocha, J. Caamano and N.D. Perkins. *Regulation of p53 tumour suppressor target gene expression by the p52 NF-kappaB subunit.* EMBO J, 2006. **25**(20): p. 4820-32.

219. Collart, M.A., P. Baeuerle and P. Vassalli. *Regulation of tumor necrosis factor alpha transcription in macrophages: involvement of four kappa B-like motifs and of constitutive and inducible forms of NF-kappa B.* Mol Cell Biol, 1990. **10**(4): p. 1498-506.

220. Hiscott, J., J. Marois, J. Garoufalis, M. D'Addario, A. Roulston, I. Kwan, N. Pepin, J. Lacoste, H. Nguyen, G. Bensi and et al. *Characterization of a functional NF-kappa B site in the human interleukin 1 beta promoter: evidence for a positive autoregulatory loop.* Mol Cell Biol, 1993. **13**(10): p. 6231-40.

221. Son, Y.H., Y.T. Jeong, K.A. Lee, K.H. Choi, S.M. Kim, B.Y. Rhim and K. Kim. *Roles of MAPK and NF-kappaB in interleukin-6 induction by lipopolysaccharide in vascular smooth muscle cells.* J Cardiovasc Pharmacol, 2008. **51**(1): p. 71-7.

222. Morris, K.R., R.D. Lutz, H.S. Choi, T. Kamitani, K. Chmura and E.D. Chan. *Role of the NF-kappaB signaling pathway and kappaB cis-regulatory elements on the IRF-1 and iNOS promoter regions in mycobacterial lipoarabinomannan induction of nitric oxide.* Infect Immun, 2003. **71**(3): p. 1442-52.

223. Song, H.Y., M. Rothe and D.V. Goeddel. *The tumor necrosis factor-inducible zinc finger protein A20 interacts with TRAF1/TRAF2 and inhibits NF-kappaB activation.* Proc Natl Acad Sci U S A, 1996. **93**(13): p. 6721-5.

224. Beg, A.A., W.C. Sha, R.T. Bronson, S. Ghosh and D. Baltimore. *Embryonic lethality and liver degeneration in mice lacking the RelA component of NF-kappa B.* Nature, 1995. **376**(6536): p. 167-70.

225. Alcamo, E., N. Hacohen, L.C. Schulte, P.D. Rennert, R.O. Hynes and D. Baltimore. *Requirement for the NF-kappaB family member RelA in the development of secondary lymphoid organs.* J Exp Med, 2002. **195**(2): p. 233-44.

226. Kontgen, F., R.J. Grumont, A. Strasser, D. Metcalf, R. Li, D. Tarlinton and S. Gerondakis. *Mice lacking the c-rel proto-oncogene exhibit defects in lymphocyte proliferation, humoral immunity, and interleukin-2 expression.* Genes Dev, 1995. **9**(16): p. 1965-77.

227. Pizzi, M., F. Goffi, F. Boroni, M. Benarese, S.E. Perkins, H.C. Liou and P. Spano. *Opposing roles for NF-kappa B/Rel factors p65 and c-Rel in the modulation of neuron survival elicited by glutamate and interleukin-1beta.* J Biol Chem, 2002. **277**(23): p. 20717-23.

228. Sha, W.C., H.C. Liou, E.I. Tuomanen and D. Baltimore. *Targeted disruption of the p50 subunit of NF-kappa B leads to multifocal defects in immune responses.* Cell, 1995. **80**(2): p. 321-30.

229. Wang, Y., A. Meng, H. Lang, S.A. Brown, J.L. Konopa, M.S. Kindy, R.A. Schmiedt, J.S. Thompson and D. Zhou. *Activation of nuclear factor kappaB In vivo selectively protects the murine small intestine against ionizing radiation-induced damage.* Cancer Res, 2004. **64**(17): p. 6240-6.

230. Inan, M.S., V. Tolmacheva, Q.S. Wang, D.W. Rosenberg and C. Giardina. *Transcription factor NF-kappaB participates in regulation of epithelial cell turnover in the colon.* Am J Physiol Gastrointest Liver Physiol, 2000. **279**(6): p. G1282-91.

231. Hunter, R.B. and S.C. Kandarian. *Disruption of either the Nfkb1 or the Bcl3 gene inhibits skeletal muscle atrophy.* J Clin Invest, 2004. **114**(10): p. 1504-11.

232. Caamano, J.H., C.A. Rizzo, S.K. Durham, D.S. Barton, C. Raventos-Suarez, C.M. Snapper and R. Bravo. *Nuclear factor (NF)-kappa B2 (p100/p52) is required for normal splenic microarchitecture and B cell-mediated immune responses.* J Exp Med, 1998. **187**(2): p. 185-96.

233. Weih, F., D. Carrasco, S.K. Durham, D.S. Barton, C.A. Rizzo, R.P. Ryseck, S.A. Lira and R. Bravo. *Multiorgan inflammation and hematopoietic abnormalities in mice with a targeted disruption of RelB, a member of the NF-kappa B/Rel family.* Cell, 1995. **80**(2): p. 331-40.

234. Weih, D.S., Z.B. Yilmaz and F. Weih. *Essential role of RelB in germinal center and marginal zone formation and proper expression of homing chemokines.* J Immunol, 2001. **167**(4): p. 1909-19.

235. Zanetti, M., P. Castiglioni, S. Schoenberger and M. Gerloni. *The role of relB in regulating the adaptive immune response.* Ann N Y Acad Sci, 2003. **987**: p. 249-57.

236. Li, Q. and I.M. Verma. *NF-kappaB regulation in the immune system.* Nat Rev Immunol, 2002. **2**(10): p. 725-34.

237. Kucharczak, J., M.J. Simmons, Y. Fan and C. Gelinas. *To be, or not to be: NF-kappaB is the answer--role of Rel/NF-kappaB in the regulation of apoptosis.* Oncogene, 2003. **22**(56): p. 8961-82.

238. Luo, J.L., H. Kamata and M. Karin. *The anti-death machinery in IKK/NF-kappaB signaling.* J Clin Immunol, 2005. **25**(6): p. 541-50.

239. Maeda, S., L. Chang, Z.W. Li, J.L. Luo, H. Leffert and M. Karin. *IKKbeta is required for prevention of apoptosis mediated by cell-bound but not by circulating TNFalpha.* Immunity, 2003. **19**(5): p. 725-37.

240. Chaisson, M.L., J.T. Brooling, W. Ladiges, S. Tsai and N. Fausto. *Hepatocyte-specific inhibition of NF-kappaB leads to apoptosis after TNF treatment, but not after partial hepatectomy.* J Clin Invest, 2002. **110**(2): p. 193-202.

241. Dutta, J., Y. Fan, N. Gupta, G. Fan and C. Gelinas. *Current insights into the regulation of programmed cell death by NF-kappaB.* Oncogene, 2006. **25**(51): p. 6800-16.

242. Mattson, M.P. and S. Camandola. *NF-kappaB in neuronal plasticity and neurodegenerative disorders.* J Clin Invest, 2001. **107**(3): p. 247-54.

243. Karin, M. and A. Lin. *NF-kappaB at the crossroads of life and death.* Nat Immunol, 2002. **3**(3): p. 221-7.

244. Liu, Z.G., H. Hsu, D.V. Goeddel and M. Karin. *Dissection of TNF receptor 1 effector functions: JNK activation is not linked to apoptosis while NF-kappaB activation prevents cell death.* Cell, 1996. **87**(3): p. 565-76.

245. Alcamo, E., J.P. Mizgerd, B.H. Horwitz, R. Bronson, A.A. Beg, M. Scott, C.M. Doerschuk, R.O. Hynes and D. Baltimore. *Targeted mutation of TNF receptor I rescues the RelA-deficient mouse and reveals a critical role for NF-kappa B in leukocyte recruitment.* J Immunol, 2001. **167**(3): p. 1592-600.

246. Li, Q., D. Van Antwerp, F. Mercurio, K.F. Lee and I.M. Verma. *Severe liver degeneration in mice lacking the IkappaB kinase 2 gene.* Science, 1999. **284**(5412): p. 321-5.

247. Tanaka, M., M.E. Fuentes, K. Yamaguchi, M.H. Durnin, S.A. Dalrymple, K.L. Hardy and D.V. Goeddel. *Embryonic lethality, liver degeneration, and impaired NF-kappa B activation in IKK-beta-deficient mice.* Immunity, 1999. **10**(4): p. 421-9.

248. Rudolph, D., W.C. Yeh, A. Wakeham, B. Rudolph, D. Nallainathan, J. Potter, A.J. Elia and T.W. Mak. *Severe liver degeneration and lack of NF-kappaB activation in NEMO/IKKgamma-deficient mice.* Genes Dev, 2000. **14**(7): p. 854-62.

249. Chen, L.W., L. Egan, Z.W. Li, F.R. Greten, M.F. Kagnoff and M. Karin. *The two faces of IKK and NF-kappaB inhibition: prevention of systemic inflammation but increased local injury following intestinal ischemia-reperfusion.* Nat Med, 2003. **9**(5): p. 575-81.

250. Greten, F.R., L. Eckmann, T.F. Greten, J.M. Park, Z.W. Li, L.J. Egan, M.F. Kagnoff and M. Karin. *IKKbeta links inflammation and tumorigenesis in a mouse model of colitis-associated cancer.* Cell, 2004. **118**(3): p. 285-96.

251. Egan, L.J., L. Eckmann, F.R. Greten, S. Chae, Z.W. Li, G.M. Myhre, S. Robine, M. Karin and M.F. Kagnoff. *IkappaB-kinasebeta-dependent NF-kappaB*

activation provides radioprotection to the intestinal epithelium. Proc Natl Acad Sci U S A, 2004. **101**(8): p. 2452-7.

252. Nenci, A., C. Becker, A. Wullaert, R. Gareus, G. van Loo, S. Danese, M. Huth, A. Nikolaev, C. Neufert, B. Madison, D. Gumucio, M.F. Neurath and M. Pasparakis. *Epithelial NEMO links innate immunity to chronic intestinal inflammation.* Nature, 2007. **446**(7135): p. 557-61.

253. Liston, P., W.G. Fong and R.G. Korneluk. *The inhibitors of apoptosis: there is more to life than Bcl2.* Oncogene, 2003. **22**(53): p. 8568-80.

254. Wright, C.W. and C.S. Duckett. *Reawakening the cellular death program in neoplasia through the therapeutic blockade of IAP function.* J Clin Invest, 2005. **115**(10): p. 2673-8.

255. Wilkinson, J.C., A.S. Wilkinson, F.L. Scott, R.A. Csomos, G.S. Salvesen and C.S. Duckett. *Neutralization of Smac/Diablo by inhibitors of apoptosis (IAPs). A caspase-independent mechanism for apoptotic inhibition.* J Biol Chem, 2004. **279**(49): p. 51082-90.

256. Duckett, C.S. *IAP proteins: sticking it to Smac.* Biochem J, 2005. **385**(Pt 1): p. e1-2.

257. Kaur, S., F. Wang, M. Venkatraman and M. Arsura. *X-linked inhibitor of apoptosis (XIAP) inhibits c-Jun N-terminal kinase 1 (JNK1) activation by transforming growth factor beta1 (TGF-beta1) through ubiquitin-mediated proteosomal degradation of the TGF-beta1-activated kinase 1 (TAK1).* J Biol Chem, 2005. **280**(46): p. 38599-608.

258. Grumont, R.J., I.J. Rourke and S. Gerondakis. *Rel-dependent induction of A1 transcription is required to protect B cells from antigen receptor ligation-induced apoptosis.* Genes Dev, 1999. **13**(4): p. 400-11.

259. Grossmann, M., L.A. O'Reilly, R. Gugasyan, A. Strasser, J.M. Adams and S. Gerondakis. *The anti-apoptotic activities of Rel and RelA required during B-cell maturation involve the regulation of Bcl-2 expression.* EMBO J, 2000. **19**(23): p. 6351-60.

260. Micheau, O. and J. Tschopp. *Induction of TNF receptor I-mediated apoptosis via two sequential signaling complexes.* Cell, 2003. **114**(2): p. 181-90.

261. Bernard, D., B. Quatannens, B. Vandenbunder and C. Abbadie. *Rel/NF-kappaB transcription factors protect against tumor necrosis factor (TNF)-related apoptosis-inducing ligand (TRAIL)-induced apoptosis by up-regulating the TRAIL decoy receptor DcR1.* J Biol Chem, 2001. **276**(29): p. 27322-8.

262. Papa, S., F. Zazzeroni, C. Bubici, S. Jayawardena, K. Alvarez, S. Matsuda, D.U. Nguyen, C.G. Pham, A.H. Nelsbach, T. Melis, E. De Smaele, W.J. Tang, L. D'Adamio and G. Franzoso. *Gadd45 beta mediates the NF-kappa B*

suppression of JNK signalling by targeting MKK7/JNKK2. Nat Cell Biol, 2004. **6**(2): p. 146-53.

263. Baetz, D., K.M. Regula, K. Ens, J. Shaw, S. Kothari, N. Yurkova and L.A. Kirshenbaum. *Nuclear factor-kappaB-mediated cell survival involves transcriptional silencing of the mitochondrial death gene BNIP3 in ventricular myocytes.* Circulation, 2005. **112**(24): p. 3777-85.

264. Neurath, M.F., C. Becker and K. Barbulescu. *Role of NF-kappaB in immune and inflammatory responses in the gut.* Gut, 1998. **43**(6): p. 856-60.

265. Berndt, U., S. Bartsch, L. Philipsen, S. Danese, B. Wiedenmann, A.U. Dignass, M. Hammerle and A. Sturm. *Proteomic analysis of the inflamed intestinal mucosa reveals distinctive immune response profiles in Crohn's disease and ulcerative colitis.* J Immunol, 2007. **179**(1): p. 295-304.

266. Lawrance, I.C., F. Wu, A.Z. Leite, J. Willis, G.A. West, C. Fiocchi and S. Chakravarti. *A murine model of chronic inflammation-induced intestinal fibrosis down-regulated by antisense NF-kappa B.* Gastroenterology, 2003. **125**(6): p. 1750-61.

267. MacMaster, J.F., D.M. Dambach, D.B. Lee, K.K. Berry, Y. Qiu, F.C. Zusi and J.R. Burke. *An inhibitor of IkappaB kinase, BMS-345541, blocks endothelial cell adhesion molecule expression and reduces the severity of dextran sulfate sodium-induced colitis in mice.* Inflamm Res, 2003. **52**(12): p. 508-11.

268. Eckmann, L., T. Nebelsiek, A.A. Fingerle, S.M. Dann, J. Mages, R. Lang, S. Robine, M.F. Kagnoff, R.M. Schmid, M. Karin, M.C. Arkan and F.R. Greten. *Opposing functions of IKKbeta during acute and chronic intestinal inflammation.* Proc Natl Acad Sci U S A, 2008. **105**(39): p. 15058-63.

269. Pai, S.Y., O. Levy, H.H. Jabara, J.N. Glickman, L. Stoler-Barak, J. Sachs, S. Nurko, J.S. Orange and R.S. Geha. *Allogeneic transplantation successfully corrects immune defects, but not susceptibility to colitis, in a patient with nuclear factor-kappaB essential modulator deficiency.* J Allergy Clin Immunol, 2008. **122**(6): p. 1113-1118 e1.

270. Pasparakis, M. *Regulation of tissue homeostasis by NF-kappaB signalling: implications for inflammatory diseases.* Nat Rev Immunol, 2009. **9**(11): p. 778-88.

271. Steinbrecher, K.A., E. Harmel-Laws, R. Sitcheran and A.S. Baldwin. *Loss of epithelial RelA results in deregulated intestinal proliferative/apoptotic homeostasis and susceptibility to inflammation.* J Immunol, 2008. **180**(4): p. 2588-99.

272. Artis, D., S. Shapira, N. Mason, K.M. Speirs, M. Goldschmidt, J. Caamano, H.C. Liou, C.A. Hunter and P. Scott. *Differential requirement for NF-kappa B*

family members in control of helminth infection and intestinal inflammation. J Immunol, 2002. **169**(8): p. 4481-7.

273. Karin, M. and F.R. Greten. *NF-kappaB: linking inflammation and immunity to cancer development and progression.* Nat Rev Immunol, 2005. **5**(10): p. 749-59.

274. Lu, H., W. Ouyang and C. Huang. *Inflammation, a key event in cancer development.* Mol Cancer Res, 2006. **4**(4): p. 221-33.

275. Shen, H.M. and V. Tergaonkar. *NFkappaB signaling in carcinogenesis and as a potential molecular target for cancer therapy.* Apoptosis, 2009. **14**(4): p. 348-63.

276. Sakamoto, K. and S. Maeda. *Targeting NF-kappaB for colorectal cancer.* Expert Opin Ther Targets, 2010. **14**(6): p. 593-601.

277. Potten, C.S. and H.K. Grant. *The relationship between ionizing radiation-induced apoptosis and stem cells in the small and large intestine.* Br J Cancer, 1998. **78**(8): p. 993-1003.

278. Boushey, R.P., B. Yusta and D.J. Drucker. *Glucagon-like peptide (GLP)-2 reduces chemotherapy-associated mortality and enhances cell survival in cells expressing a transfected GLP-2 receptor.* Cancer Res, 2001. **61**(2): p. 687-93.

279. Bowen, J.M., R.J. Gibson, A.M. Stringer, T.W. Chan, A.S. Prabowo, A.G. Cummins and D.M. Keefe. *Role of p53 in irinotecan-induced intestinal cell death and mucosal damage.* Anticancer Drugs, 2007. **18**(2): p. 197-210.

280. Gibson, R.J., J.M. Bowen, E. Alvarez, J. Finnie and D.M. Keefe. *Establishment of a single-dose irinotecan model of gastrointestinal mucositis.* Chemotherapy, 2007. **53**(5): p. 360-9.

281. Hu, Y., J. Martin, R. Le Leu and G.P. Young. *The colonic response to genotoxic carcinogens in the rat: regulation by dietary fibre.* Carcinogenesis, 2002. **23**(7): p. 1131-7.

282. Hu, Y., R.K. Le Leu and G.P. Young. *Sulindac corrects defective apoptosis and suppresses azoxymethane-induced colonic oncogenesis in p53 knockout mice.* Int J Cancer, 2005. **116**(6): p. 870-5.

283. Cheung, K.L., T.O. Khor, M.T. Huang and A.N. Kong. *Differential in vivo mechanism of chemoprevention of tumor formation in azoxymethane/dextran sodium sulfate mice by PEITC and DBM.* Carcinogenesis. **31**(5): p. 880-5.

284. Hamamoto, N., K. Maemura, I. Hirata, M. Murano, S. Sasaki and K. Katsu. *Inhibition of dextran sulphate sodium (DSS)-induced colitis in mice by*

intracolonically administered antibodies against adhesion molecules (endothelial leucocyte adhesion molecule-1 (ELAM-1) or intercellular adhesion molecule-1 (ICAM-1)). Clin Exp Immunol, 1999. **117**(3): p. 462-8.

285. Murthy, S.N., H.S. Cooper, H. Shim, R.S. Shah, S.A. Ibrahim and D.J. Sedergran. *Treatment of dextran sulfate sodium-induced murine colitis by intracolonic cyclosporin.* Dig Dis Sci, 1993. **38**(9): p. 1722-34.

286. Cooper, H.S., S.N. Murthy, R.S. Shah and D.J. Sedergran. *Clinicopathologic study of dextran sulfate sodium experimental murine colitis.* Lab Invest, 1993. **69**(2): p. 238-49.

287. Bauer, C., P. Duewell, C. Mayer, H.A. Lehr, K.A. Fitzgerald, M. Dauer, J. Tschopp, S. Endres, E. Latz and M. Schnurr. *Colitis induced in mice with dextran sulfate sodium (DSS) is mediated by the NLRP3 inflammasome.* Gut, 2010. **59**(9): p. 1192-9.

288. Bergin, I.L., R.C. Smedley, D.G. Esplin, W.L. Spangler and M. Kiupel. *Prognostic evaluation of Ki67 threshold value in canine oral melanoma.* Vet Pathol, 2011. **48**(1): p. 41-53.

289. Kumar, L.D. and A.R. Clarke. *Gene manipulation through the use of small interfering RNA (siRNA): from in vitro to in vivo applications.* Adv Drug Deliv Rev, 2007. **59**(2-3): p. 87-100.

290. Weiser, M.M. *Intestinal epithelial cell surface membrane glycoprotein synthesis. I. An indicator of cellular differentiation.* J Biol Chem, 1973. **248**(7): p. 2536-41.

291. Potten, C.S., G. Owen and S.A. Roberts. *The temporal and spatial changes in cell proliferation within the irradiated crypts of the murine small intestine.* Int J Radiat Biol, 1990. **57**(1): p. 185-99.

292. van der Woude, C.J., J.H. Kleibeuker, P.L. Jansen and H. Moshage. *Chronic inflammation, apoptosis and (pre-)malignant lesions in the gastro-intestinal tract.* Apoptosis, 2004. **9**(2): p. 123-30.

293. Fearon, E.R. and B. Vogelstein. *A genetic model for colorectal tumorigenesis.* Cell, 1990. **61**(5): p. 759-67.

294. Bernal-Mizrachi, L., C.M. Lovly and L. Ratner. *The role of NF-{kappa}B-1 and NF-{kappa}B-2-mediated resistance to apoptosis in lymphomas.* Proc Natl Acad Sci U S A, 2006. **103**(24): p. 9220-5.

295. Nishimura, T., A. Andoh, T. Hashimoto, A. Kobori, T. Tsujikawa and Y. Fujiyama. *Cellobiose Prevents the Development of Dextran Sulfate Sodium (DSS)-Induced Experimental Colitis.* J Clin Biochem Nutr, 2010. **46**(2): p. 105-10.

296. Beg, A.A. and D. Baltimore. *An essential role for NF-kappaB in preventing TNF-alpha-induced cell death.* Science, 1996. **274**(5288): p. 782-4.

297. Iimuro, Y., T. Nishiura, C. Hellerbrand, K.E. Behrns, R. Schoonhoven, J.W. Grisham and D.A. Brenner. *NFkappaB prevents apoptosis and liver dysfunction during liver regeneration.* J Clin Invest, 1998. **101**(4): p. 802-11.

298. Baichwal, V.R. and P.A. Baeuerle. *Activate NF-kappa B or die?* Curr Biol, 1997. **7**(2): p. R94-6.

299. Baldwin, A.S., Jr., J.C. Azizkhan, D.E. Jensen, A.A. Beg and L.R. Coodly. *Induction of NF-kappa B DNA-binding activity during the G0-to-G1 transition in mouse fibroblasts.* Mol Cell Biol, 1991. **11**(10): p. 4943-51.

300. Ishikawa, H., D. Carrasco, E. Claudio, R.P. Ryseck and R. Bravo. *Gastric hyperplasia and increased proliferative responses of lymphocytes in mice lacking the COOH-terminal ankyrin domain of NF-kappaB2.* J Exp Med, 1997. **186**(7): p. 999-1014.

301. Finnberg, N., S.H. Kim, E.E. Furth, J.J. Liu, P. Russo, D.A. Piccoli, A. Grimberg and W.S. El-Deiry. *Non-invasive fluorescence imaging of cell death in fresh human colon epithelia treated with 5-Fluorouracil, CPT-11 and/or TRAIL.* Cancer Biol Ther, 2005. **4**(9): p. 937-42.

302. Siegmund, D., A. Hausser, N. Peters, P. Scheurich and H. Wajant. *Tumor necrosis factor (TNF) and phorbol ester induce TNF-related apoptosis-inducing ligand (TRAIL) under critical involvement of NF-kappa B essential modulator (NEMO)/IKKgamma.* J Biol Chem, 2001. **276**(47): p. 43708-12.

303. Lamkanfi, M., W. Declercq, M. Kalai, X. Saelens and P. Vandenabeele. *Alice in caspase land. A phylogenetic analysis of caspases from worm to man.* Cell Death Differ, 2002. **9**(4): p. 358-61.

304. Kalai, M., M. Lamkanfi, G. Denecker, M. Boogmans, S. Lippens, A. Meeus, W. Declercq and P. Vandenabeele. *Regulation of the expression and processing of caspase-12.* J Cell Biol, 2003. **162**(3): p. 457-67.

305. Mineva, N.D., T.L. Rothstein, J.A. Meyers, A. Lerner and G.E. Sonenshein. *CD40 ligand-mediated activation of the de novo RelB NF-kappaB synthesis pathway in transformed B cells promotes rescue from apoptosis.* J Biol Chem, 2007. **282**(24): p. 17475-85.

306. Wang, X., K. Belguise, N. Kersual, K.H. Kirsch, N.D. Mineva, F. Galtier, D. Chalbos and G.E. Sonenshein. *Oestrogen signalling inhibits invasive phenotype by repressing RelB and its target BCL2.* Nat Cell Biol, 2007. **9**(4): p. 470-8.

307. Sayer, B., J. Lu, C. Green, J.D. Soderholm, M. Akhtar and D.M. McKay. *Dextran sodium sulphate-induced colitis perturbs muscarinic cholinergic*

control of colonic epithelial ion transport. Br J Pharmacol, 2002. **135**(7): p. 1794-800.

308. Diaz-Granados, N., K. Howe, J. Lu and D.M. McKay. *Dextran sulfate sodium-induced colonic histopathology, but not altered epithelial ion transport, is reduced by inhibition of phosphodiesterase activity.* Am J Pathol, 2000. **156**(6): p. 2169-77.

309. Cepek, K.L., S.K. Shaw, C.M. Parker, G.J. Russell, J.S. Morrow, D.L. Rimm and M.B. Brenner. *Adhesion between epithelial cells and T lymphocytes mediated by E-cadherin and the alpha E beta 7 integrin.* Nature, 1994. **372**(6502): p. 190-3.

310. Beg, A.A., W.C. Sha, R.T. Bronson and D. Baltimore. *Constitutive NF-kappa B activation, enhanced granulopoiesis, and neonatal lethality in I kappa B alpha-deficient mice.* Genes Dev, 1995. **9**(22): p. 2736-46.

311. Acharyya, S., S.A. Villalta, N. Bakkar, T. Bupha-Intr, P.M. Janssen, M. Carathers, Z.W. Li, A.A. Beg, S. Ghosh, Z. Sahenk, M. Weinstein, K.L. Gardner, J.A. Rafael-Fortney, M. Karin, J.G. Tidball, A.S. Baldwin and D.C. Guttridge. *Interplay of IKK/NF-kappaB signaling in macrophages and myofibers promotes muscle degeneration in Duchenne muscular dystrophy.* J Clin Invest, 2007. **117**(4): p. 889-901.

312. Greten, F.R., M.C. Arkan, J. Bollrath, L.C. Hsu, J. Goode, C. Miething, S.I. Goktuna, M. Neuenhahn, J. Fierer, S. Paxian, N. Van Rooijen, Y. Xu, T. O'Cain, B.B. Jaffee, D.H. Busch, J. Duyster, R.M. Schmid, L. Eckmann and M. Karin. *NF-kappaB is a negative regulator of IL-1beta secretion as revealed by genetic and pharmacological inhibition of IKKbeta.* Cell, 2007. **130**(5): p. 918-31.

313. Lawrence, T., D.W. Gilroy, P.R. Colville-Nash and D.A. Willoughby. *Possible new role for NF-kappaB in the resolution of inflammation.* Nat Med, 2001. **7**(12): p. 1291-7.

314. Karban, A.S., T. Okazaki, C.I. Panhuysen, T. Gallegos, J.J. Potter, J.E. Bailey-Wilson, M.S. Silverberg, R.H. Duerr, J.H. Cho, P.K. Gregersen, Y. Wu, J.P. Achkar, T. Dassopoulos, E. Mezey, T.M. Bayless, F.J. Nouvet and S.R. Brant. *Functional annotation of a novel NFKB1 promoter polymorphism that increases risk for ulcerative colitis.* Hum Mol Genet, 2004. **13**(1): p. 35-45.

315. Zou, Y.F., F. Wang, X.L. Feng, J.H. Tao, J.M. Zhu, F.M. Pan and H. Su. *Association of NFKB1 -94ins/delATTG promoter polymorphism with susceptibility to autoimmune and inflammatory diseases: a meta-analysis.* Tissue Antigens, 2011. **77**(1): p. 9-17.

316. Borm, M.E., A.A. van Bodegraven, C.J. Mulder, G. Kraal and G. Bouma. *A NFKB1 promoter polymorphism is involved in susceptibility to ulcerative colitis.* Int J Immunogenet, 2005. **32**(6): p. 401-5.

317. Andersen, V., J. Christensen, A. Ernst, B.A. Jacobsen, A. Tjonneland, H.B. Krarup and U. Vogel. *Polymorphisms in NF-kappaB, PXR, LXR, PPARgamma and risk of inflammatory bowel disease.* World J Gastroenterol, 2011. **17**(2): p. 197-206.

318. Oliver, J., M. Gomez-Garcia, L. Paco, M.A. Lopez-Nevot, A. Pinero, F. Correro, L. Martin, J.A. Brieva, A. Nieto and J. Martin. *A functional polymorphism of the NFKB1 promoter is not associated with ulcerative colitis in a Spanish population.* Inflamm Bowel Dis, 2005. **11**(6): p. 576-9.

319. Latiano, A., O. Palmieri, M.R. Valvano, F. Bossa, T. Latiano, G. Corritore, E. DeSanto, A. Andriulli and V. Annese. *Evaluating the role of the genetic variations of PTPN22, NFKB1, and FcGRIIIA genes in inflammatory bowel disease: a meta-analysis.* Inflamm Bowel Dis, 2007. **13**(10): p. 1212-9.

320. Lees, C.W., J.C. Barrett, M. Parkes and J. Satsangi. *New IBD genetics: common pathways with other diseases.* Gut, 2011. **60**(12): p. 1739-53.

321. Janse, M., L.E. Lamberts, L. Franke, S. Raychaudhuri, E. Ellinghaus, K. Muri Boberg, E. Melum, T. Folseraas, E. Schrumpf, A. Bergquist, E. Bjornsson, J. Fu, H. Jan Westra, H.J. Groen, R.S. Fehrmann, J. Smolonska, L.H. van den Berg, R.A. Ophoff, R.J. Porte, T.J. Weismuller, J. Wedemeyer, C. Schramm, M. Sterneck, R. Gunther, F. Braun, S. Vermeire, L. Henckaerts, C. Wijmenga, C.Y. Ponsioen, S. Schreiber, T.H. Karlsen, A. Franke and R.K. Weersma. *Three ulcerative colitis susceptibility loci are associated with primary sclerosing cholangitis and indicate a role for IL2, REL, and CARD9.* Hepatology, 2011. **53**(6): p. 1977-85.

322. Papadakis, K.A. and S.R. Targan. *Role of cytokines in the pathogenesis of inflammatory bowel disease.* Annu Rev Med, 2000. **51**: p. 289-98.

323. Reimund, J.M., C. Wittersheim, S. Dumont, C.D. Muller, R. Baumann, P. Poindron and B. Duclos. *Mucosal inflammatory cytokine production by intestinal biopsies in patients with ulcerative colitis and Crohn's disease.* J Clin Immunol, 1996. **16**(3): p. 144-50.

324. Ligumsky, M., P.L. Simon, F. Karmeli and D. Rachmilewitz. *Role of interleukin 1 in inflammatory bowel disease--enhanced production during active disease.* Gut, 1990. **31**(6): p. 686-9.

325. Youngman, K.R., P.L. Simon, G.A. West, F. Cominelli, D. Rachmilewitz, J.S. Klein and C. Fiocchi. *Localization of intestinal interleukin 1 activity and protein and gene expression to lamina propria cells.* Gastroenterology, 1993. **104**(3): p. 749-58.

326. Mahida, Y.R., K. Wu and D.P. Jewell. *Enhanced production of interleukin 1-beta by mononuclear cells isolated from mucosa with active ulcerative colitis of Crohn's disease.* Gut, 1989. **30**(6): p. 835-8.

327. Arai, Y., H. Takanashi, H. Kitagawa and I. Okayasu. *INVOLVEMENT OF INTERLEUKIN-1 IN THE DEVELOPMENT OF ULCERATIVE COLITIS INDUCED BY DEXTRAN SULFATE SODIUM IN MICE.* Cytokine, 1998. **10**(11): p. 890-896.

328. Ishiguro, Y. *Mucosal proinflammatory cytokine production correlates with endoscopic activity of ulcerative colitis.* J Gastroenterol, 1999. **34**(1): p. 66-74.

329. Woywodt, A., D. Ludwig, P. Neustock, A. Kruse, K. Schwarting, G. Jantschek, H. Kirchner and E.F. Stange. *Mucosal cytokine expression, cellular markers and adhesion molecules in inflammatory bowel disease.* Eur J Gastroenterol Hepatol, 1999. **11**(3): p. 267-76.

330. Raab, Y., R. Hallgren and B. Gerdin. *Enhanced intestinal synthesis of interleukin-6 is related to the disease severity and activity in ulcerative colitis.* Digestion, 1994. **55**(1): p. 44-9.

331. Gay, J., E. Kokkotou, M. O'Brien, C. Pothoulakis and K.P. Karalis. *Interleukin-6 genetic ablation protects from trinitrobenzene sulfonic acid-induced colitis in mice. Putative effect of antiinflammatory cytokines.* Neuroimmunomodulation, 2006. **13**(2): p. 114-21.

332. naito, Y., T. Takagi, K. Uchiyama, M. Kuroda, S. Kokura, H. Ichikawa, R. Yanagisawa, K. Inoue, H. Takano, M. Satoh, N. Yoshida, T. Okanoue and T. Yoshikawa. *Reduced intestinal inflammation induced by dextran sodium sulfate in interleukin-6-deficient mice.* Int J Mol Med, 2004. **14**(2): p. 191-6.

333. Grigoriadis, G., Y. Zhan, R.J. Grumont, D. Metcalf, E. Handman, C. Cheers and S. Gerondakis. *The Rel subunit of NF-kappaB-like transcription factors is a positive and negative regulator of macrophage gene expression: distinct roles for Rel in different macrophage populations.* EMBO J, 1996. **15**(24): p. 7099-107.

334. Wu, L., A. D'Amico, K.D. Winkel, M. Suter, D. Lo and K. Shortman. *RelB is essential for the development of myeloid-related CD8alpha- dendritic cells but not of lymphoid-related CD8alpha+ dendritic cells.* Immunity, 1998. **9**(6): p. 839-47.

335. Podolsky, D.K. *Inflammatory bowel disease.* N Engl J Med, 2002. **347**(6): p. 417-29.

336. Atreya, R. and M.F. Neurath. *New therapeutic strategies for treatment of inflammatory bowel disease.* Mucosal Immunol, 2008. **1**(3): p. 175-82.

337. te Velde, A.A., R.J. Huijbens, K. Heije, J.E. de Vries and C.G. Figdor. *Interleukin-4 (IL-4) inhibits secretion of IL-1 beta, tumor necrosis factor alpha, and IL-6 by human monocytes.* Blood, 1990. **76**(7): p. 1392-7.

338. Schreiber, S., T. Heinig, U. Panzer, R. Reinking, A. Bouchard, P.D. Stahl and A. Raedler. *Impaired response of activated mononuclear phagocytes to interleukin 4 in inflammatory bowel disease.* Gastroenterology, 1995. **108**(1): p. 21-33.

339. Togawa, J., H. Nagase, K. Tanaka, M. Inamori, T. Umezawa, A. Nakajima, M. Naito, S. Sato, T. Saito and H. Sekihara. *Lactoferrin reduces colitis in rats via modulation of the immune system and correction of cytokine imbalance.* Am J Physiol Gastrointest Liver Physiol, 2002. **283**(1): p. G187-95.

340. Stevceva, L., P. Pavli, A. Husband, A. Ramsay and W.F. Doe. *Dextran sulphate sodium-induced colitis is ameliorated in interleukin 4 deficient mice.* Genes Immun, 2001. **2**(6): p. 309-16.

341. Van Kampen, C., J. Gauldie and S.M. Collins. *Proinflammatory properties of IL-4 in the intestinal microenvironment.* Am J Physiol Gastrointest Liver Physiol, 2005. **288**(1): p. G111-7.

342. Coussens, L.M. and Z. Werb. *Inflammation and cancer.* Nature, 2002. **420**(6917): p. 860-7.

343. Onizawa, M., T. Nagaishi, T. Kanai, K. Nagano, S. Oshima, Y. Nemoto, A. Yoshioka, T. Totsuka, R. Okamoto, T. Nakamura, N. Sakamoto, K. Tsuchiya, K. Aoki, K. Ohya, H. Yagita and M. Watanabe. *Signaling pathway via TNF-alpha/NF-kappaB in intestinal epithelial cells may be directly involved in colitis-associated carcinogenesis.* Am J Physiol Gastrointest Liver Physiol, 2009. **296**(4): p. G850-9.

344. Ekbom, A., C. Helmick, M. Zack and H.O. Adami. *Ulcerative colitis and colorectal cancer. A population-based study.* N Engl J Med, 1990. **323**(18): p. 1228-33.

345. Eaden, J. *Review article: colorectal carcinoma and inflammatory bowel disease.* Aliment Pharmacol Ther, 2004. **20 Suppl 4**: p. 24-30.

346. Salcedo, R., A. Worschech, M. Cardone, Y. Jones, Z. Gyulai, R.M. Dai, E. Wang, W. Ma, D. Haines, C. O'HUigin, F.M. Marincola and G. Trinchieri. *MyD88-mediated signaling prevents development of adenocarcinomas of the colon: role of interleukin 18.* J Exp Med, 2010. **207**(8): p. 1625-36.

347. Matsumoto, S., T. Hara, K. Mitsuyama, M. Yamamoto, O. Tsuruta, M. Sata, J. Scheller, S. Rose-John, S. Kado and T. Takada. *Essential roles of IL-6 trans-signaling in colonic epithelial cells, induced by the IL-6/soluble-IL-6 receptor derived from lamina propria macrophages, on the development of colitis-associated premalignant cancer in a murine model.* J Immunol, 2010. **184**(3): p. 1543-51.

348. Li, H., W.K. Wu, Z.J. Li, K.M. Chan, C.C. Wong, C.G. Ye, L. Yu, J.J. Sung, C.H. Cho and M. Wang. *2,3',4,4',5'-Pentamethoxy-trans-stilbene, a resveratrol*

derivative, inhibits colitis-associated colorectal carcinogenesis in mice. Br J Pharmacol, 2010. **160**(6): p. 1352-61.

349. Neurath, M.F., S. Pettersson, K.H. Meyer zum Buschenfelde and W. Strober. *Local administration of antisense phosphorothioate oligonucleotides to the p65 subunit of NF-kappa B abrogates established experimental colitis in mice.* Nat Med, 1996. **2**(9): p. 998-1004.

350. Balkwill, F. and A. Mantovani. *Inflammation and cancer: back to Virchow?* Lancet, 2001. **357**(9255): p. 539-45.

351. de Visser, K.E. and L.M. Coussens. *The interplay between innate and adaptive immunity regulates cancer development.* Cancer Immunol Immunother, 2005. **54**(11): p. 1143-52.

352. Zaki, M.H., P. Vogel, R.K. Malireddi, M. Body-Malapel, P.K. Anand, J. Bertin, D.R. Green, M. Lamkanfi and T.D. Kanneganti. *The NOD-like receptor NLRP12 attenuates colon inflammation and tumorigenesis.* Cancer Cell, 2011. **20**(5): p. 649-60.

353. Allen, I.C., J.E. Wilson, M. Schneider, J.D. Lich, R.A. Roberts, J.C. Arthur, R.M. Woodford, B.K. Davis, J.M. Uronis, H.H. Herfarth, C. Jobin, A.B. Rogers and J.P. Ting. *NLRP12 suppresses colon inflammation and tumorigenesis through the negative regulation of noncanonical NF-kappaB signaling.* Immunity, 2012. **36**(5): p. 742-54.

354. Adli, M., E. Merkhofer, P. Cogswell and A.S. Baldwin. *IKKalpha and IKKbeta each function to regulate NF-kappaB activation in the TNF-induced/canonical pathway.* PLoS One, 2010. **5**(2): p. e9428.

355. Zarnegar, B., S. Yamazaki, J.Q. He and G. Cheng. *Control of canonical NF-kappaB activation through the NIK-IKK complex pathway.* Proc Natl Acad Sci U S A, 2008. **105**(9): p. 3503-8.

356. Okamoto, T., T. Sanda and K. Asamitsu. *NF-kappa B signaling and carcinogenesis.* Curr Pharm Des, 2007. **13**(5): p. 447-62.

357. Renehan, A.G., S.P. Bach and C.S. Potten. *The relevance of apoptosis for cellular homeostasis and tumorigenesis in the intestine.* Can J Gastroenterol, 2001. **15**(3): p. 166-76.

358. Hong, M.Y., J.R. Lupton, J.S. Morris, N. Wang, R.J. Carroll, L.A. Davidson, R.H. Elder and R.S. Chapkin. *Dietary fish oil reduces O6-methylguanine DNA adduct levels in rat colon in part by increasing apoptosis during tumor initiation.* Cancer Epidemiol Biomarkers Prev, 2000. **9**(8): p. 819-26.

359. Baron, J.A. and R.S. Sandler. *Nonsteroidal anti-inflammatory drugs and cancer prevention.* Annu Rev Med, 2000. **51**: p. 511-23.

360. Barnes, C.J., I.L. Cameron, W.E. Hardman and M. Lee. *Non-steroidol anti-inflammatory drug effect on crypt cell proliferation and apoptosis during initiation of rat colon carcinogenesis.* Br J Cancer, 1998. **77**(4): p. 573-80.

361. Reddy, B.S., T. Kawamori, R.A. Lubet, V.E. Steele, G.J. Kelloff and C.V. Rao. *Chemopreventive efficacy of sulindac sulfone against colon cancer depends on time of administration during carcinogenic process.* Cancer Res, 1999. **59**(14): p. 3387-91.

362. Hayden, M.S., A.P. West and S. Ghosh. *NF-kappaB and the immune response.* Oncogene, 2006. **25**(51): p. 6758-80.

363. Perkins, N.D. and T.D. Gilmore. *Good cop, bad cop: the different faces of NF-kappaB.* Cell Death Differ, 2006. **13**(5): p. 759-72.

364. Gilmore, T.D. and S. Gerondakis. *The c-Rel Transcription Factor in Development and Disease.* Genes Cancer, 2011. **2**(7): p. 695-711.

365. Gugasyan, R., A. Voss, G. Varigos, T. Thomas, R.J. Grumont, P. Kaur, G. Grigoriadis and S. Gerondakis. *The transcription factors c-rel and RelA control epidermal development and homeostasis in embryonic and adult skin via distinct mechanisms.* Mol Cell Biol, 2004. **24**(13): p. 5733-45.

366. LA, O.R., L. Tai, L. Lee, E.A. Kruse, S. Grabow, W.D. Fairlie, N.M. Haynes, D.M. Tarlinton, J.G. Zhang, G.T. Belz, M.J. Smyth, P. Bouillet, L. Robb and A. Strasser. *Membrane-bound Fas ligand only is essential for Fas-induced apoptosis.* Nature, 2009. **461**(7264): p. 659-63.

367. Chen, L., S.M. Park, A.V. Tumanov, A. Hau, K. Sawada, C. Feig, J.R. Turner, Y.X. Fu, I.L. Romero, E. Lengyel and M.E. Peter. *CD95 promotes tumour growth.* Nature, 2010. **465**(7297): p. 492-6.

368. Liu, F., K. Bardhan, D. Yang, M. Thangaraju, V. Ganapathy, J.L. Waller, G.B. Liles, J.R. Lee and K. Liu. *NF-kappaB directly regulates Fas transcription to modulate Fas-mediated apoptosis and tumor suppression.* J Biol Chem, 2012. **287**(30): p. 25530-40.

369. Barnes, P.J. and M. Karin. *Nuclear factor-kappaB: a pivotal transcription factor in chronic inflammatory diseases.* N Engl J Med, 1997. **336**(15): p. 1066-71.

370. Kopp, E. and S. Ghosh. *Inhibition of NF-kappa B by sodium salicylate and aspirin.* Science, 1994. **265**(5174): p. 956-9.

371. Yang, J.P., J.P. Merin, T. Nakano, T. Kato, Y. Kitade and T. Okamoto. *Inhibition of the DNA-binding activity of NF-kappa B by gold compounds in vitro.* FEBS Lett, 1995. **361**(1): p. 89-96.

372. Bantel, H., C. Berg, M. Vieth, M. Stolte, W. Kruis and K. Schulze-Osthoff. *Mesalazine inhibits activation of transcription factor NF-kappaB in inflamed mucosa of patients with ulcerative colitis.* Am J Gastroenterol, 2000. **95**(12): p. 3452-7.

373. Itzkowitz, S.H. and X. Yio. *Inflammation and cancer IV. Colorectal cancer in inflammatory bowel disease: the role of inflammation.* Am J Physiol Gastrointest Liver Physiol, 2004. **287**(1): p. G7-17.

374. Berg, D.J., N. Davidson, R. Kuhn, W. Muller, S. Menon, G. Holland, L. Thompson-Snipes, M.W. Leach and D. Rennick. *Enterocolitis and colon cancer in interleukin-10-deficient mice are associated with aberrant cytokine production and CD4(+) TH1-like responses.* J Clin Invest, 1996. **98**(4): p. 1010-20.

375. Ohsie, S.J., G.P. Sarantopoulos, A.J. Cochran and S.W. Binder. *Immunohistochemical characteristics of melanoma.* J Cutan Pathol, 2008. **35**(5): p. 433-44.

376. Thiagalingam, S. *A cascade of modules of a network defines cancer progression.* Cancer Res, 2006. **66**(15): p. 7379-85.

8 Appendix

8.1 List of published abstracts

1. **Hanedi, A**., M.D. Burkitt, C.A. Duckworth, R. Dimaline, J.H. Caamano and D.M. Pritchard. *Altered trail, CASPASE12, BAK and FAS-l expressions are associated with increased susceptibility to radiation induced intestinal epithelial apoptosis in NF-κ b1-null and NF-κ b2-null mice.* Gut, 2012. **61** (Suppl 2): p. A8-A9 (Oral presentation).

2. **Hanedi, A**., M.D. Burkitt, C.A. Duckworth, R. Dimaline, J.H. Caamano and D.M. Pritchard. *NF-κB2 deletion protects murine colon against DSS-induced colitis and this is associated with reduced expression of TNF-α and IL14.* Gut, 2012. **61** (Suppl 2): p. A165-A166 (Poster).

3. **Hanedi, A**., C.A. Duckworth, M.D. Burkitt, J.H. Caamano and D.M. Pritchard. *NF-κB1 and NF-κB2 regulate susceptibility to DNA damage induced intestinal epithelial apoptosis in vivo.* Gut, 2011. **60** (Suppl 1): p. A19-A20 (Oral presentation).